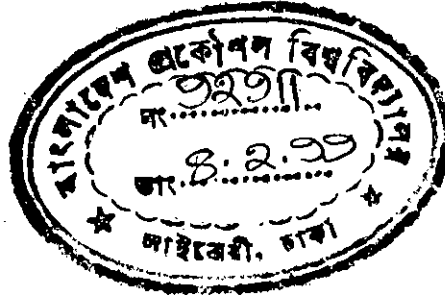


**STUDYING THE BEHAVIOUR OF SHEAR WALL-FLOOR SLAB  
CONNECTIONS USING ARTIFICIAL NEURAL NETWORK (ANN)**



**BY  
MD.SHAFIQUL ISLAM**

**A thesis submitted to the Department of Civil Engineering of Bangladesh University  
of Engineering and Technology, Dhaka in partial fulfilment of the requirement  
for the degree of**

**MASTER OF SCIENCE IN ENGINEERING (CIVIL)**



#92911#

**December, 1998**



**STUDYING THE BEHAVIOUR OF SHEAR WALL-FLOOR SLAB  
CONNECTIONS USING ARTIFICIAL NEURAL NETWORK (ANN)**

**BY**

**MD.SHAFIQUL ISLAM**

**A thesis approved as to style and content for the degree of M. Sc. Engg.(Civil)**

  
30/02/98

**Dr. Md. Shafiqul Bari**

**Professor**

**Department of Civil Engineering,**

**BUET, Dhaka-1000**

**: Chairman**

**(Supervisor)**

  
30.12.98

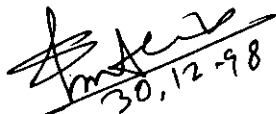
**Dr. M. Hossain Ali**

**Professor and Head,**

**Department of Civil Engineering,**

**BUET, Dhaka-1000**

**: Member**

  
30,12-98

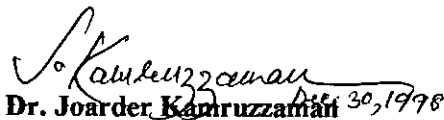
**Dr. M. S. A. Siddiquee**

**Associate Professor,**

**Department of Civil Engineering,**

**BUET, Dhaka-1000**

**: Member**

  
Dec. 30, 1998

**Dr. Joarder Kamruzzaman**

**Associate Professor,**

**Department of Electrical & Electronic Engineering,**

**BUET, Dhaka-1000**

**: Member**

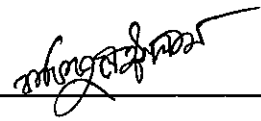
**(External)**

**December, 1998**

## DECLARATION

**I hereby certify that the research work reported in this thesis has been performed by me and that this work has not been submitted elsewhere for any other purpose (except for publication).**

**30 December, 1998**



---

**(MD.SHAFIQUL ISLAM)**

## ACKNOWLEDGEMENT

The author wishes to express his deepest gratitude to Dr. Md. Shafiq Bari, Professor, Department of Civil Engineering, BUET for his continuous guidance, invaluable suggestions and affectionate encouragement at every stage of this study.

The author wishes to express his profound gratitude to Dr. Joarder Kamruzzaman, Associate Professor, Department of Electrical & Electronic Engineering, BUET and Dr. M. S. A. Siddiquee, Associate Professor, Department of Civil Engineering, BUET for the interest taken by them in this research and for their advice and co-operation in developing the ANN.

The author wishes to express his deep feeling to his wife and daughters for their co-operation in completing the thesis work.

## ABSTRACT

The behaviour of shear wall-floor slab connections has been studied by using artificial neural network (ANN). An artificial neural network is an information-processing system based on the observed behaviour of biological nervous systems. A neural net consists of a large number of simple processing elements called neurones. Each neurone is connected to another neurone by means of direct communication links, each with an associated weight. The strength of the connections is dictated by the weights, which connect different neurones. Each neurone accepts a set of inputs from other neurones and also from external sources and generates an output. Structural design requires engineering judgement, intuition, experience and creative abilities in addition to number of options available to the designer. The ANN approach has the capabilities to incorporate some of the above-mentioned requirements for development of computer programs in structural design. ANN has been used in this thesis to

- (i) to determine the effective width of slabs coupling walls of different shapes and
- (ii) to determine the critical perimeter and ultimate punching shear capacity of the shear wall-floor slab junction,

A computer program is also developed for determining the effective width and the ultimate punching shear capacity of the shear wall-floor slab junction.

The effective width and ultimate failure load of slabs coupling walls of different shapes as predicted by ANN is compared with the experimental and theoretical results available. The agreement is found very good. The effect of shear wall thickness, opening between shear walls, effect of flange wall etc. on effective width and ultimate failure load of slabs are also analyzed. Once the neural network is developed, it will be able to predict the effective width and ultimate failure load for different new parameters within fraction of minute.

It has been revealed that application of ACI and British Code in case of shear wall structures for calculating punching shear strength may lead to an overestimation of strength. In most practical cases, the formula proposed by Bari M. S. gives a conservative estimation of punching shear strength of shear wall structures.

# CONTENTS

	Page
Declaration	iii
Acknowledgement	iv
Abstract	v
Contents	vi
List of Figures	x
List of Tables	xiii
List of Symbols	xv
List of Abbreviations	xvii

## Chapter 1: INTRODUCTION

1.1 Artificial Neural Networks	1
1.2 Shear Wall-Floor Slab Connections	2
1.3 Purpose of this Study	5

## Chapter 2: LITERATURE REVIEW

2.1 General	6
2.2 Effective Width of Floor Slab	7
2.2.1 Empirical Relationships for Effective Slab Width	9
2.3 Analysis of Shear Wall Structure	12
2.3.1 Strength of Slab-Wall Junction	14
2.3.2 Strength of Slab-Column Connections with Shear Reinforcement Transferring Shear only	15
2.3.3 Shear Strength of Slabs with Moments Transferred to Column	16

2.3.4 Shear Strength Predicted by Codes of Practice	16
2.3.4.1 BNBC/ACI Code	16
2.3.4.2 British Code BS 8110	21
2.4 Application of ANN	22
2.5 General Discussion	24

### **Chapter 3: ARTIFICIAL NEURAL NETWORKS**

3.1 Introduction	25
3.2 Artificial Neural Networks	25
3.3 Backpropagation (BP) Algorithm	30
3.4 Points to be Considered to Develop the Net	34
3.4.1 Selection of Activation Function	34
3.4.2 Learning Rate	35
3.4.3 Momentum Factor	35
3.4.4 Configuring Hidden Layer (s)	36
3.4.5 Initialisation of Weights and Biases	37
3.4.6 Evaluation of the Net Performance	37

### **Chapter 4: EFFECTIVE WIDTH OF FLOOR SLAB**

4.1 Introduction	38
4.2 Plane Wall Configurations	41
4.2.1 Development of the Net and Design Curves	42
4.3 Flanged Wall Configurations–Equal Width	45
4.3.1 Development of the Net and Design Curves	55

4.4	Results and Discussions	67
4.4.1	Effect of Wall Thickness	67
4.4.2	Effect of Opening Between Walls	67
4.4.3	Effect of Flange (Equal) Width	68
4.4.4	Comparison of ANN with Other Published Results	69
4.5	Computer Program	69

## **Chapter 5: PUNCHING SHEAR OF WALL – SLAB CONNECTIONS**

5.1	Introduction	71
5.2	Punching Shear Design in Flat Plates and Flat Slabs	71
5.3	Calculation of Critical Perimeter for Punching Shear	73
5.3.1	Development of the Net and Design Curves	73
5.3.2	Results and Discussions	89
5.3.2.1	Effect of Web Wall and Flange Thickness	89
5.3.2.2	Effect of Web Wall Length	89
5.3.2.3	Effect of Flange Width	90
5.3.2.4	Effect of Considering $t_f/W$ instead of $t_f/X$ for Plotting the Graph	90
5.3.2.5	Comparison Between ANN, ACI and British Code	91
5.4	Calculation of Punching Shear Strength of Shear Wall–Floor Slab Connections	91
5.4.1	General	91
5.4.2	Calculation of Shear Strength	93
5.4.3	Development of the Net and Design Curves	95
5.4.4	Results and Discussions	104
5.4.4.1	Effect of Flange Width ( $Z$ )	104
5.4.4.2	Effect of Web Wall Length ( $W$ )	112
5.4.4.3	Effect of Effective Slab Thickness ( $d$ )	114
5.4.4.4	Effect of Slab Opening Length ( $L$ )	114
5.4.4.5	Comparison of ANN with Other Results	115



5.4.4.6 Calculation of Punching Shear Strength using	
Design Curves	115
5.4.4.6.1 Example 1: Flanged Shear Wall	117
5.4.4.6.2 Example 2: Plane Shear Wall	120
5.5 Computer Program	121

## **Chapter 6: CONCLUSIONS AND RECOMMENDATIONS**

6.1 General	123
6.2 Effective Slab Width of Floor Slab	123
6.3 Punching Shear Strength of Wall-Slab Connections	124
6.4 Recommendations for Future Study	125

<b>REFERENCES</b>	126
-------------------	-----

<b>APPENDIX A</b>	A-1
-------------------	-----

<b>APPENDIX B</b>	B-1
-------------------	-----

<b>APPENDIX C</b>	C-1
-------------------	-----

<b>APPENDIX D</b>	D-1
-------------------	-----

## LIST OF FIGURES

	page
Fig 1.1 (a) Perspective view of a shear wall building	4
(b) Plan of a typical shear wall building	4
Fig 1.2 Different wall configurations	4
Fig 2.1 Structural action of coupled shear wall-slab structure	8
Fig 2.2 Coupled shear wall configurations analysed	10
Fig 2.3 A typical shear wall with openings	13
Fig 2.4 Shear wall with idealised continuous connection of laminae	13
Fig 2.5 Theory of linear variation in shear stress	17
Fig 2.6 Moment-shear interaction relationship for interior column connection	20
Fig 3.1 Biological neurone	26
Fig 3.2 An artificial neurone	28
Fig 3.3 Nodal function	28
Fig 3.4 Three layer feed forward network	31
Fig 3.5 Flow chart of dynamic back propagation algorithm	33
Fig 4.1 Structural action of coupled shear wall-slab structure	39
Fig 4.2 Coupled shear wall configurations analysed	40
Fig 4.3 Comparative study of $Y_e/Y$ for plane wall configurations for varying Y keeping X, L and t constant	46
Fig 4.4 Comparative study of $Y_e/Y$ for plane wall configurations for varying L keeping X, Y and t constant	47
Fig 4.5 Comparative study of $Y_e/Y$ for plane wall configurations for varying t keeping X, L and Y constant	48
Fig 4.6 Schematic diagram of ANN for calculation of effective slab width for plane wall configurations	49
Fig 4.7 Flow diagram for calculation of effective slab width for plane wall configurations	50
Fig 4.8 Effective slab width for plane wall configurations for $Y/X = 0.6$	51
Fig 4.9 Effective slab width for plane wall configurations for $Y/X = 0.8$	52

Fig 4.10 Effective slab width for plane wall configurations for $Y/X = 1.0$	53
Fig 4.11 Comparative study of $Y_e/Y$ for flanged (equal width) wall configurations for Varying Y keeping X, L and Z constant	59
Fig 4.12 Comparative study of $Y_e/Y$ for flanged (equal width) wall configurations for Varying L keeping X, Y and Z constant	60
Fig 4.13 Comparative study of $Y_e/Y$ for flanged (equal width) wall configurations for Varying Z keeping X, L and Y constant	61
Fig 4.14 Schematic diagram of ANN for calculation of effective slab width for flanged (equal width) wall configurations	62
Fig 4.15 Flow diagram for calculation of effective slab width for flanged (equal width) wall configurations	63
Fig 4.16 Effective slab width for flanged (equal width) wall configurations for $Y/X = 0.40$	64
Fig 4.17 Effective slab width for flanged (equal width) wall configurations for $Y/X = 0.60$	65
Fig 4.18 Effective slab width for flanged (equal width) wall configurations for $Y/X = 0.75$	66
Fig 5.1 Failure surface defined by punching shear	72
Fig 5.2 Proposed critical section	72
Fig 5.3 Comparative study of $b_p/d$ for varying $t_f$ keeping d, Z and W constant	78
Fig 5.4 Comparative study of $b_p/d$ for varying d keeping $t_f$ , Z and W constant	79
Fig 5.5 Comparative study of $b_p/d$ for varying Z keeping d, $t_f$ and W constant	80
Fig 5.6 Comparative study of $b_p/d$ for varying W keeping d, $t_f$ and Z constant	81
Fig 5.7 Schematic diagram of ANN for calculation of critical perimeter of shear wall and edge column-slab connection	82
Fig 5.8 Flow diagram for calculation of critical perimeter of shear wall and edge column-slab connection	83
Fig 5.9 $b_p/d$ as a function of $d/Z$ and $t_f/W$ for $d/t_f = 0.3$	84
Fig 5.10 $b_p/d$ as a function of $d/Z$ and $t_f/W$ for $d/t_f = 0.5$	85
Fig 5.11 $b_p/d$ as a function of $d/Z$ and $t_f/W$ for $d/t_f = 0.7$	86

Fig 5.12 $b_p/d$ as a function of $d/Z$ and $t_f/W$ for $d/t_f = 0.9$	87
Fig 5.13 $b_p/d$ as a function of $d/Z$ and $t_f/W$ for $d/t_f = 1.2$	88
Fig 5.14 Comparative study of $V_c/V_0$ for varying $t_f$ keeping $d$ , $Z$ and $W$ constant	98
Fig 5.15 Comparative study of $V_c/V_0$ for varying $d$ keeping $t_f$ , $Z$ and $W$ constant	99
Fig 5.16 Comparative study of $V_c/V_0$ for varying $Z$ keeping $d$ , $t_f$ and $W$ constant	100
Fig 5.17 Comparative study of $V_c/V_0$ for varying $W$ keeping $d$ , $t_f$ and $Z$ constant	101
Fig 5.18 Schematic diagram of ANN for calculation of critical perimeter of shear wall and edge column-slab connection	102
Fig 5.19 Flow diagram for calculation of punching shear strength of shear wall and edge column-slab connection by using computer program	103
Fig 5.20 $V_c/V_0$ as a function of $t_f/Z$ and $d/W$ for $f'_c = 15 \text{ N/mm}^2$ $L = 2000\text{mm}$ , $Z/L = 0.10$	105
Fig 5.21 $V_c/V_0$ as a function of $t_f/Z$ and $d/W$ for $f'_c = 15 \text{ N/mm}^2$ $L = 2000\text{mm}$ , $Z/L = 0.20$	106
Fig 5.22 $V_c/V_0$ as a function of $t_f/Z$ and $d/W$ for $f'_c = 15 \text{ N/mm}^2$ $L = 2000\text{mm}$ , $Z/L = 0.30$	107
Fig 5.23 $V_c/V_0$ as a function of $t_f/Z$ and $d/W$ for $f'_c = 15 \text{ N/mm}^2$ $L = 2000\text{mm}$ , $Z/L = 0.40$	108
Fig 5.24 $V_c/V_0$ as a function of $t_f/Z$ and $d/W$ for $f'_c = 15 \text{ N/mm}^2$ $L = 2000\text{mm}$ , $Z/L = 0.50$	109
Fig 5.25 Multiplying factor as a function of $f'_c$	110
Fig 5.26 Multiplying factor as a function of $L$	111
Fig 5.27 Conversion factor from $f'_c$ to $f_{cu}$	116
Fig 5.28 Flow diagram for calculation of punching shear strength of shear wall and edge column-slab connection by using graph	118
Fig 5.29 Typical plan of a shear wall structure	119

## LIST OF TABLES

	Page
<b>Table 4.1</b> Percentage difference between values of $Y_e/Y$ calculated by formula and ANN	43
<b>Table 4.2</b> Percentage difference between values of $Y_e/Y$ calculated by formula and ANN (ANN after 35000 iterations having 15 hidden neurones, learning rate = 0.90 & momentum factor = 0.3)	44
<b>Table 4.3</b> Comparison between results proposed by Coull & Wong, Anwar and ANN for plane wall configurations	54
<b>Table 4.4</b> Percentage difference between values of $Y_e/Y$ (for flanged wall) calculated by formula (Eqns. 4.5 & 4.6) and ANN	56
<b>Table 4.5</b> Percentage difference between values of $Y_e/Y$ (for flanged wall) calculated by formula (Eqns. 4.5 & 4.6) and ANN (ANN after 40000 iterations having 15 hidden neurones, learning rate = 0.90 & momentum factor = 0.7)	57
<b>Table 4.6</b> Comparison between ANN and finite element results for flanged wall configuration-equal width	58
<b>Table 4.7</b> Comparative study of the rate of increase of $Y_e/Y$ for different values of $Z/Y$ to see the effect of flange width	68
<b>Table 5.1</b> Percentage difference between values of $b_p/d$ calculated by formula and ANN	74
<b>Table 5.2</b> Percentage difference between values of $b_p/d$ calculated by formula and ANN (ANN after 150000 iterations having 15 hidden neurones, learning rate = 0.20 & momentum factor = 0.10)	76
<b>Table 5.3</b> Effect of considering $t_f/W$ instead of $t_f/X$ for plotting the graph	90
<b>Table 5.4</b> Values of $b_p$ calculated by formula (Eqn. 5.1) ACI and British Code	92
<b>Table 5.5</b> Percentage difference between values of $V_e/V_0$ calculated by formula and ANN	96

<b>Table 5.6</b> Percentage difference between values of $V_c/V_0$ calculated by formula and ANN (ANN after 125000 iterations having 12 hidden neurones, learning rate = 0.005 & momentum factor = 0.10)	97
<b>Table 5.7</b> Rate of increase of $V_c/V_0$ due to increase of $Z/L$	112
<b>Table 5.8</b> Comparison between results calculated by ANN, formula (Eqn. 5.9), ACI and British Code for punching shear strength	113

## LIST OF SYMBOLS

$A_s$	Area of steel reinforcement
$A_{cp}$	Area of the critical perimeter for punching failure
$b_p$	Length of the critical perimeter
$C_1, C_2$	Dimensions of column
$d$	Effective depth of the slab
$D$	Slab flexural rigidity
$E$	Elastic modulus
$f_{cu}$	Cube crushing strength of concrete
$f'_c$	Cylinder crushing strength of concrete
$h$	Thickness of the slab
$I$	Second moment of inertia
$j$	Neurone of ANN
$J$	Property of the critical perimeter analogous to the polar moment of inertia
$K$	Rotational stiffness factor of slab
$K_s$	Translational stiffness factor of slab
$K.M$	A portion of the unbalanced moment transferred by torsion
$L$	Clear opening between walls
$M$	Amount of unbalanced moment
$M_0$	Capacity of the critical section for moment transfer only
$q$	Shear force per unit height of the coupled wall
$R_{ls}$	Ratio of long side to short side of a rectangular column
$R_f$	Rectangularity factor of the junction
$t$	Thickness of the wall
$T$	Integral shear force in the wall = $\int q dx$
$t_f$	Thickness of the flange of the wall
$t_w$	Thickness of the web of the wall
$V$	Applied shear force
$V_c$	Shear strength without shear reinforcement

$V_0$	$V_0 = f_c' * b_p * d$
$V_{d,ACI}$	Ultimate shear strength predicted by ACI Code
$V_{d,BS}$	Ultimate shear strength predicted by British Code
$V_{shear}$	Shear stress due to direct shear
$V_{torsion}$	Shear stress due to torsion
$v$	Shear stress
$V_{eff}$	Effective shear stress at the perimeter
$V_0$	Capacity of the critical section for shear transfer only
$v_c$	Allowable shear stress in concrete
$V_c$	Punching shear strength of concrete
$W$	Length of the web of the wall
$w_{ij}$	Weight of ANN
$X$	Total slab length
$x_i$	Input of ANN
$X_1$	Length of the side of perimeter considered parallel to the axis
$Y$	Total slab width or longitudinal wall spacing
$Y_e$	Effective width of the slab
$Z$	Flange width of the wall
$\nu$	Poisson's ratio
$\gamma_m$	Partial safety factor
$y_j$	Output of ANN
$\eta$	Learning rate of ANN
$\alpha, \beta, \gamma$	Coefficients in continuum connection method
$\theta$	Angle of the yield line to the x-axis



## LIST OF ABBREVIATION

ACI	American Concrete Institute
ANN	Artificial neural network
BNBC	Bangladesh National Building Code
BP	Backpropagation
Eqn.	Equation
Eqns.	Equations
FFN	Feed forward network
Fig.	Figure
Figs.	Figures
Ref.	Reference
Refs.	References
SDF	single-degree of freedom

# CHAPTER ONE

## INTRODUCTION



### 1.1 Artificial Neural Networks

An artificial neural network (ANN) is an information-processing system that has certain performance characteristics in common with biological neural networks. Artificial neural networks have been developed as generalisations of mathematical models of human cognition or neural biology, based on the assumptions that:

- (i) Information processing occur at many simple elements called neurones.
- (ii) Signals are passed between neurones over connection links.
- (iii) Each connection link has associated weight, which, in a typical neural net, multiplies the signal transmitted.
- (iv) Each neurone applies an activation function (usually non-linear) to its net input (sum of weighted input signals) to determine its output signal.

Again a neural network is characterised by :

- a. Its pattern of connections between the neurones (called its architecture),
- b. Its method of determining the weights on the connections (called its training or learning algorithm) and
- c. Its activation function.

Since what distinguishes (artificial) neural networks from other approaches to information processing provides an introduction to both how and when to use neural networks. A neural net consists of a large number of simple processing elements called neurones or nodes. Each neurone is connected to other neurones by means of directed communication links each with an associated weight. The weights represent information being used by the net to solve a problem. Neural nets can be applied to a wide variety problems, such as storing and recalling data or patterns, performing general mappings from input patterns to output patterns, grouping similar patterns, or finding solution to constrained optimisation problems [1].

## 1.2 Shear Wall-Floor Slab Connections

Shear walls may be defined as structural elements, which provide strength, stiffness and stability against lateral loads, deriving their strength and stiffness mainly from their shape. They are vertical stiffening members designed to resist lateral loads due to wind and earthquake. The walls may be either planar open section or close sections around elevator and stair cores.

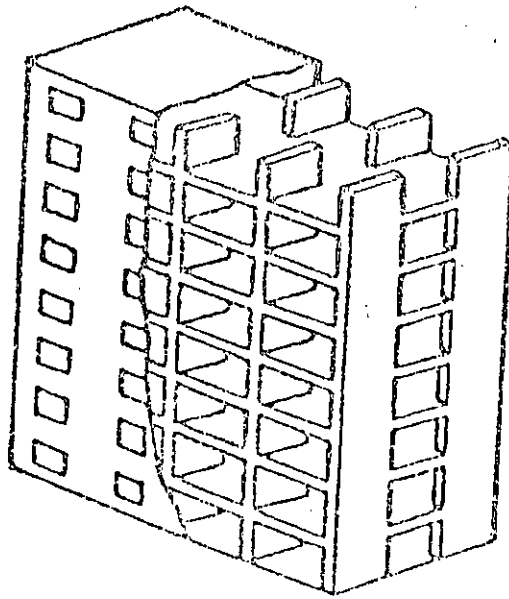
BS 8110 defines a shear wall as a vertical load-bearing member whose length exceeds four times its thickness. If the ratio of length to thickness of the section does not exceed four times, the member is defined as a column, which is a vertical member designed primarily to resist axial compression. ACI Code has no clear definition to differentiate between column and shear wall.

Shear wall buildings consist of series of parallel walls that resist all the vertical and horizontal loads. In the longitudinal direction lateral loads are resisted by additional shear walls, elevator shafts and by tube action.

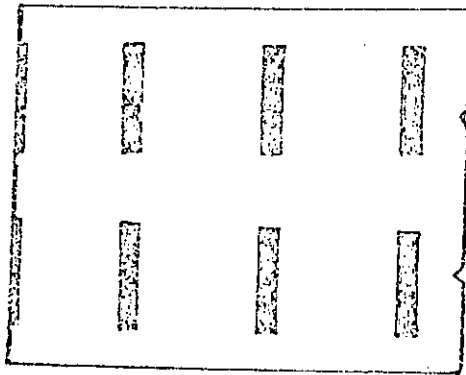
A popular form of high rise structure, especially for hotel and apartment use, is a slab-coupled shear wall structure. The reason for this is economy resulting from reduced floor heights and simplified formwork. From the constructional and architectural points, it is relatively easy to make the final structure aesthetically pleasing.

Fig. 1.1(a) shows a pictorial view of a shear wall structure and Fig. 1.1(b) shows a typical (idealised) floor plan of an apartment building in which self-contained units are arranged side by side along the length of the building. This arrangement naturally results in parallel assemblies of division walls running perpendicular to the face of the building, with intersecting longitudinal walls along the corridor and façade. The cross-walls are employed not only as division walls but also as load bearing walls. The longitudinal corridor and façade walls are provided with openings for access to the living areas and balconies and for window framing, this longitudinal wall act effectively as flanges for the primary cross-walls. In addition to its use as structural partition walls, shear walls are used to enclose lift shafts and stair wells to form partially open box structures which act as strong points in the building. Thus, in practice, shear walls of various shapes such as planar, flanged or box-shaped may be coupled together in cross wall structures (Fig. 1.2).

In slab-coupled shear walls, both the gravity load and wind load has to be finally transmitted to the walls at the wall-slab junction. The transfer of moments from slab to columns may further increase these shear stresses, and requires concentration of negative flexural steel in the slab in the region close to the columns. The region of a slab in the vicinity of a support could fail in shear by developing a failure surface in the form of a truncated cone or pyramid. This type of failure, called a 'punching shear failure', is usually the source of collapse of flat slab and slab-coupled shear wall structures. In recent years, some form of shear reinforcement is used in the slab to increase the punching shear strength of the connections. Certain problems associated with flat plate construction require special attention. Shear stresses near the columns may be very high, requiring the use of special forms of slab reinforcement there.



(a) Perspective view of a shear wall building.



(b) Plan of a typical shear wall building.

Figure (1.1)

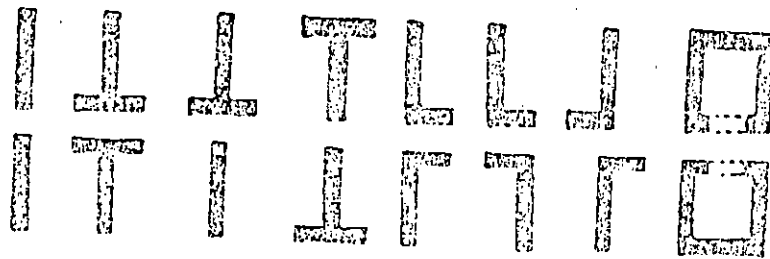


Figure (1.2) : Different wall configurations.

### **1.3 Purpose of this Study**

The structural analysis and design of slab-coupled shear wall structure can be performed if the behaviour of slab in the system is adequately known. As we know that the shear walls are provided to give lateral rigidity to the structure and connecting slabs play a significant role in resisting lateral load.

When a shear wall structure is subjected to gravity and lateral loads, substantial bending moment, twisting moment and shear force are transferred at the slab-wall junction. During an earthquake the slab-wall junctions of a shear wall structure will be subjected to repeated reversal of loads. This may lead to shear failure in the slab around the wall due to degradation of shear strength.

The object of the work, reported in this thesis is to

- (i) Prepare non-dimensional design curves to determine the effective width of slab for different wall slab configuration,
- (ii) Prepare non-dimensional design curves to determine the critical perimeter and ultimate punching shear capacity of the shear wall-floor slab junction,
- (iii) Develop a computer program for determining the effective width of floor slab and ultimate punching shear capacity of the shear wall-floor slab junction using the ANN.

# CHAPTER TWO

## LITERATURE REVIEW

### 2.1 General

The structural analysis and design of a slab-coupled shear wall system can be conveniently performed using the techniques developed for beam-coupled shear wall systems provided the effective width of the slab can be established. In a coupled-wall system, the stresses are not uniform across the width of the slab. In order to design the slab safely, it is necessary to know the magnitude and distribution of the stresses developed through the coupling action and it is also essential to determine accurately the interactive forces developed at the slab-wall junction.

In the 1950s and 1960s, a group of researchers combined biological and psychological insights to produce the first artificial neural networks. After about two decades, interest in artificial neural networks has grown rapidly over the past few years. Professionals from such diverse fields as engineering, philosophy, psychology and physiology are intrigued by the potential offered by this technology and are seeking applications within their disciplines.

In this chapter, a brief critical review of previous experimental and analytical research work done in the following fields is given:

- (i) Effective width of floor slab,
- (ii) Analysis of shear wall structures,
- (iii) Application of ANN.

## 2.2 Effective Width of Floor Slab

The shear wall-slab structures subjected to lateral loads deflect and the rotation of the wall generates moments in the slab. The portion of the slab, which acts as a beam connecting the walls and is active in resisting the moment is called effective width of the slab (Fig. 2.1(a)).

The resistance of the floor slab against the displacements imposed by the shear walls is a measure of its coupling stiffness, which can be defined in terms of the displacements at its ends and the forces producing them. Thus, referring to Figs 2.1(c) and 2.1(d), the stiffness of the slab may be defined either as a rotational stiffness  $M/\theta$  or as a translational stiffness  $V/\delta$  as the two are related as shown in Eqns. 2.3 and 2.4. Due to the non-uniform bending across the width, the force-displacement relationship can be evaluated only from a two dimensional plate-bending analysis. The rotational and translational slab stiffness factors  $K$  and  $K_\delta$  are given by

$$K = \frac{M}{\theta} \frac{1}{D} \quad (2.1)$$

$$K_\delta = \frac{V}{\delta} \frac{L^2}{D} \quad (2.2)$$

Where  $L$  is the clear opening between the walls and  $D$  is the flexural rigidity of the slab  $Et^3/12(1 - \nu^2)$ . The effective width of slab may be established by equating the rotational and translational stiffness of the slab with those of the equivalent beam

$$\frac{M}{\theta} = \frac{6EI}{L^3} (L + W)^2 \quad (2.3)$$

$$\frac{V}{\delta} = \frac{12EI}{L^3} \quad (2.4)$$

where  $W$  is the web length of the wall and  $I$  ( $Y_e t^3/12$ ) is the second moment of inertia of the beam of effective width  $Y_e$  and thickness  $t$ .



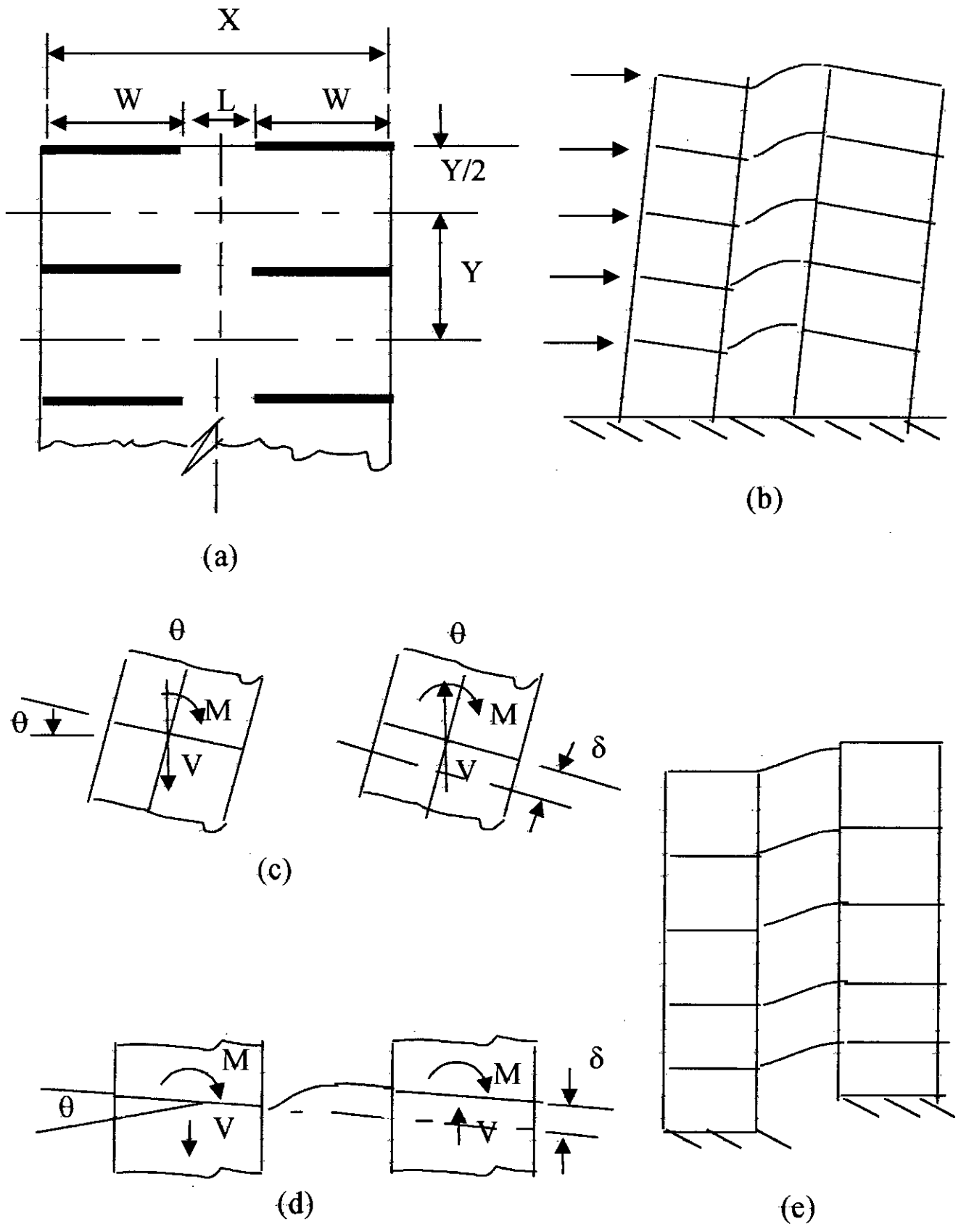


Fig. 2.1 Structural action of coupled shear wall-slab structure

The effective width may then be expressed in terms of the rotational and translational stiffness factors, in non-dimensional form, as

$$\frac{Y_e}{Y} = \frac{K}{6(1-\nu^2)} \left(\frac{L}{Y}\right) \left(\frac{L}{L+W}\right)^2 \quad (2.5)$$

or

$$\frac{Y_e}{Y} = \frac{K_\delta}{12(1-\nu^2)} \left(\frac{L}{Y}\right) \quad (2.6)$$

where  $Y$  is the bay width or longitudinal wall spacing (Fig.2.1(a)) and  $\nu$  is Poisson's ratio for the slab material.

Theoretical and experiment studies have shown that the main coupling actions take place in corridor area and at the inner edges of the coupled walls. For walls with external façade flanges (Fig. 2.2c), the flange has a negligible effect on the coupling stiffness and the walls may be treated as plane walls (Fig.2.2a). In the case of walls with internal flanges (Fig. 2.2d), very little bending of the slab occurs in the regions behind the flanges, and so the influence of wall length may generally be disregarded.

### 2.2.1 Empirical Relationships for Effective Slab Width

Comprehensive sets of design curves have been presented in Refs. [2], [3] and [4]. However, Coull and Wong [2] proposed simple empirical relationship that fit the design curves fairly accurately, and that may be used for design calculation. These are considered for the various cross-sectional forms of shear walls commonly encountered in practice. For a slab coupling a pair of plane walls as shown in Fig. 2.2(a) the effective slab width ratio  $Y_e/Y$  may be taken to be

$$Y_e/Y = t/Y + L/Y [1 - 0.4 (L/Y)'] \text{ for } 0 \leq (L/Y)' \leq 1 \quad (2.7)$$

and

$$Y_e/Y = t/Y + Y/Y [1 - 0.4 (L/Y)'^{-1}] \text{ for } 1 \leq (L/Y)' \leq \infty \quad (2.8)$$

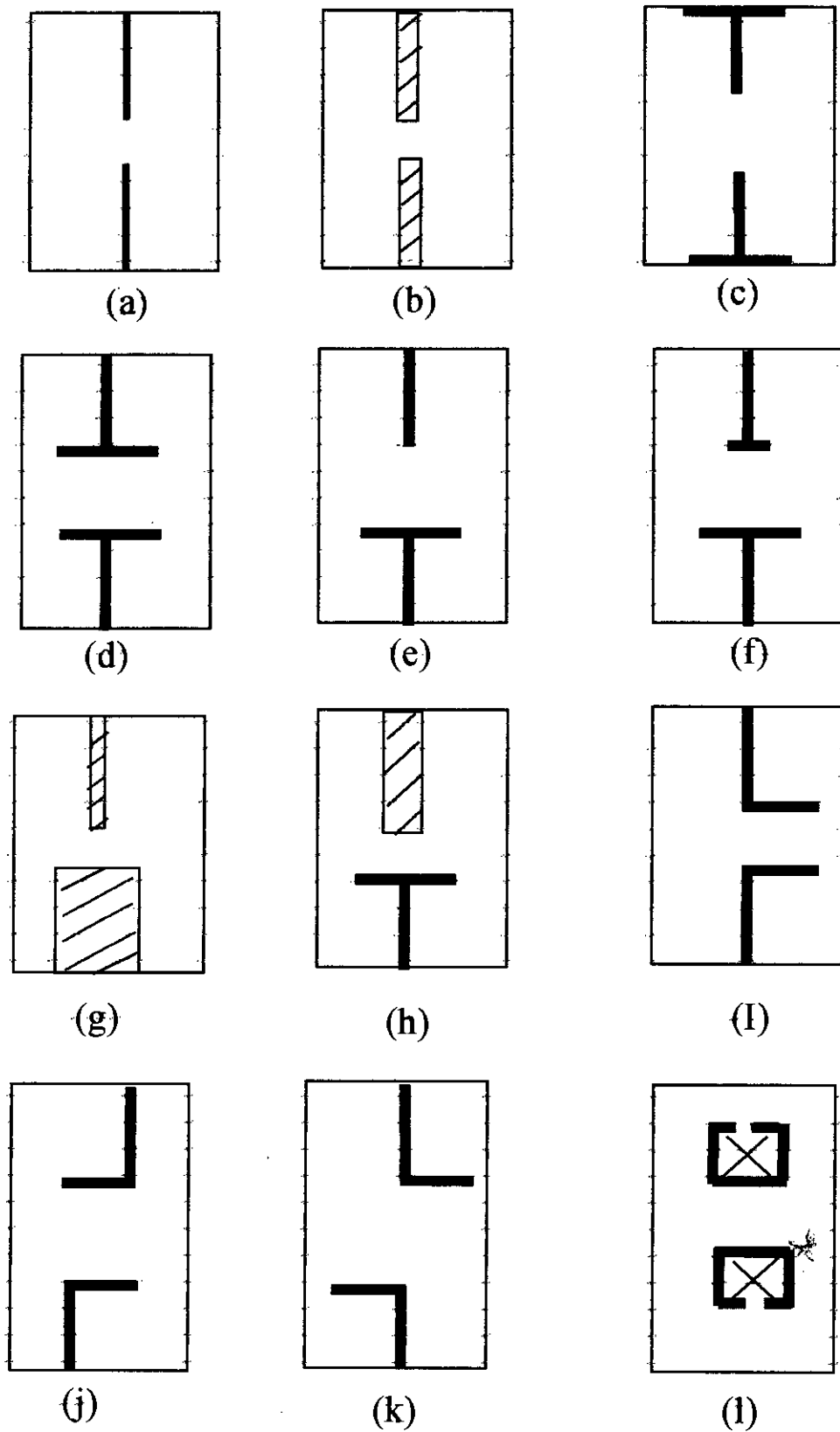


Fig. 2.2 Coupled shear wall configurations analyzed

in which

$t$  = wall thickness

$Y$  = bay width

$Y' = Y - t$

$L$  = length of opening between walls.

If the wall thickness is neglected as being small, Eqns. (2.7 & 2.8) reduce to the simpler expressions.

$$Y_e/Y = L/Y [1 - 0.4 (L/Y)] \text{ for } 0 \leq L/Y \leq 1 \quad (2.9)$$

and

$$Y_e/Y = 1 - 0.4 (L/Y)^{-1} \text{ for } 1 \leq L/Y \leq \infty \quad (2.10)$$

The effective width of slab coupling wall of different shapes was investigated theoretically by Coull and Wong [2] and Tso and Mahmoud [3]. They produced design curves suitable for use in an engineering office. The curves generally show the variation of the effective slab width or stiffness with different geometrical parameters.

End bay occur at the two gable ends of the building, where the gable walls are coupled by the floor slab on one side of the wall only. With the asymmetric coupling of the slab, gable walls will generally undergo some out-of-plane bending that will depend on the relative stiffness of the wall. Since the gable edge of the slab is less restrained against transverse rotation than a continuous interior edge, the coupling stiffness of the end bay will be less than half the stiffness of an internal bay slab.

Coull & Wong [2] suggested that for a practical range of wall configurations, the effective width of an end bay varies between 44% to 47% of the value for an interior bay. As a convenient rule, the effective width of an end bay should be taken to be 45% of the corresponding interior value given by Eqns. (2.7 and 2.8).

## 2.3 Analysis of Shear Wall Structures

The analysis of uniform walls pierced with regular sets of similar openings i.e. coupled shear walls, has attracted several investigators. A simplified analysis has been produced by assuming that the discrete system of connections, formed by lintel beams or floor slabs as shown in Fig. (2.3) may be replaced by an equivalent continuous medium, as shown in Fig. (2.4). By assuming that the axially rigid lintel beams have a point of contraflexure at mid-span, the behaviour of the system can be defined by a single second order differential equation. A general closed form solution of the problem can be obtained.

Using above simplified approach Rosman [5] first derived solutions for a wall with one or two symmetric bands of opening, with various conditions of support at the lower end (piers rigid basement, on separate foundation, and on various form of column supports). Deformations due to bending moment and normal forces in the walls and flexural and shear deformation in the connecting beam were also taken into account. The axial force in the walls was chosen as the statically redundant function. So if  $q$  is the shear force related to the unit length, the axial force in wall is

$$T = \int_0^x q \cdot dx \quad (2.11)$$

Where  $x$  is abscissa, measured from the top of the wall as shown in Fig. (2.3). Making use of certain simplifying assumptions, the governing differential equation takes the form

$$d^2T/dx^2 - \alpha^2T = -\gamma x \quad (2.12)$$

A direct mathematical solution of above equation can be obtained for any loading case. Eqns. (2.13 and 2.14) show the general solutions of above differential equation for the case of concentrated lateral load at the top and uniformly distributed lateral load respectively.

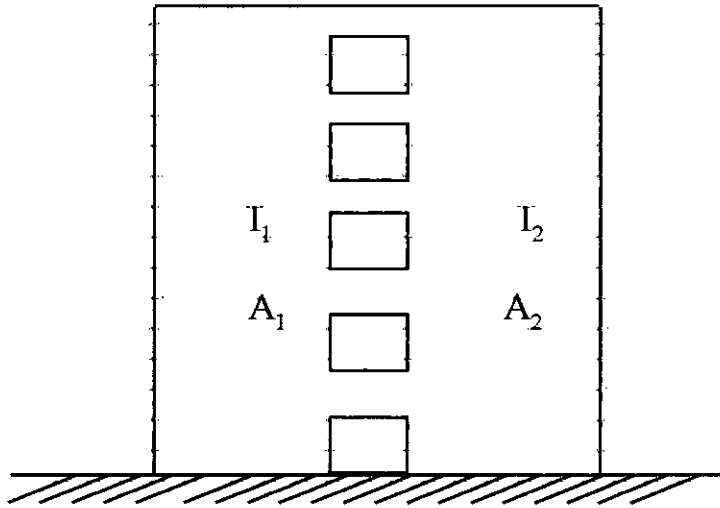


Fig. 2.3 : A typical shear wall with openings

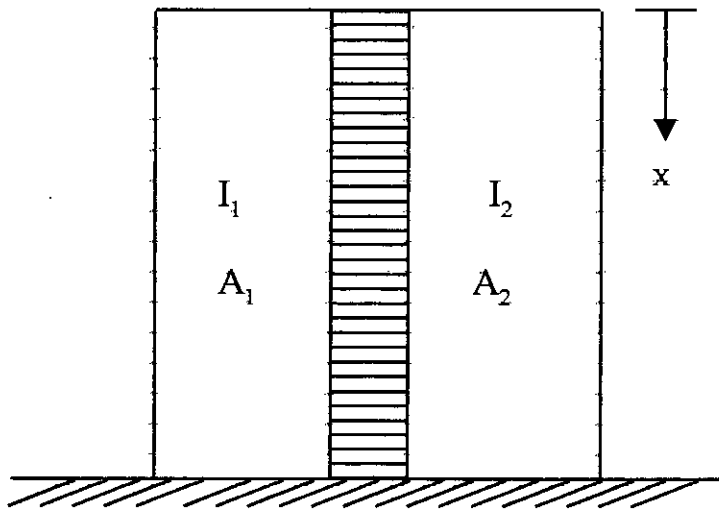


Fig. 2.4 : Shear wall with idealized continuous connection of laminae.

$$T = C_1 \sinh \alpha x - (\gamma/\alpha^2) x \quad (2.13)$$

$$T = C_1 \sinh \alpha x - (2\beta/\alpha^4)(\cosh \alpha x - 1) + (\beta/\alpha^2) x^2 \quad (2.14)$$

The coefficients  $\alpha$ ,  $\beta$ , and  $\gamma$  depend on the load and the geometrical properties of the shear wall. Once the value of  $T$  is known, the shear force and bending moment in the connecting beams can be easily calculated using equilibrium considerations.

### 2.3.1 Strength of Slab-Wall Junction

The region of a slab in the vicinity of a support could fail in shear by developing a failure surface in the form of a truncated cone or pyramid. This type of failure, called a 'punching shear failure', is usually the source of collapse of flat slab and slab-coupled shear wall structures. Design of this region of slab is therefore of paramount importance.

Comprehensive test data and reliable design criteria exist to estimate shear strength of slabs at interior slab-column junction loaded by reasonably concentric loads. In contrast, limited experimental results are available regarding shear strength of slabs at exterior column junctions and shear wall junctions. In recent years, some form of shear reinforcement is used in the slab to increase the punching shear strength of the connections. But detailed design methods are not available for proportioning shear reinforcement around the slab-column connections where both shear and moment are transferred.

Bari M. S. [6] has critically reviewed all major publications on the shear strength of slab-column connections with or without shear reinforcement, transferring both shear and moment or shear only to column. Works on each field are briefly discussed below based on Ref. [6].

### **2.3.2 Strength of Slab-Column Connections with Shear Reinforcement Transferring Shear only**

A large number of tests have been carried out of slabs with shear reinforcement subjected to shearing action only i.e. when the load is considered to be applied without eccentricity with respect to the critical section of the slab. These tests have led to several semi-empirical design procedures. An extensive review of the available data concerning the shearing strength of slabs with shear reinforcement in the form of structural steel sections, bent up bars, stirrups, prefabricated wire cages etc. was made by Hawkins [7]. He concluded that for slabs with properly detailed bent up bars or stirrups and transferring shear only, the shear capacity equals the lesser of the following strengths:

- (i) The shear strength for a slab without shear reinforcement calculated on the basis of ACI Code 318-71 for a critical section located  $d/2$  beyond the end of the stirrups or the bend in the bent up bars, where  $d$  is effective depth of slab.
- (ii) Half the shear capacity for a slab without shear reinforcement for a critical section at a distance  $d/2$  from the column perimeter plus the vertical component of the yield strength of the shear reinforcement intersected by a crack inclined at 45 degrees to the horizontal.

It was apparent from the observed behaviour of tested specimens that adequate anchorage for the shear reinforcement is essential to obtain sufficient ductility. Shear reinforcement, where needed, must extend to a distance of at least  $1.5 d$  from the column perimeter. Bars must be bent down within a distance  $0.5d$  of the column at an angle not less than 30 degrees to the horizontal. The maximum spacing between vertical stirrups should be  $0.5 d$ .



### **2.3.3 Shear Strength of Slabs with Moments Transferred to Column**

The state of knowledge about the strength of column-slab connections transferring moments, that increase monotonically to failure, has been summarised by ACI-ASCE committee 426 [8]. Available methods of predicting the ultimate strength of such connections can be divided into four groups:

- (1) Analysis based on a linear variation in shear stress,
- (2) Analysis based on thin plate theory,
- (3) Beam analogies, and
- (4) Finite element based procedures.

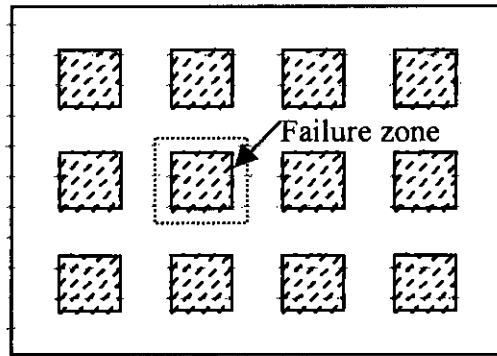
Detail comparison with the summary of the essential features of the four methods is presented in Ref. [6].

### **2.3.4 Shear Strength Predicted by Codes of Practice**

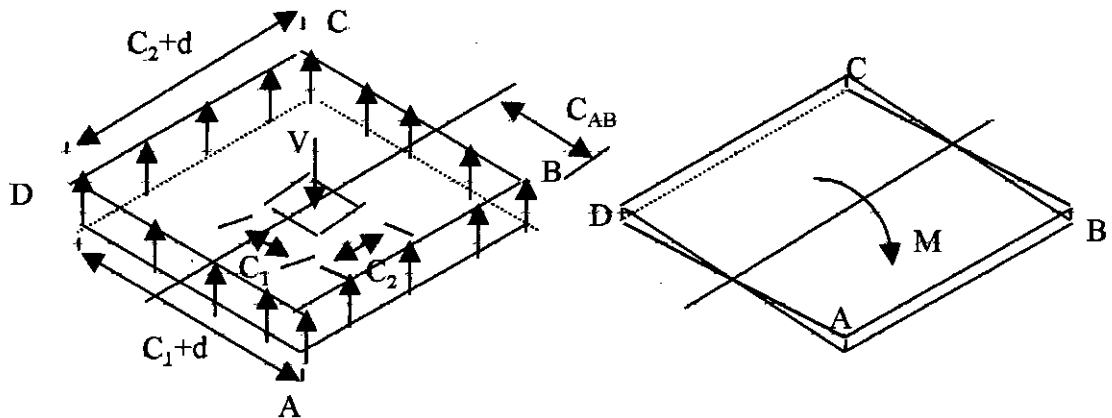
The formulae given for exterior edge column-slab connections of different Codes can be applied for estimating the punching shear strength of shear wall-floor slab connections. Punching shear strength as predicted by Bangladesh National Building Code (BNBC), ACI Code and British Code BS 8110 are discussed below:

#### **2.3.4.1 BNBC/ACI Code**

The shear strength prediction by Bangladesh National Building Code (BNBC) and the ACI Code is almost same. The ACI Code 318 and Commentary [9] specify the use of a linear variation in shear stress approach for predicting the limited shear capacity of connections transferring shear and moment. This procedure was first proposed as a working stress method by Di Stasio and Van Buren [10] in 1960. Fig. (2.5) shows the model proposed by them. They divided the resisting mechanism of the connections into two parts. As shown in Fig. (2.5-b), one part was an uniform shear field that resisted the shear force. The other part was a linear shear field, Fig. (2.5-c) which resisted the torsion part of the applied bending moment. This approach was subsequently utilised by Moe [11], & Hanson and Hanson [12] whose procedure was first incorporated into the ACI

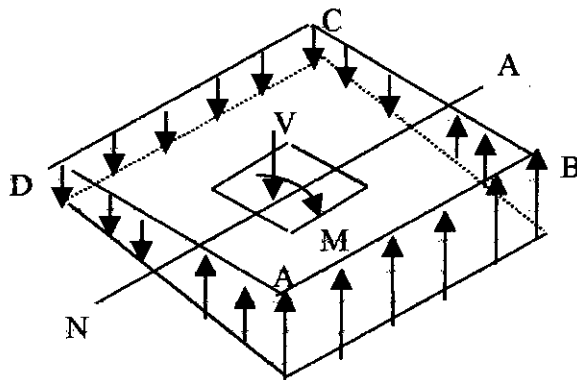


(a) Plan of a typical flat-slab column structure



(b) Uniform shear stress due to axial force,  $V$

(c) Shear stress (torsional) due to applied bending moment,  $M$



(d) Net shear stress around the critical perimeter

Fig. 2.5 Theory of linear variation in shear stress.

building Code in 1963 and carried over essentially unchanged into ACI Codes 318-71, 318-77, 318-83 and 318-89. For an interior slab-to-column connections, as shown in Fig. (2.5-a), it is assumed in this approach that around the column periphery, at some distance from it, there exists a pseudo-critical section. ACI Code specifies this critical perimeter at a distance  $d/2$  from the column periphery, where  $d$  is the effective depth of the slab. The resultant forces acting on this perimeter is due to the axial force and bending moment in column. The axial force,  $V$ , is transmitted to the column by uniform shear along the perimeter as shown in Fig. (2.5-b). The resultant moment,  $M$ , in column is transferred partly by bending of slab (normal frame action) and partly by linear shear stress distribution (torsion) at the perimeter as shown in Fig. (2.5-c). Therefore, the maximum shear stress according to Fig. (2.5-d) will be

$$\begin{aligned} V_{AB} &= V_{\text{shear}} + V_{\text{torsion}} \\ &= V/A_{cp} + K.M C_{AB}/J \end{aligned} \quad (2.15)$$

where  $A_{cp}$  = area of the critical perimeter.

$K.M$  = is the fraction of the total moment,  $M$ , transferred by torsion and

$C_{AB}$  = is the distance from the centre of rotation to the section AB.

$J$  = a property of the critical perimeter analogous to the polar moment of inertia.

$J$  (for interior rectangular column) =  $[(C_1+d)*h^3]/6 + [(C_1+d)^3*h]/6 + [(C_1+d)^2*h*(C_2+d)]/2$ , where  $h$  is the thickness of slab.

$J$  (for exterior rectangular column) =  $[(C_1+d/2)*h^3]/6 + [(C_1+d/2)^3*h]/6 + [2*(C_1+d/2)*h\{(C_1+d/2)(C_2+d)/(4C_1+2d) + (2C_2+2d)\}^2] + (C_2+d)*h\{(C_1+d/2)/2 - (C_1+d/2)(C_2+d)/(4C_1+2d) + (2C_1+2d)\}^2]$

where  $C_1, C_2$  = dimension of the column as shown in Fig. 2.5.

ACI Code 318-89 specifies that the fraction,  $K$ , of the total moment  $M$ , transferred by shear across the critical perimeter is given by

$$K = 1 - \frac{1}{1 + \frac{2}{3}\sqrt{(C_1+d)(C_2+d)}} \quad (2.16)$$

The remaining fraction of unbalanced moment  $(1-K)M$  must be transferred by reinforcement within lines  $1.5h$ , where  $h$  is the slab thickness on either side of the column. For ACI Code 318- 89 the maximum value of shear stress is limited to

$$v_c = 0.17(1+2/R_{ls}) \sqrt{f'_c} N / mm^2 \quad (2.17)$$

but not greater than  $0.33 \sqrt{f'_c} N / mm^2$ .  $R_{ls}$  is the ratio of long side to short side of a rectangular column and  $f'_c$  is the cylinder crushing strength of concrete.

The moment-shear interaction relationship predicted by the ACI Code procedure is shown in Fig. (2.6) for an interior column connection. Ordinate,  $V_u/V_o$ , is the ratio of the direct shear transferred to the column to the capacity of the section for shear transfer only. Abscissa,  $K.M/M_o$ , is the ratio of the moment transferred by shear to the same capacity for moment transfer only.  $V_o$  and  $M_o$  are calculated from the following Eqns. :

$$V_o = v_c A_{cp} \quad (2.18-a)$$

$$M_o = v_c J/C_{AB} \quad (2.18-b)$$

Line ab on Fig. (2.6) represent the condition for which the maximum shear stress is limited to  $v_c$ . Diagrams on Fig. (2.6) indicate idealised shear stress distributions for different points along line ab. Line cd represents the possible limitation imposed by the flexural reinforcement which must transfer the moment  $(1 - K)M$ .

The geometric properties of the connection and the concrete strength are the factors dictating the position of the line ab. The amount of reinforcement within lines  $1.5h$  either side of the column affects only the position of line cd. Test results [8] indicate a behaviour not far from that idealisation. Hawkins et. al. [13] have shown that measured ultimate shear strengths of the specimens when converted to the shear stress lie along curve such as amn, for a  $21 \text{ N/mm}^2$  (3000 psi) concrete. That curve lies progressively further outside the envelope acd as the reinforcement ratio within lines  $1.5h$  either side of the column increases above 0.8%. The reverse is true as ratios decrease below 0.8%.

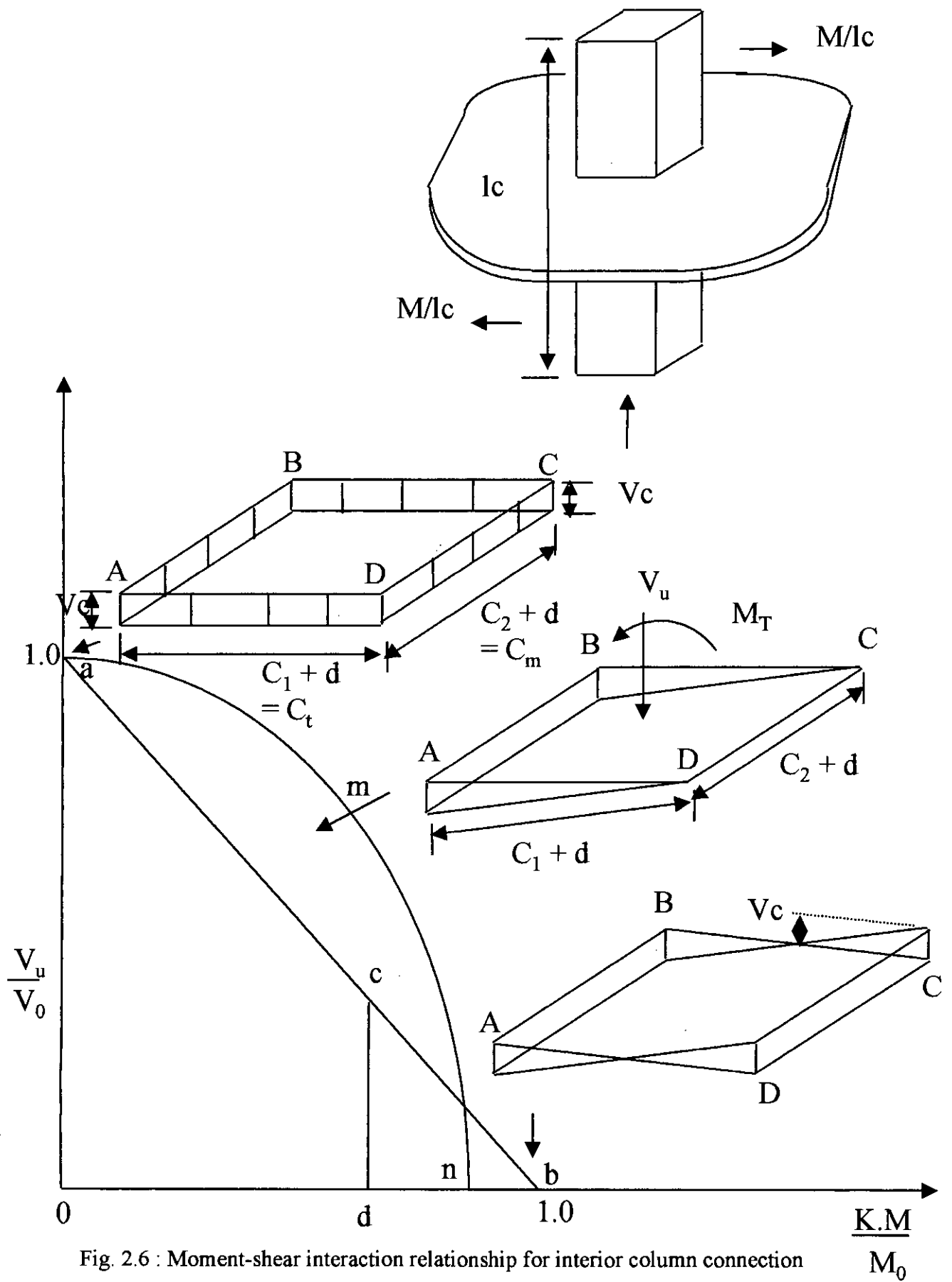


Fig. 2.6 : Moment-shear interaction relationship for interior column connection

### 2.3.4.2 British Code BS 8110

Regan [14] proposed a simple modified linear shear stress approach which was incorporated in the British Code CP 110 [15] and carried over the slight modification into BS 8110 [16]. The British Code BS 8110 specifies the critical section at a distance  $1.5d$  from the perimeter and it has square corners whether the column is square or circular. The treatment of moment transfer accounted in this Code is also different from that in ACI Code. The bending moment is assumed to be carried entirely by uneven shear along the critical perimeter. In presence of unbalanced moment,  $M$ , the effective shear stress at the critical perimeter of internal column connection is taken as:

$$v_{eff} = \left(\frac{V}{A_{cp}}\right)\left(1 + \frac{1.5M}{VX_1}\right) \quad (2.19)$$

Where  $X_1$  is the length of the side of perimeter considered parallel to the axis of bending. According to Fig. (2.5)  $X_1$  is equal to  $(C_2 + 3d)$ . In the absence of calculation, it is suggested that  $V$  can be taken  $(1/1.15)$  times of  $v_c A_{cp}$  for internal columns in braced structures with approximately equal spans.

At corner columns and at edge columns where bending about an axis parallel to the free edge is being considered, the design effective shear is calculated from  $V = (1/1.25)$  times of  $v_c A_{cp}$ . For edge columns where bending about an axis perpendicular to the edge is being considered, the design effective shear is calculated from  $V = (1/1.40)$  times of  $v_c A_{cp}$ . The maximum value of shear stress for British Code BS 8110 is limited to

$$v_c = 0.79(f_{cu}/25)^{1/3}(100A_s/bd)^{1/3}(400/d)^{1/4}/\gamma_m \quad (2.20)$$

Where  $f_{cu}$  is the cube crushing strength of concrete. Value of  $(100A_s/bd)$  is calculated for widths equal to those of the column plus  $1.5d$  of slab to either side of it. Further  $0.15 \leq (100A_s/bd) \leq 3.0$  and  $(400/d) \geq 1$  and  $\gamma_m$  is the partial factor of safety.

For the purpose of making comparisons between the shear strength predicted by Codes of practice, Eqns. (2.15) and (2.19) can be written in the form of design equations as follows:

$$V_d, ACI = v_c \cdot A_{cp} / [1 + (M / Vd) \left( \frac{K.C_{AB} \cdot A_{cp} \cdot d}{J} \right)] \quad (2.21)$$

$$V_d, BS = v_c \cdot A_{cp} / \left\{ 1 + (M / Vd) \left( \frac{1.5d}{X_1} \right) \right\} \quad (\text{for interior column}) \quad (2.22)$$

$$V_d, BS = \frac{v_c \cdot A_{cp}}{1.25} \quad (\text{for corner/edge columns where bending about an axis parallel to the free edge is being considered}) \quad (2.23)$$

$$V_d, BS = \frac{v_c \cdot A_{cp}}{1.40} \quad (\text{for corner/edge columns where bending about an axis perpendicular to the free edge is being considered}) \quad (2.24)$$

Where permissible maximum shear stress,  $v_c$ , is given by Eqn. (2.17) for ACI Code and by Eqn. (2.20) for British Code.

## 2.4 Application of ANN

In the past few years enormous progress has been made in research on ANNs and their applications. In the field of control, ANN has been successfully applied to the control of robot arms and manufacturing process. However, applying ANNs to structural problem is still in the early development stages. The potential of applying ANNs with a back propagation (BP) algorithm to civil engineering structural problem was explored [17]. In their study two ANNs were used. One was used to predict the structural response subjected to the control force alone, and the other to predict the ground acceleration. The control force was then set equal in magnitude, but in the opposite direction of the product of the mass and ground acceleration to nullify the excitation. To the best of the author's knowledge, other research works done in this field are:

The use of an artificial neural network has been made by A. Mukherjee and J. M. Deshpande [18] to arrive at an initial or the preliminary design model with an example of optimum design of RC beams. The application of ANN in the preliminary design of RC beams has been proposed.

A neural dynamics model for structural optimisation (application to plastic design of structures) was proposed by Hyo Seon Park and H. Adeli [19]. They applied the model to optimum plastic design of low-rise steel frames. They formulated the plastic design of low-rise frames as a linear programming problem. But, the neural dynamics model for structural optimisation is general and can be applied to non-linear programming problems.

An artificial neural network and genetic algorithm for the design optimisation of industrial roofs was written by J. V. Ramasamy and S. Rajasekaran [20]. They applied an expert system to the design of industrial roofs. All the codal knowledge was considered in the design. A database containing different sections and their properties are used in the design. Five different types of trusses were designed using the expert system and grouping the members into six regions. Three loading cases were considered in the analysis of the truss. The same five types of trusses were optimised using genetic algorithm. The stress and displacement constrains for the three loading cases were considered. They concluded that the design results using the expert system compare favourably with results of genetic algorithm.

A study of seismic activity control using an artificial neural networks (ANN) was done by Yu Tang [21]. He trained an ANN to recognise a linear single-degree of freedom (SDF) system subjected to base excitations. This trained ANN was then used to control systems with different natural frequencies, systems with non-linearity and systems subjected to larger input motions. It is a study of the application of artificial neural networks to activate structural control. A simple effective strategy for the on-line control of single-degree of freedom (SDF) structures was proposed by him.



## **2.5 General Discussion**

Experimental as well as theoretical work have been reported on slab-wall junction for shear walls with or without flanges, with or without using shear reinforcement in the slab. To the best of the author's knowledge, no non-dimensional design curves are available for predicting the critical perimeter as well as punching shear strength of the slab-wall junction. No attempt has been made to study the behaviour of shear wall-floor slab junction and effective width of floor slab coupling shear walls using artificial neural network. It is for this reason that the present work reported in this thesis is undertaken.

# **CHAPTER THREE**

## **ARTIFICIAL NEURAL NETWORKS**

### **3.1 Introduction**

Among the various intelligent systems ANN is one of the potential tools. The neural computing approach began more than four decades ago. It has attracted significant attention in several disciplines such as signal processing, pattern recognition, and control. Considerable activity can also be observed in the application of ANN for structural problems. The success of this tool is mainly attributed due to the unique feature of the neural networks, such as:

- (i) Learning ability by adjusting their network interconnection weights and biases based on a learning algorithm.
- (ii) Parallel structure with distributed storage and processing of information.

Neural network models inspired by the biological nervous systems are providing a new approach to problem solving. The neural network applications in structural engineering reported so far are based on backpropagation and counter propagation [17] – [21]. The following sections describe the basic theory of ANN and learning algorithms.

### **3.2 Artificial Neural Networks**

An artificial neurone is a very approximately simulated mathematical model of a biological neurone. A biological neurone is the basic functional unit of a human brain. Human brain is capable of parallel processing of many activities at a time due to a massively parallel huge network of neurones. A human brain functions with 100 billion of neurones, which are interconnected by a highly complex network. One such biological neurone is illustrated in Fig. 3.1, together with axons from two other neurones (from which the illustrated neurone could receive signals) and dendrites for two other neurones (to which the original neurone would send signals).

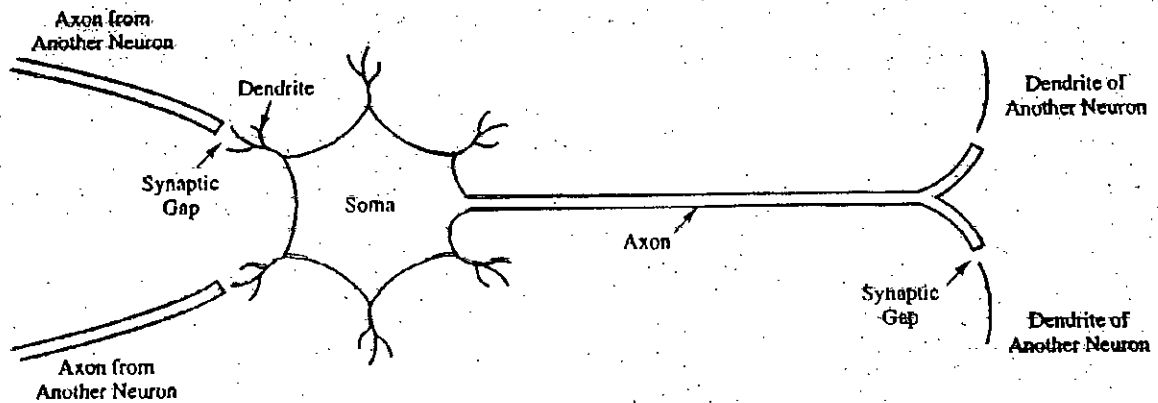


Fig. 3.1 Biological neuron.

Several key features of the processing elements of artificial neural networks are suggested by the properties of biological neurones, viz., that:

- (i) The processing element receives many signals.
- (ii) Signals may be modified by a weight at the receiving synapse.
- (iii) The processing element sums the weighted inputs.
- (iv) Under appropriate circumstances (sufficient input), the neurone transmits a single output.
- (v) The output from a particular neurone may go to many other neurones (the axon branches).

Other features of artificial neural networks that are suggested by biological neurones are:

- (vi) Information processing is local (although other means of transmission, such as the action of hormones, many suggest means of overall process control).
- (vii) Memory is distributed:
  - a. Long-term memory resides in the neurones' synapses or weights.
  - b. Short-term memory corresponds to the signals sent by the neurones.
- (viii) A synapse's strength may be modified by experience.
- (ix) Neurotransmitters for synapses may be excitatory or inhibitory.

A typical biological neurone receives the input through dendrites. Different dendrites meet a particular point called synapse. All the input from the different neurones is essentially summed up in the cell body called soma. If the summation at a given time is greater than a particular threshold value, then the neurone fires, i.e. a signal is sent down the axon. In a similar fashion, an artificial neurone also receives signals from other neurone through the connections between them (Fig. 3.2). Each connection has 'synaptic' connection strength, which is represented by a weight of that connection. The incoming signal is multiplied by this connection strength. Thus an artificial neurone receives a weighted sum of outputs of all the neurones to which it is connected. This weighted sum is then compared with the threshold for the artificial neurone and if it exceeds this threshold, the artificial neurone also fires. When an artificial neurone is fired, it goes to a higher excitation state and a signal is sent down to other connected neurones. The output ( $y_j$ ) of a typical neurone ( $j$ ) is obtained as a result of a non-linear function of weighted sum as follows:

$$Y_j = F(\sum x_i w_{ij} - \theta_j) \quad (3.1)$$

Where  $F$  is a non-linear function,  $x_i$  and  $w_{ij}$  are the inputs and the weights from the  $i$ -th input node to  $j$ -th node and  $\theta_j$  is the threshold value for the  $j$ -th artificial neurone.

The node characteristics of an artificial neurone are thus determined by Eqn. 3.1. Various node functions used for obtaining the output are shown in Fig. 3.3.

- (i) Hard limiter: having binary states, i.e. +1 and -1.
- (ii) Threshold logic: having variation as continuous values between 0 and +1 with linear variation.
- (iii) Sigmoid: having sigmoid nature between 0 to +1.

The choice of the threshold function depends on the nature of the application problem.

Existing neural network architecture can be divided into three basic categories: feed forward, recurrent, and self-organising neural networks. In feed forward networks the signals flow from the input units to the output units in a forward direction. But in recurrent

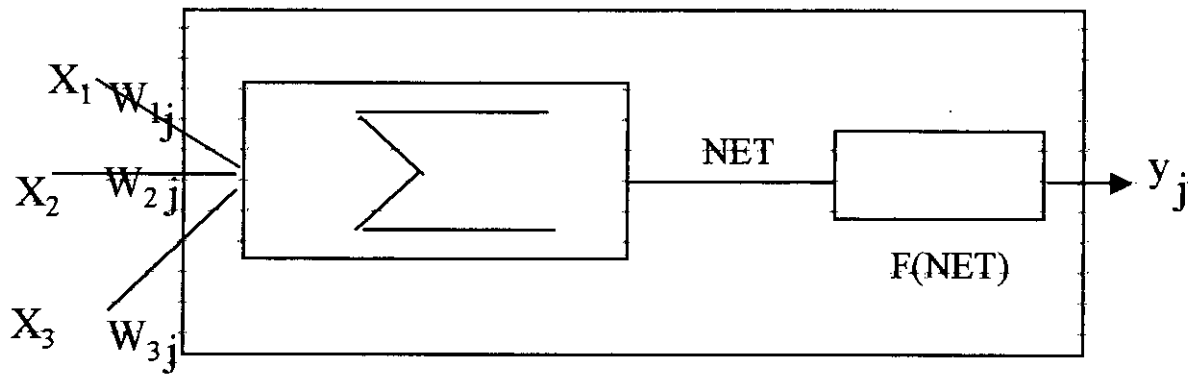


Fig. 3.2 An artificial neuron

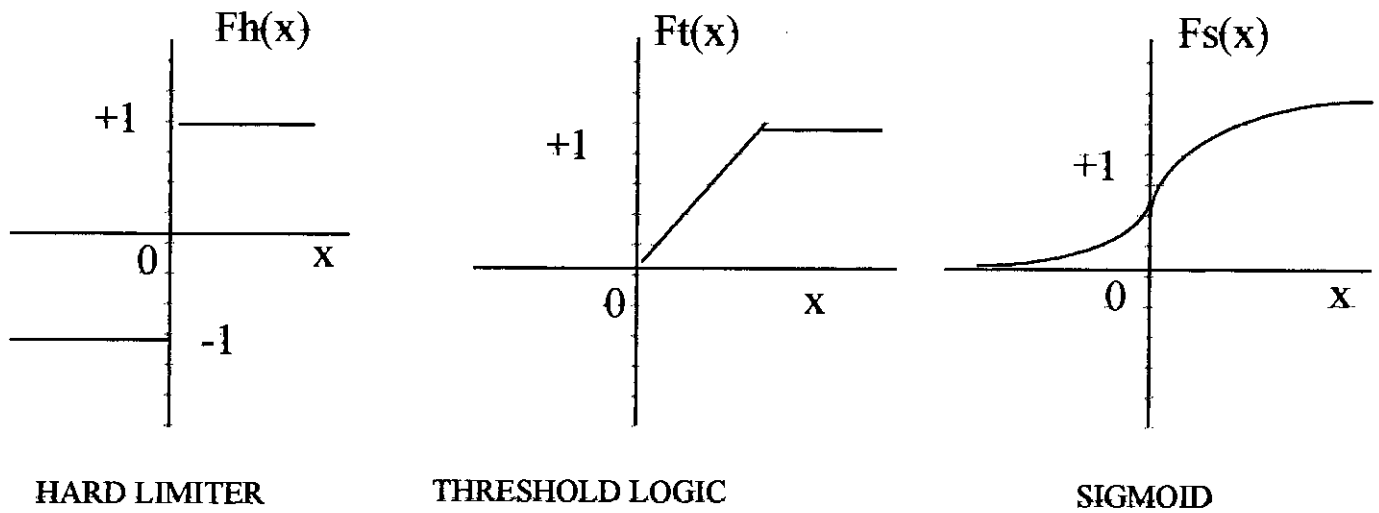


Fig. 3.3 Nodal function

network the output signal of a neurone is fed back to its input. In a self - organising neural network, neighbouring units compete in their activation by means of mutual lateral interactions, and develop adaptively into specific detectors of different signal patterns. Again each categories can be subdivided as single layer and multilayer connection. A single layer net has one layer of connection weight whereas a multilayer net has two or more layers of nodes (called hidden units) between the input units and the output units. Multilayer nets can solve more complicated problems than single layer nets, but training may be more difficult. Sometimes it is possible to solve a problem by multilayer nets which can not be trained to perform correctly at all by single layer net [22].

There are three general learning schemes in neural net works such as:

- (i) Supervised learning in which the correct output signal for each input vector to be specified.
- (ii) Unsupervised or self organising learning in which the network self-adjusts its parameters and structure to capture the regularities of input vector, without receiving explicit information from external environment.
- (iii) Reinforcement or graded learning in which the network receives implicit scalar evaluations of previous inputs.

Among these three learning schemes, supervised learning is used for real-time learning controller function, non-linear mappings and process parameter identification for adaptive and intelligent control of dynamic systems. The most useful learning algorithm of supervised learning is back propagation technique.

Feed forward network architecture has been chosen for the present work. For output neurones of the network, the non-linear sigmoid function is used as an activation function. The backpropagation (BP) algorithm has been chosen as learning algorithm for the network. The mathematical background of the algorithm has been described in the following section.

### 3.3 Backpropagation (BP) Algorithm

The backpropagation training algorithm is an iterative gradient descent algorithm designed to minimise the mean square error between the actual computed output and the desired output. The training of a network by back propagation involves three stages:

- (i) To propagate the training pattern and calculate the actual output of the network,
- (ii) Back propagate the associate error and
- (iii) The adjustments of weights.

A three layer Feed Forward Network (FFN) architecture is shown in Fig. 3.4. The layers are fully interconnected. When signals are applied to the input layer of the network, it propagates towards the output layer through the interconnections of the middle layer, known as hidden layer. The propagated signal will finally produce an output. This output is then compared with the desired output for each node. The error signals (measured at the output layer) are transmitted backward from the output layer to each node in the intermediate layer. Each unit in the intermediate layer receives only a portion of the total error signal, based roughly on the relative contribution the unit made to the original output. This process repeats, layer by layer, until each node in the network has received an error signal that describes its relative contribution to the total error. Based on the error signal received, connection weights are then updated.

All the relevant equations for the BP are presented in the order in which they would be used during training for a single input-output vector pair [22]. A flow chart of this algorithm is shown in Fig. 3.5.

- An input vector,  $\mathbf{X}_P = (x_{P1}, x_{P2}, \dots, x_{PN})$ , is applied to the input layer of the network. The subscript "P" refers to the p-th training vector. The input units distribute the values to the hidden layer units.
- The net input to the j-th hidden unit is given as

$$\text{net}_{pj}^h = \sum_{i=1}^N w_{ji}^h x_{pi} + \theta_j^h \quad (3.2)$$

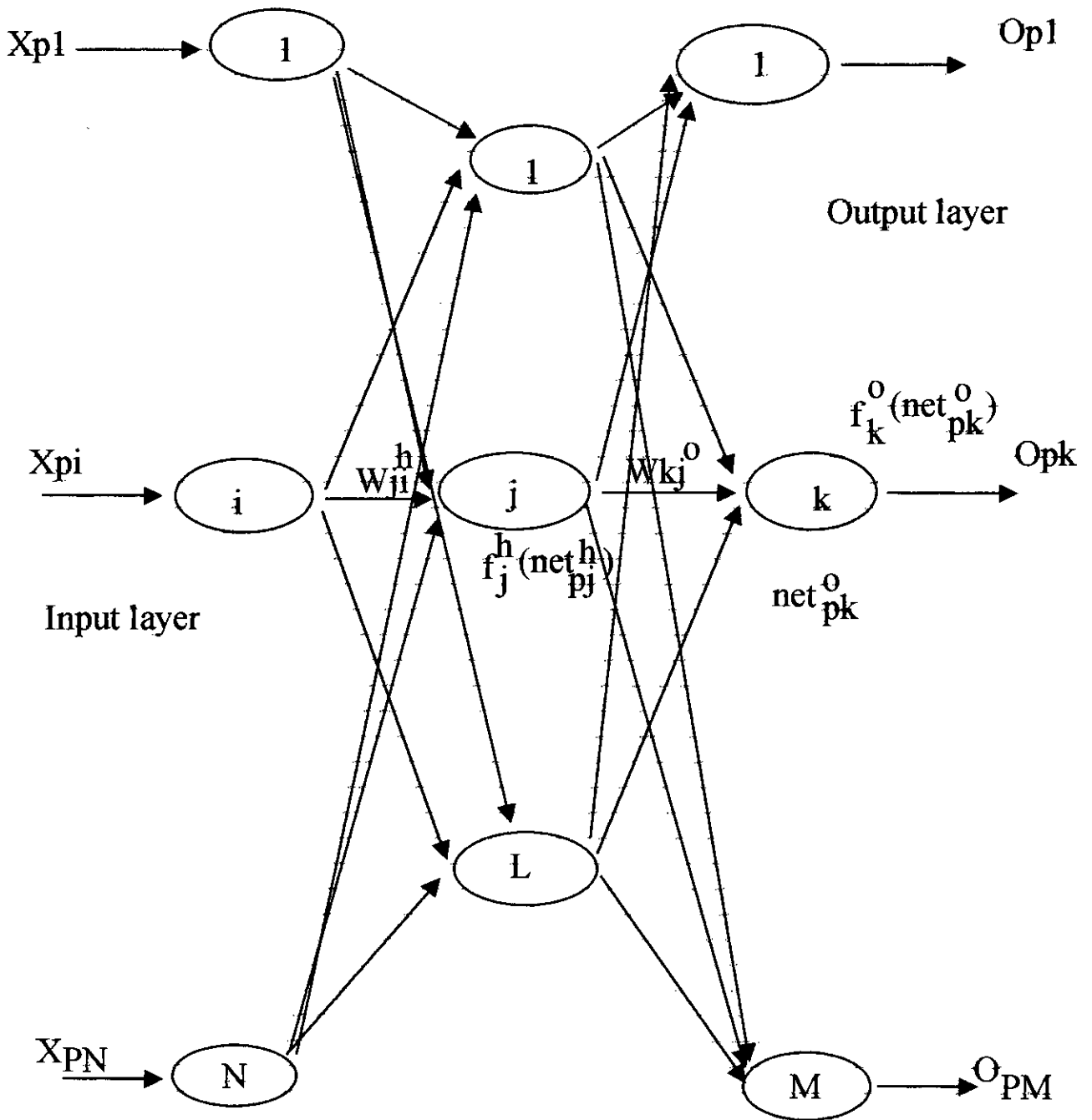


Fig. 3.4 Three layer feed forward network



Where  $w_{ji}^h$  is the weight on the connection from the  $i$ -th input unit to the  $j$ -th hidden unit, and  $\theta_j^h$  is the bias term of  $j$ -th hidden unit. The superscript “h” refers to quantities on the hidden layer.

- The output of this node becomes

$$h_{pj} = f_j^h(\text{net}_{pj}^h) \quad (3.3)$$

Where the function  $f_j^h(\cdot)$  is referred to as an activation function.

- All the hidden units feed their output to each unit in output layer. Net input to  $k$ -th output unit can be written as

$$\text{net}_{pk}^0 = \sum_{j=1}^L w_{kj}^0 h_{pj} + \theta_k^0 \quad (3.4)$$

- Output of  $k$ -th output unit is given by

$$O_{pk} = f_k^0(\text{net}_{pk}^0) \quad (3.5)$$

Where subscript “0” refers to quantities on the output layer.

- The calculated error terms for the output units

$$\delta_{pk}^0 = (y_{pk} - O_{pk}) f_k^{0'}(\text{net}_{pk}^0) \quad (3.6)$$

$y_{pk}$  is the desired output value.

The calculated error signal for  $j$ -th hidden units

$$\delta_{pj}^h = f_j^h(\text{net}_{pj}^h) \sum_{k=1}^M \delta_{pk}^0 w_{kj}^0 \quad (3.7)$$

Point to note that the error terms on the hidden units are calculated before the connection weights to the output-layer units have been updated.

- The update weights of the output layer becomes

$$W_{kj}^0(t+1) = W_{kj}^0(t) + \eta \delta_{pk}^0 h_{pj} \quad (3.8)$$

Where “t” refers to  $t$ -th iteration and  $\eta$  is the learning rate.

- The update weights of the hidden layer becomes

$$W_{ji}^h(t+1) = W_{ji}^h(t) + \eta \delta_{pj}^h x_{pi} \quad (3.9)$$

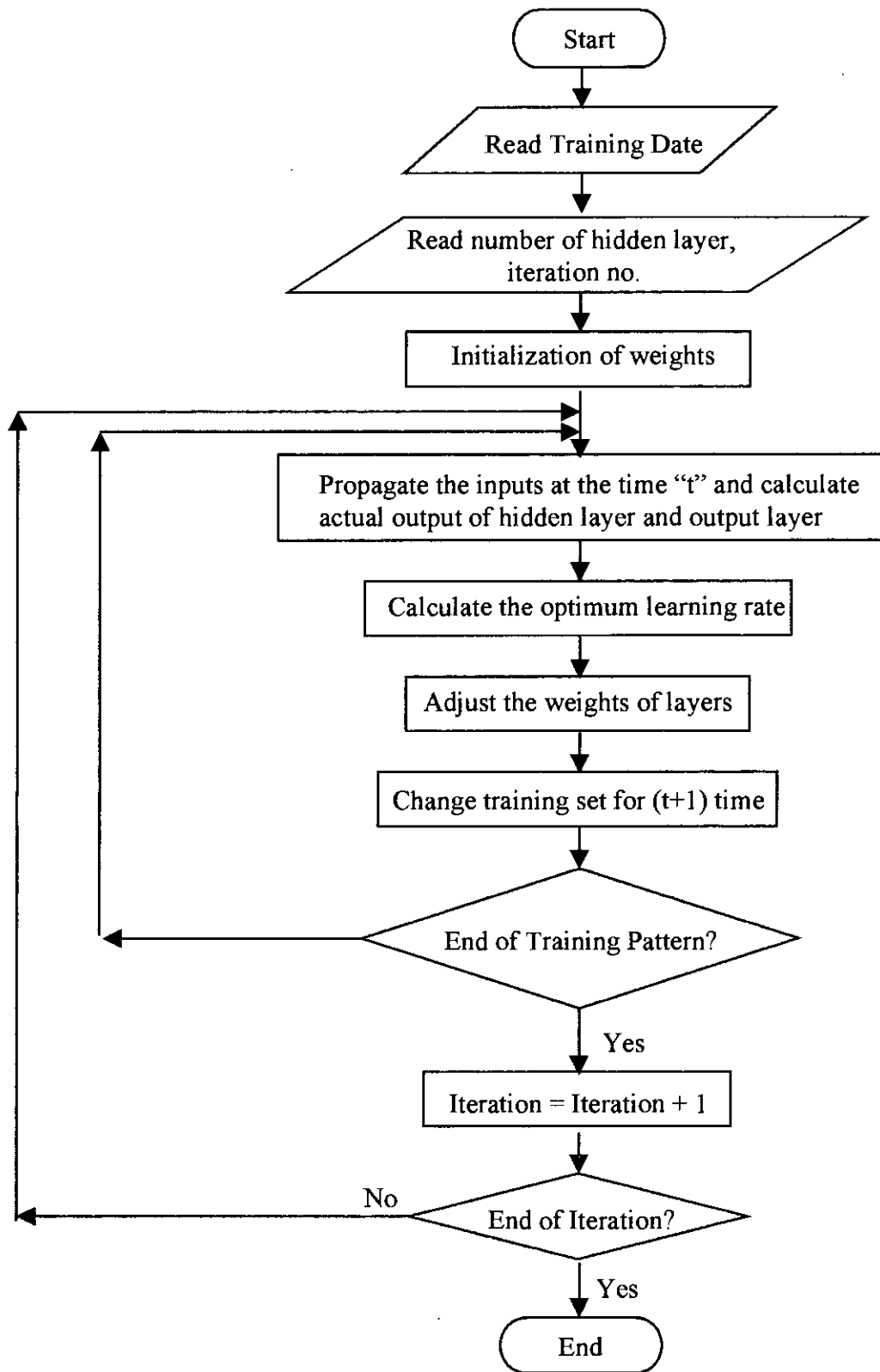


Fig. 3.5 Flow chart of back propagation

The error to be minimised is the sum of the squares of the errors of all the output units.

$$E_p = \frac{1}{2} \sum_{k=1}^M (y_{pk} - o_{pk})^2 \quad (3.10)$$

This quantity is the measure of how well the network is learning. When the error is acceptably small for each of the training-vector pairs, training can be discontinued.

### 3.4 Points to be Considered to Develop the Net

Faster convergence with minimum error and desired response depends on many training parameters. The selection of the training parameters is discussed in the following sub sections.

#### 3.4.1 Selection of Activation Function

The selection of activation function mainly depends on the intended use of the network and method of learning. For example, when the backpropagation algorithm is used to train the feed forward network, which is intended for a prediction problem, then the sigmoidal non-linear nodal function is normally used. The three types of nodal function, which are commonly used, are shown in Fig. 3.3. As it can be seen from the figure, the hard limiter non-linearity has only two states, i.e. 0 and +1 or -1 and +1. The activation logic has a linearly varying part and the sigmoidal function has low output for the low input and high output for sufficiently high input. Implementation of BP algorithm requires the activation function to be differentiable throughout the active region. Sigmoid function is the most commonly used activation function in backpropagation learning and is expressed as follows

$$Y = f(x) = \frac{1}{1 + e^{-x}} \quad (3.11)$$

### 3.4.2 Learning Rate

Selection of a value for the learning rate parameter has a significant effect on the network performance. The learning rate ( $\eta$ ) is used to control the amount of weight adjustment in each step of training. Usually,  $\eta$  is a small number-on the order of 0.05 to 0.25 to ensure that the network will settle to a solution without much oscillation during training. Small value of  $\eta$  means that the network will have to make a large number of iterations, but that is the price to be paid. It is often possible to increase the value of  $\eta$  as learning proceeds. The network error decreases for increasing value of  $\eta$  and will often help to speed convergence by increasing the value of  $\eta$  as the error reaches a minimum, but the network may bounce around too far from the actual minimum value if  $\eta$  gets too large. However it is well accepted that a small learning rate makes the learning slow but more likely to converge, while large learning rate makes the system unstable and sometimes the network may not learn at all.

### 3.4.3 Momentum Factor

Another way to increase the speed of convergence is to use a technique called momentum. Momentum factor allows the network to make reasonably large weight adjustment as long as the corrections are in the same general direction for several inputs while using a small value of learning rate to prevent a large response to the error from any training input. It also reduces the likelihood that the network will settle to a set of weights that corresponds to a local minimum, not global one. With momentum factor the network proceeds not only in the direction of the gradient but also in the direction of a combination of current gradient and the previous direction of weight correction. Thus the use of momentum factor, along with the learning rate, accelerates the training speed to achieve faster convergence. When calculating weight-change value,  $\Delta_p w$ , we add a fraction of the previous change. This additional term tends to keep the weight changes going to the same direction-hence the term momentum. The weight-change equations on the input layer then become

$$w_{kj}^0(t+1) = w_{kj}^0(t) + \eta \cdot \delta_{pk}^0 \cdot i_{pj} + \alpha \Delta_p w_{kj}^0(t-1) \quad (3.12)$$

with a similar equation on the hidden layer. In Eqn. 3.12  $\alpha$  is the momentum parameter and it is usually set to a positive value less than 1. However, there are no guidelines to determine the optimum momentum factor for a given task. The use of momentum term is also optional.

### **3.4.4 Configuring Hidden Layer (s)**

The selection of the number of hidden layer(s) and the number of nodes in the hidden layer(s) are the most challenging part in the total network development process. Unfortunately, there is no fixed guideline available for this purpose and hence this has to be done by the trial and error method. Although some investigators have tried to arrive at an approximate formula, still, there is no reliable method available. Therefore, generally the decision about this takes a long time and sometimes it may take weeks to train the network. It is proved that with a sufficient number of units in a single hidden layer any functional relationship can be mapped. But an increase in the number of hidden layers may improve the generalisation capacity.

Determining the number of units to use in the hidden layer is not usually as straightforward as it is for the input and output layers. The main idea is to use as few hidden layer units as possible, because each unit adds to the load on the CPU during simulations. Of course, in a system that is fully implemented in hardware (one processor per processing element), additional CPU loading is not as much of a consideration (inter processor communication may be a problem, however). From experience it can be said that for networks of reasonable size (hundreds or thousands of inputs), the size of hidden layer needs to be only a relatively small fraction of that of the input layer. If the network fails to converge to a solution it may be that more hidden nodes are required. If it does converge, fewer hidden nodes may be used to try and settle on the basis of overall system performance.

### **3.4.5 Initialisation of Weights and Biases**

The choice of initial weights will influence whether the net reaches a global (or only a local) minimum of error and, if so, how quickly it reaches the minimum. The update of the weight between two units depends on both the derivative of the upper unit's activation function and the output of the lower unit. For this reason, it is important to avoid choices of initial weights that would make it likely that either activation or derivations of activation are zero. The values for the initial weights must not be too large, or the initial input signal to each hidden or output unit will likely to fall in the region where the derivative of the sigmoid function has a very small value. On the other hand, if the initial weights are too small, the net input to a hidden or output unit will be near zero, which also cause extremely slow learning. Thus all the weights and biases are initialised by random numbers between  $-0.5$  and  $0.5$ .

### **3.4.6 Evaluation of the Net Performance**

The performance of the net is tested by watching it's behaviour towards unseen examples. When a net is successfully trained, it is supposed to have mapped the desired functional relation between the given input and output vectors in the solution space. But there is every possibility of the net having mapped a different relationship than the desired one, which still gives the correct output for the training pairs. This may happen if both the desired relation and the one that net has mapped have some common points in the solution space which happened to be training set pairs. Hence to make sure that the network has learnt the desired function only, it is important to evaluate the performance of the net by submitting it to a number of unseen examples. A neurone basically computes by classification. Therefore, the network can only try to approximate the desired output values as accurately as possible. Hence a small tolerance limit should be allowed while evaluating the performance of the network. Comparison of the percentage error in the values desired and those, the network has predicted may be a better choice.

## CHAPTER FOUR

### EFFECTIVE WIDTH OF FLOOR SLAB

#### 4.1 Introduction

A common form of construction for multi-story residential buildings consists of assemblies of shear walls and floor slabs, in which the coupling of the cross-walls by the floor slabs provides a more efficient structural system of resisting lateral forces. Fig. 2.1 [reproduced as Fig.4.1] (a) shows a floor plan of a slab block where apartment units are placed side by side. Division walls perpendicular to the length of the building, intersecting longitudinal walls along the corridor and façade enclosing the living spaces are employed as load bearing walls and can efficiently transmit both gravity and lateral loads to the structural elements. Any longitudinal corridor and façade walls, if they are designed to be load-bearing act effectively as flanges for the primary cross-walls. In addition to the partition walls, shear walls are used to resist the lateral load due to wind and earthquake. Shear walls, if used for lift shafts and stairwells act as strong points for the structure. Thus, in practice, shear walls of various shapes such as planar, flanged or box shaped may be coupled together in cross wall structures (Fig.2.2) [reproduced as Fig.4.2].

The shear walls resist the lateral load due to wind or earthquake effects, by cantilever bending action, which results in rotations of the wall cross-sections. The free bending of a pair of shear walls is resisted by the floor slab, which is forced to rotate and bend out of plane where it is connected rigidly to the walls (Fig. 4.1(b)). Due to large depth of the wall, considerable differential shearing action is imposed to the connecting slab, which develops transverse reactions to resist the wall deformation (Fig. 4.1(c)), and induces tensile and compressive axial forces into the walls. As a result of the larger lever arm involved, relatively small axial forces can give rise to substantial moments of resistance, thereby reducing greatly the wind moments in the walls and the resulting tensile stresses at the windward edges. The lateral stiffness of the structure is also considerably increased.

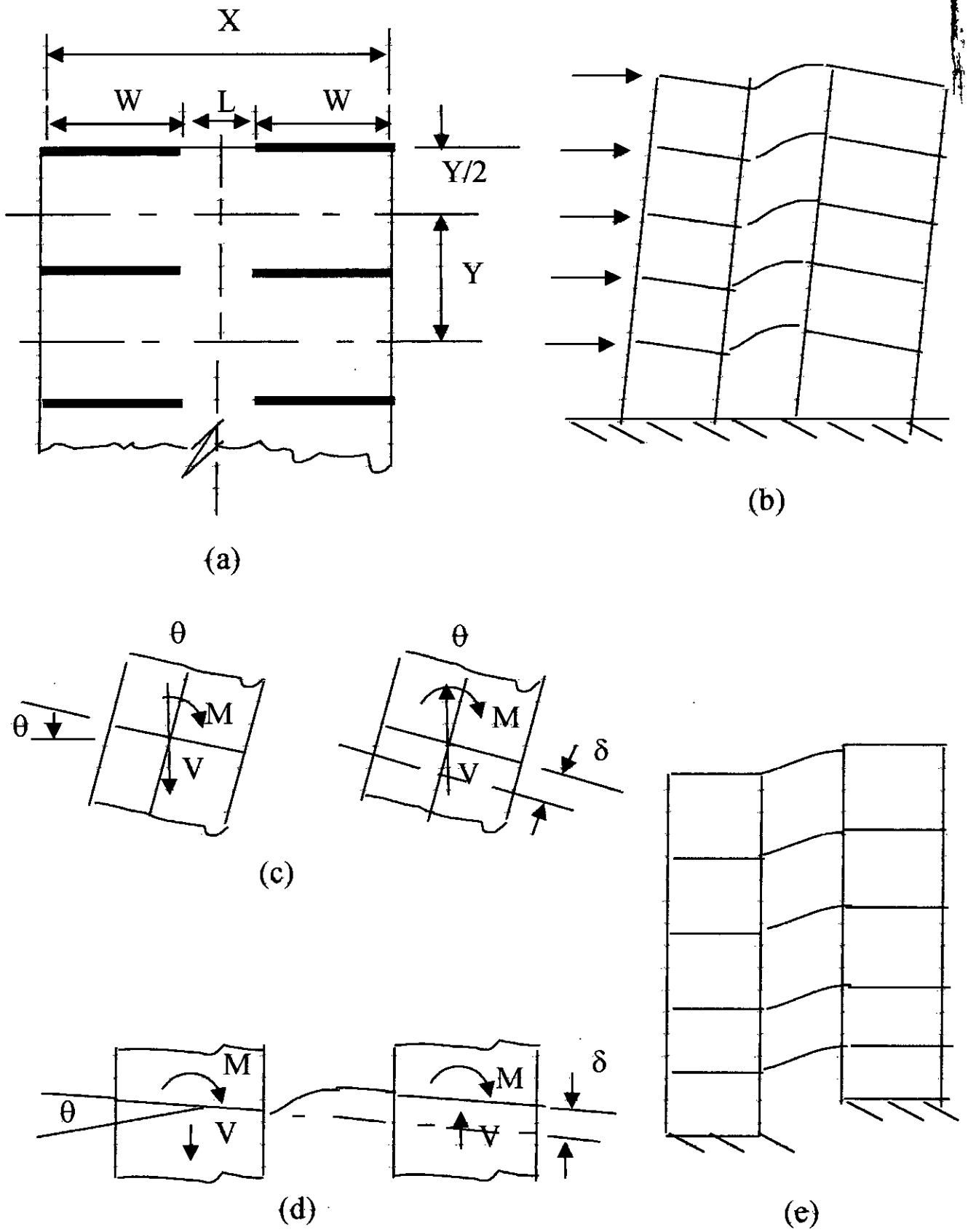


Fig. 4.1 Structural action of coupled shear wall-slab structure



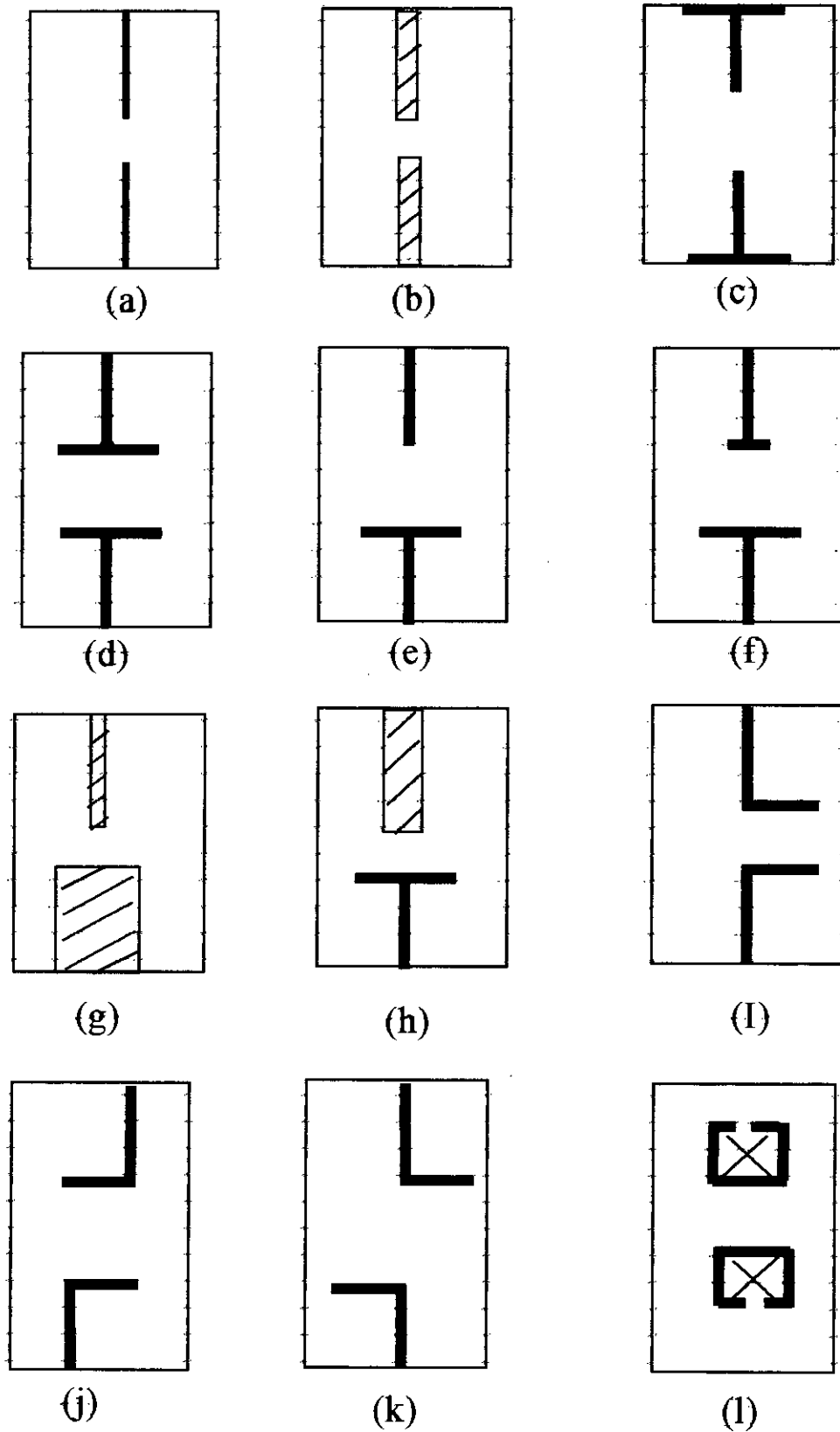


Fig. 4.2 Coupled shear wall configurations analyzed

A similar situation arises if relative vertical deformation of the walls occurs, due to unequal vertical loading on the walls or to differential foundation settlement. The effect on the slab is similar to that produced by parallel wall rotation caused by bending as shown in Figs 4.1(d) and 4.1(e).

The structural analysis and design of a slab-coupled shear wall system may readily be performed using existing techniques for beam-coupled wall structures, provided that the equivalent width of the slab which acts effectively as a wide coupling beam, or its corresponding structural stiffness, can be assessed.

This chapter presents a comprehensive set of design curves to determine the effective width using ANN. Input data are generated based on simple empirical formulae of Reference [2] to enable the effective bending stiffness of a floor slab coupling a pair of cross-walls to be determined quickly and accurately. The curves apply to all common wall cross-sections in practical structures.

The finite element technique and method of analysis used are described in Reference [23]. The accuracy of the results obtained by ANN is checked by comparing with those published data of Reference [2] & [4].

## 4.2 Plane Wall Configurations

For a slab coupling a pair of plane walls as shown in Fig. 4.2(a), the effective slab width ratio  $Y_e/Y$  [23] may be taken to be

$$Y_e/Y = t/Y + L/Y [1 - 0.4(L/Y')] \text{ for } 0 \leq (L/Y') \leq 1 \quad (4.1)$$

and

$$Y_e/Y = t/Y + Y'/Y [1 - 0.4(L/Y')^{-1}] \text{ for } 1 \leq (L/Y') \leq \infty \quad (4.2)$$

in which

$t$  = wall thickness

$Y$  = bay width

$Y' = Y - t$

$L$  = length of opening between walls.

Above Eqns. (4.1 and 4.2) will generally yield results that are within a small percentage of the accurate values obtain directly from a finite element analysis.



The values from which the empirical relationships were derived based on a Poisson's ratio for concrete of 0.15. The effective width is not sensitive to small difference in the value of Poisson's ratio, but, if desired, the value of  $Y_e/Y$  may be corrected approximately for the actual value of Poisson's ratio  $\nu$  by multiplying by the factor  $(1 - 0.15^2)/(1 - \nu^2)$ .

If the wall thickness is neglected as being small, Eqns. (4.1 and 4.2) reduce to the simpler expressions.

$$Y_e/Y = L/Y [1 - 0.4(L/Y)] \text{ for } 0 \leq (L/Y) \leq 1 \quad (4.3)$$

and

$$Y_e/Y = [1 - 0.4(L/Y)^{-1}] \text{ for } 1 \leq (L/Y) \leq \infty \quad (4.4)$$

#### 4.2.1 Development of the Net and Design Curves

To develop the net, values of learning rate, momentum factor and hidden neurones were varied to get the best fit net. To begin with, different values of learning rate such as 0.05, 0.3, and 0.9 are chosen to train the network with a constant momentum 0.1. Table 4.1 shows the percentage difference to a set of data between values of  $Y_e/Y$  calculated by Eqns. (4.1 and 4.2) and ANN. We can see that the minimum error is achieved at the learning rate of 0.9. Thus the value of the learning rate is chosen as 0.9.

During the training process various values of momentum factor such as 0.1, 0.2, and 0.3 are taken to choose the best one. At this stage, the same set of data is again used to show the percentage difference between values of  $Y_e/Y$  calculated by Eqns. (4.1 and 4.2) and ANN. From table 4.1 it is found that the value of momentum factor has little effect on the system. Thus 0.3 is taken as the momentum factor for training the network.

In this work a neural network having a single hidden layer with various number of neurones such as 12, 15 and 18 is trained individually. Their training history is also shown in table 4.1. Network with 15 neurones having learning rate 0.9 and momentum factor 0.3 after 35000 iteration is chosen to develop the network with an input file having 319 sets of data [Appendix A]. Network weights and bias are also given in appendix A. The output response of finally accepted parameters for the network to the set of data (which was used for table 4.1) is shown in table 4.2.

The range of various parameters for input data are as follows :

X = 12.00 meter,

Y = 7.20 meter to 12.00 meter,

L = 1.00 meter to 11.00 meter,

t = 0.10 meter to 0.50 meter.

**Table 4.1** Percentage difference between  $Y_c/Y$  calculated by formula and ANN.

Sl No	Learning rate	Momentum factor	Hidden neurones	No of iteration	Average % difference
1	0.05	0.1	15	20000	0.53 (-0.78 to +1.58)
2	0.30	0.1	15	20000	0.54 (-0.71 to +1.43)
3	0.90	0.1	15	20000	0.51 (-0.75 to +1.37)
4	0.90	0.2	15	20000	0.50 (-0.71 to +1.40)
5	0.90	0.3	15	20000	0.48 (-0.67 to +1.42)
6	0.90	0.3	12	20000	0.51 (-1.14 to +1.32)
7	0.90	0.3	18	20000	0.53 (-1.09 to +1.35)
8	0.90	0.3	15	25000	0.48 (-0.62 to +1.42)
9	0.90	0.3	15	30000	0.48 (-0.56 to +1.42)
10	0.90	0.3	15	35000	0.48 (-0.52 to +1.42)

**Table 4.2** Percentage difference between values of  $Y_c/Y$  calculated by formula and ANN (ANN after 35000 iterations having 15 hidden neurones, learning rate = 0.90 & momentum factor = 0.30).

X (meter)	Y (meter)	L (meter)	t (meter)	Y <sub>c</sub> /Y Calculated by		% difference
				Formula	ANN	
12.00	8.00	10.50	0.15	0.7066	0.7051	-0.21
12.00	11.50	2.50	0.15	0.2113	0.2106	-0.33
12.00	9.50	8.50	0.15	0.5852	0.5874	+0.38
12.00	10.00	7.50	0.15	0.5366	0.5338	-0.52
12.00	11.50	3.50	0.25	0.2882	0.2896	+0.49
12.00	8.00	7.50	0.25	0.6058	0.6123	+1.07
12.00	10.50	11.50	0.25	0.6520	0.6507	-0.20
12.00	9.00	4.50	0.25	0.4249	0.4251	+0.02
12.00	9.00	7.50	0.35	0.5832	0.5837	+0.09
12.00	7.50	9.50	0.35	0.7130	0.7110	-0.28
12.00	10.00	4.50	0.35	0.4011	0.4033	+0.55
12.00	8.50	11.50	0.35	0.7282	0.7260	-0.30
12.00	10.00	9.50	0.45	0.6170	0.6257	+1.41
12.00	8.50	6.50	0.45	0.5707	0.5689	-0.32
12.00	8.00	7.50	0.45	0.6212	0.6300	+1.42
12.00	9.25	10.25	0.45	0.6733	0.6729	-0.06

Average % difference = 0.48  
(-0.52 to +1.42)

From the above testing data set, it is seen that the network gives the maximum error when  $X = 12.00$  meter,  $Y = 8.0$  meter,  $L = 7.50$  meter &  $t = 0.45$  meter. For this set of data, the comparative study of effective width is given in Figs. 4.3 to 4.5 by varying a single parameter when other parameters remain constant. The schematic and flow diagram of ANN for plane wall configurations are shown in Figs. 4.6 & 4.7.

The set of curves given in Figs. 4.8, 4.9, and 4.10 show the variation of effective width ratio ( $Y_e/Y$ ) for a range of wall opening ratios  $L/X$  for varying wall thickness ratio  $t/Y$  for plane wall configurations. The numerical results (for a constant ratio of  $Y/X = 0.6$ ) which are calculated by ANN for plane wall configurations is compared with the results proposed by Coull & Wong [2] and Hossain M. A. [4], which is given in table 4.3. The effective width ratio predicted by ANN is found slightly higher than the values given in Ref. 2 and 4. In ANN wall thickness has been considered but Coull & Wong [2] and Hossain M. A. [4] neglected the wall thickness, this may be one of the reason of slight variation of results.

### 4.3 Flanged Wall Configurations-Equal Width

It has been demonstrated both theoretically and experimentally that the main coupling actions in the slab take place in the corridor region between the internal edges of the walls. The coupling actions are dependent only on the flange dimensions, since the regions behind the flanges are essentially stress free. Consequently, the effective width is unaffected by the location of the web wall, and the results presented are equally appropriate for offset web walls provided the flanges are located opposite each other as shown in Fig. 4.2(i) and (j).

For the configuration shown in Fig. 4.2(d), the effective width of a slab coupling two walls with equal flange width may be taken to be [23]:

$$Y_e/Y = Z/Y + L/Y [1 - 0.4(L/Y')] \text{ for } 0 \leq (L/Y') \leq 1 \quad (4.5)$$

and

$$Y_e/Y = Z/Y + Y'/Y [1 - 0.4(L/Y')^{-1}] \text{ for } 1 \leq (L/Y') \leq \infty \quad (4.6)$$

in which  $Z =$  flange width and  $Y' = Y - Z$

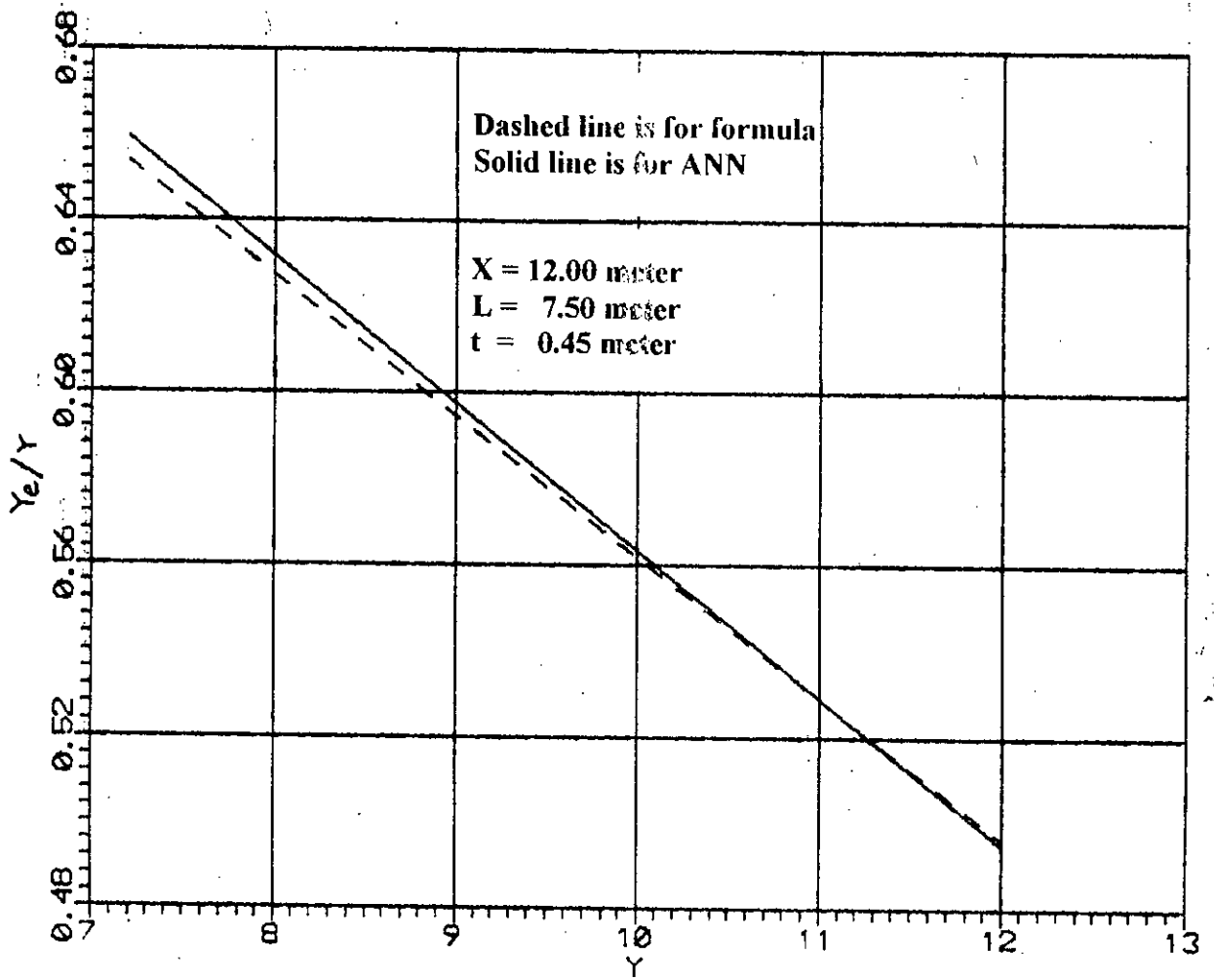


Fig. 4.3 Comparative study of  $Y_c/Y$  for plane wall configurations for varying  $Y$  keeping  $X$ ,  $L$  and  $t$  constant

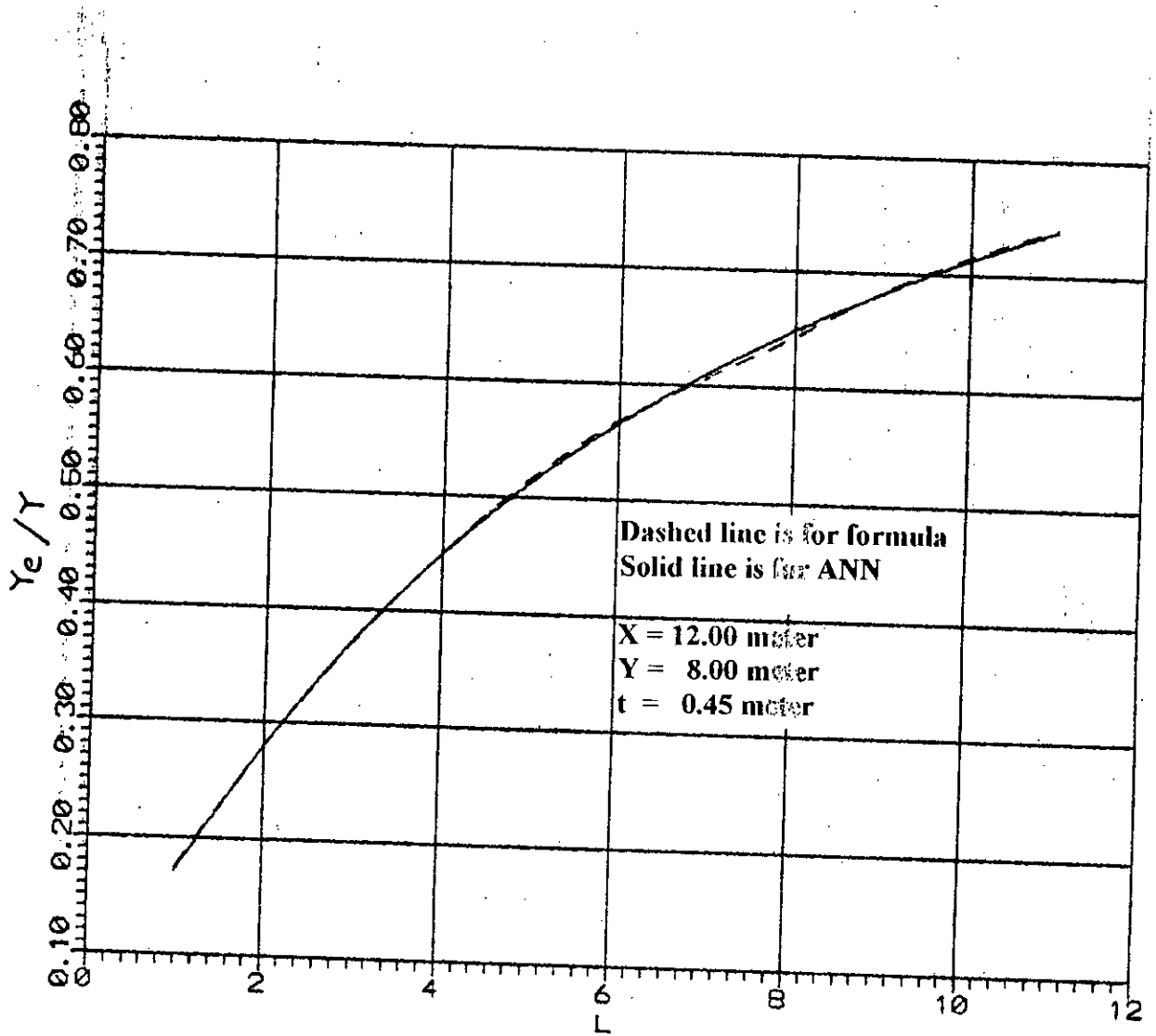


Fig. 4.4 Comparative study of  $Y_e/Y$  for plane wall configurations for varying  $L$  keeping  $X$ ,  $Y$  and  $t$  constant



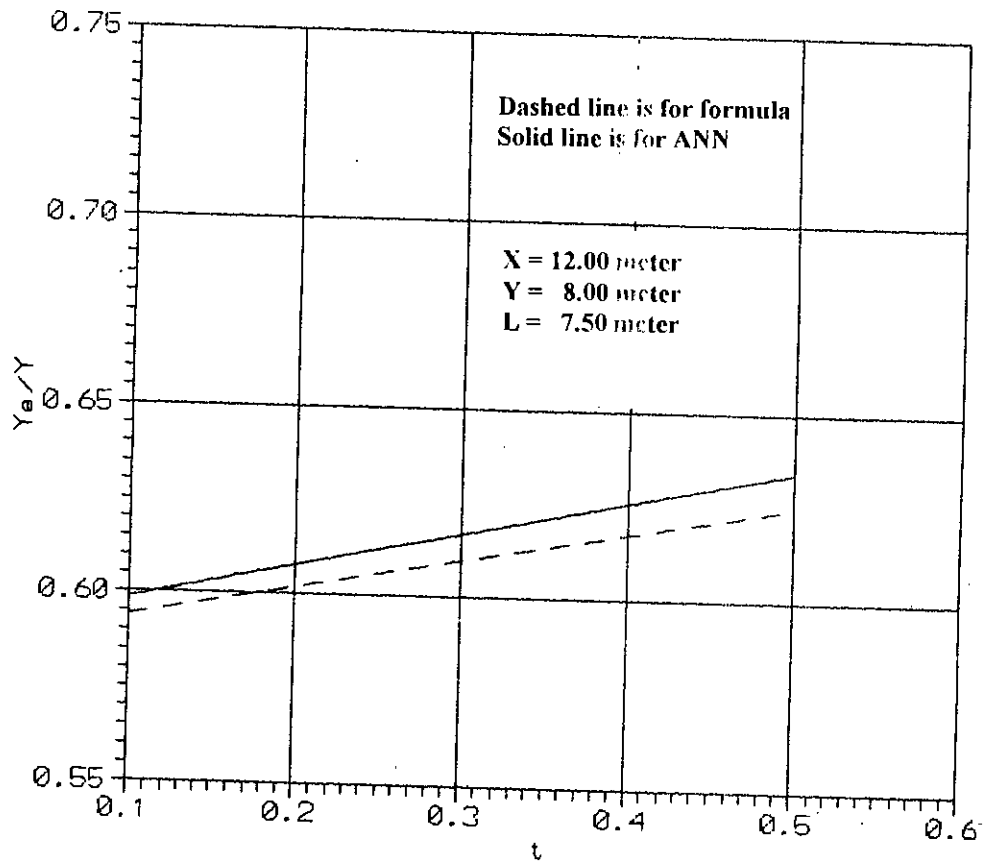


Fig. 4.5 Comparative study of  $Y_e/Y$  for plane wall configurations for varying  $t$  keeping  $X$ ,  $L$  and  $Y$  constant

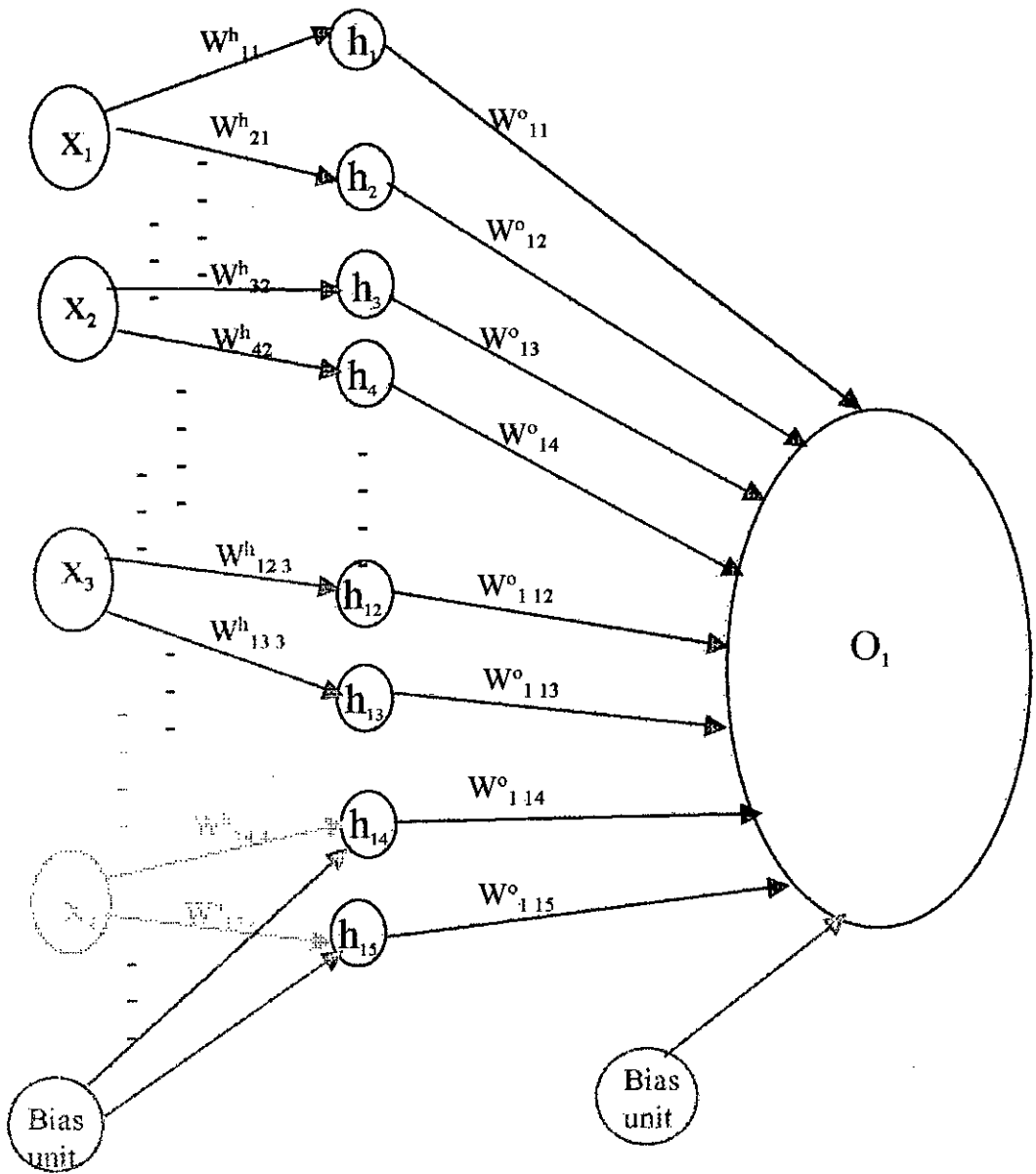


Fig. 4.6 Schematic diagram of ANN for calculation of effective slab width for plane wall configurations

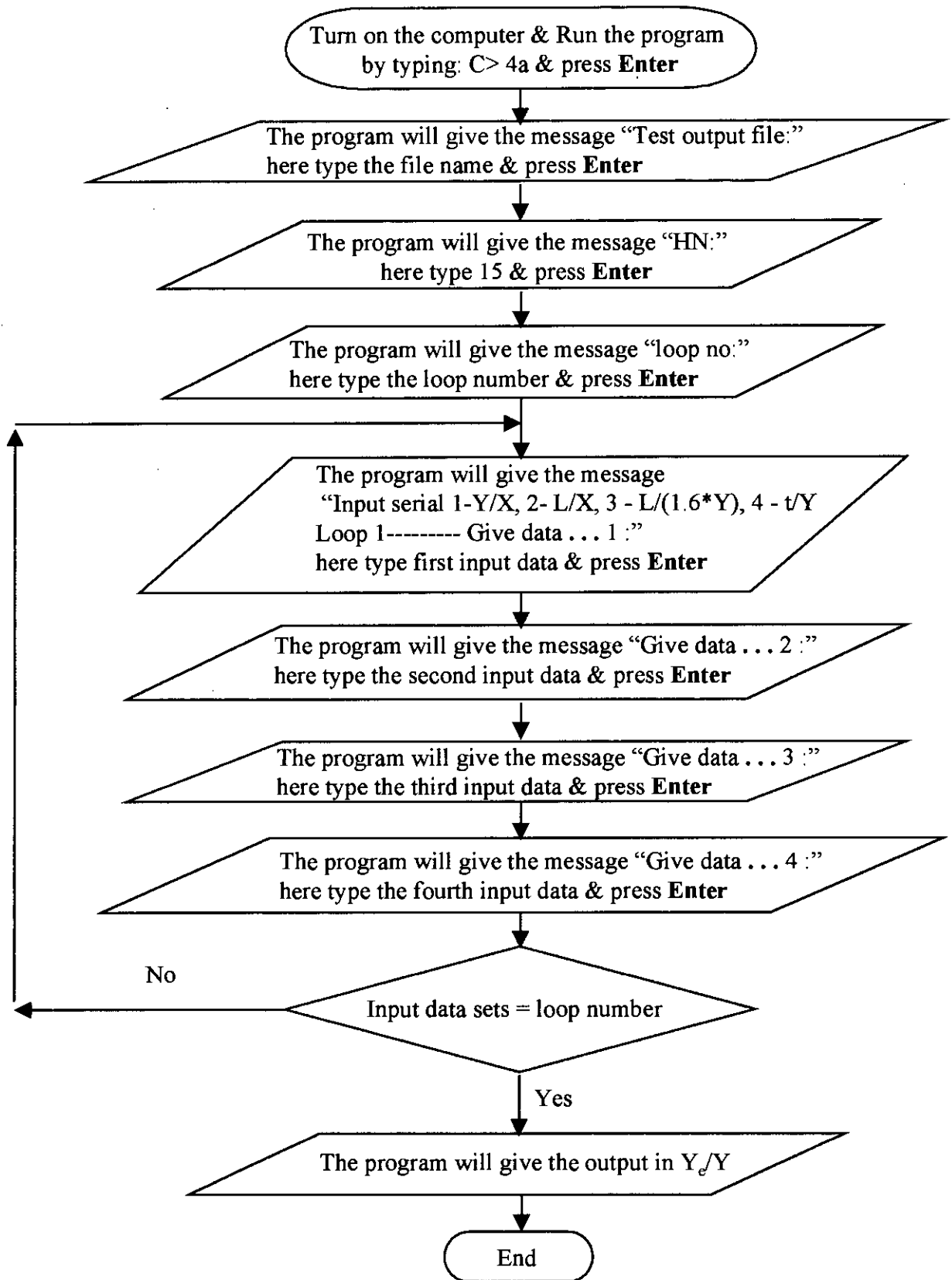


Fig. 4.7 Flow diagram for calculation of effective slab width for plane wall configurations

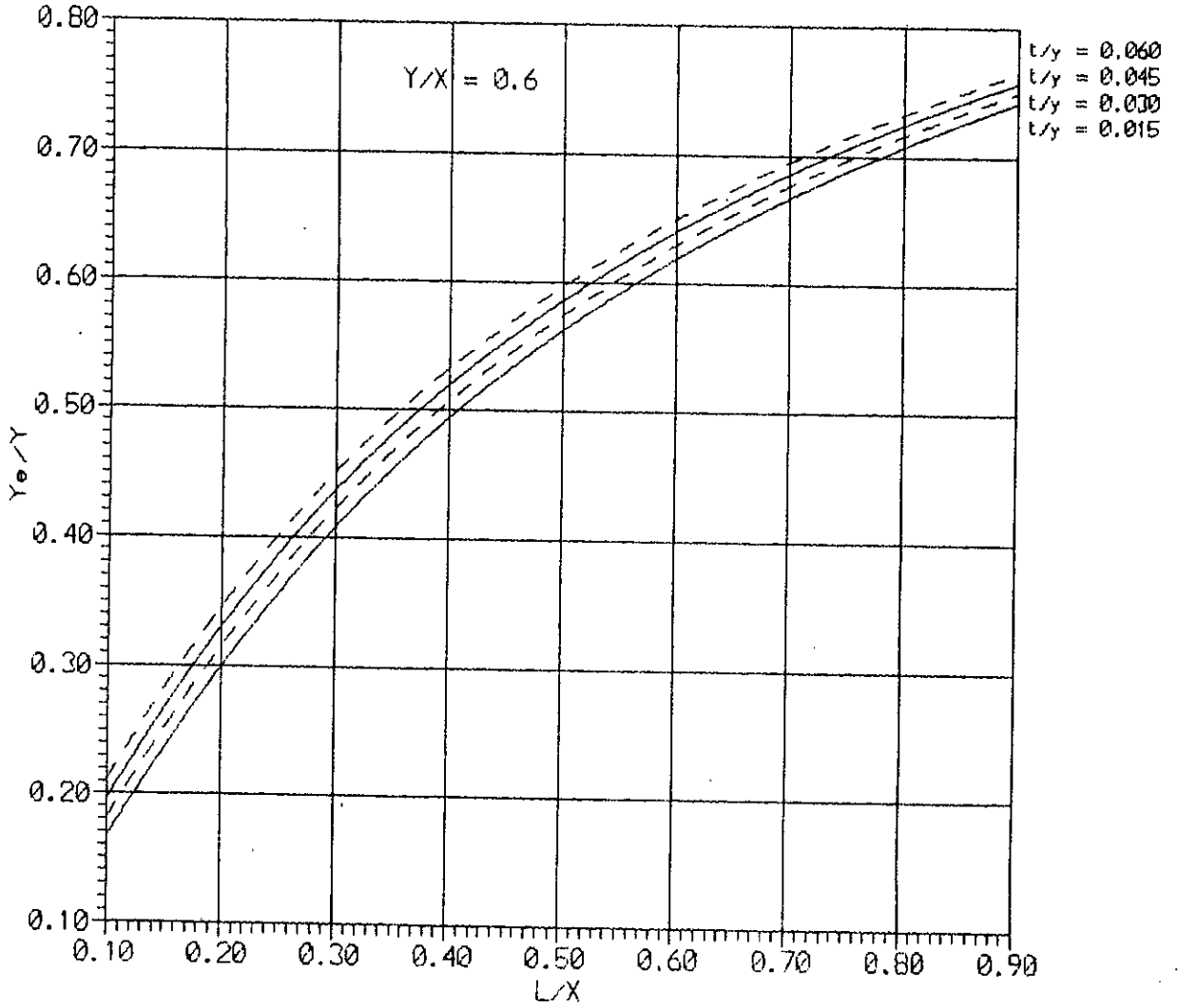
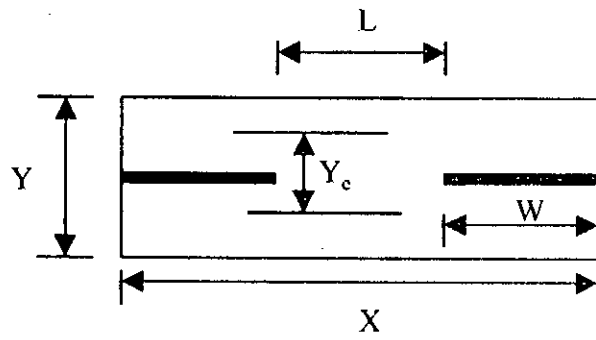


Fig. 4-8 Effective slab width for plane wall configuration for  $Y/X = 0.6$

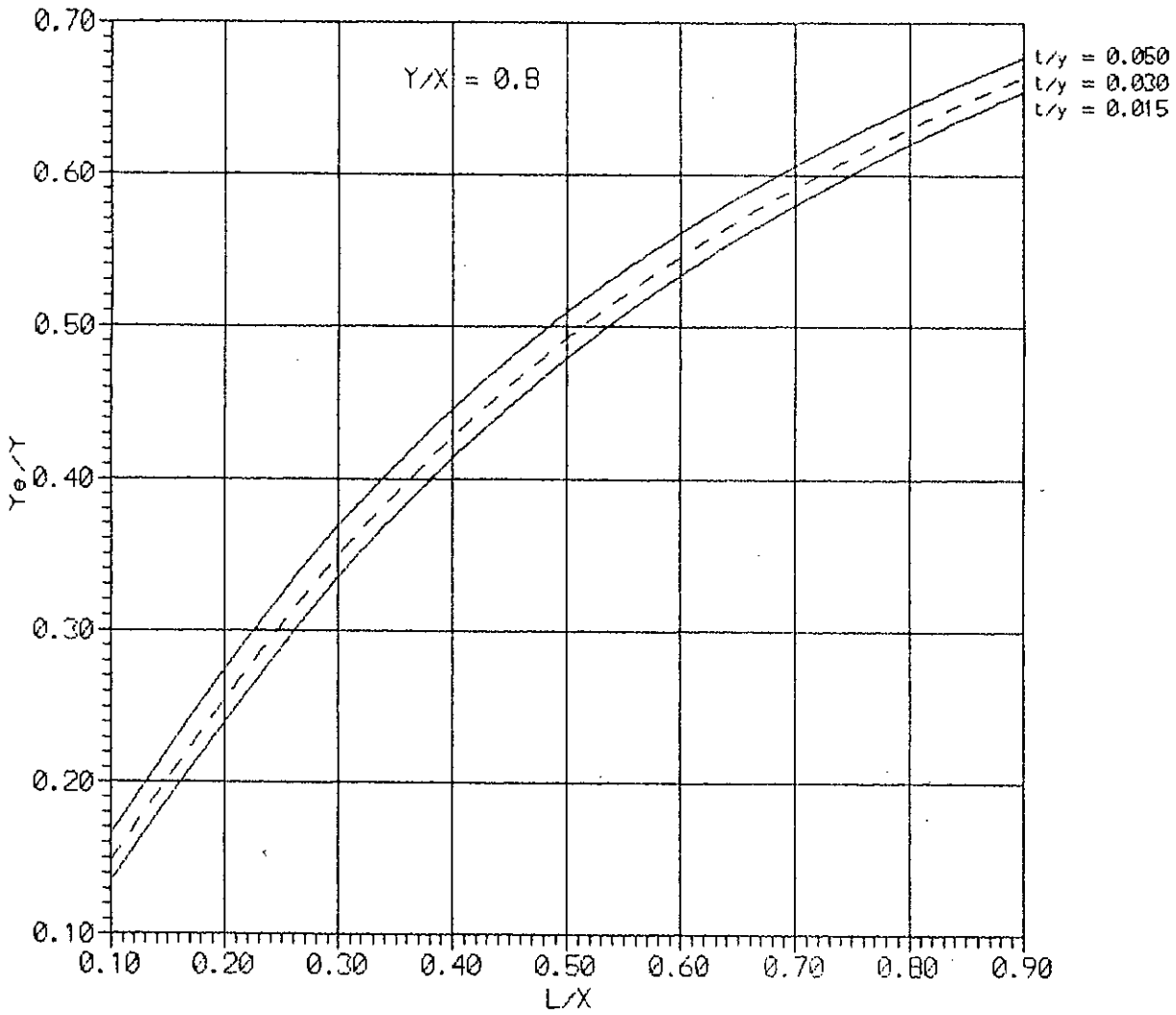
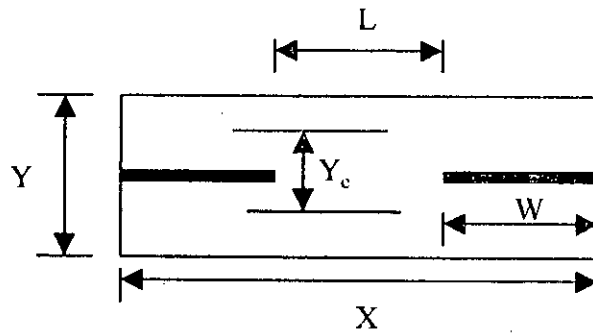


Fig. 4.9 Effective slab width for plane wall configuration for  $y/x = 0.8$

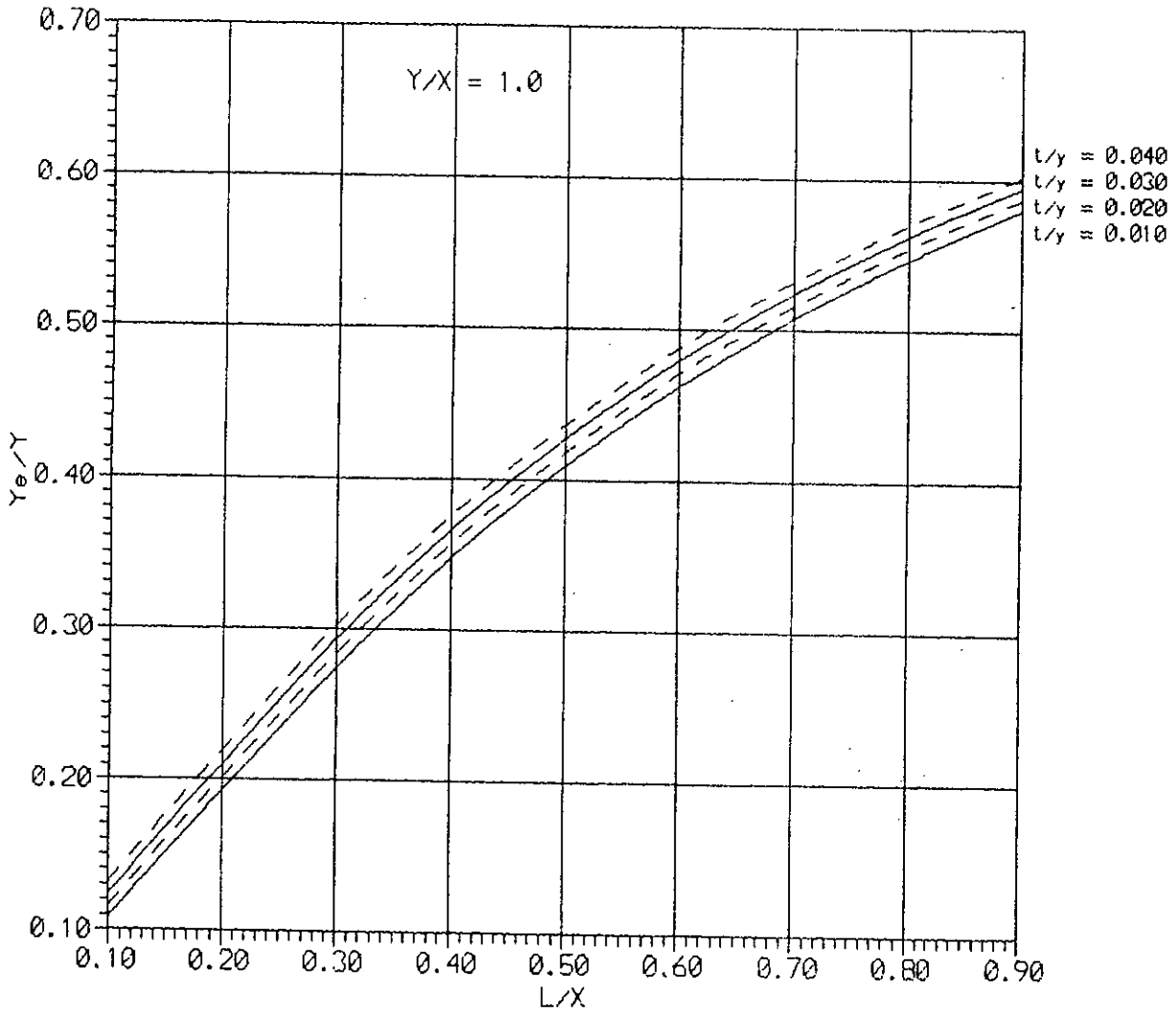
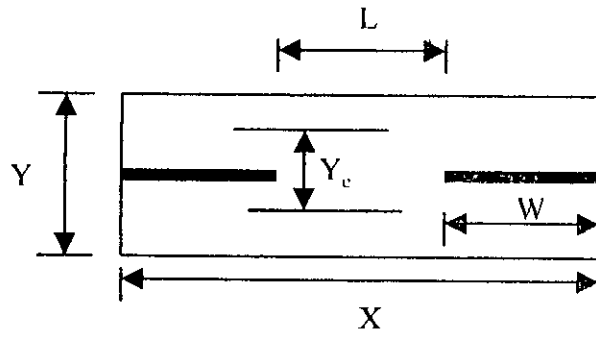


Fig. 4.10 Effective slab width for plane wall configuration for  $y/x = 1.0$

**Table 4.3** Comparison between results proposed by Coull & Wong, Hossain M. A. and ANN for plane wall configurations.

Y/X	Values of			Y <sub>e</sub> /Y Calculated by		
	L/X	L/Y	t/Y	ANN	Coull & Wong	Hossain M. A.
0.6000	0.1000	0.1667	-	-	0.1500	0.1600
			0.0150	0.1667	-	-
			0.0300	0.1812	-	-
			0.0450	0.1962	-	-
			0.0600	0.2116	-	-
0.6000	0.2000	0.3333	-	-	0.2800	0.2900
			0.0150	0.2997	-	-
			0.0300	0.3151	-	-
			0.0450	0.3305	-	-
			0.0600	0.3459	-	-
0.6000	0.3000	0.5000	-	-	0.3800	0.3800
			0.0150	0.4086	-	-
			0.0300	0.4229	-	-
			0.0450	0.4370	-	-
			0.0600	0.4510	-	-
0.6000	0.4000	0.6667	-	-	0.4700	0.4700
			0.0150	0.4940	-	-
			0.0300	0.5069	-	-
			0.0450	0.5197	-	-
			0.0600	0.5322	-	-
0.6000	0.5000	0.8333	-	-	0.5200	0.4800
			0.0150	0.5626	-	-
			0.0300	0.5743	-	-
			0.0450	0.5857	-	-
			0.0600	0.5970	-	-
0.6000	0.6000	0.9999	-	-	0.5800	0.5800
			0.0150	0.6192	-	-
			0.0300	0.6298	-	-
			0.0450	0.6402	-	-
			0.0600	0.6502	-	-

### 4.3.1 Development of the Net and Design Curves

Various values of learning rate, momentum factor and hidden neurones were taken to develop the net for selecting learning rate. Different values of learning rate such as 0.50, 0.70, and 0.90 are chosen to train the network with a constant momentum 0.6. Table 4.4 shows the percentage difference between values of  $Y_j/Y$  calculated by Eqns. (4.5 and 4.6) and ANN for a set of data. We can see that the minimum error is achieved at the learning rate of 0.90. Thus the value of the learning rate is chosen as 0.90.

During the training process various values of momentum factor such as 0.50, 0.60, 0.70 and 0.80 are taken to choose the best one. At this stage, the same set of data is again used to show the percentage difference between values of  $Y_j/Y$  calculated by Eqns. (4.5 and 4.6) and ANN. From table 4.4, it is found that the value of momentum factor has negligible effect on the system. Thus 0.70 is taken as the momentum factor for training the network.

In this work a neural network having a single hidden layer with various number of neurones such as 12, 15 and 18 is trained individually. Their training history is also shown in table 4.4. Network with 15 neurones having learning rate 0.90 and momentum factor 0.70 after 40000 iteration is chosen to develop the network with an input file having 339 sets of data [Appendix B]. Network weights and bias are also given in appendix B. The output response of finally accepted parameters for network for the set of data (which was used for table 4.4) is shown in table 4.5. The range of various parameters for input data are as follows :

X = 12.00 meter,

Y = 3.50 meter to 9.00 meter,

L = 1.00 meter to 9.00 meter,

Z = 0.10 meter to 4.00 meter.



**Table 4.4** Percentage difference between values of  $Y_p/Y$  (for flanged wall- equal width) calculated by formula (Eqns. 4.5 & 4.6) and ANN.

Sl No	Learning rate	Momentum factor	Hidden neurones	No of iteration	Mean % difference
1	0.50	0.6	15	20000	0.32 (-0.51 to +1.45)
2	0.70	0.6	15	20000	0.27 (-0.39 to +1.25)
3	0.90	0.6	15	20000	0.24 (-0.39 to +1.32)
4	0.90	0.7	15	20000	0.21 (-0.26 to +1.12)
5	0.90	0.5	15	20000	0.26 (-0.30 to +1.26)
6	0.90	0.8	15	20000	0.21 (-0.23 to +1.20)
7	0.90	0.7	12	20000	0.22 (-0.35 to +1.09)
8	0.90	0.7	18	20000	0.29 (-0.42 to +1.15)
9	0.90	0.7	15	40000	0.18 (-0.39 to +0.95)

**Table 4.5** Percentage difference between values of  $Y_p/Y$  (for flanged wall- equal width) calculated by formula (Eqns. 4.5 & 4.6) and ANN (ANN after 40000 iterations having 15 hidden neurones, learning rate = 0.90 & momentum factor = 0.70).

X (meter)	Y (meter)	L (meter)	Z (meter)	Y <sub>p</sub> /Y Calculated by		% difference
				Formula	ANN	
12.00	8.50	1.20	1.0625	0.2571	0.2561	-0.39
12.00	6.50	1.20	1.6250	0.4164	0.4178	+0.34
12.00	4.50	1.20	1.6875	0.5962	0.5952	-0.17
12.00	7.50	1.20	3.7500	0.6395	0.6386	-0.14
12.00	3.50	1.20	2.6250	0.9271	0.9268	-0.03
12.00	8.50	4.80	1.0625	0.5439	0.5437	-0.04
12.00	6.50	4.80	1.6250	0.6976	0.7042	+0.95
12.00	4.50	4.80	1.6875	0.8535	0.8533	-0.02
12.00	7.50	4.80	3.7500	0.8438	0.8416	-0.26
12.00	3.50	4.80	2.6250	0.9818	0.9830	+0.12
12.00	2.50	6.50	2.2500	0.9985	0.9987	+0.02
12.00	5.50	8.50	3.6250	0.9699	0.9705	+0.06
12.00	3.50	2.50	2.6750	0.9689	0.9685	-0.04
12.00	7.50	7.50	3.2500	0.8716	0.8715	-0.01
12.00	5.50	5.50	2.3750	0.8709	0.8703	-0.06

Average % difference = 0.18  
(+0.95 to -0.39)

From the above testing data set, it is seen that the network gives the maximum error when  $X = 12.00$  meter,  $Y = 6.50$  meter,  $L = 4.80$  meter &  $Z = 1.625$  meter. For this set of data, the comparative study of effective width is given in Figs. 4.11 to 4.13 by varying a single parameter when other parameters remain constant. The schematic and flow diagram of ANN for flanged wall configurations- equal width are shown in Figs. 4.14 & 4.15.

The set of curves given in Fig. 4.16, 4.17, and 4.18 show the variation of effective width ratio ( $Y_e/Y$ ) for a range of wall opening ratios  $L/X$  for varying flange width ratio  $Z/Y$ . The numerical results which are calculated by ANN is compared with the results calculated by finite element [23], which is given in table 4.6. The agreement is found very good. In this comparison the value of  $Y$  is taken equal to 4.8 meter.

**Table 4.6** Comparison between finite element, formula and ANN results for flanged wall configurations-equal width.

L/X	Z/Y	Y <sub>e</sub> /Y Calculated by			% difference with finite element
		finite element (Ref. 2)	Formula	ANN	
0.10	0.125	0.3388	0.3464	0.3503	+3.39
0.10	0.250	0.4603	0.4667	0.4691	+0.51
0.10	0.375	0.5804	0.5850	0.5841	+0.64
0.10	0.500	0.6985	0.7000	0.6983	-0.03
0.10	0.750	0.9176	0.9000	0.9052	-1.26
0.40	0.125	0.6950	0.6938	0.6950	0.00
0.40	0.250	0.7666	0.7750	0.7741	+0.98
0.40	0.375	0.8325	0.8437	0.8430	+1.26
0.40	0.500	0.8918	0.9000	0.8996	+0.88
0.40	0.750	0.9906	0.9750	0.9764	-1.43

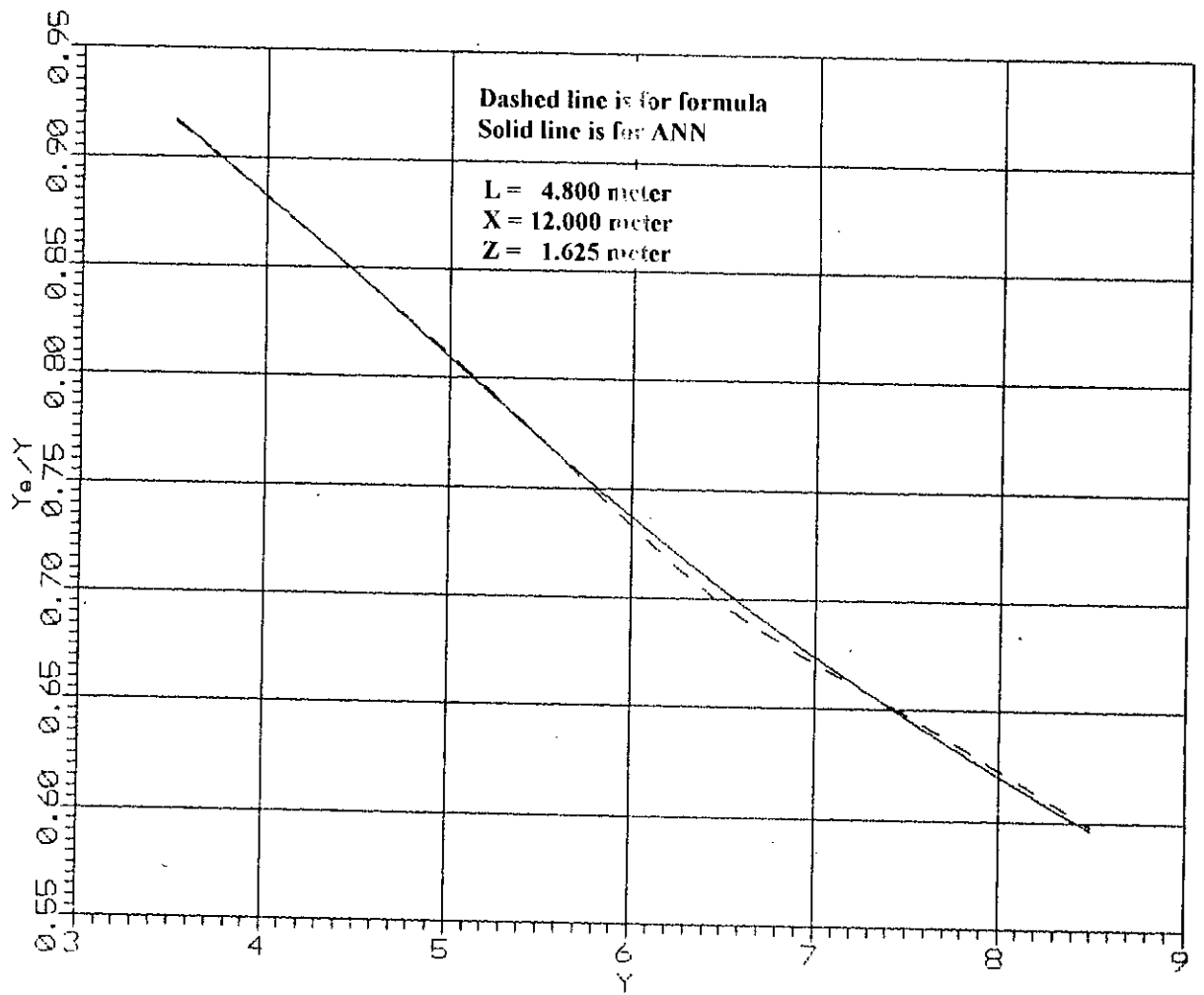


Fig. 4.11 Comparative study of  $Y_e/Y$  for flanged (equal width) wall configurations for varying  $Y$  keeping  $X$ ,  $L$  and  $Z$  constant

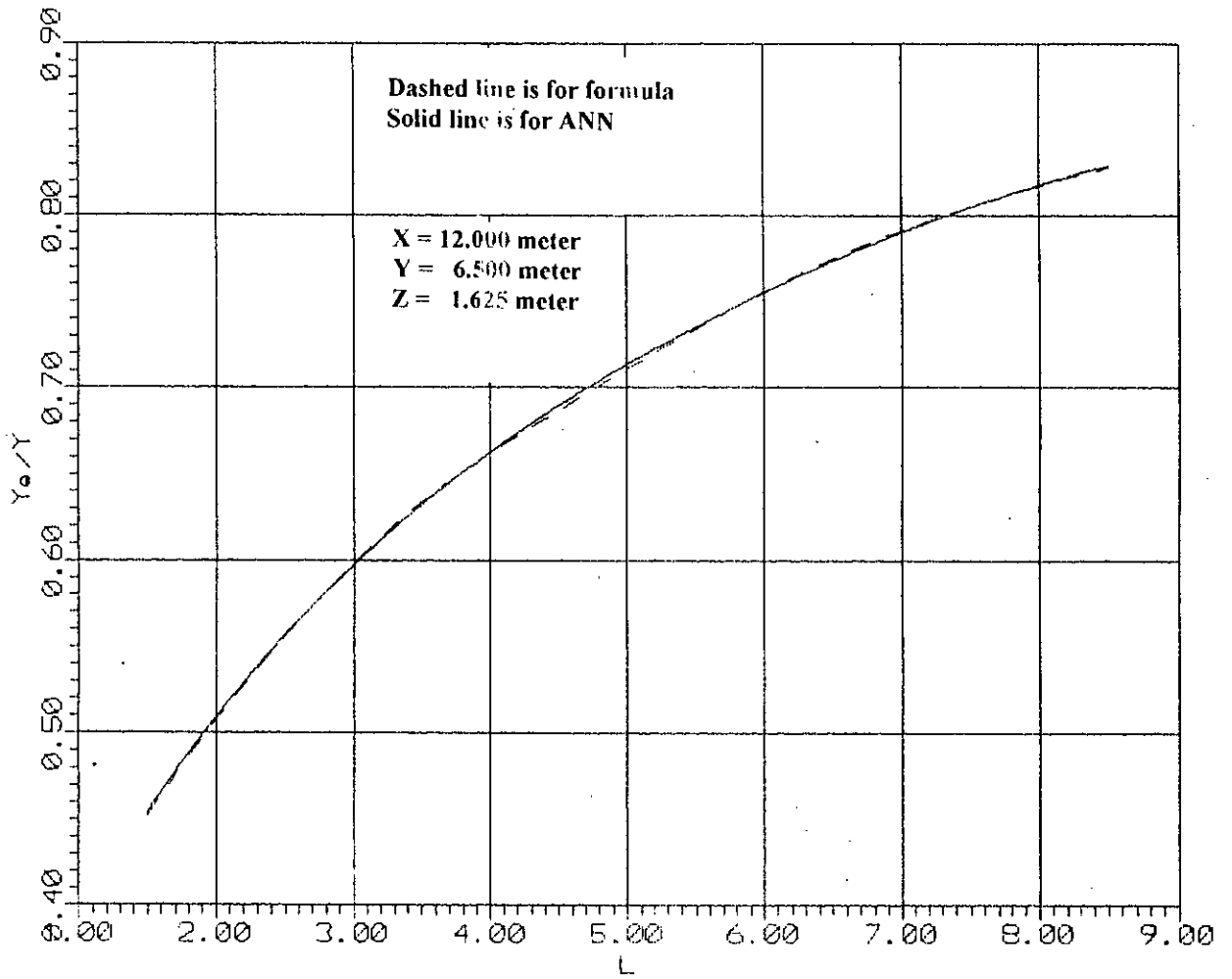


Fig. 4.12 Comparative study of  $Y_0/Y$  for flanged (equal width) wall configurations for varying  $L$  keeping  $X$ ,  $Y$  and  $Z$  constant

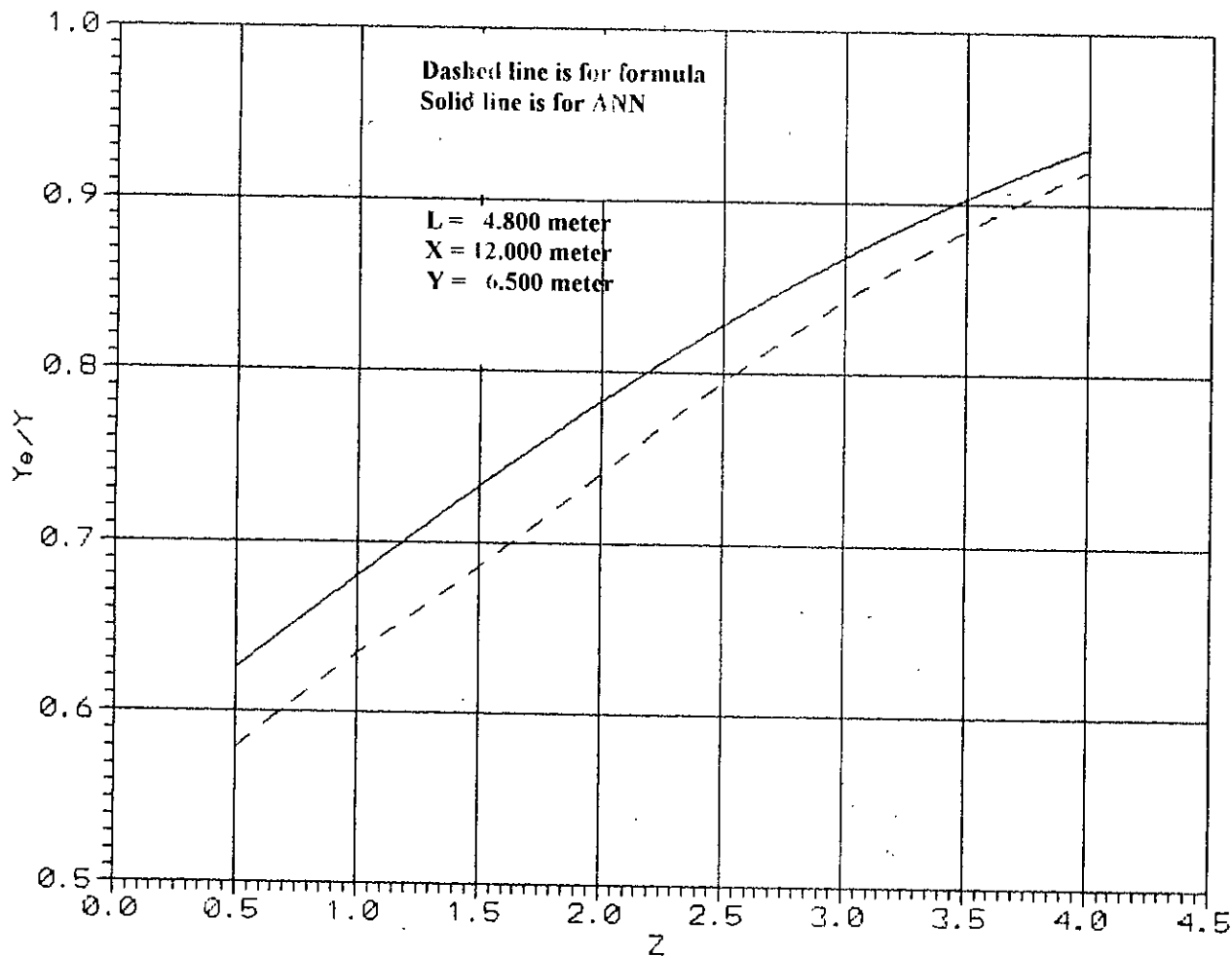


Fig. 4.13 Comparative study of  $Y_e/Y$  for flanged (equal width) wall configurations for varying  $Z$  keeping  $X$ ,  $L$  and  $Y$  constant

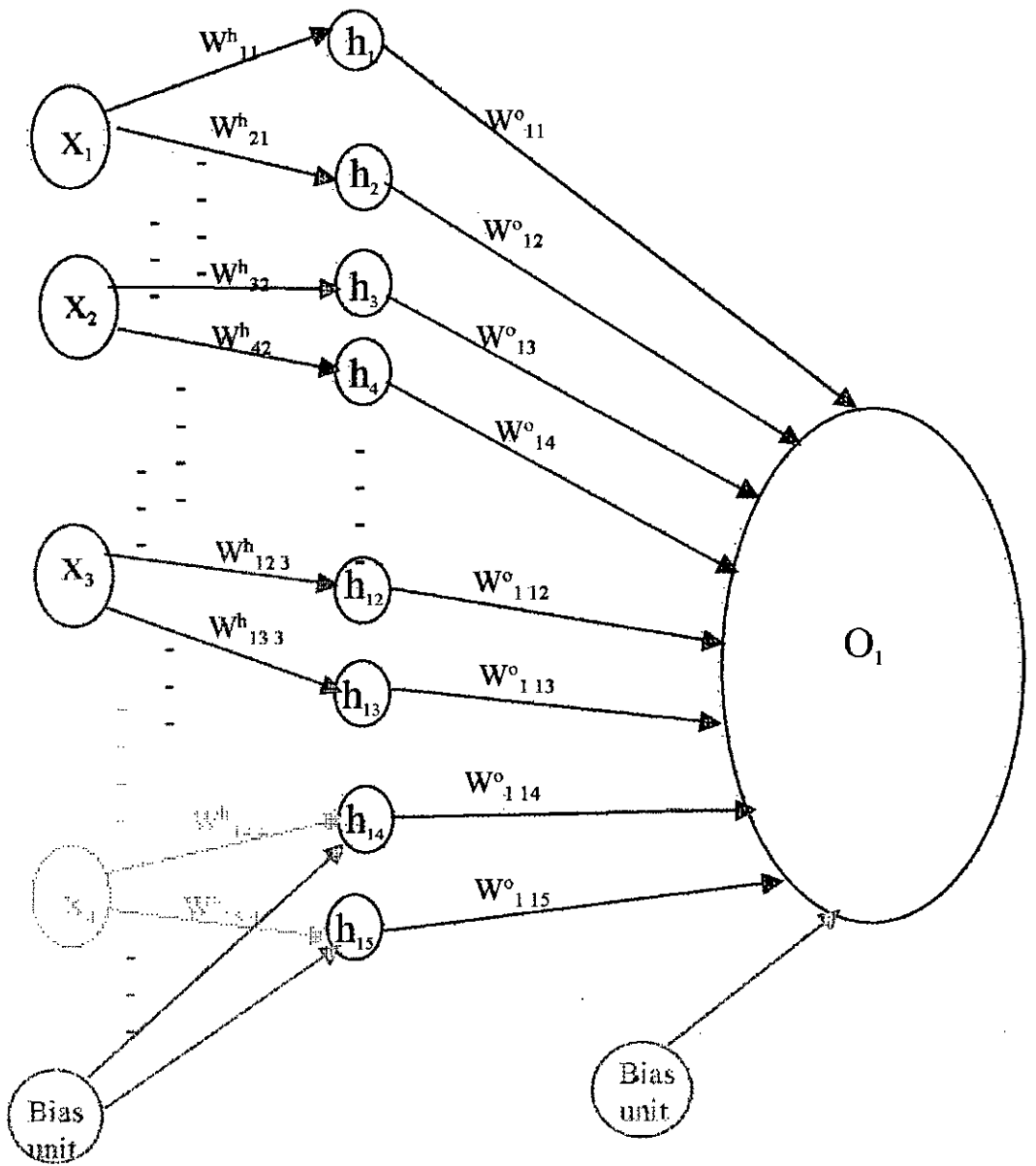


Fig. 4.14 Schematic diagram of ANN for calculation of effective slab width for flanged wall (equal width) configurations

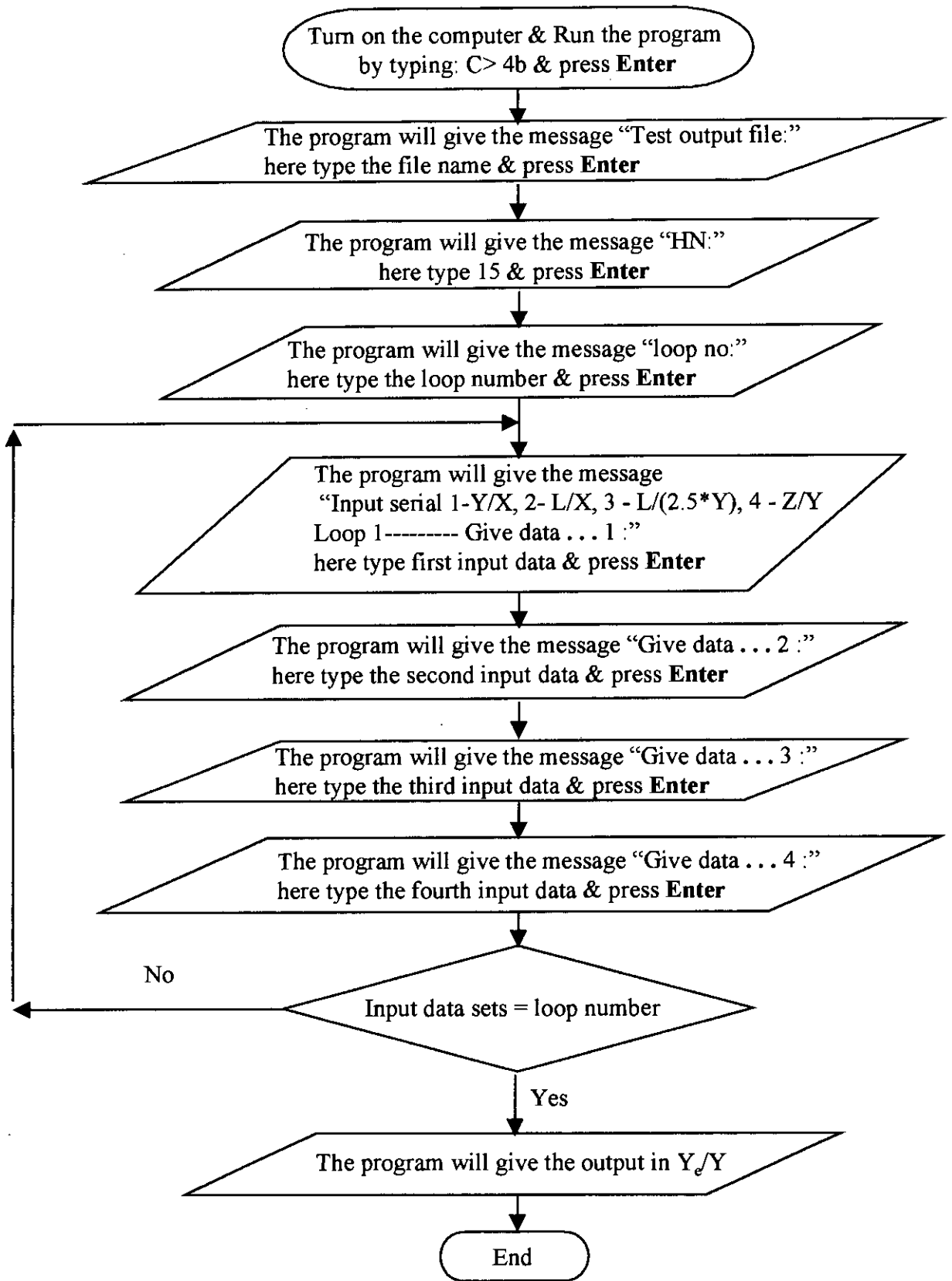


Fig. 4.15 Flow diagram for calculation of effective slab width for flanged wall (equal width) configurations



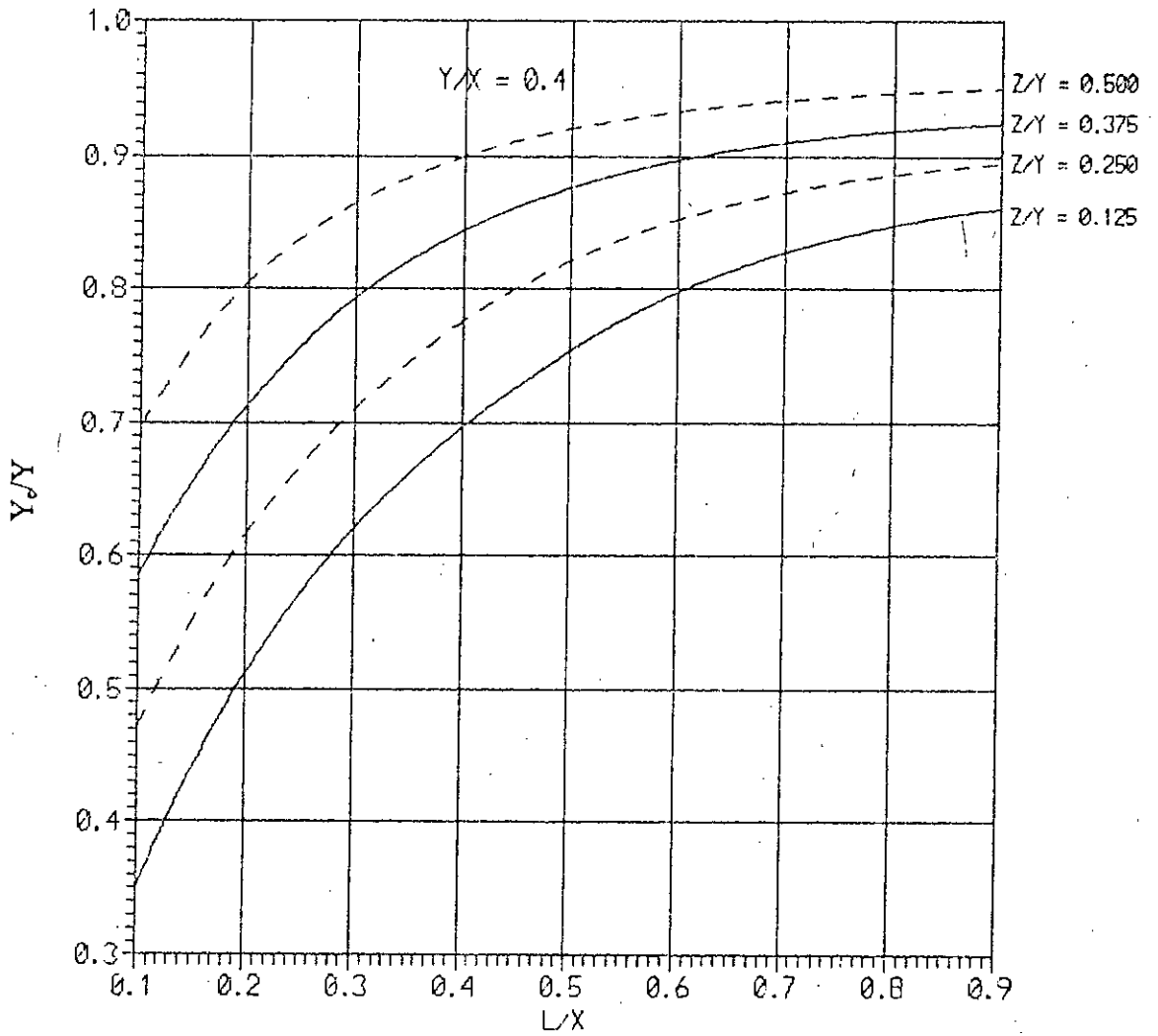
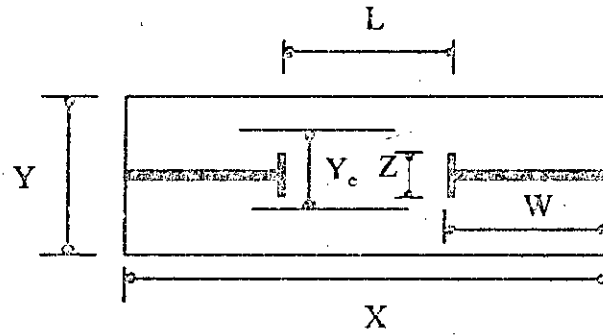


Fig. 4/16 Effective slab width for flanged (equal width) wall configurations for  $Y/X = 0.40$

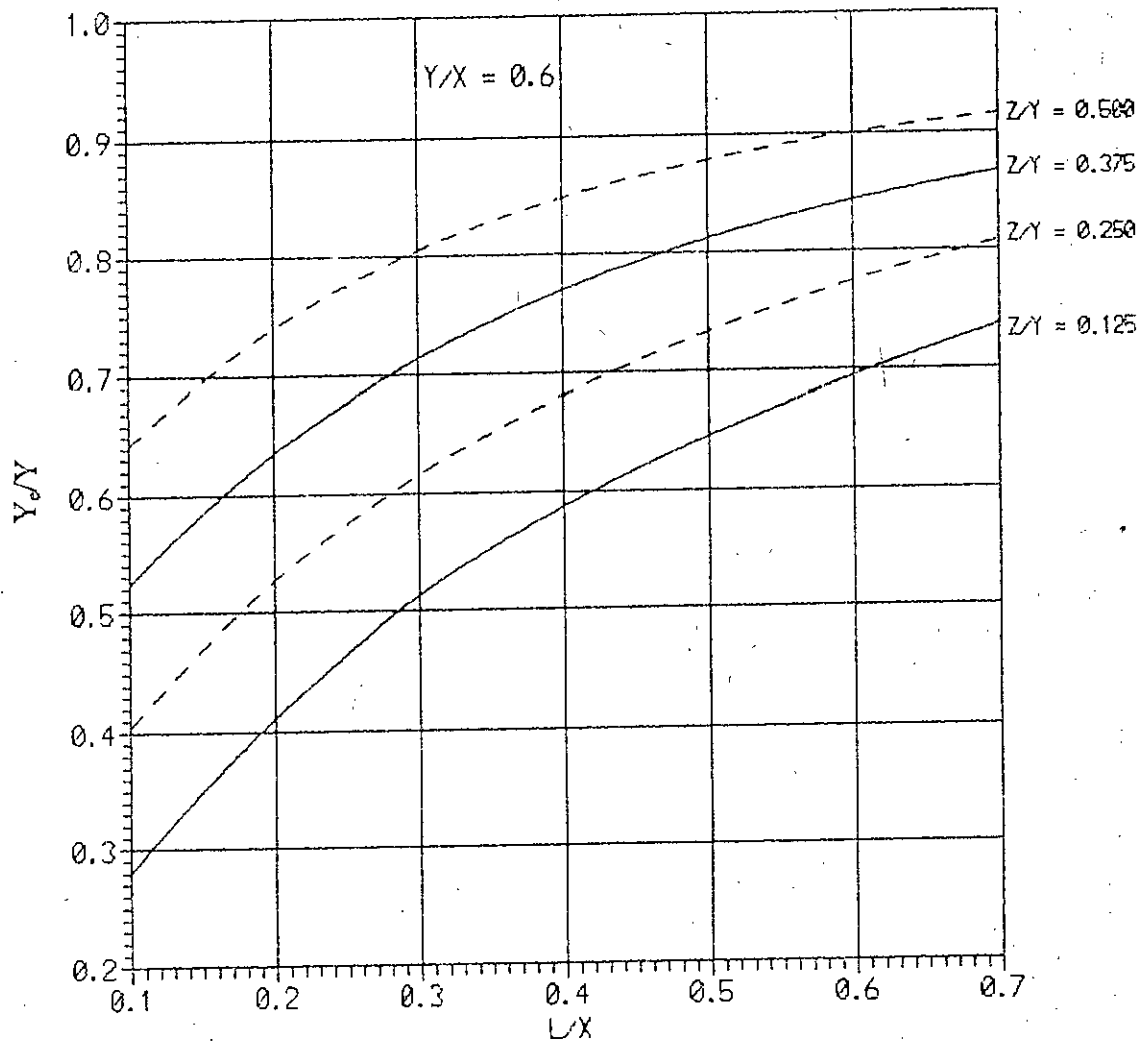
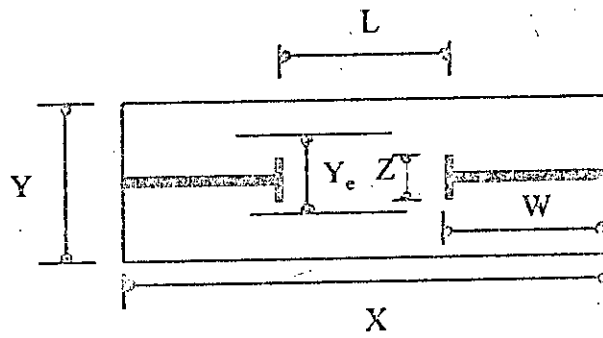


Fig. 4.17 Effective slab width for flanged (equal width) wall configurations for  $Y/X = 0.60$

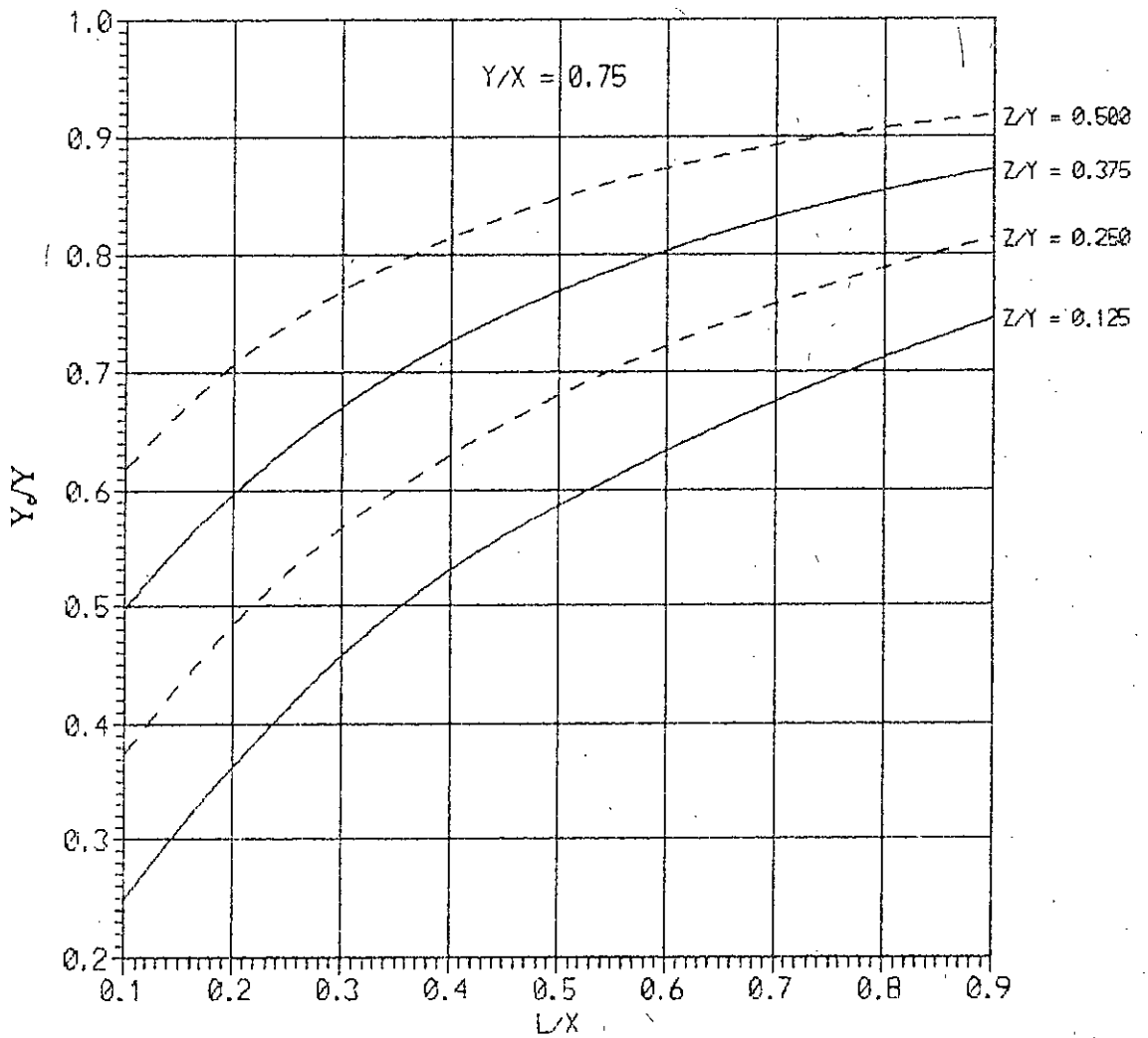
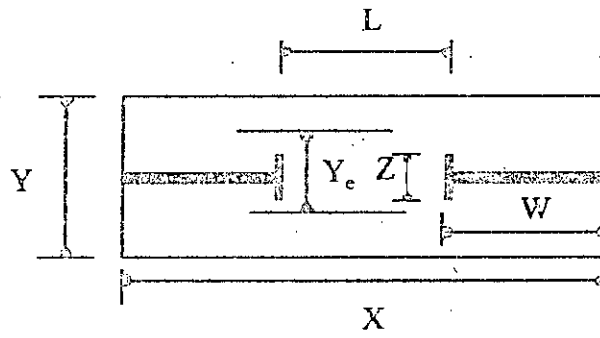


Fig. 418 Effective slab width for flanged (equal width) wall configurations for  $Y/X = 0.75$

## 4.4 Results and Discussions

The curves show the variation of the effective slab width or stiffness with different geometric layout parameters. However, as many variables are concerned (slab thickness, wall lengths, wall spacing, size of opening, wall thickness and wall flanged width), many curves are required to cover all likely practical situations. The influence of important parameters are discussed below:

### 4.4.1 Effect of Wall Thickness (t)

In examining the influence of wall thickness of shear wall on the effective width ratio,  $Y_e/Y$ , curves are plotted (Figs. 4.8 to 4.10) for varying  $t/Y$  ratio, keeping slab width (Y) constant. For the same value of Y, the ratio,  $t/Y$  increases with the increase of wall thickness. It is seen from the graph that with the increase of wall thickness the effective width ratio,  $Y_e/Y$  also increases. The rate of increase of  $Y_e/Y$  is maximum when length of opening between walls (L) and slab length (X) ratio,  $L/X$ , is minimum. When  $t/Y$  is increased from 0.015 to 0.045, the effective width ratio,  $Y_e/Y$  increases by 18% for  $L/X$  equal to 0.10 and  $Y_e/Y$  increases by 3% only for  $L/X$  equal to 0.60 for the same value of  $Y/X$  ( $Y/X = 0.60$ ). Graphs for various values of slab width (Y) have been plotted keeping the slab length (X) constant, which was assumed 12.00 meter. The rate of increase of effective width ratio is almost same for different values of Y.

### 4.4.2 Effect of Opening Between Walls (L)

Effect of opening between walls (L) can be examined when other parameters i.e. shear wall thickness (t), slab width (Y) and slab length (X) are constant. So curves have been plotted for varying values of L, keeping all other constant. When L is increased, the ratio  $L/X$  also increases. From the Figs. 4.8 to 4.10, it is seen that with the increase of  $L/X$ , the effective width ratio  $Y_e/Y$  also increases. When  $L/X$  is increased from 0.10 to 0.60, the effective width ratio  $Y_e/Y$  increases by 3.71 times for  $t/Y$  equal to 0.015. The effective width ratio  $Y_e/Y$  is maximum for higher values of  $L/X$ .

### 4.4.3 Effect of Flange (Equal) Width

The influence of flange width ( $Z$ ) on the effective width ratio,  $Y_e/Y$  is quite prominent. In examining the effect of flange width, curves are plotted in Figs.4.16 to 4.18 for varying  $Z/Y$  ratio, keeping slab width ( $Y$ ) constant. For a constant value of  $Y$ , the ratio  $Z/Y$  increases with the increase of flange width ( $Z$ ). When  $Z/Y$  is increased from 0.125 to 0.50, the effective width ratio,  $Y_e/Y$  increases by 2.29 times for  $L/X$  equal to 0.10 and  $Y/X$  equal to 0.60. The rate of increase of  $Y_e/Y$  is maximum/sharp when  $L/X$  is minimum and the increment is negligible as the value of  $L/X$  exceeds 0.50. That is the influence of the flange width ( $Z$ ) and finite wall thickness ( $t$ ) are practically identical. Table 4.7 gives a comparative study of the rate of increase of  $Y_e/Y$ .

**Table 4.7** Comparative study of the rate of increase of  $Y_e/Y$  for different values of  $Z/Y$  to see the effect of flange width.

Y/X	L/X	Y <sub>e</sub> /Y Calculated when			
		Z/Y = 0.125	Z/Y = 0.250	Z/Y = 0.375	Z/Y = 0.500
0.60	0.10	0.2801	0.4046	0.5237	0.6427
0.60	0.20	0.4117	0.5266	0.6351	0.7400
0.60	0.30	0.5126	0.6157	0.7134	0.8045
0.60	0.40	0.5873	0.6815	0.7697	0.8483
0.60	0.50	0.6457	0.7328	0.8117	0.8788
0.60	0.60	0.6946	0.7742	0.8436	0.9004
0.60	0.70	0.7362	0.8074	0.8673	0.9154

#### 4.4.4 Comparison of ANN with Other Published Results

To illustrate the accuracy of the ANN, when they are applied to plane and flanged wall configurations, the ANN results are compared with the Coull & Wong [2], Hossain M. A. [4] and finite element results [23] in table 4.3 and 4.6 respectively. The agreement with the results of Coull & Wong [2] and Hossain M. A. [4] is found very good. The results agree with the accurate finite element values to within 3.5%. Once the artificial neural network is developed, the effective width ratio ( $Y_e/Y$ ) can be found out accurately and within fraction of minute, when the required input parameters such as  $Y/X$ ,  $L/X$ ,  $t/Y$  or  $Z/Y$  and  $L/Y$  are known for a particular problem.

#### 4.5 Computer Program

There are two different sets of program. These are:

- a. First set of program consists of two files: 4a.wt and 4a.exe files. These are used to calculate the effective width of plane wall configurations. The listing of files 4a.wt and 4a.exe are given in appendix A.
- b. Second set of program also consists of two files: 4b.wt and 4b.exe files. These are used to calculate the effective width of flanged wall (equal width) configurations. The listing of files 4b.wt and 4b.exe are given in appendix B.

##### *Use of the computer program:*

Once the program files are copied, we can start it by simply typing 4a or 4b (as applicable) at the root directory and pressing **Enter**.

“Test output file” writing will appear on the screen. Here the output file name is to be given. File name can be alphabetical or numerical. File name will have an extension “out”. Example of file name: A.out or 1.out. After typing output file name **Enter** is to be pressed.

“HN” writing will appear on the screen. Number of hidden neurones, which was used during training must be given here. Otherwise output value will not be correct. The value of HN for plane and flanged wall configurations is 15. After typing 15 **Enter** is to be pressed.

“Loop no” and “Give data ... 1” writing will appear on the screen. It is the number of sets of data one wants to calculate. After loop number input data is given. During data input, input serial must be maintained, input serial will appear on the screen. Otherwise output value will not be correct. After typing first input data **Enter** is to be pressed. “Give data ... 2” writing will appear on the screen. Here second input data is given and **Enter** is to be pressed. “Give data ...” writing will continue to appear on the screen until data input is completed.

Output writing along with output will appear on the screen. Output is given in the same sequence of loop number. The output for the effective width of plane and flanged wall configurations is in the form of  $Y/Y$ . So to get the effective width the computed value should be multiplied by total slab width or longitudinal wall spacing (Y).

## CHAPTER FIVE

### PUNCHING SHEAR OF WALL-SLAB CONNECTIONS

#### 5.1 Introduction

The region of a slab in the vicinity of a support could fail in shear by developing a failure surface in the form of a truncated cone or pyramid. This type of failure, called a 'punching shear failure', is usually the source of collapse of flat slab and slab-coupled shear wall structures. In slab-coupled shear walls, both the gravity load and wind load has to be finally transmitted to the walls at the wall-slab junction. The transfer of moments from slab to columns may further increase these shear stresses, and requires concentration of negative flexural steel in the slab in the region close to the columns. Again when two-way slabs are supported directly by columns, as in flat slabs and flat plates, or when slabs carry concentrated loads, as in footings, shear near the columns is of critical importance. Tests of flat plate structures indicate that, in most practical cases, the capacity is governed by shear.

#### 5.2 Punching Shear Design in Flat Plates and Flat Slabs

Two kinds of shear may be critical in the design of flat slabs, flat plates or footings. The first is the familiar beam-type shear leading to diagonal tension failure. Alternatively, failure may occur by punching shear, with the potential diagonal crack following the surface of a truncated cone or pyramid around the column capital or drop panel, as shown in Fig. 5.1a. The failure surface extends from the bottom of the slab, at the support, diagonally upward to the top surface. The angle of inclination with the horizontal,  $\theta$  (Fig. 5.1b), depends upon the nature and amount of reinforcement in the slab. It may range between about  $20^\circ$  to  $45^\circ$ . The critical section for shear is taken perpendicular to the plane of the slab and a distance  $d/2$  from the periphery of the support, as shown in Fig. 5.2. The shear force  $V_u$  to be resisted can be calculated as the total factored load on the area bounded by panel centreline around the column less the load applied within the area defined by the critical shear perimeter, unless significant moments must be transferred from the slab to the column.



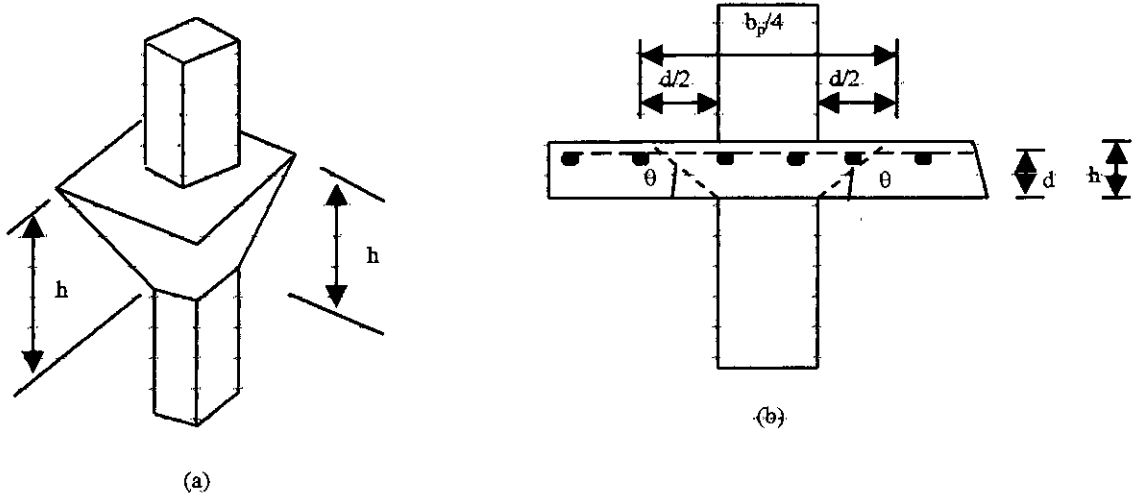


Fig. 5.1 Failure surface defined by punching shear

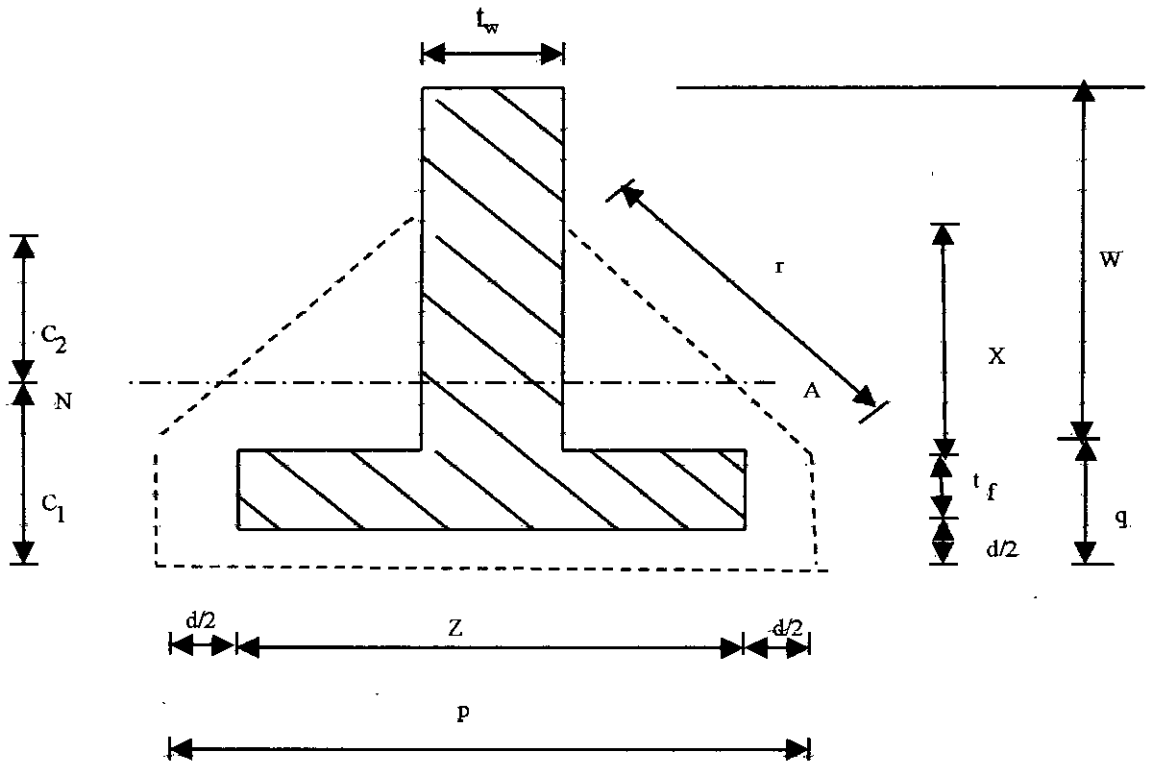


Fig. 5.2 Proposed critical section

At such a section, in addition to the shearing stresses and horizontal compressive stresses due to negative bending moment, vertical or somewhat inclined compressive stress is present, owing to the reaction of the column. The simultaneous presence of vertical and horizontal compression increases the shear strength of concrete.

### 5.3 Calculation of Critical Perimeter for Punching Shear

According to the study reported in Reference [6], the length of critical perimeter,  $b_p$  for critical section in Fig. 5.2 may be taken as:

$$b_p = p + 2(r + q) \quad (5.1)$$

Where

$$p = Z + d$$

$Z$  = flange width for T-section shear walls  
 = equal to wall thickness for plane models

$d$  = effective depth of tension reinforcement

$$q = t_f + d/2$$

$t_f$  = flange thickness

$r$  = length of inclined portion of the section

$x$  = distance behind flange up to which the critical section extends

$t_w$  = web thickness

$$x/Z = 4.0 e^{-0.465(Z/t_w)} \quad (5.2)$$

$$r^2 = x^2 + 0.25(p - t_w)^2 \quad (5.3)$$

#### 5.3.1 Development of the Net and Design Curves

Different values of learning rate such as 0.1, 0.2, and 0.3 are chosen to train the network with a constant momentum 0.3. After 150,000 iterations for each network (for learning rate = 0.1, 0.2 & 0.3), the weight of the network is saved for calculating the error of a set of data having known output. Comparison between the output response of the network (ANN) and values calculated by Eqn. 5.1 to the set of data is shown in table 5.1. From table 5.1, it is seen that minimum average percentage difference is achieved at the learning rate of 0.2. Thus the value of the learning rate is chosen as 0.2.

**Table 5.1** Percentage difference between  $b_p/d$  calculated by formula and ANN.

Sl no	Learning rate	Momentum factor	Hidden neurones	No of iteration	Average % difference
1.	0.10	0.30	15	150000	1.24 (+1.91 to -3.47)
2.	0.20	0.30	15	150000	1.20 (+1.43 to -4.66)
3.	0.30	0.30	15	150000	1.26 (+1.12 to -4.99)
4.	0.20	0.30	15	150000	1.19 (+1.37 to -4.20)
5.	0.20	0.10	15	150000	1.21 (+1.40 to -4.03)
6.	0.20	0.30	18	150000	1.32 (+1.58 to -4.07)
7.	0.20	0.30	12	150000	1.50 (+1.91 to -4.21)
8.	0.20	0.20	15	125000	1.21 (+2.82 to -4.20)
9.	0.20	0.20	15	175000	1.18 (+1.57 to -4.20)
10.	0.20	0.10	15	175000	1.18 (+1.37 to -4.05)

During the training process various values of momentum factor such as 0.1, 0.2, and 0.3 are taken to choose the best one. Comparison between the results calculated by formula (Eqn. 5.1) and ANN at different momentum factors to the same set of data is shown in table 5.1. The minimum average percentage difference is achieved at momentum factor 0.1. Thus 0.1 is taken as the momentum factor for training the network.

In this work a neural network having a single hidden layer with various number of neurones such as 12, 15 and 18 is trained individually. After 150,000 iterations for each network, the weight of the network is saved for calculating the error of the set of data having known output. Comparison between the output response of all the networks are shown in table 5.1. From the table it is seen that the output response of the net having 15 neurones is the best. Again the weight of the network having 15 neurones is saved after 150,000 and 175,000 iterations. Between the output responses of the later networks the average percentage difference is very small. So the network with single hidden layer having 15 neurones after 150,000 iterations is selected to develop the network with an input file having 239 sets of data [Appendix C]. Network weights and bias are also given in appendix C. Detail of the output response of finally accepted parameters for the network for the set of data having known output is shown in table 5.2.

**Table 5.2** Percentage difference between values of  $b_p/d$  calculated by formula and ANN. (ANN after 150000 iterations having 15 hidden units, learning rate = 0.20 and momentum factor = 0.10)

$t_f$ (cm)	d (cm)	Z (cm)	W (cm)	$b_p/d$ Calculated by		% difference
				Formula	ANN	
20.00	18.00	30.00	55.00	12.19	11.90	-2.38
25.00	15.00	50.00	50.00	15.85	16.07	+1.38
23.00	18.00	70.00	70.00	16.82	16.35	-2.78
27.00	22.00	90.00	60.00	15.23	15.28	+0.33
30.00	24.00	65.00	90.00	15.10	14.59	-3.36
35.00	25.00	45.00	75.00	12.76	12.76	0.00
32.00	29.00	75.00	85.00	13.16	13.14	-0.15
35.00	21.00	50.00	90.00	16.46	16.02	-2.65
38.00	15.00	30.00	45.00	15.08	15.01	-0.48
42.00	29.00	95.00	65.00	13.47	13.40	-0.49
48.00	18.00	100.00	68.00	21.39	21.27	-0.55
25.00	22.00	20.00	79.00	10.25	10.20	-0.45
50.00	17.00	95.00	55.00	20.90	20.90	0.00
38.00	26.00	65.00	70.00	13.18	13.36	+1.40
50.00	15.00	90.00	90.00	27.21	27.16	-0.18
25.00	22.00	85.00	60.00	14.74	14.76	+0.11
35.00	26.00	59.00	80.00	13.41	13.50	+0.70
45.00	18.00	30.00	60.00	15.34	15.12	-1.43
38.00	28.00	35.00	85.00	12.10	11.61	-4.03
45.00	27.00	50.00	70.00	12.50	12.66	+1.25

Average % difference = 1.21  
Range (+1.40 to -4.03)

From the above testing data set, it is seen that the network gives the maximum error when  $t_f = 38.00$  cm,  $d = 28.00$  cm,  $Z = 35.00$  cm &  $W = 85.00$  cm. For this set of data, the comparative study of effective width is given in Figs. 5.3 to 5.6 by varying a single parameter when other parameters remain constant. The schematic and flow diagram of ANN for calculation of critical perimeter are shown in Figs. 5.7 & 5.8.

The length of critical perimeter ( $b_p$ ) can be evaluated satisfactorily by equation 5.1. In selecting the range of input data emphasis is given to cover the range that is frequently encountered in practical design. The range of input data for various parameters are as follows:

$$t_f = t_w = 200 \text{ to } 500 \text{ mm.}$$

$$d = 150 \text{ to } 300 \text{ mm.}$$

$$Z = 200 \text{ to } 1000 \text{ mm.}$$

$$W = 500 \text{ to } 1000 \text{ mm.}$$

Fig. 5.9 shows the critical perimeter ( $b_p$ ) for a constant ratio of  $d/t_f = 0.3$ . Similarly Figs. 5.10, 5.11, 5.12 and 5.13 show the critical perimeter ( $b_p$ ) for a constant ratio of  $d/t_f = 0.5$ , 0.7, 0.9 and = 0.1.2 respectively. For easy consulting all the curves are presented in non-dimensional form. Following points are observed in calculating critical perimeter:

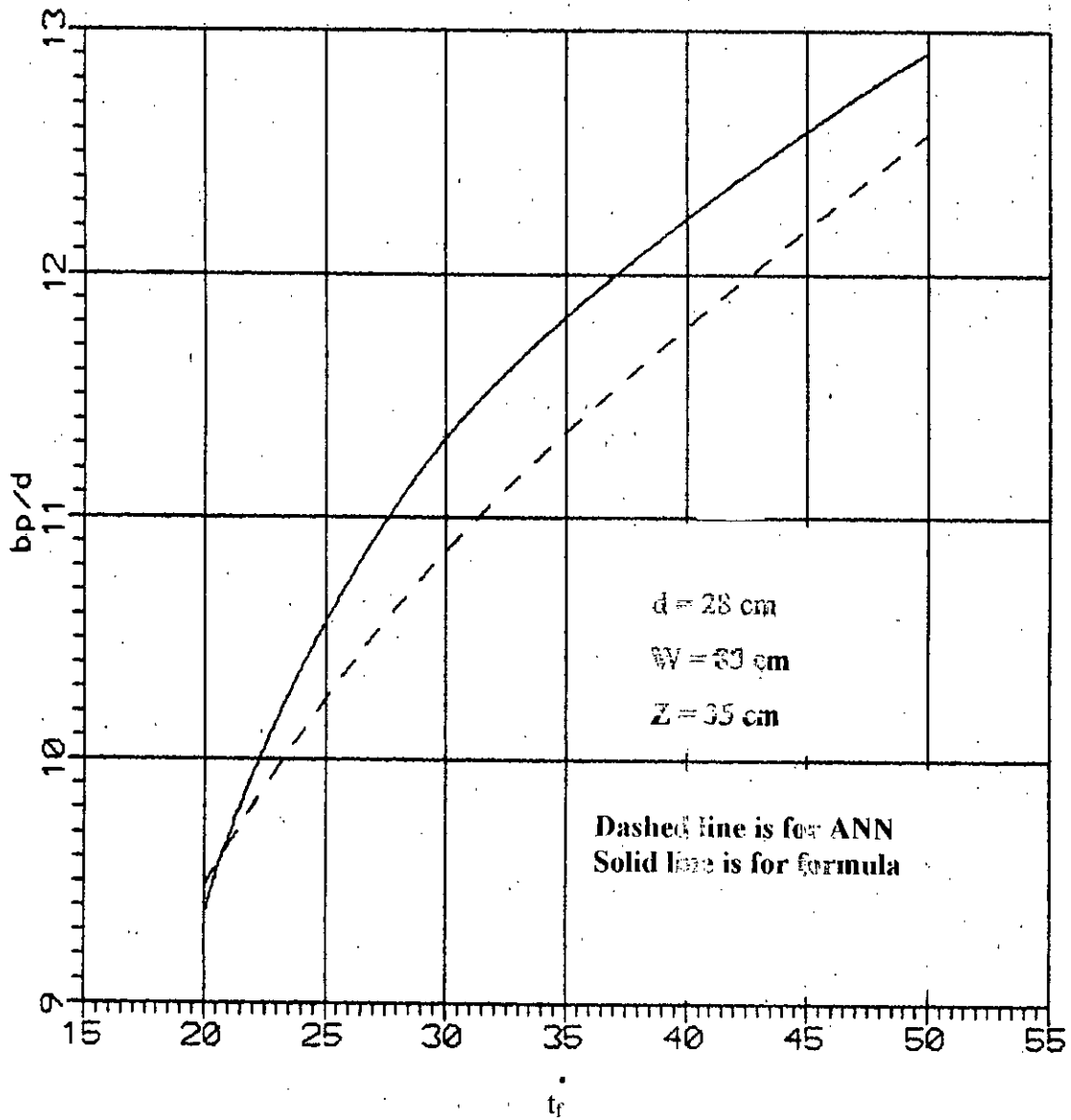


Fig. 5.3 Comparative study of  $b_p/d$  for varying  $t_r$  keeping  $d$ ,  $W$  and  $Z$  constant

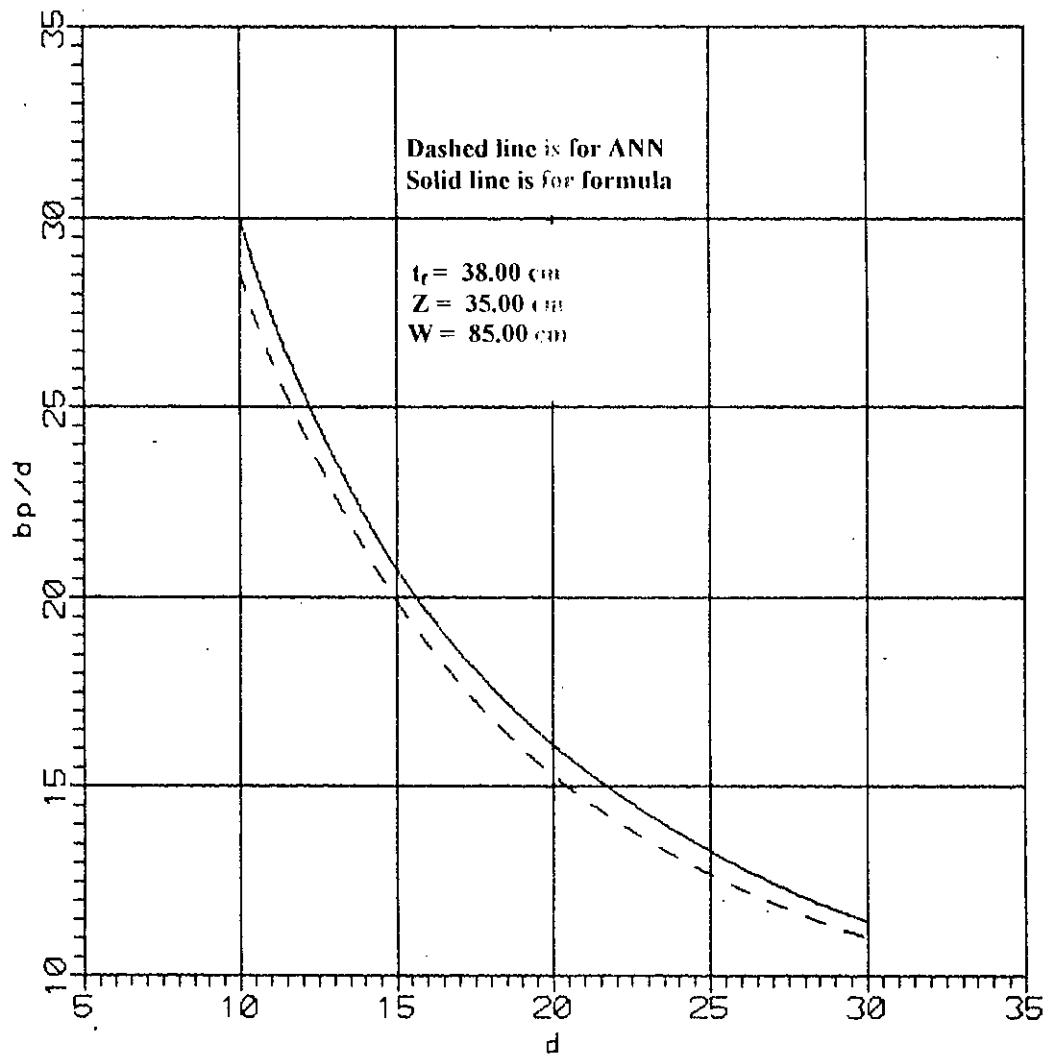


Fig. 5.4 Comparative study of  $b_p/d$  for varying  $d$  keeping  $t_r$ ,  $Z$  and  $W$  constant



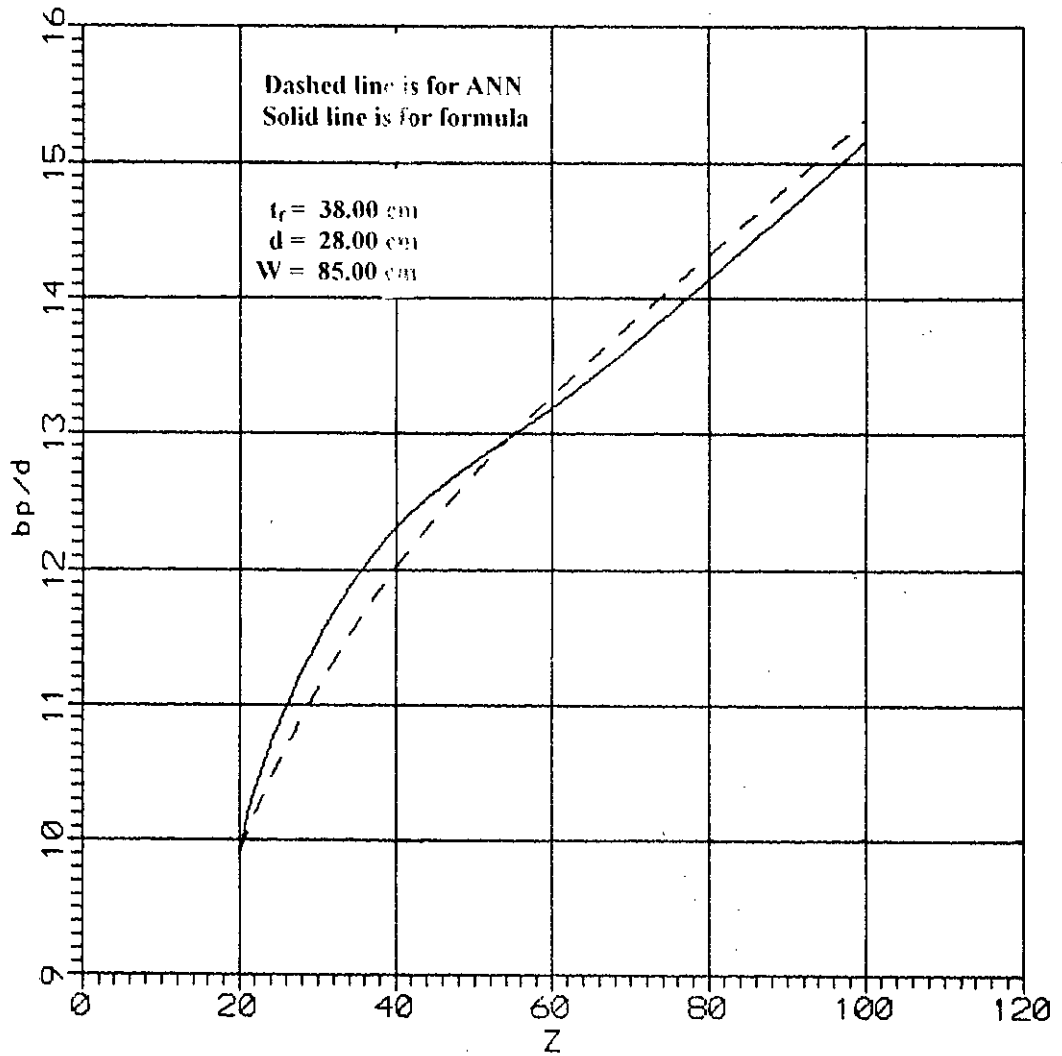


Fig. 5.5 Comparative study of  $b_p/d$  for varying  $Z$  keeping  $d$ ,  $t_r$  and  $W$  constant

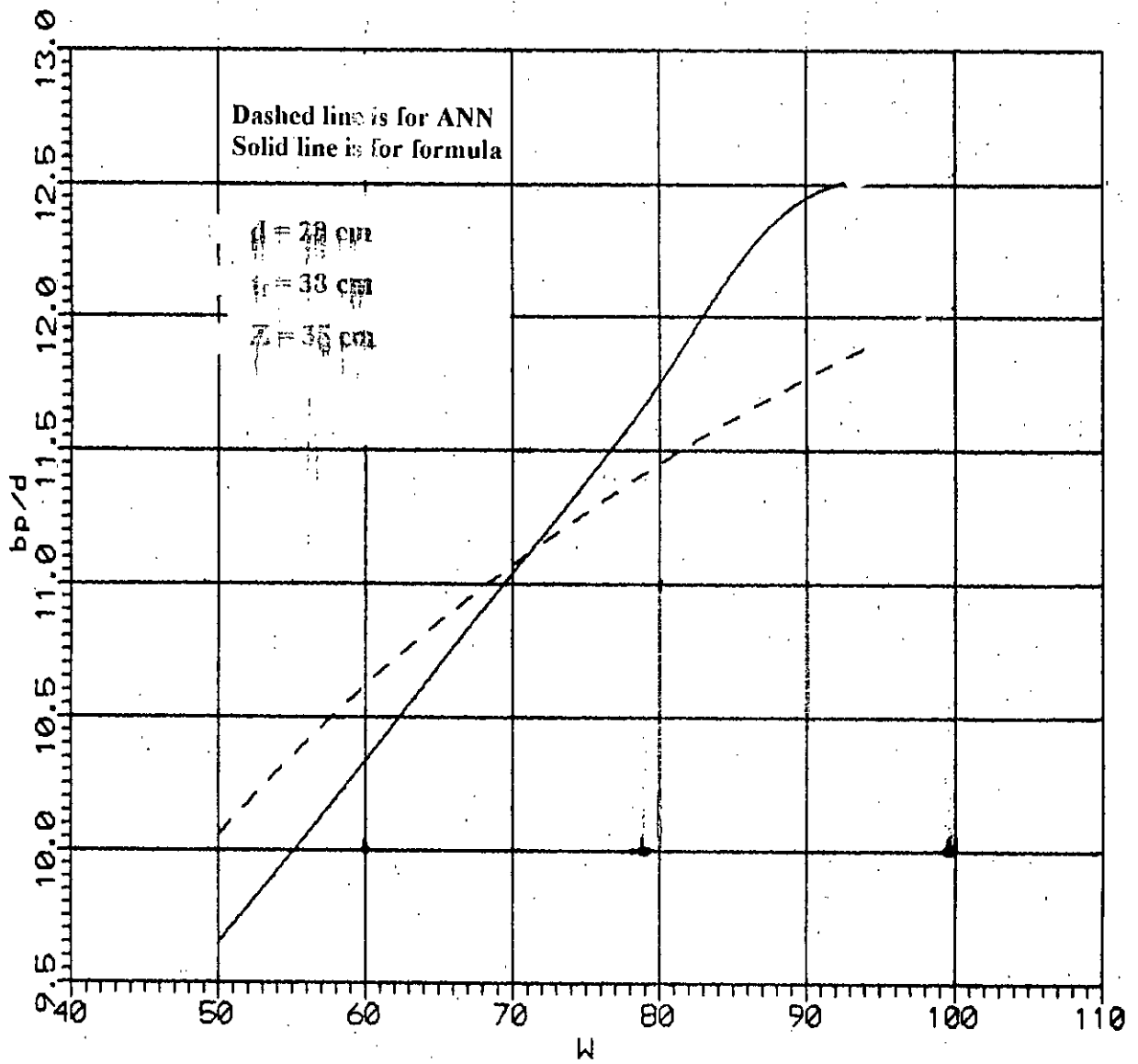


Fig. 5.6 Comparative study of  $b_p/d$  for varying  $W$  keeping  $d$ ,  $t_r$  and  $Z$  constant

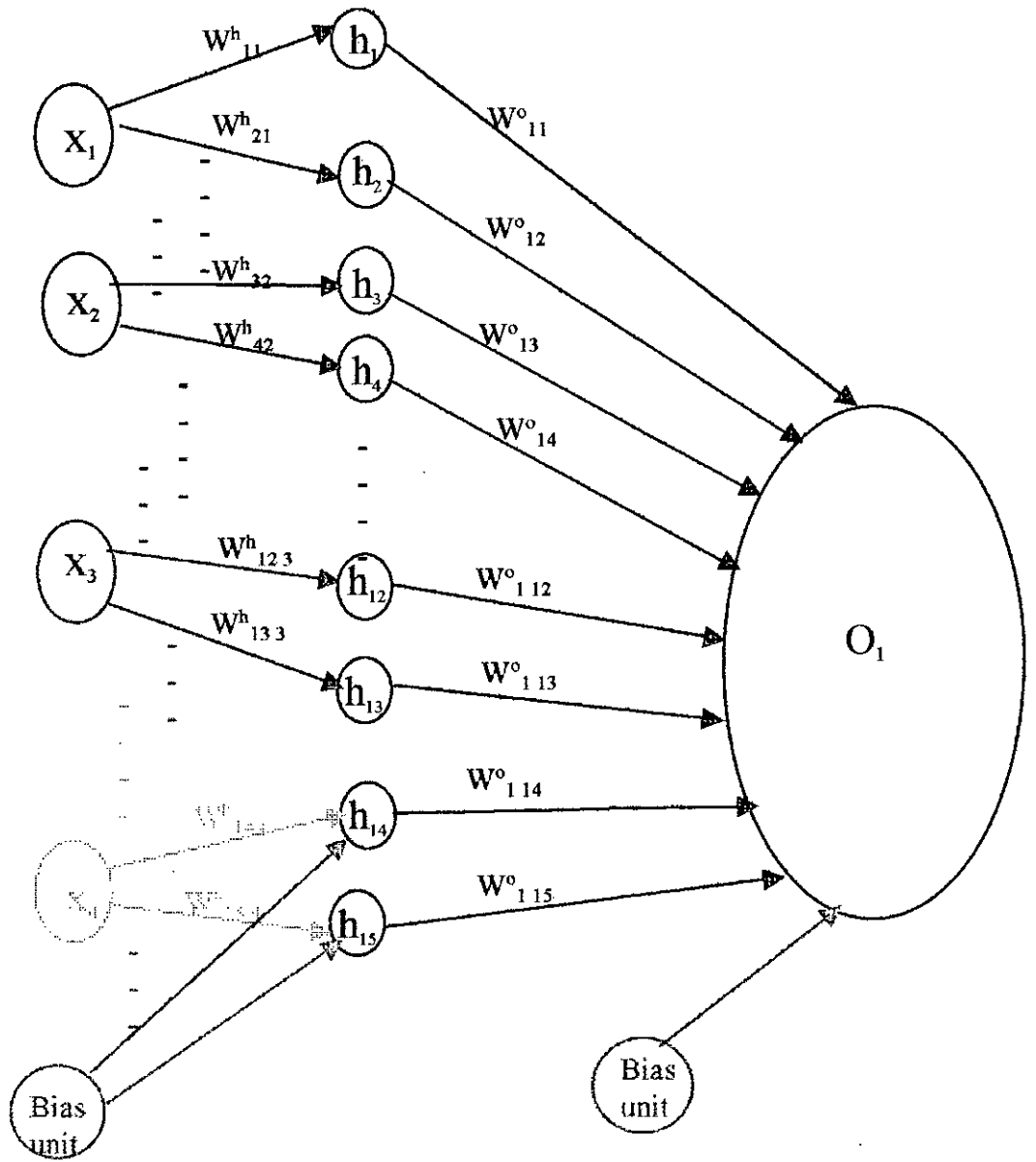


Fig. 5.7 Schematic diagram of ANN for calculation of critical perimeter of shear wall-floor slab connections

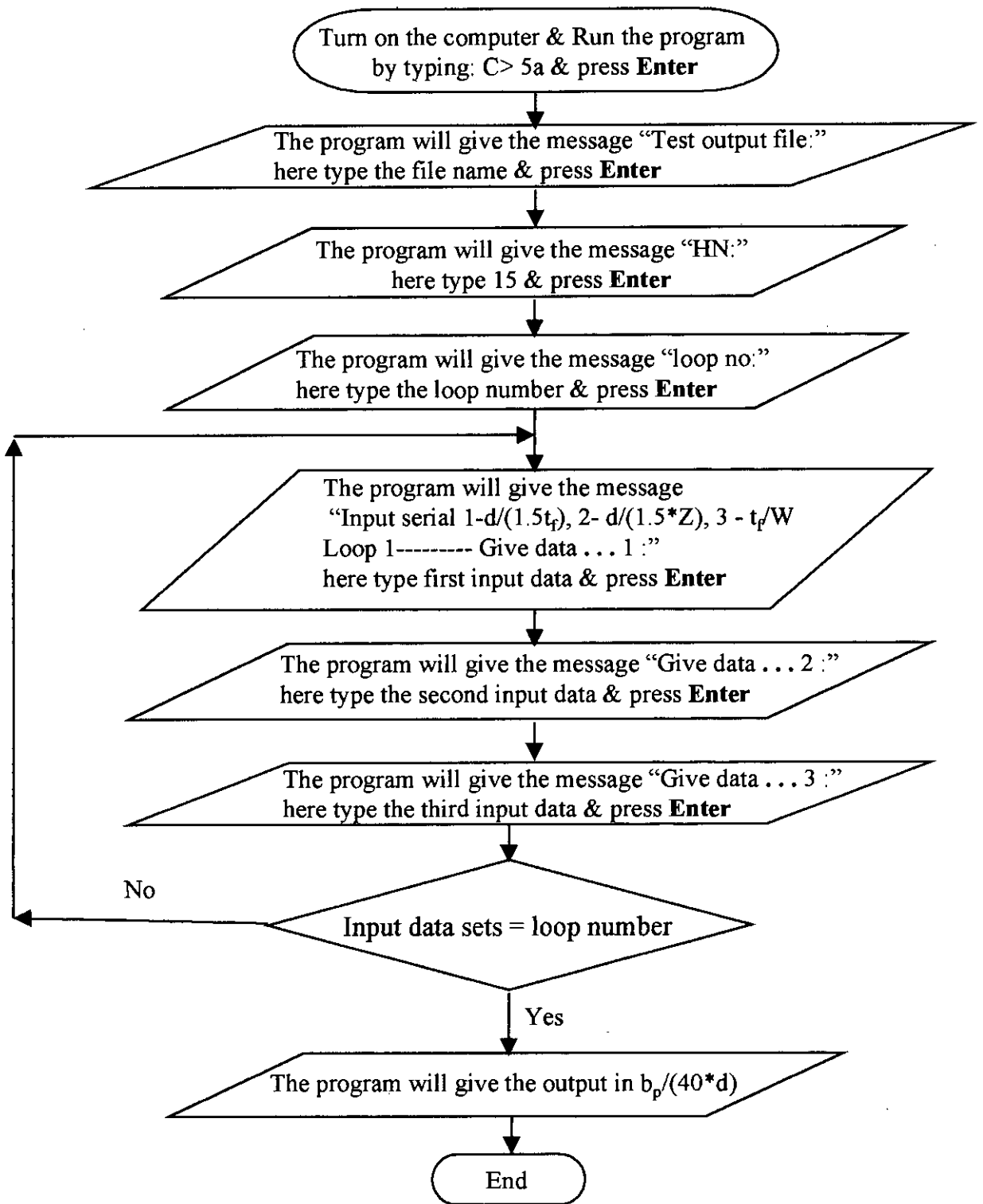


Fig. 5.8 Flow diagram for calculation of critical perimeter of shear wall and edge column-slab connection

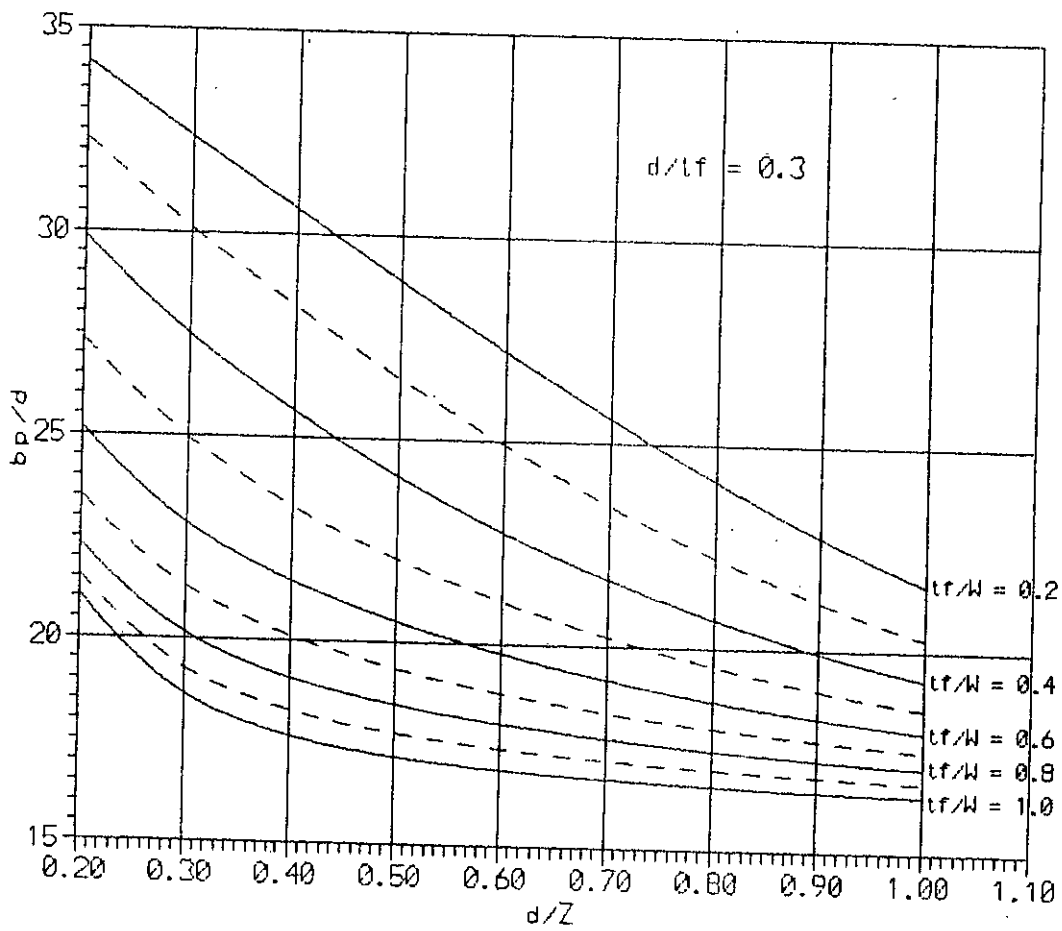
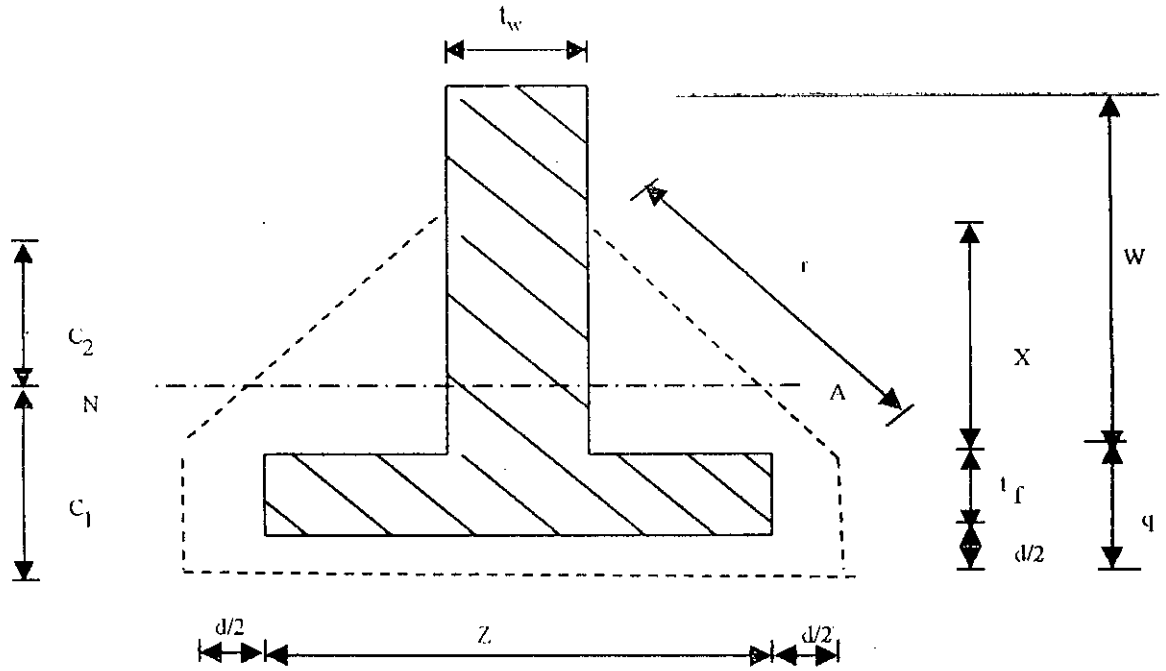


Fig. 5.9  $b_p/d$  as a function of  $d/Z$  and  $t_f/W$  for  $d/t_f = 0.3$

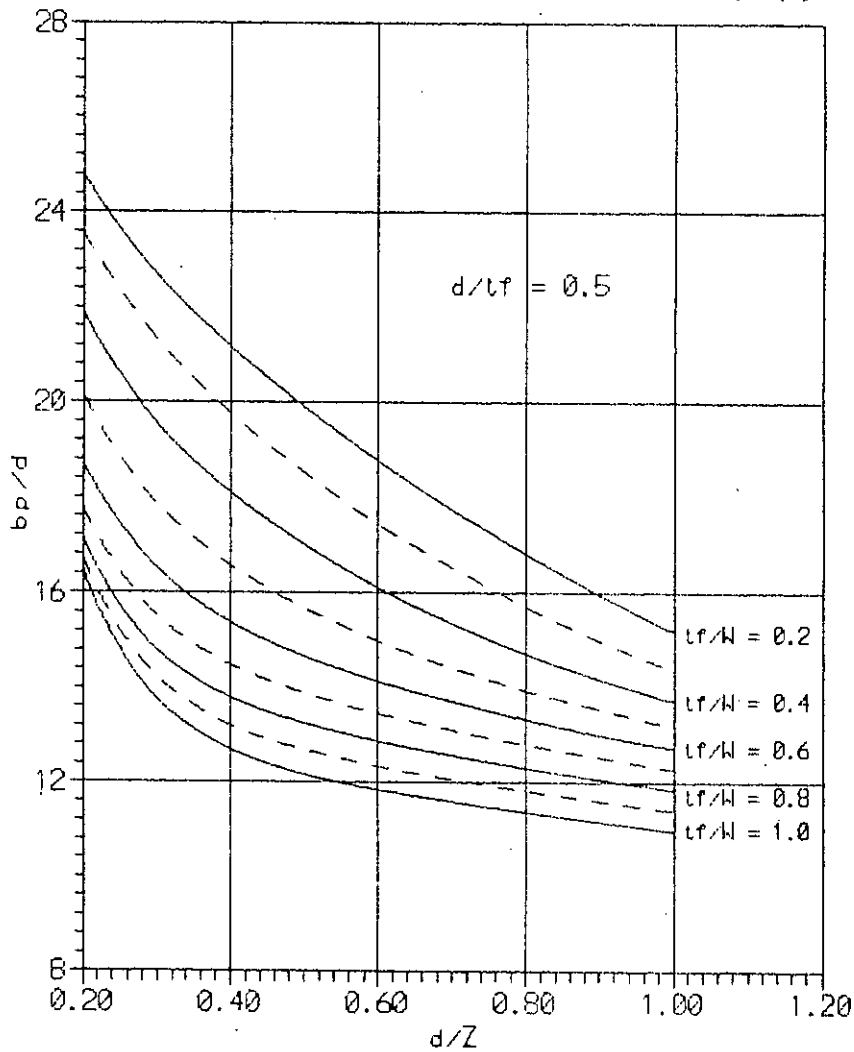
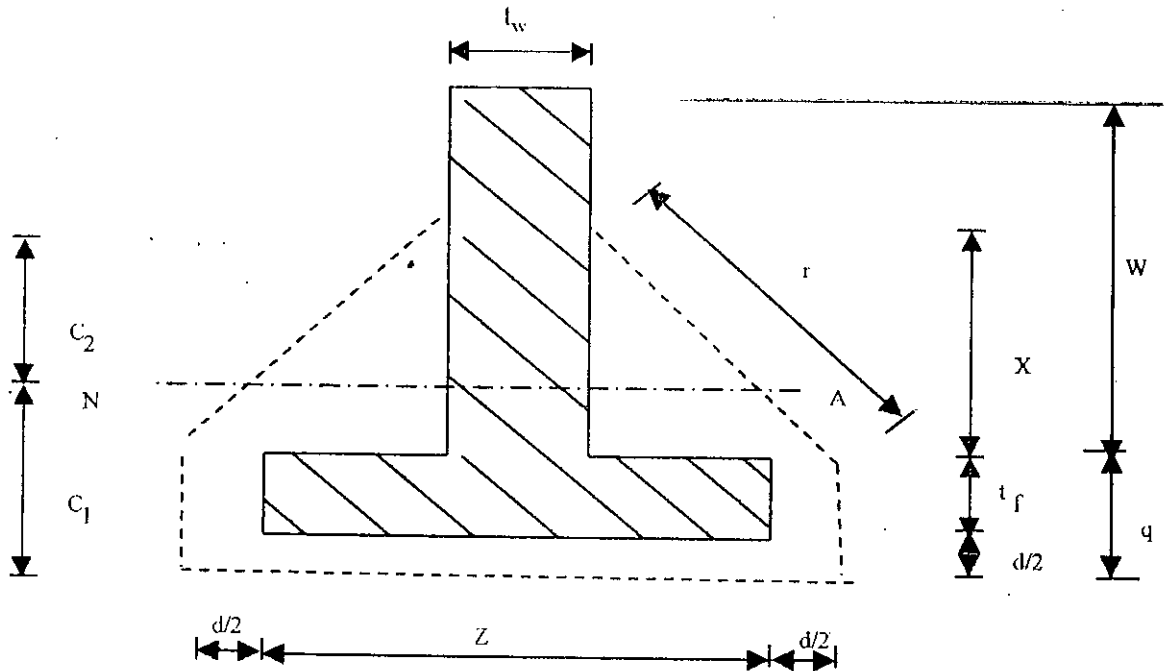


Fig. 5.10  $b_p/d$  as a function of  $d/Z$  and  $t_f/W$  for  $d/t_f = 0.5$

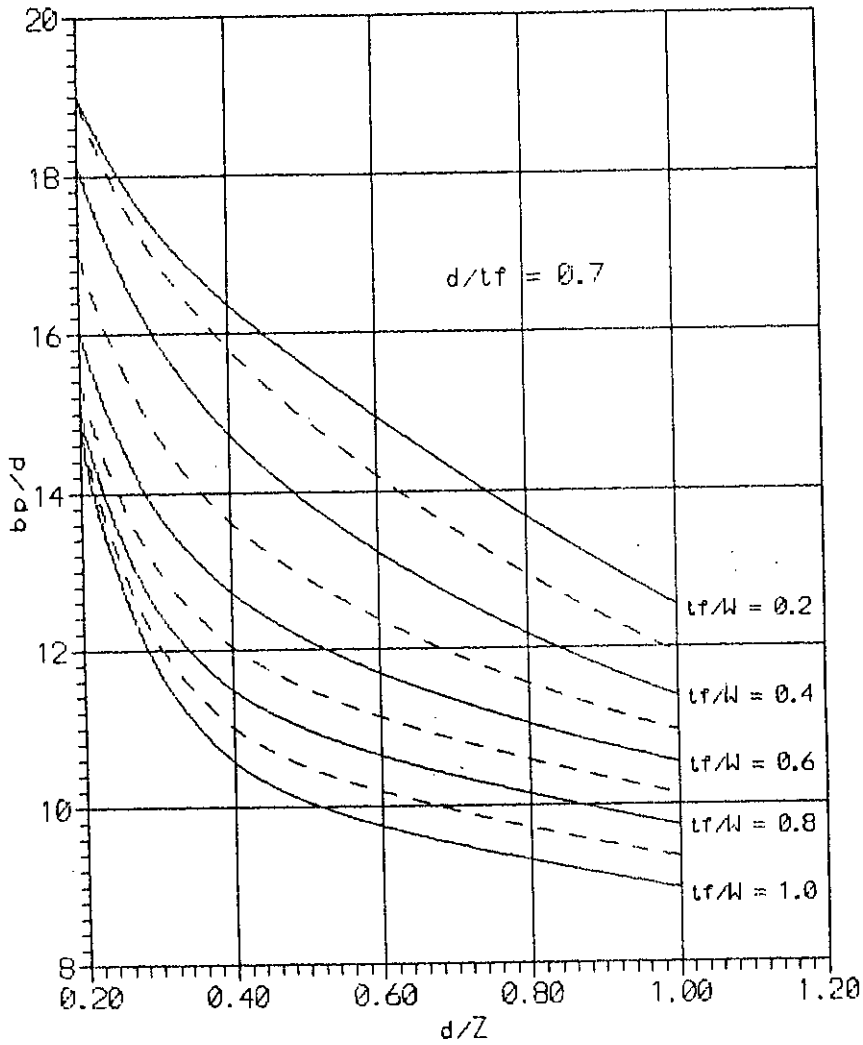
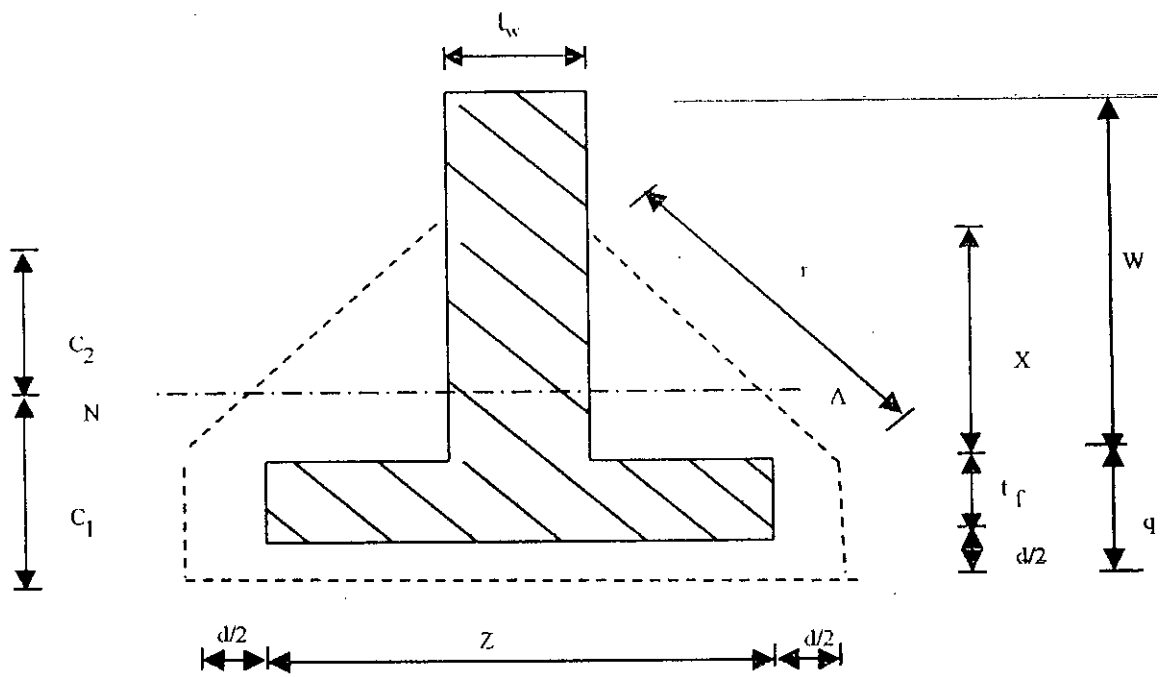


Fig. 5.11  $b_p/d$  as a function of  $d/Z$  and  $t_f/W$  for  $d/t_f = 0.7$

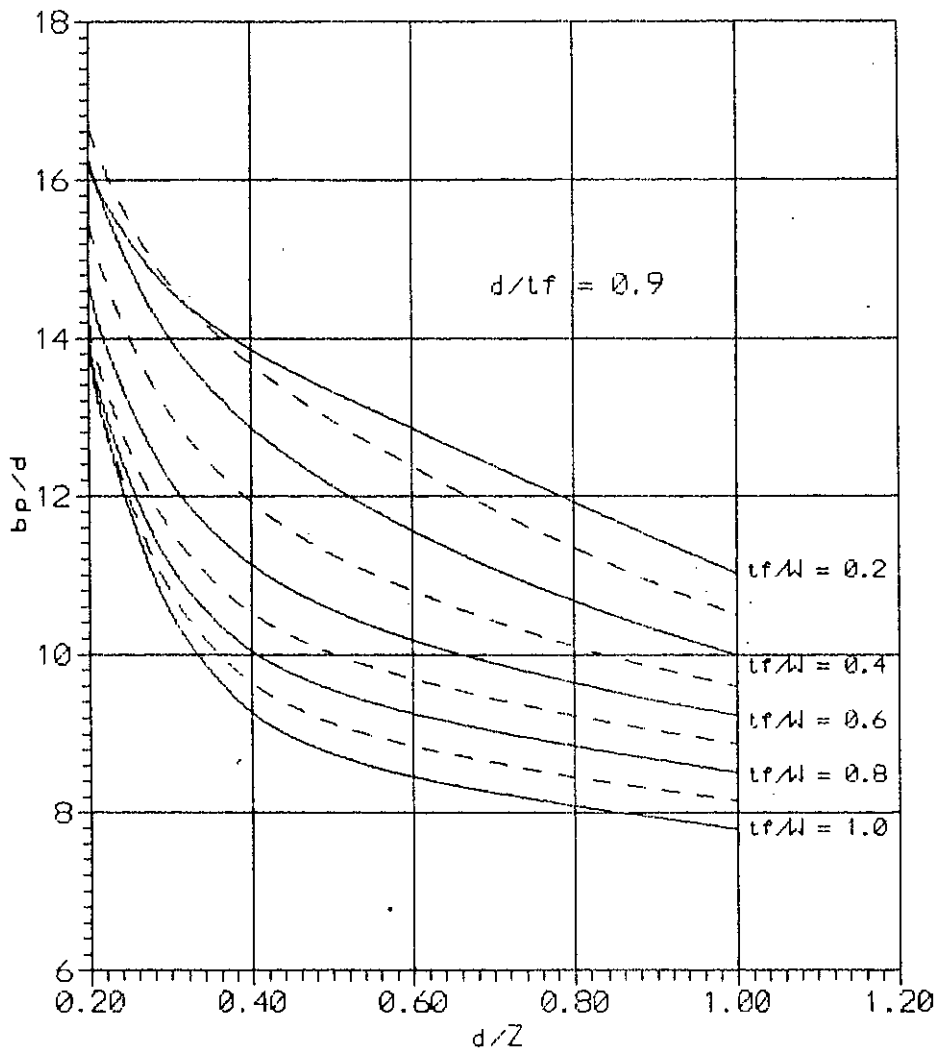
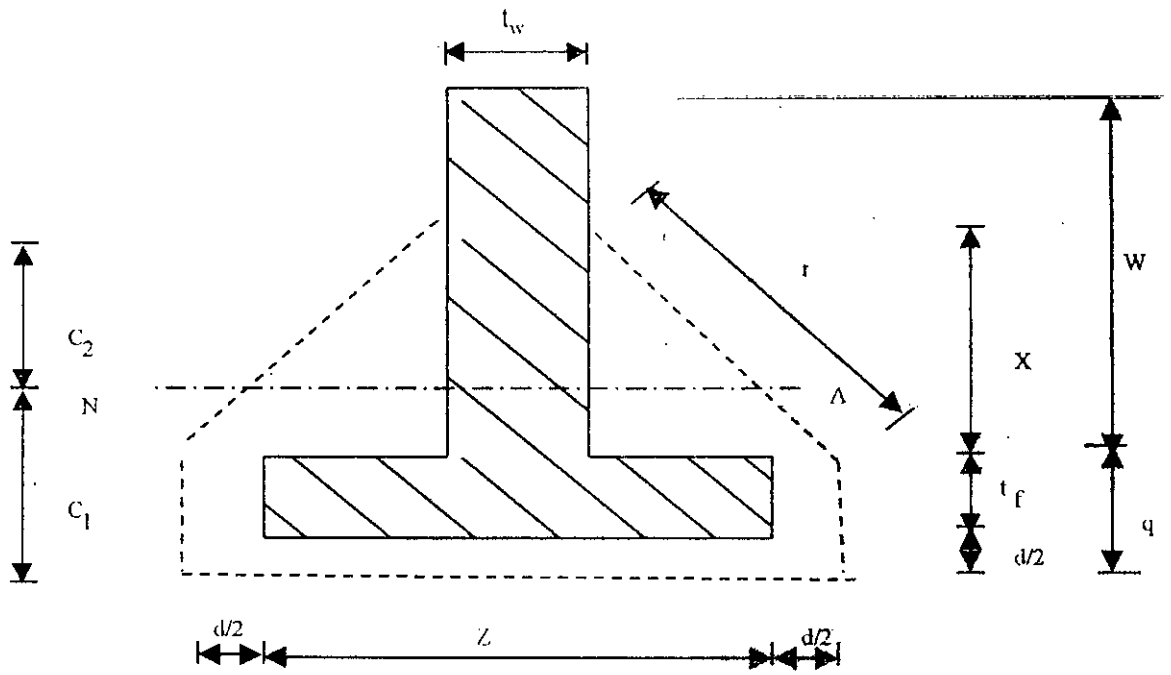


Fig. 5.12  $b_p/d$  as a function of  $d/Z$  and  $t_f/W$  for  $d/t_f = 0.9$



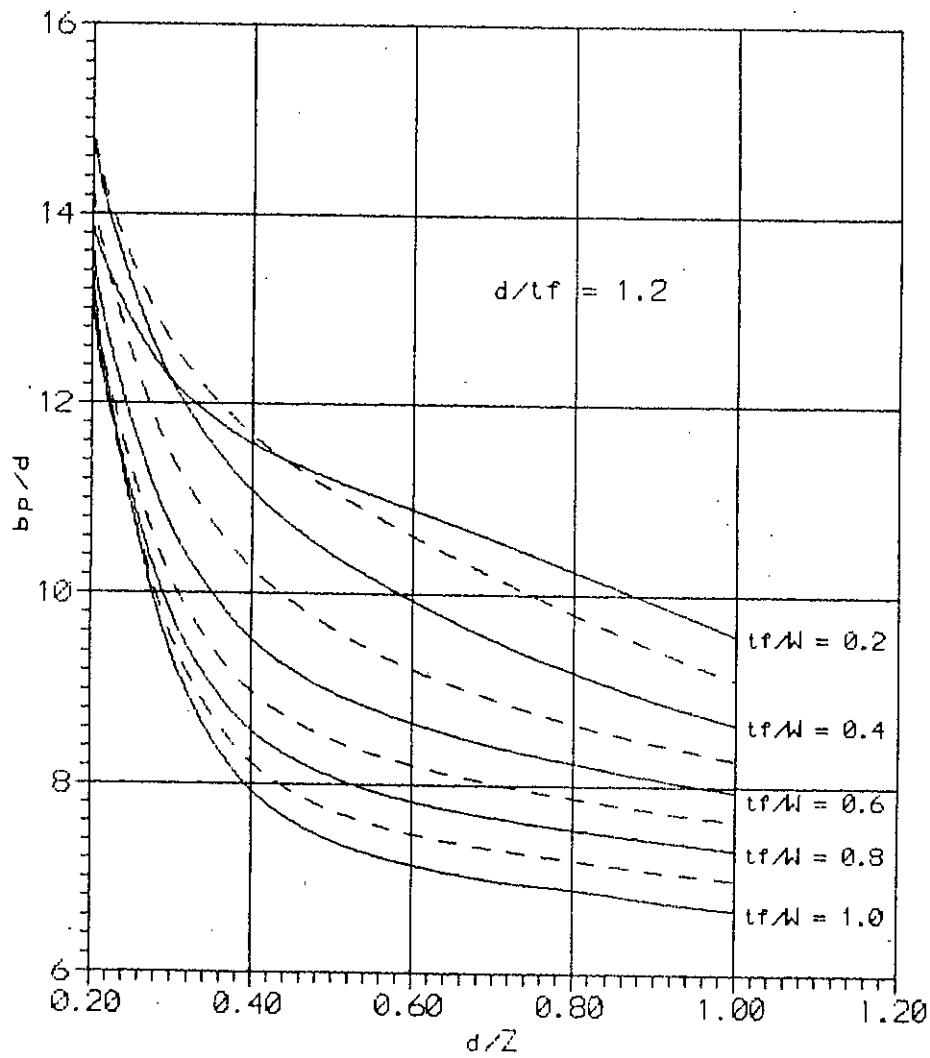
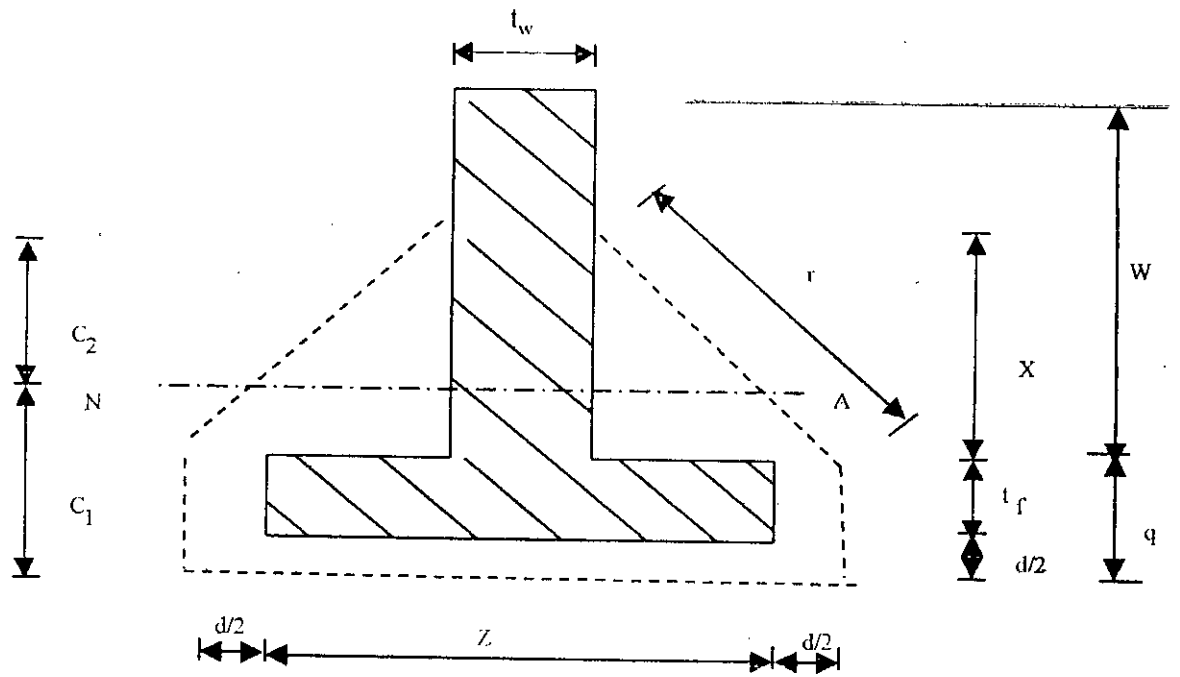


Fig. 5.13  $b_p/d$  as a function of  $d/Z$  and  $t_f/W$  for  $d/t_f = 1.2$

## 5.3.2 Results and Discussions

To produce non-dimensional design curves, different ratios are selected in plotting the curves. The influence of various parameters is discussed based on these ratios.

### 5.3.2.1 Effect of Web Wall and Flange Thickness

In calculating critical perimeter,  $b_p$ , web wall thickness,  $t_w$  and flange wall thickness,  $t_f$  are always taken to be equal. This is also true for maximum practical design problem. Curves are plotted in Figs. 5.9 to 5.13 for various  $d/t_f$  ratios [0.30 to 1.20]. From the curves it is seen that the critical perimeter ratio,  $b_p/d$  is maximum when the ratio  $d/t_f$  is minimum. For a constant effective slab width,  $d$ , the ratio  $d/t_f$  decreases when flange wall thickness increases. That is when web wall thickness or flange wall thickness increases, the critical perimeter ratio,  $b_p/d$  also increases. The critical perimeter ratio,  $b_p/d$  increases by 2.47 times when  $d/t_f$  is decreased by 4.0 times for a constant  $t_f/W$  ratio ( $t_f/W = 0.20$ ).

### 5.3.2.2 Effect of Web Wall Length (W)

Effect of web wall length,  $W$  can be examined when other parameters i.e. flange thickness,  $t_f$  flange width,  $Z$  and slab thickness,  $d$  is constant. When  $W$  is increased, the ratio  $t_f/W$  decreases. From the curves in Figs. 5.9 to 5.13, it is seen that with the increase of the ratio  $t_f/W$ , the critical perimeter ratio,  $b_p/d$  decreases for various values of  $d/Z$  and  $d/t_f$ . The critical perimeter ratio,  $b_p/d$  is maximum when the ratio  $t_f/W$  is minimum. The critical perimeter ratio,  $b_p/d$  increases by 64% when  $t_f/W$  is decreased by 500% [from 1.0 to 0.20] for a constant  $d/t_f$  ratio ( $d/t_f = 0.30$ ). But the critical perimeter ratio,  $b_p/d$  increases only by 9% for the value of  $d/t_f$  equal to 1.20 when  $t_f/W$  is decreased from 1.0 to 0.20.

### 5.3.2.3 Effect of Flange Width (Z)

The influence of flange width,  $Z$  on the critical perimeter ratio,  $b_p/d$  is quite prominent for smaller  $d/Z$  ratio. In examining the effect of flange width, curves are plotted for varying  $d/Z$  ratio.  $d/Z$  is minimum for maximum flange width. Other values remaining constant, the critical perimeter ratio,  $b_p/d$  increases with the increase of flange width,  $Z$ . The rate of increase is maximum/sharp for lower values of  $d/Z$ . The rate of increase is very small for values of  $d/Z$  greater than 0.50.

### 5.3.2.4 Effect of Considering $t_f/W$ instead of $t_f/X$ for Plotting the Graph

From the discussion in 5.3.2.2, it is clear that the increase of the critical perimeter ratio,  $b_p/d$  with the increase of web wall length,  $W$  has also some limitation. In calculation of critical perimeter "X" (distance behind flange up to which the critical section extends) is considered, not the total web wall length,  $W$ . It is because, if  $W$  is too long, web wall length influence in calculation of critical perimeter reduces greatly. But for ease of consulting the graph,  $t_f/W$  has been used for plotting the graphs, since  $X$  can not be found out directly without calculation. For considering  $t_f/W$  instead of  $t_f/X$  for plotting the graphs, in Fig. 5.12, it is seen that line for  $t_f/W = 0.3$  has crossed the line for  $t_f/W = 0.2$ . In Fig. 5.13 the crossing of lines is more than that of Fig. 5.12. This situation would not have arisen if  $t_f/X$  could also be considered for preparing the graphs. Table 5.3 shows the effect of this in calculating critical perimeter by using the graphs.

**Table 5.3** Effect of considering  $t_f/W$  instead of  $t_f/X$  for plotting the graph.

d (cm)	$t_f = t_w$ (cm)	Z (cm)	W (cm)	b <sub>p</sub> /d Calculated by		% difference
				formula	graph	
20.00	22.22	100.00	111.11	16.17	16.15	-0.12
20.00	22.22	100.00	74.04	16.17	16.65	+2.96
15.00	12.50	75.00	62.50	14.39	13.89	-3.47
15.00	12.50	75.00	41.67	14.39	14.81	+2.92
15.00	12.50	75.00	31.25	14.39	14.82	+2.99
15.00	12.50	75.00	25.00	14.39	14.28	-0.76

From the table it is seen that maximum percentage difference is 3.47 which is acceptable. So it is concluded that use of graph is quite logical for calculating critical perimeter, more so it is to be remembered that safety factor is not considered here.

### **5.3.2.5 Comparison Between ANN, ACI and British Code**

The value of critical perimeter obtained from design curves (ANN), ACI Code and British Code are compared in table 5.4. In BS 8110, the critical section is defined as being at a distance equal to  $1.5d$ , where  $d$  is the effective depth of the slab, in ACI 318-83, the critical perimeter is located at a distance  $d/2$  from the column faces. For ANN, it is considered that the critical perimeter is located at a distance  $d/2$  from the column faces. Due to this reason the value of critical perimeter obtained from design curves (ANN), ACI Code and British Code varies too much from one another.

## **5.4 Calculation of Punching Shear Strength of Shear Wall-Floor Slab Connections**

### **5.4.1 General**

So far research work on theory of punching for slab-wall connections is very limited. The design curves given in Figs. 5.20 to 5.24 are based on empirical formulas proposed by Bari M. S. in his Ph.D. thesis [6]. Code recommendations on the calculation of punching shear strength of slab-column connections differ in regard to the distance from the column faces to the critical perimeter, and in the expression used to define the limiting value of the shearing stress.

When the perimeter is drawn close to the column the corresponding stresses are very high. If the perimeter is moved outward, the stresses reduce. In BS 8110, the critical section is defined as being at a distance equal to  $1.5d$ , where  $d$  is the effective depth of the slab, in ACI 318-83, the critical perimeter is located at a distance  $d/2$  from the column faces.

**Table 5.4** Values of  $b_p$  calculated by formula (Eqn. 5.1), ACI and British Code

$t_f$ (mm)	$d$ (mm)	$Z$ (mm)	$W$ (mm)	$L$ (mm)	$b_p$ (in mm) calculated by		
					formula	ACI Code	British Code
200.00	125.00	200.00	600.00	2000.00	1862.76	2050.00	2550.00
200.00	125.00	200.00	700.00	2000.00	1862.76	2250.00	2750.00
200.00	125.00	200.00	800.00	2000.00	1862.76	2450.00	2950.00
200.00	125.00	200.00	900.00	2000.00	1862.76	2650.00	3150.00
200.00	125.00	200.00	1000.00	2000.00	1862.76	2850.00	3350.00
200.00	175.00	200.00	600.00	2000.00	1970.14	2150.00	2850.00
200.00	175.00	200.00	700.00	2000.00	1970.14	2350.00	3050.00
200.00	175.00	200.00	800.00	2000.00	1970.14	2550.00	3250.00
200.00	175.00	200.00	900.00	2000.00	1970.14	2750.00	3450.00
200.00	175.00	200.00	1000.00	2000.00	1970.14	2950.00	3650.00
200.00	175.00	200.00	600.00	3000.00	1970.14	2150.00	2850.00
200.00	175.00	200.00	700.00	3000.00	1970.14	2350.00	3050.00
200.00	175.00	200.00	800.00	3000.00	1970.14	2550.00	3250.00
200.00	175.00	200.00	900.00	3000.00	1970.14	2750.00	3450.00
200.00	175.00	200.00	1000.00	3000.00	1970.14	2950.00	3650.00
200.00	175.00	200.00	600.00	4000.00	1970.14	2150.00	2850.00
200.00	175.00	200.00	700.00	4000.00	1970.14	2350.00	3050.00
200.00	175.00	200.00	800.00	4000.00	1970.14	2550.00	3250.00
200.00	175.00	200.00	900.00	4000.00	1970.14	2750.00	3450.00
200.00	175.00	200.00	1000.00	4000.00	1970.14	2950.00	3650.00

The proposed method [6] is, in fact, based on the shear criteria of failure in which punching is assumed to occur when the shear stress around a critical perimeter reaches a limiting value. The shear capacity is estimated from the product of three terms – a critical area term, a critical shear stress term and a moment transfer reduction factor.

### 5.4.2 Calculation of Shear Strength

A typical shape of the critical section is shown in Fig. 5.2. The thickness of the wall is assumed as flange width for the models with plane walls. The properties of this section are :

$$p = Z + d$$

$$Z = \text{flange width for models with T-section shear walls}$$

$$= \text{equal to wall thickness for plane shear walls}$$

$$d = \text{effective depth of tension reinforcement}$$

$$q = t_f + d/2$$

$$t_f = \text{flange thickness}$$

$$r = \text{length of inclined portion of the section}$$

$$x = \text{distance behind flange up to which the critical section extends}$$

$$t_w = \text{web thickness}$$

$$x/Z = 4.0 e^{-0.465(Z/t_w)}$$

$$r^2 = x^2 + 0.25(p - t_w)^2$$

$$C_1 = \{ q^2 + r(x + 2q) \} / [ p + 2(q + r) ] \quad (5.4)$$

$$C_2 = q + x - C_1$$

Where  $C_1, C_2$  determine the location of neutral axis

$$b_p = \text{length of critical perimeter}$$

$$= p + 2(r + q) \quad (5.5)$$

$$A_{cp} = \text{area of critical perimeter}$$

$$= d \cdot b_p$$

$$J = \text{similar to polar moment of inertia}$$

$$= d C_1 [ p C_1 + q(C_1 - q/3) + \frac{3xrq(c_1 - q)(c_1 - 2q/3) + 2r^2(c_1 - q)^3 + c_2^3}{3x(xq + r(c_1 - q))} ] \quad (5.6)$$

The shear stress value for critical section in Fig. 5.2 is

$$v_c = 0.17 (1 + 2/R_f)(f_c')^{1/3}$$

where rectangularity factor,  $R_f = (x + q) \geq 2.0$

To incorporate the effect of flexural reinforcement, it is assumed that an increase of every 0.5% in the ratio of flexural steel in the slab above 0.8%, the calculated value of  $v_c$  should be increased by  $0.05 \text{ N/mm}^2$ . Thus

$$v_c = 0.17 (1 + 2/R_f)(f_c')^{1/3} + 0.1 (100A_s/bd - 0.8) \quad (5.7)$$

where value of  $(100A_s/bd)$  are calculated for width  $(Z + 3d)$  and  $0.8 \leq (100A_s/bd) \leq 2.0$

For the second part of Eqn. 5.7, a constant value of 0.12 is taken during calculation of input data assuming value of  $100A_s/bd = 2.0$ . Two approaches are usually adopted for punching shear capacity of slab column connections transferring shear and unbalanced bending moment. The first approach calculates the increase in shear stress caused by moment transfer (e.g. ACI) and then compares it with the permissible shear value. The second approach calculates the punching capacity for no moment transfer and then applies a reduction factor (e.g. BS 8110). The first approach is followed in this study. The net shear stress is around the slab-wall junction is given by:

$$v_c = V_d/A_{cp} + (K.M.C_1)/j$$

Where 
$$K = 1 - \frac{1}{1 + \frac{1}{2}\sqrt{R_f}} \quad (5.8)$$

and  $R_f = (x + q)/p$

For the present study  $M = 0.5(V_c.L)$ . Therefore,

$$V_c = V_{\text{without shear steel}} = \frac{v_c \cdot A_{cp}}{1 + \frac{K.L}{2} \cdot \frac{A_{cp}}{(J/C_1)}} \quad (5.9)$$

Based on experimental observation, Bari M. S. proposed [6] that an increase in ultimate strength can be obtained by the use of properly designed shear reinforcement in the slab. In addition, the failure mode can be changed from brittle to ductile mode, using shear reinforcement in the slab. The punching shear strength,  $V_c$  i.e.  $V_{\text{without shear steel}}$ , can be increased by 50% by the provision of closed vertical stirrup as required in the slab. So, the punching shear strength of the shear wall-floor slab connections with shear reinforcement in the slab can be calculated from:

$$V = 1.5 * V_{\text{without shear steel}} \quad (5.10)$$

### 5.4.3 Development of the Net and Design Curves

Different values of momentum factor, learning rate and neurones were chosen to train the network having single hidden layer. The training history at different values of momentum factor, learning rate and neurones is shown in table 5.5. Detail of the output response of finally accepted parameters for the network for a set of data having known output is shown in table 5.6. From the above testing data set, it is seen that the network gives the maximum error when  $t_f = 21.00$  cm,  $d = 10.00$  cm,  $Z = 54.00$  cm &  $W = 45.00$  cm. For this set of data, the comparative study of effective width is given in Figs. 5.14 to 5.17 by varying a single parameter when other parameters remain constant. The schematic and flow diagram of ANN for calculation of punching shear strength are shown in Figs. 5.18 & 5.19.

The numerical results as evaluated by the Eqn. 5.9 have been used as input data for ANN (Appendix D). Network weights and bias are also given in appendix D. In selecting the range of input data emphasis is given to cover the range that is frequently encountered in practical design. Point to note that  $Z$  is always more or equal to  $t_f$ . During calculation of the input data the range of various parameters are as follows:



$t_f = 150$  to  $400$  mm.

$d = 100$  to  $250$  mm.

$Z = 200$  to  $1000$  mm.

$W = 400$  to  $1000$  mm.

$L = 2000$  mm.

$f'_c = 15$  N/mm<sup>2</sup>

**Table 5.5** Percentage difference between  $V_d/V_o$  calculated by formula (Eqn. 5.9) and ANN.

Sl No	Learning rate	Momentum factor	Hidden neurones	No of iteration	Average % difference
1.	0.003	0.10	10	20000	5.15 (-9.59 to +1.37)
2.	0.005	0.10	10	20000	3.62 (-8.92 to +8.96)
3.	0.009	0.10	10	20000	3.77 (-8.87 to +9.19)
4.	0.005	0.10	8	20000	3.61 (-9.02 to +8.79)
5.	0.005	0.10	12	20000	3.54 (-8.82 to +8.69)
5.	0.005	0.10	12	20000	3.54 (-8.82 to +8.69)
6.	0.005	0.10	15	20000	3.65 (-9.44 to +8.71)
7.	0.005	0.15	12	50000	3.57 (-8.80 to +8.75)
8.	0.005	0.08	12	20000	3.53 (-8.85 to +8.64)
9.	0.005	0.10	12	125000	3.36 (-7.85 to +8.10)
10.	0.005	0.10	12	150000	3.47 (-7.05 to +8.75)

**Table 5.6** Percentage difference between  $V/V_0$  calculated by formula (Eqn. 5.9) and ANN (ANN after 125000 iterations having 12 hidden units, learning rate = 0.005 and momentum factor = 0.10)

$t_r$ (mm)	d (mm)	Z (mm)	W (mm)	L (mm)	$f_c'$ (N/mm <sup>2</sup> )	12*( $V/V_0$ ) Calculated by		% diffe- rence
						Formula	ANN	
160	190	500	900	2000	15	0.4771	0.4707	-1.34
210	100	540	850	2000	15	0.5070	0.4951	-2.35
210	180	300	850	2000	15	0.4801	0.4424	-7.85
160	190	500	700	2000	15	0.4771	0.4744	-0.57
375	140	375	700	2000	15	0.4998	0.5181	+3.66
210	180	300	650	2000	15	0.4801	0.4455	-7.21
210	100	540	650	2000	15	0.5062	0.4974	-1.74
375	190	375	600	2000	15	0.5284	0.5232	-0.98
375	110	375	500	2000	15	0.4838	0.5190	+7.28
375	190	375	500	2000	15	0.5086	0.5259	+3.40
160	190	500	500	2000	15	0.4771	0.4809	+0.80
210	100	540	450	2000	15	0.4640	0.5016	+8.10
210	180	300	450	2000	15	0.4420	0.4512	+2.08
200	220	230	410	2000	15	0.4290	0.4369	+1.84
170	240	240	430	2000	15	0.4357	0.4267	-2.07
160	200	210	490	2000	15	0.4173	0.4099	-1.77
330	240	400	400	2000	15	0.5045	0.5286	+4.78
170	200	200	400	2000	15	0.4035	0.4165	+3.22
200	175	400	550	2000	15	0.4805	0.4671	-2.79

Average % difference = 3.36  
(+8.10 to -7.85)

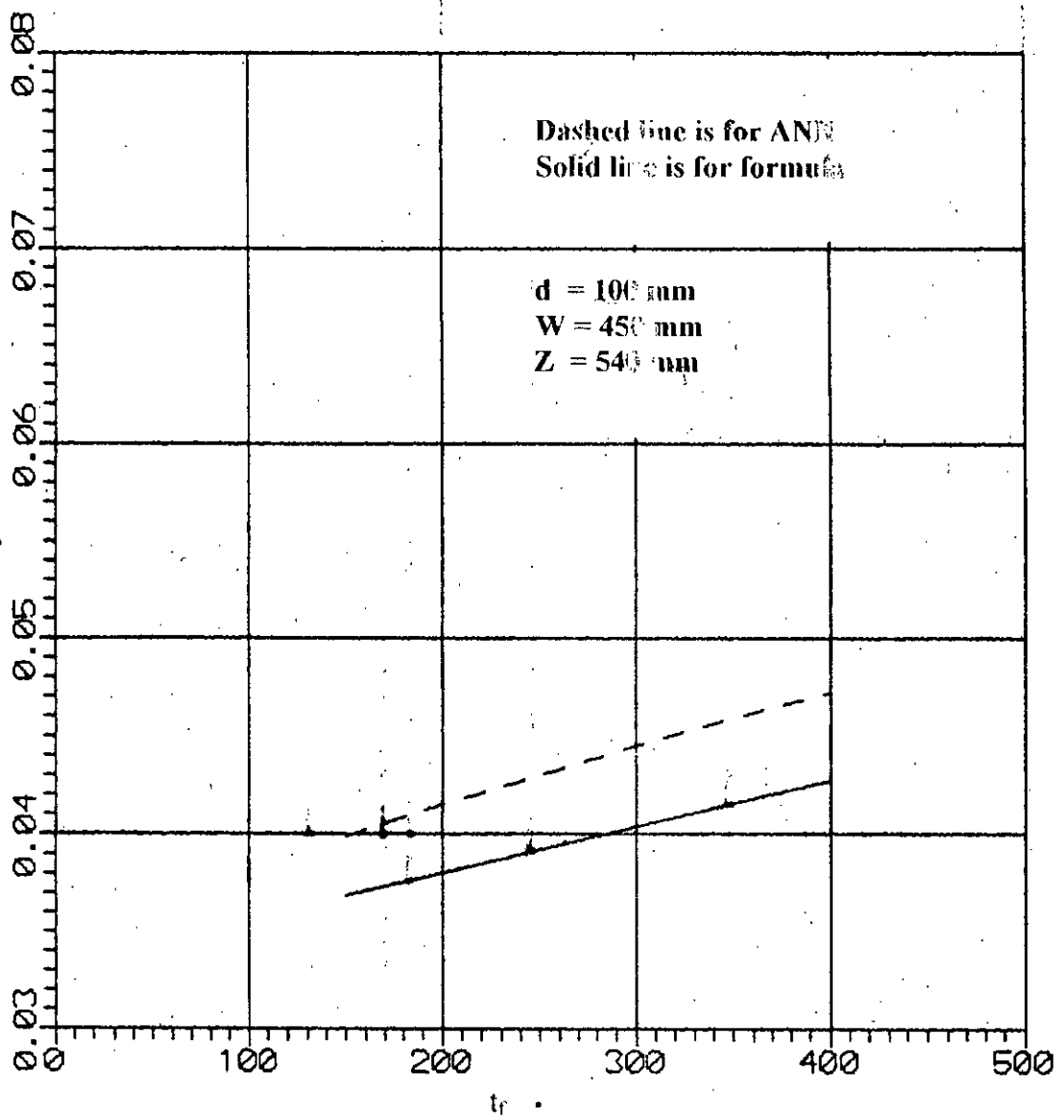


Fig. 5.14 Comparative study of  $V_c/V_o$  for varying  $t_r$  keeping  $d$ ,  $W$  and  $Z$  constant

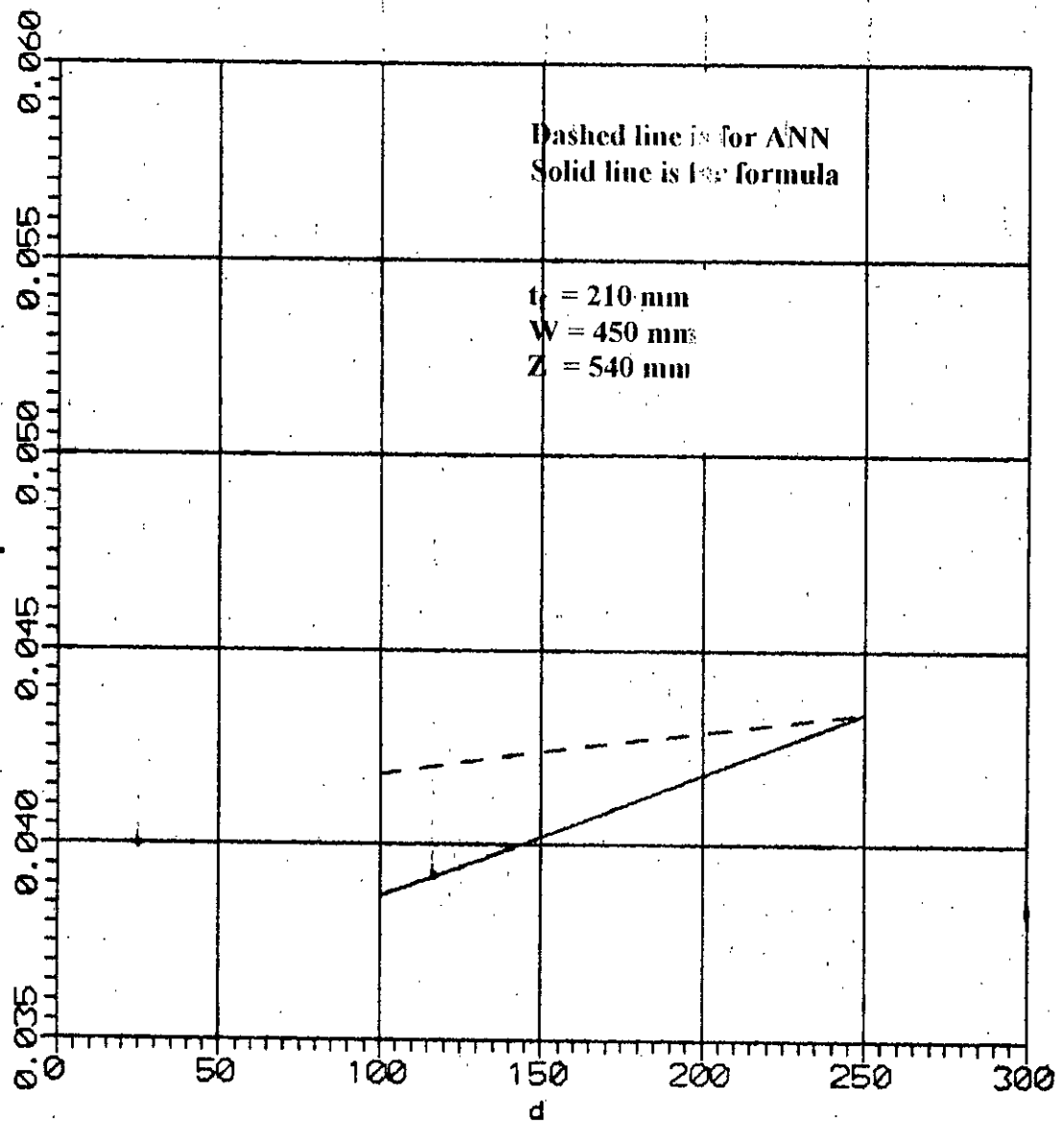


Fig. 5.15 Comparative study of  $V_c/V_o$  for varying  $d$  keeping  $t_s$ ,  $W$  and  $Z$  constant

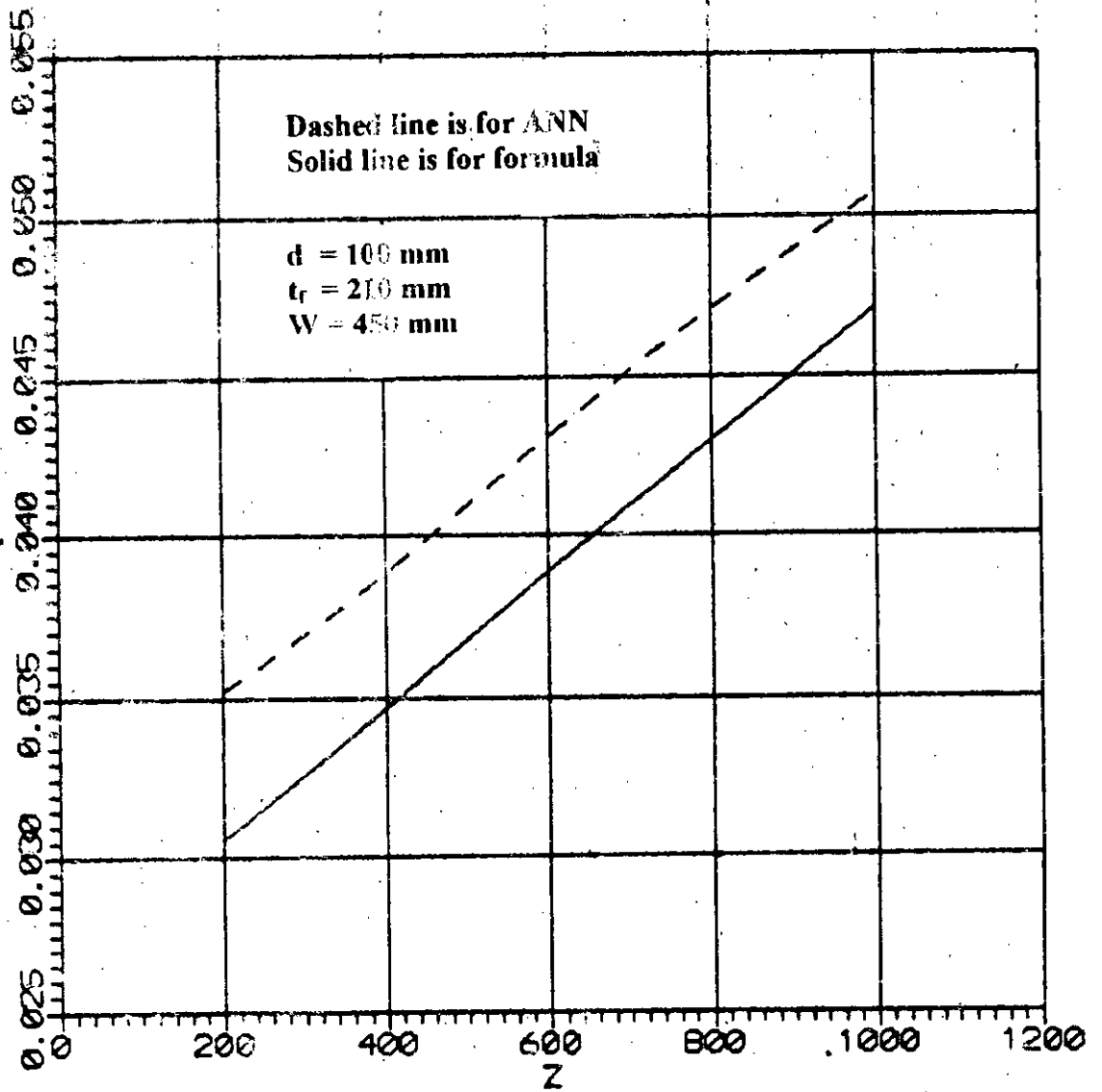


Fig. 5.16 Comparative study of  $V_c/V_o$  for varying  $Z$  keeping  $d$ ,  $t_r$ , and  $W$  constant

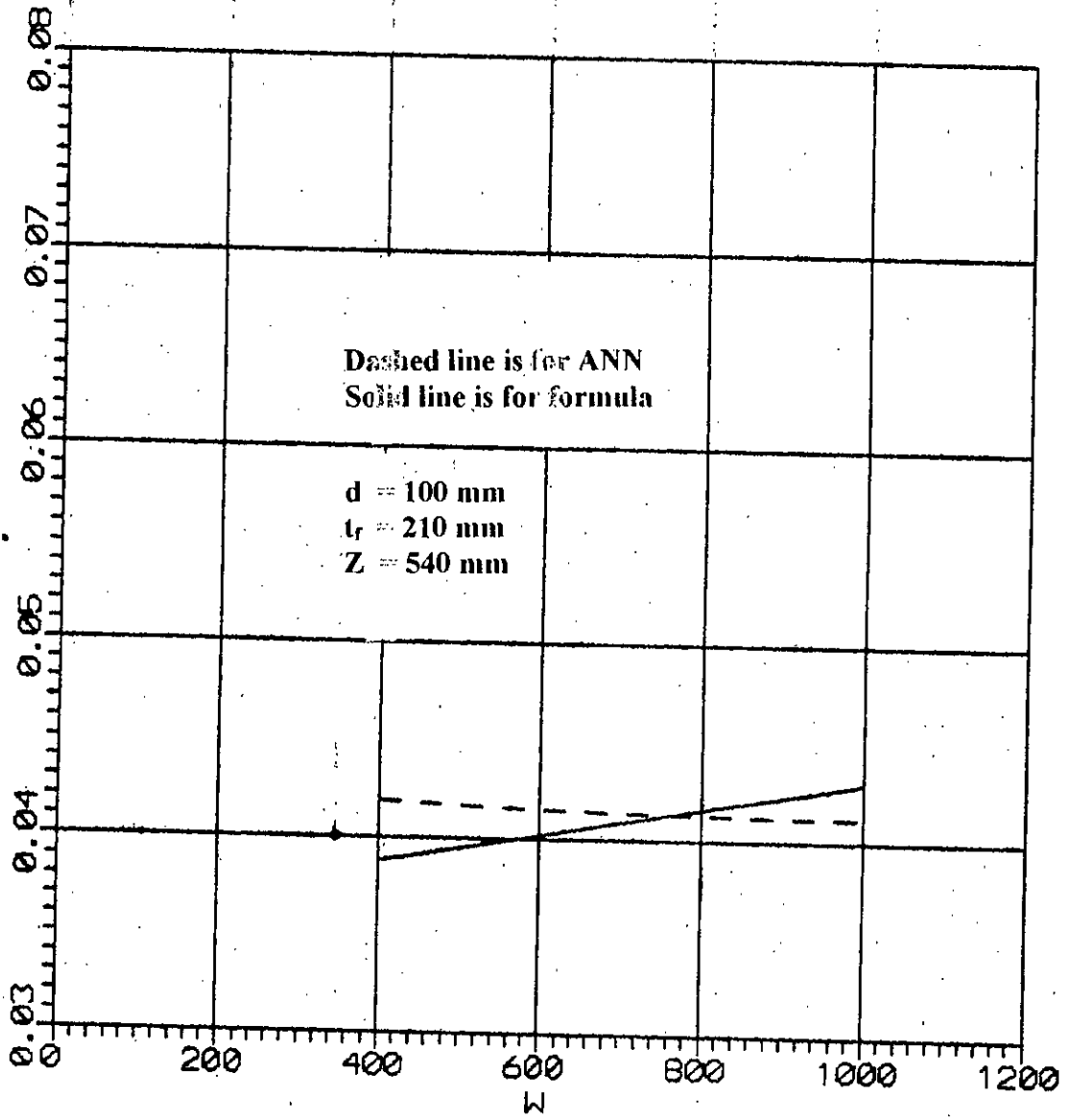


Fig. 5.17 Comparative study of  $V_c/V_o$  for varying  $W$  keeping  $d$ ,  $t_f$ , and  $Z$  constant

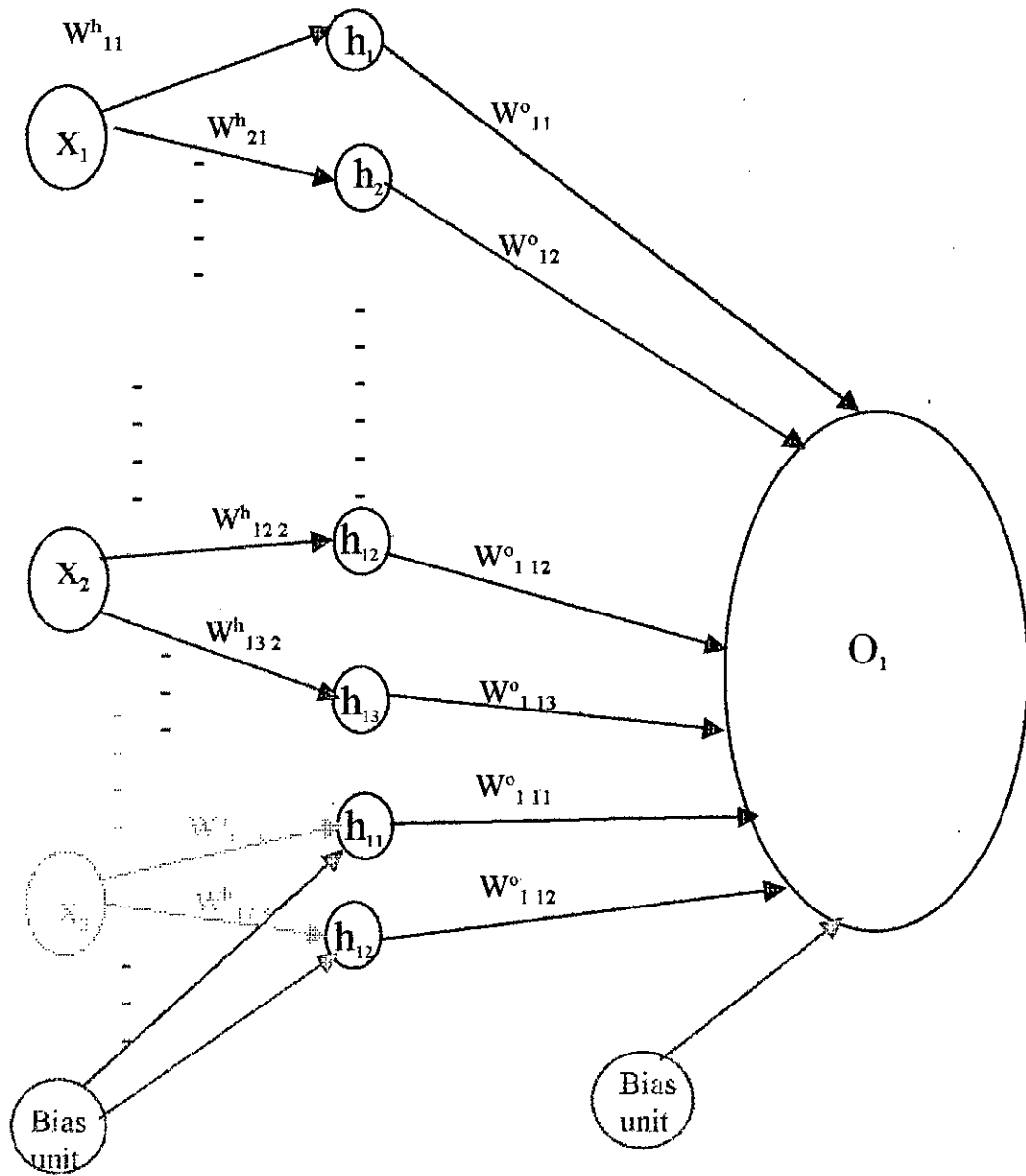


Fig. 5.18 Schematic diagram of ANN for calculation of punching shear strength of shear wall-floor slab connections

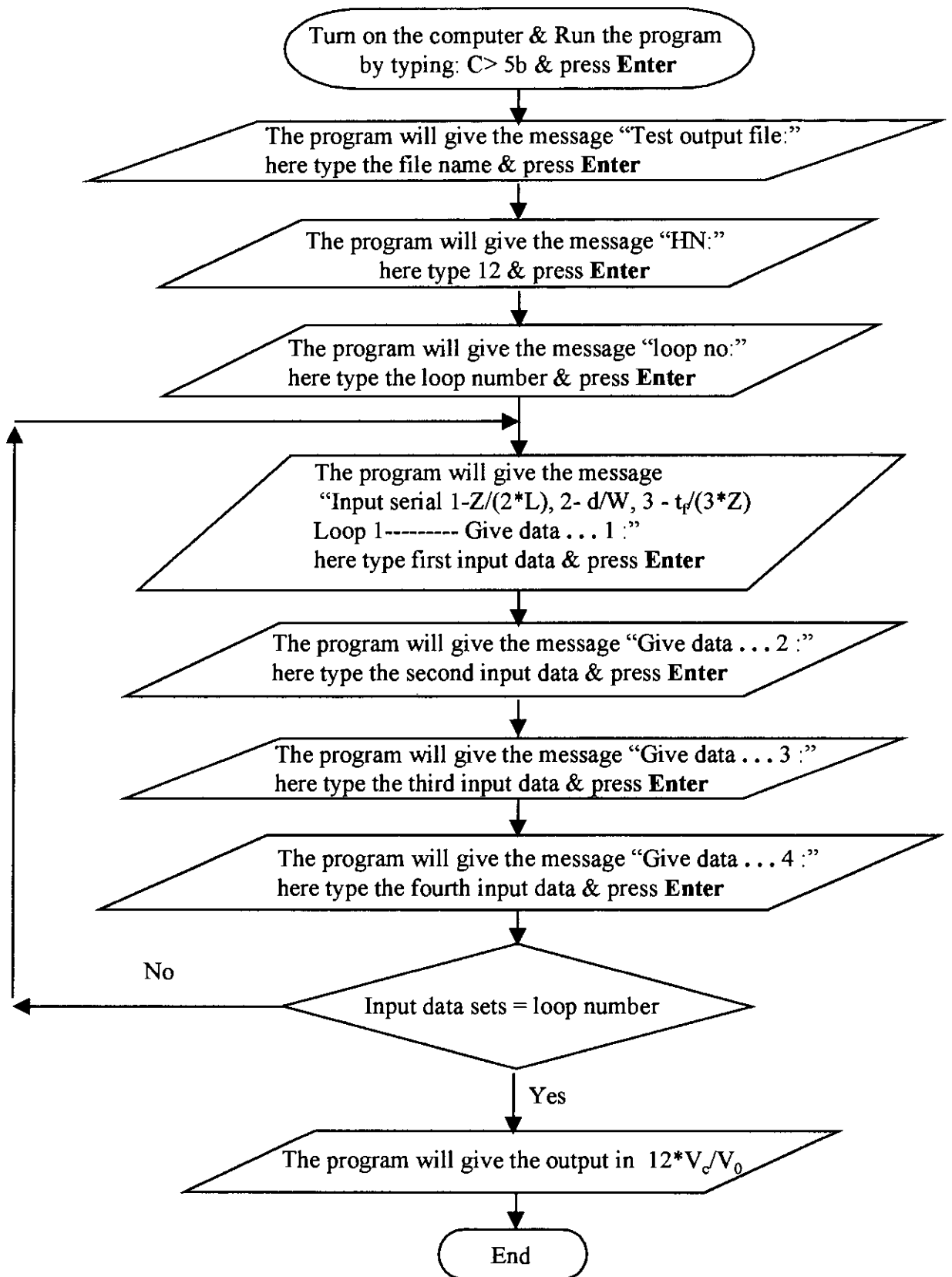


Fig. 5.19 Flow diagram for calculation of punching shear strength of shear wall and edge column-slab connection by using computer program



The punching shear strength,  $V_c$ , is given in the form of  $V_c/V_0$  to make the curves non-dimensional, where  $V_0 = f'_c \cdot b_p \cdot d$ . Figs. 5.20 to 5.24 show the punching shear strength ratio ( $V_c/V_0$ ) as a function of  $d/W$  and  $t_f/Z$  for  $L = 2000$  mm and  $f'_c = 15$  N/mm<sup>2</sup>.

The punching shear strength for other than  $f'_c = 15$  N/mm<sup>2</sup> and  $L = 2000$  mm, the value of  $V_c/V_0$  obtained from the graph should be multiplied by multiplying factors. The multiplying factor for different  $f'_c$  and  $L$  can be calculated from Fig. 5.25 and Fig. 5.26. The multiplying factor is introduced to avoid a large number of curves.

#### 5.4.4 Results and Discussions

The ultimate shear strength for exterior edge column-slab connections or shear wall-floor slab connections,  $V_c$  is expressed as the ratio of  $V_c/V_0$  to make the design curves non-dimensional. The ultimate shear strength ratio,  $V_c/V_0$  of exterior edge column-slab connections or slab-wall connections are given in Figs. 5.20 to 5.24 for a range of flange width ratio  $Z/L$  of 0.10 to 0.50 respectively. In all the figures, the value of  $f'_c$  is taken as 15 N/mm<sup>2</sup> and  $L$  equal to 2000 mm. Web wall thickness  $t_w$  is always equal to flange wall thickness  $t_f$ . Results based on these figures are discussed below:

##### 5.4.4.1 Effect of Flange Width (Z)

Effect of flange width ( $Z$ ) is expressed in terms of  $Z/L$  to make the curves non-dimensional. With the increase of flange width ( $Z$ ), the ratio between flange width and opening between walls,  $Z/L$  increases, when  $L$  is constant. From the figures, it is seen that with the increase of  $Z/L$  ratio the punching shear strength increases, when all other parameters are constant. The rate of increase of  $V_c/V_0$  is higher for lower values of  $d/W$  &  $t_f/Z$  and the rate of increase is lower for higher values of  $d/W$  &  $t_f/Z$ . The rate of increase of  $V_c/V_0$  due to increase of  $Z/L$ ,  $d/W$  &  $t_f/Z$  is shown in table 5.7. It can be concluded that the punching shear strength ratio,  $V_c/V_0$  increases with the increase of flange width ( $Z$ ) and it is very prominent for lower values of  $d/W$  &  $t_f/Z$ .

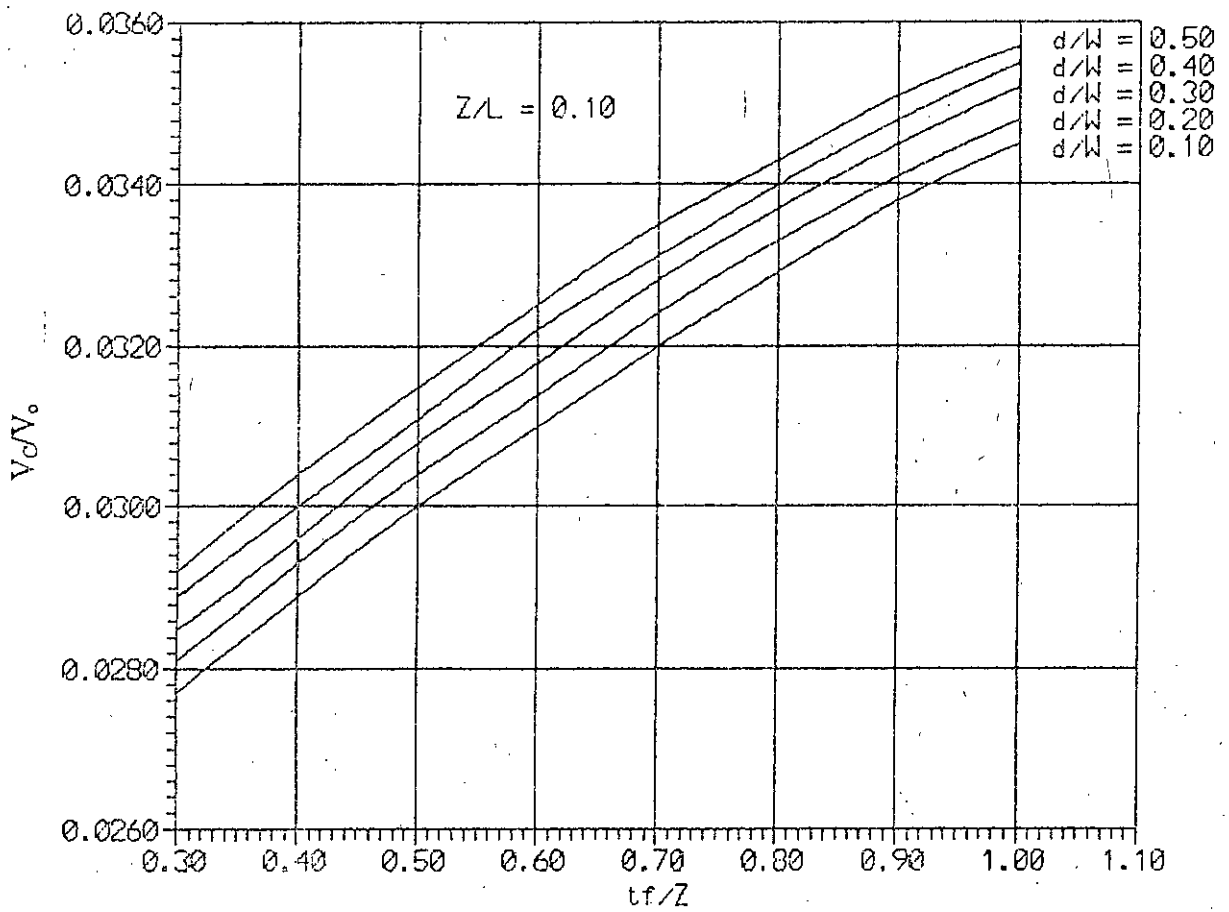
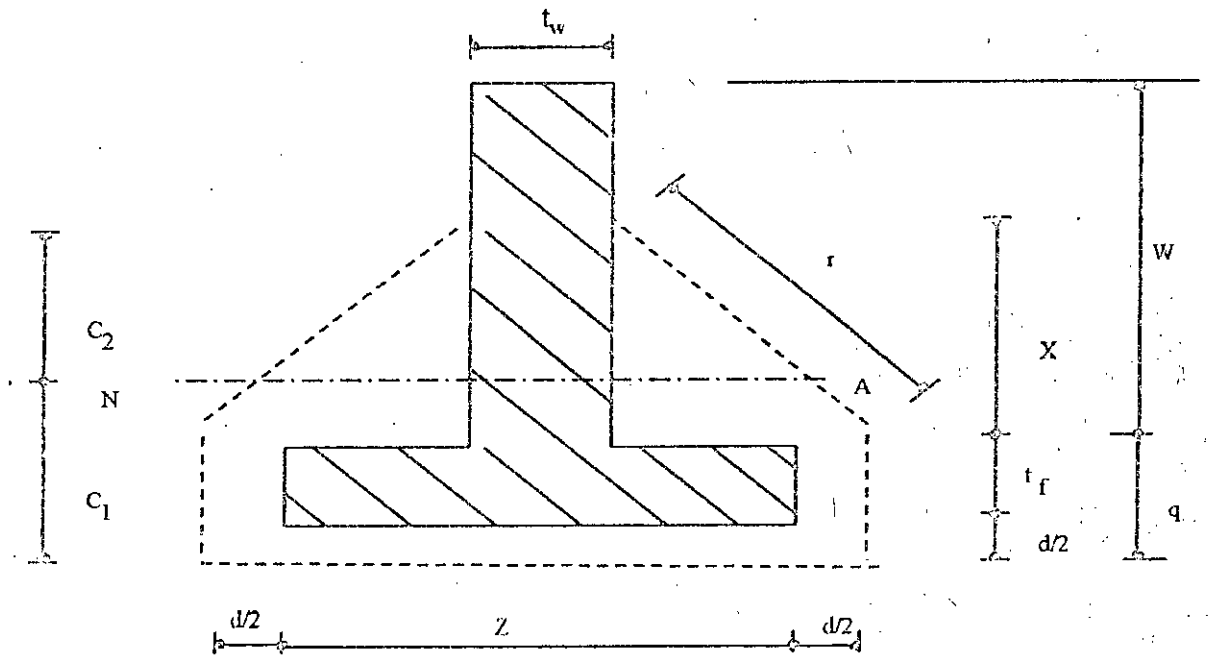


Fig. 5.20  $V_c/V_o$  as a function of  $t_f/Z$  and  $d/W$  for  $f'_c = 15 \text{ N/mm}^2$ ,  $L = 2000 \text{ mm}$  and  $Z/L = 0.10$

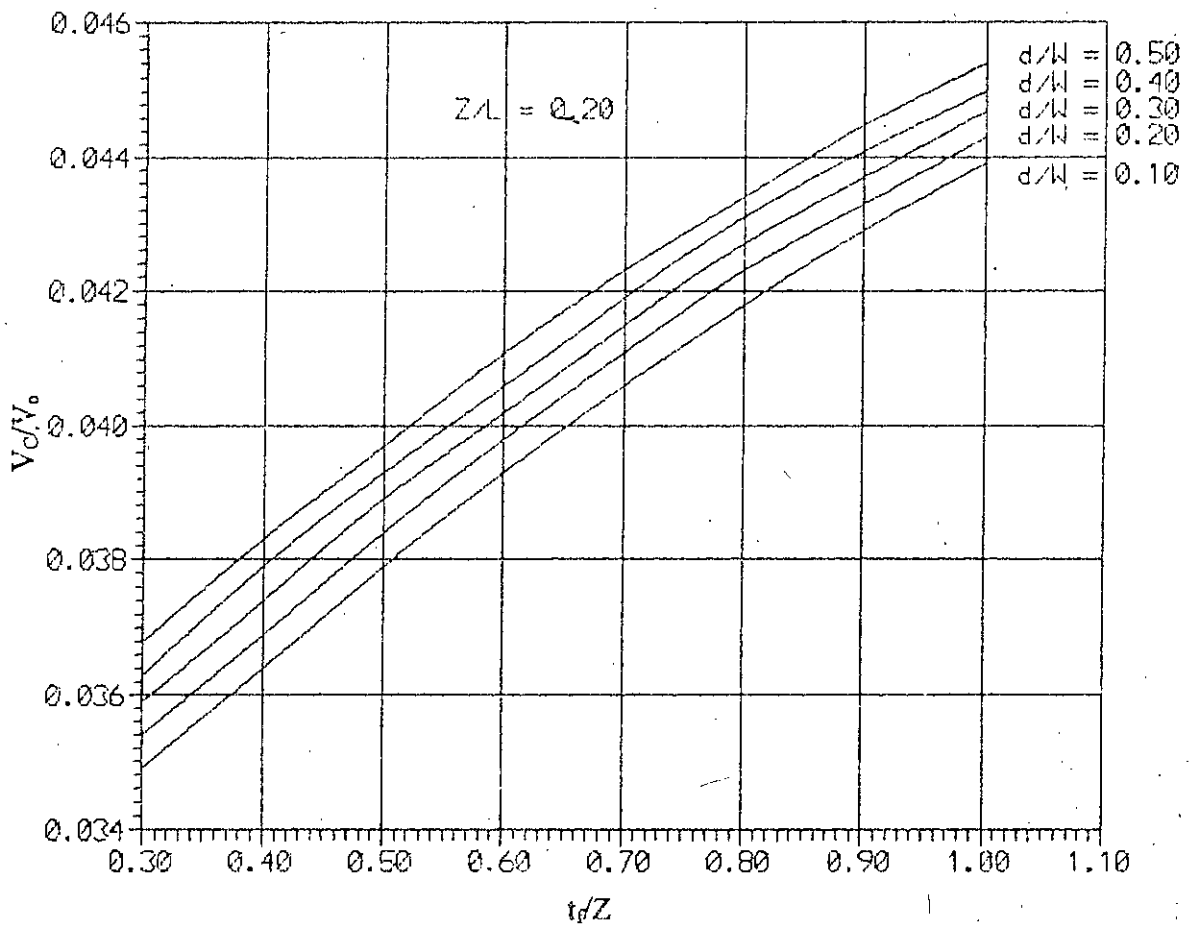
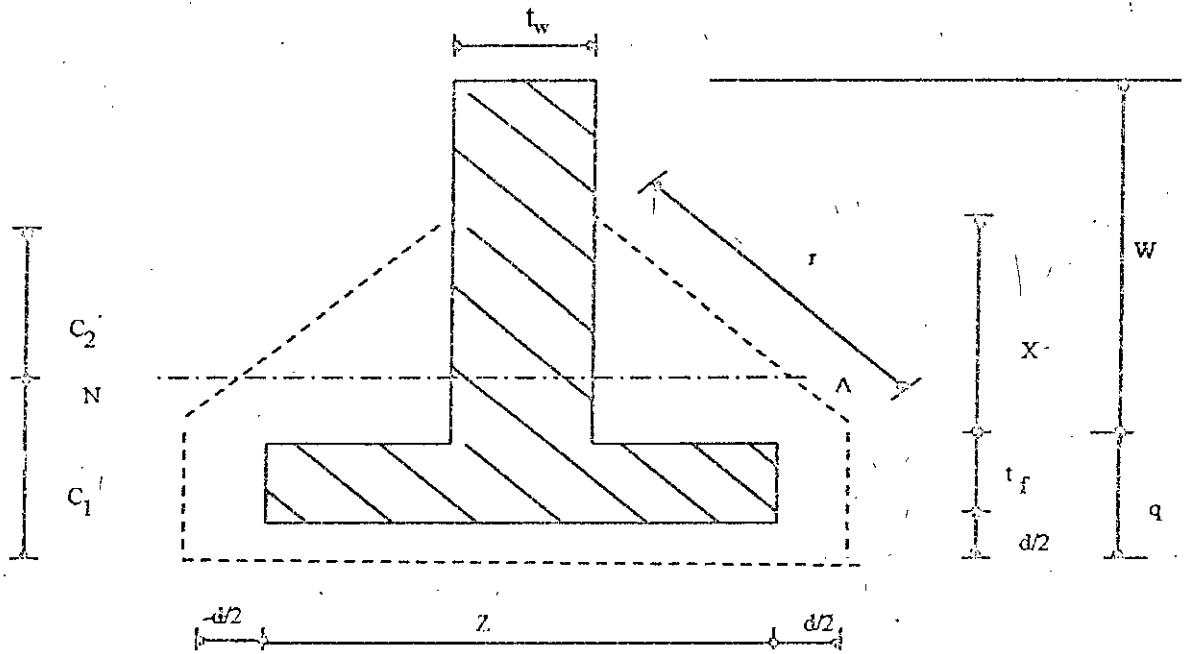


Fig. 5.21  $V_c/V_0$  as a function of  $t_f/Z$  and  $d/W$  for  $f'_c = 15 \text{ N/mm}^2$ ,  $L = 2000 \text{ mm}$  and  $Z/L = 0.20$

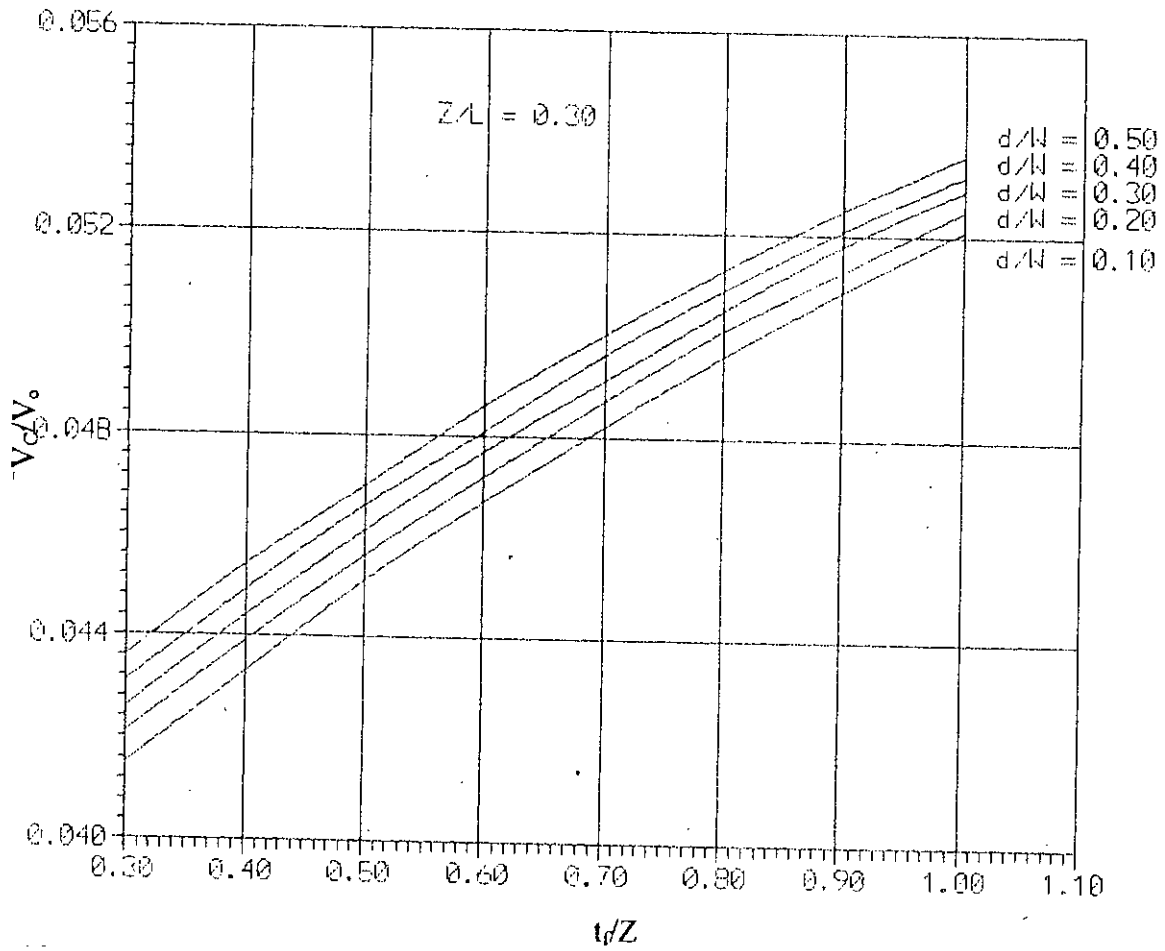
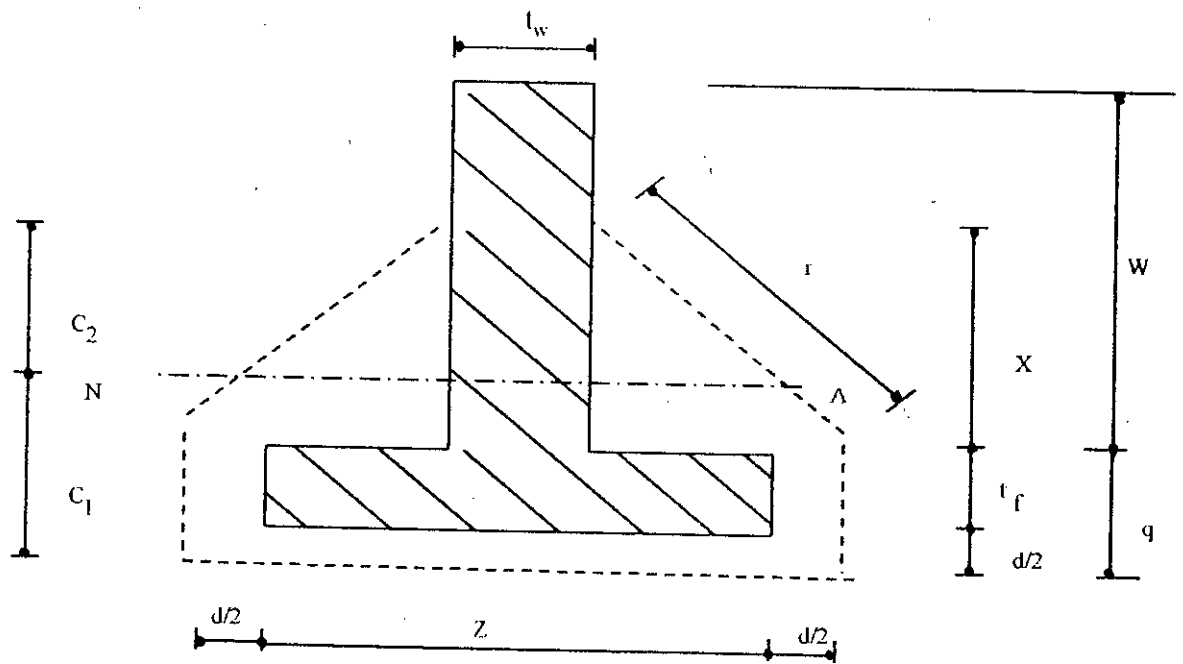


Fig. 5.22  $V_c/V_0$  as a function of  $t_f/Z$  and  $d/W$  for  $f'_c = 15 \text{ N/mm}^2$ ,  $L = 2000 \text{ mm}$  and  $Z/L = 0.30$

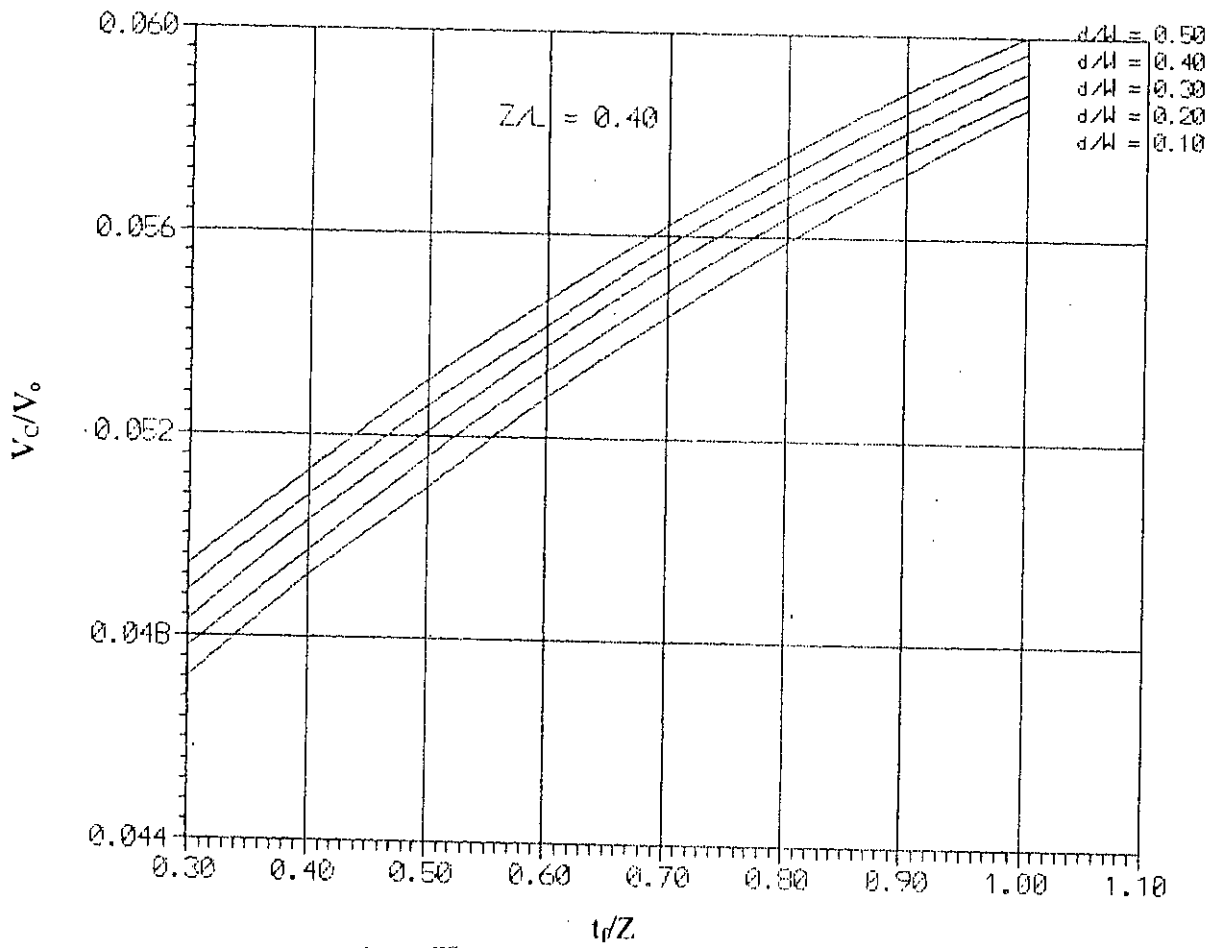
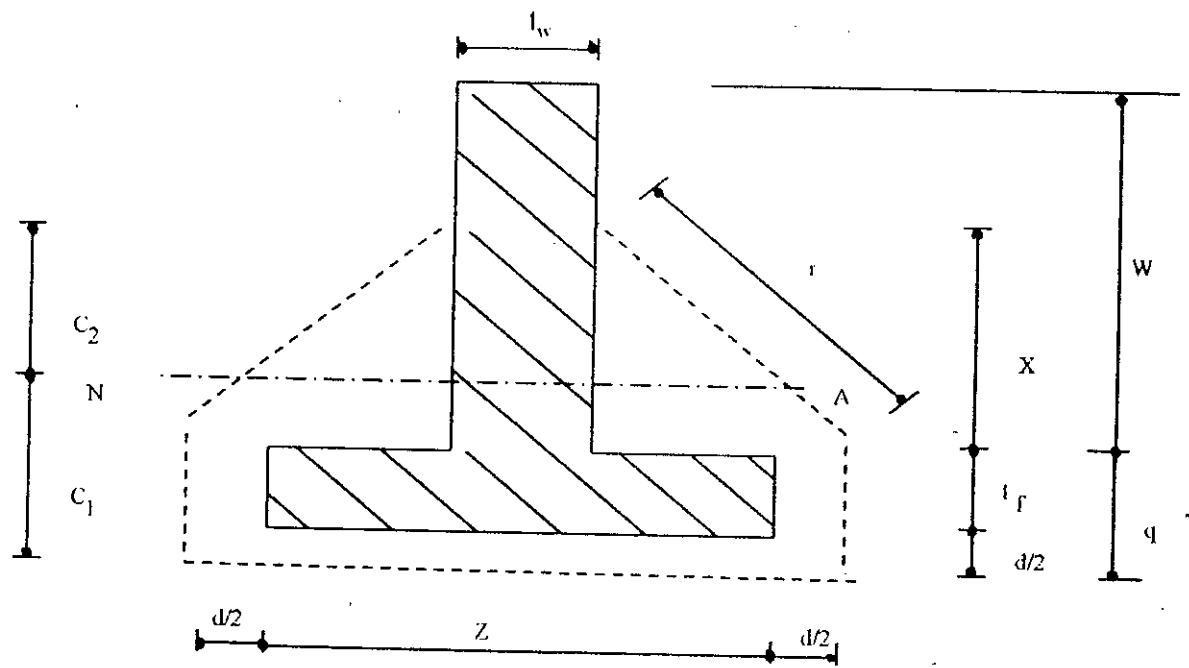


Fig. 5.23  $V_c/V_0$  as a function of  $t_f/Z$  and  $d/W$  for  $f'_c = 15 \text{ N/mm}^2$ ,  $L = 2000 \text{ mm}$  and  $Z/L = 0.40$

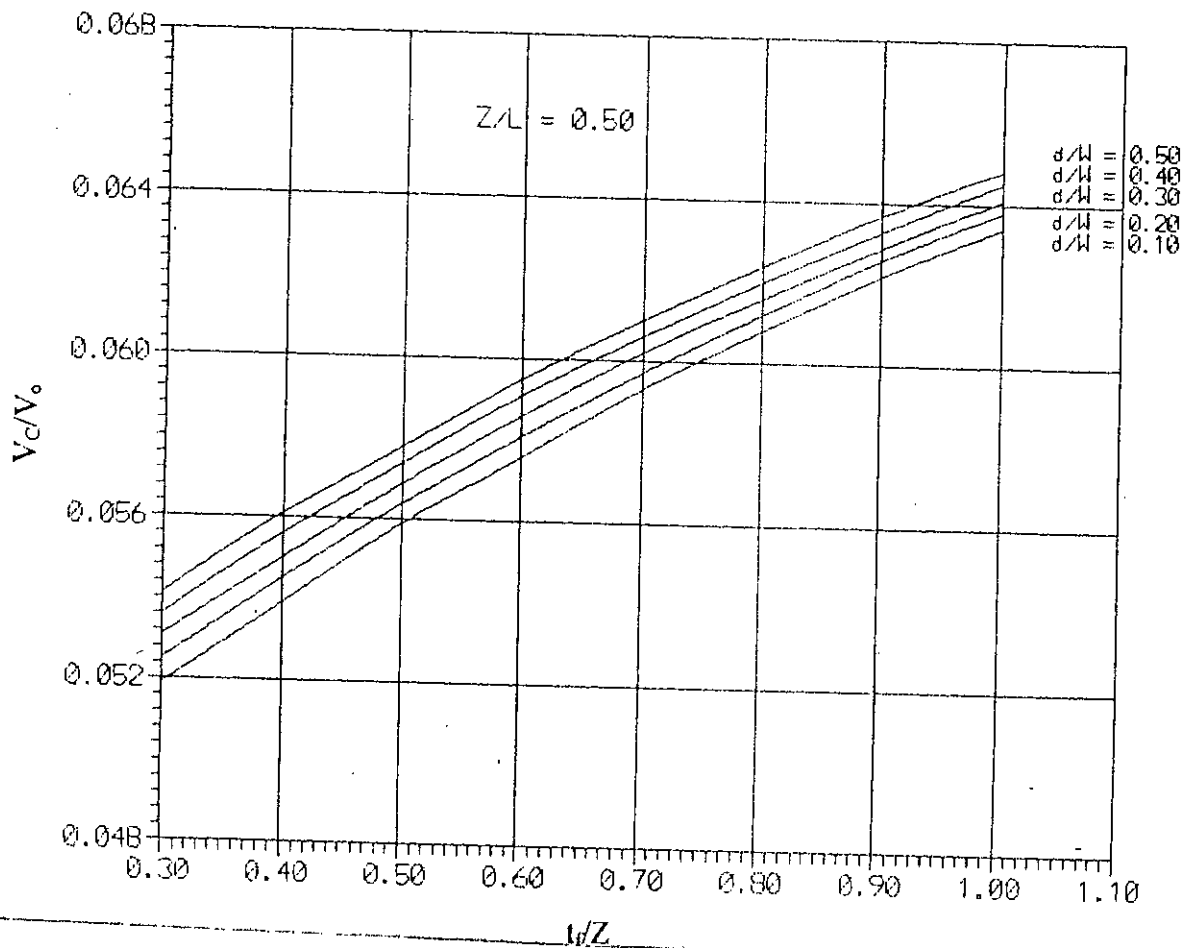
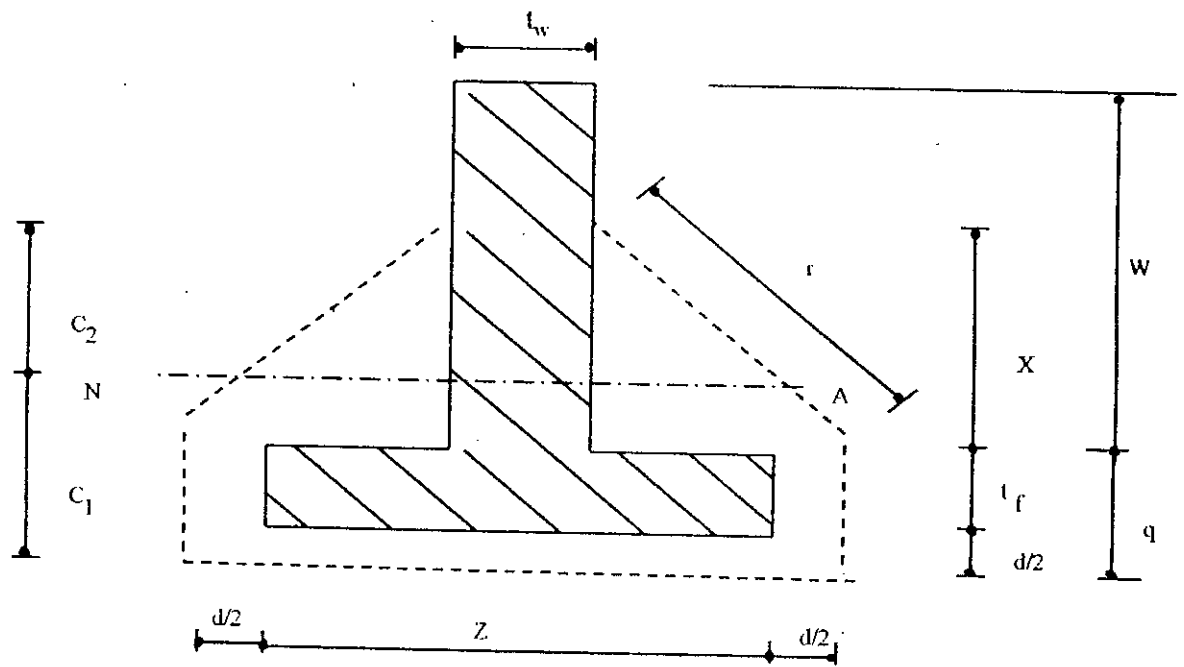


Fig. 5.24  $V_c/V_0$  as a function of  $t_f/Z$  and  $d/W$  for  $f'_c = 15 \text{ N/mm}^2$ ,  
 $L = 2000 \text{ mm}$  and  $Z/L = 0.50$

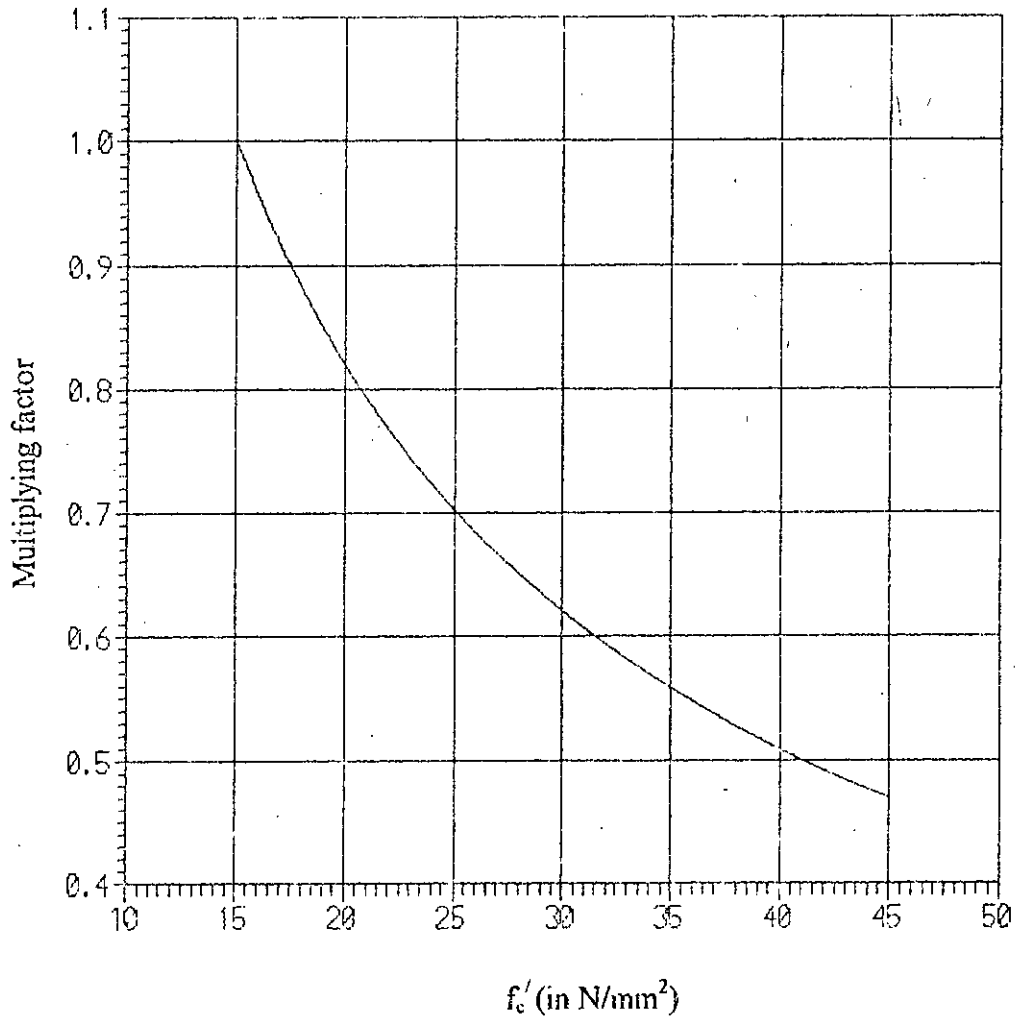


Fig. 5.25 Multiplying factor as a function of  $f'_c$

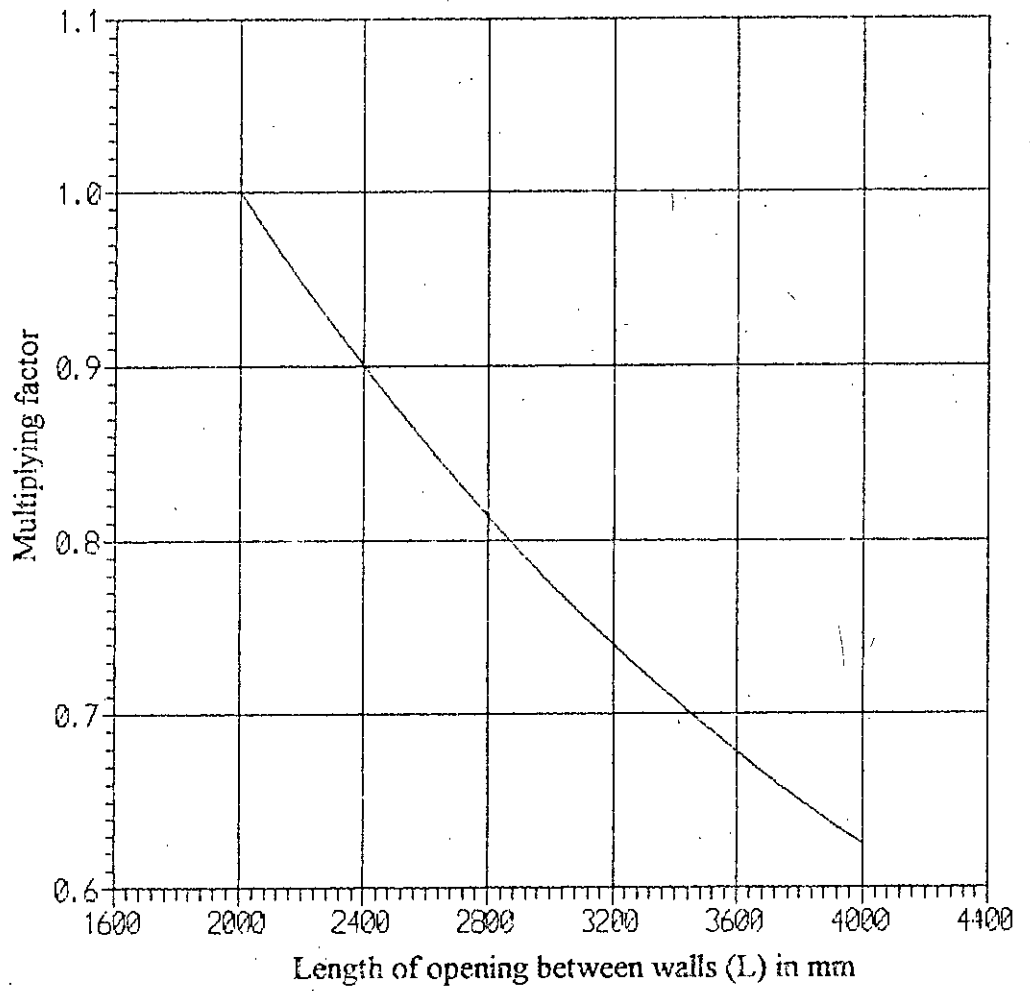


Fig. 5.26 Multiplying factor as a function of L



**Table 5.7** Rate of increase of  $V_c/V_0$  due to increase of  $Z/L$ .

d/W	$t_f/Z$	Values of $V_c/V_0$				
		Z/L = 0.10	Z/L = 0.20	Z/L = 0.30	Z/L = 0.40	Z/L = 0.50
0.10	0.60	0.0310	0.0393	0.0467	0.0528	0.0576
0.20	0.60	0.0314	0.0398	0.0472	0.0533	0.0581
0.30	0.60	0.0318	0.0402	0.0477	0.0538	0.0586
0.40	0.60	0.0322	0.0406	0.0481	0.0542	0.0591
0.50	0.60	0.0325	0.0411	0.0486	0.0547	0.0595
0.10	0.80	0.0329	0.0418	0.0496	0.0559	0.0608
0.20	0.80	0.0333	0.0423	0.0501	0.0564	0.0612
0.30	0.80	0.0337	0.0427	0.0505	0.0568	0.0616
0.40	0.80	0.0340	0.0431	0.0509	0.0572	0.0620
0.50	0.80	0.0343	0.0434	0.0513	0.0576	0.0624
0.10	1.00	0.0345	0.0439	0.0521	0.0586	0.0634
0.20	1.00	0.0348	0.0443	0.0525	0.0589	0.0638
0.30	1.00	0.0352	0.0447	0.0529	0.0593	0.0641
0.40	1.00	0.0355	0.0450	0.0532	0.0597	0.0645
0.50	1.00	0.0357	0.0454	0.0536	0.0600	0.0648

#### 5.4.4.2 Effect of Web Wall Length (W)

Punching shear strength, when calculated by the formula (Eqn. 5.9), increases with the increase of web wall length (W) and it remains constant, if W is more than three times of  $t_w$  (table 5.8). The test results [6] also show that the punching shear strength does not increase if W is increased more than three times of  $t_w$ . But the calculated punching shear strength by ANN shows slight decrease in strength, when W is more than three times of  $t_w$ , considering d/W instead of d/X in plotting the graph is one of the reasons of this variation. The design curves can only be applied to calculate the ultimate shear strength for exterior edge column-slab connections if W is more than 2.5 times of  $t_f$ .

**Table 5.8** Comparison between results calculated by ANN, formula (Eqn. 5.9), ACI and British code for punching shear strength.

$t_f$ (mm)	d (mm)	Z (mm)	W (mm)	L (mm)	$f'_c/f_{cu}$ (N/mm <sup>2</sup> )	V calculated by				% difference with formula		
						ANN (KN)	formula (KN)	ACI code (KN)	British code (KN)	ACI code	British code	ANN
200.00	125.00	200.00	600.00	2000.00	20.00/25.55	132.93	117.24	122.54	271.40	+4.53	+131.50	+13.38
200.00	125.00	200.00	700.00	2000.00	20.00/25.55	132.55	117.24	139.52	292.68	+19.01	+149.66	+13.06
200.00	125.00	200.00	800.00	2000.00	20.00/25.55	132.27	117.24	157.15	313.97	+34.05	+167.81	+12.82
200.00	125.00	200.00	900.00	2000.00	20.00/25.55	132.08	117.24	175.39	335.26	+49.61	+185.97	+12.66
200.00	125.00	200.00	1000.00	2000.00	20.00/25.55	131.88	117.24	194.22	356.54	+65.66	+204.12	+12.49
200.00	175.00	200.00	600.00	2000.00	20.00/25.55	198.34	194.76	181.53	390.40	-6.79	+100.45	+1.84
200.00	175.00	200.00	700.00	2000.00	20.00/25.55	197.59	194.76	205.66	417.79	+5.60	+114.52	+1.45
200.00	175.00	200.00	800.00	2000.00	20.00/25.55	197.02	194.76	230.63	445.19	+18.42	+128.58	+1.16
200.00	175.00	200.00	900.00	2000.00	20.00/25.55	196.60	194.76	256.41	472.59	+31.65	+142.65	+0.95
200.00	175.00	200.00	1000.00	2000.00	20.00/25.55	196.22	194.76	282.94	499.98	+45.28	+156.72	+0.75
200.00	175.00	200.00	600.00	3000.00	20.00/25.55	139.31	145.93	135.82	390.40	-6.93	+167.52	-4.54
200.00	175.00	200.00	700.00	3000.00	20.00/25.55	138.80	145.93	154.56	417.79	+5.91	+186.29	-4.86
200.00	175.00	200.00	800.00	3000.00	20.00/25.55	138.36	145.93	174.07	445.19	+19.28	+205.06	-5.19
200.00	175.00	200.00	900.00	3000.00	20.00/25.55	138.07	145.93	194.32	472.59	+33.16	+223.84	-5.39
200.00	175.00	200.00	1000.00	3000.00	20.00/25.55	137.82	145.93	215.28	499.98	+47.52	+242.61	-5.56
200.00	175.00	200.00	600.00	4000.00	20.00/25.55	106.61	116.68	108.50	390.40	-7.01	+234.58	-8.63
200.00	175.00	200.00	700.00	4000.00	20.00/25.55	106.20	116.68	123.81	417.79	+6.10	+258.06	-8.98
200.00	175.00	200.00	800.00	4000.00	20.00/25.55	105.88	116.68	139.79	445.19	+19.81	+281.54	-9.26
200.00	175.00	200.00	900.00	4000.00	20.00/25.55	105.64	116.68	156.44	472.59	+34.07	+305.02	-9.46
200.00	175.00	200.00	1000.00	4000.00	20.00/25.55	105.44	116.68	173.73	499.98	+48.89	+328.50	-9.64

### 5.4.4.3 Effect of Effective Slab Thickness (d)

For examining the influence of effective slab thickness (d) on  $V_c/V_0$  the ratio between effective slab thickness and web wall length,  $d/W$  is increased. With the increase of d, the ratio  $d/W$  increases, when W remains constant. When the ratio  $d/W$  is increased,  $V_c/V_0$  also increases as evident from the curves. That is the punching shear strength ratio,  $V_c/V_0$  increases with the increase of effective slab thickness. The rate of increase is maximum for lower values of  $d/W$ . As the value of  $d/W$  increases, the rate of increase of the punching shear strength ratio,  $V_c/V_0$  decreases (table 5.7).

### 5.4.4.4 Effect of Slab Opening Length (L)

The ultimate shear strength ratio,  $V_c/V_0$  of slab-wall connections are given in Figs. 5.20 to 5.24. All these Figs. are for  $L = 2000$  mm. For other values of L (i.e.  $L = 2000$  mm to 4000 mm), the calculated ultimate shear strength value is to be multiplied by a factor which is given in Fig. 5.26. There is no unique relation between the ultimate shear strength for various values of L. All parameters remain constant except L, when L equals to 3000 mm, the ultimate shear strength is 0.735 to 0.81 times of the ultimate shear strength of L equals to 2000 mm. For L equals to 4000 mm, the ultimate shear strength is 0.58 to 0.67 times of the ultimate shear strength of L equals to 2000 mm. In plotting the graph for multiplying factor of L (Fig. 5.26), the average value is taken. The factor depends on the value of various parameters. Normally it is seen that the value of this factor is small when the value of  $t_f$ , d, Z etc are small and the value of this factor increases as the value of  $t_f$ , d, Z etc are increased. In British Code effect of L on ultimate shear strength is not at all considered. But practically the effect of L on ultimate shear strength is very prominent. So British Code should not be used when the value of L is high.

#### 5.4.4.5 Comparison of ANN with Other Results

The punching shear strength for exterior edge column-slab connections or shear wall-floor slab connections obtained by ANN are compared in table 5.8 with the results calculated by formula (Eqn. 5.9), ACI and British Code. In ACI Code the cylinder strength is used and in British Code the cube strength is used. According to BS.1881.1970, the strength of a cylinder is equal to four-fifth of the strength of a cube, but experiments have shown that there is no unique relation between the strength of the specimens of the two shapes. The cylinder strength/cube strength ratio depends primarily on the level of strength of the concrete. It is suggested in Ref. 24 that the ratio of the strengths of the cylinder and a cube can be taken as

$$0.76 + 0.2 \log_{10} f_{cu}/2840 \quad (5.11)$$

where  $f_{cu}$  is the strength of the cube in lbs/in<sup>2</sup>. Based on Eqn. 5.11 a curve (Fig. 5.27) is drawn to find out conversion factor from  $f_c'$  to  $f_{cu}$ .

It is seen from the table 5.8 that the values calculated by ACI and British Code gives much higher value than the values calculated by formula, where ratio of long side to short side of a rectangular column is greater than 2.5 times of  $t_f$ .

When compared with the formula, the maximum percentage difference is 65.66% for ACI Code and 328.50% for British Code (table 5.8). The ANN results agree with the values calculated by formula (Eqn. 5.9) to within 14%. The test results [6] also show that the punching shear strength is very close to the value calculated by formula. Once the artificial neural network is developed, the punching shear strength can be found out within minutes, when the required input parameters for ANN such as  $(d/t_f)$ ,  $(d/Z)$ ,  $(t_f/W)$ ,  $(Z/L)$ ,  $(d/W)$  and  $(t_f/Z)$  are known for a particular problem.

#### 5.4.4.6 Calculation of Punching Shear Strength using Design Curves

The punching shear strength for any structure can be calculated satisfactorily by the design curves shown in Figs. 5.20 to 5.27, if the various parameters of the structure fall within the following range:

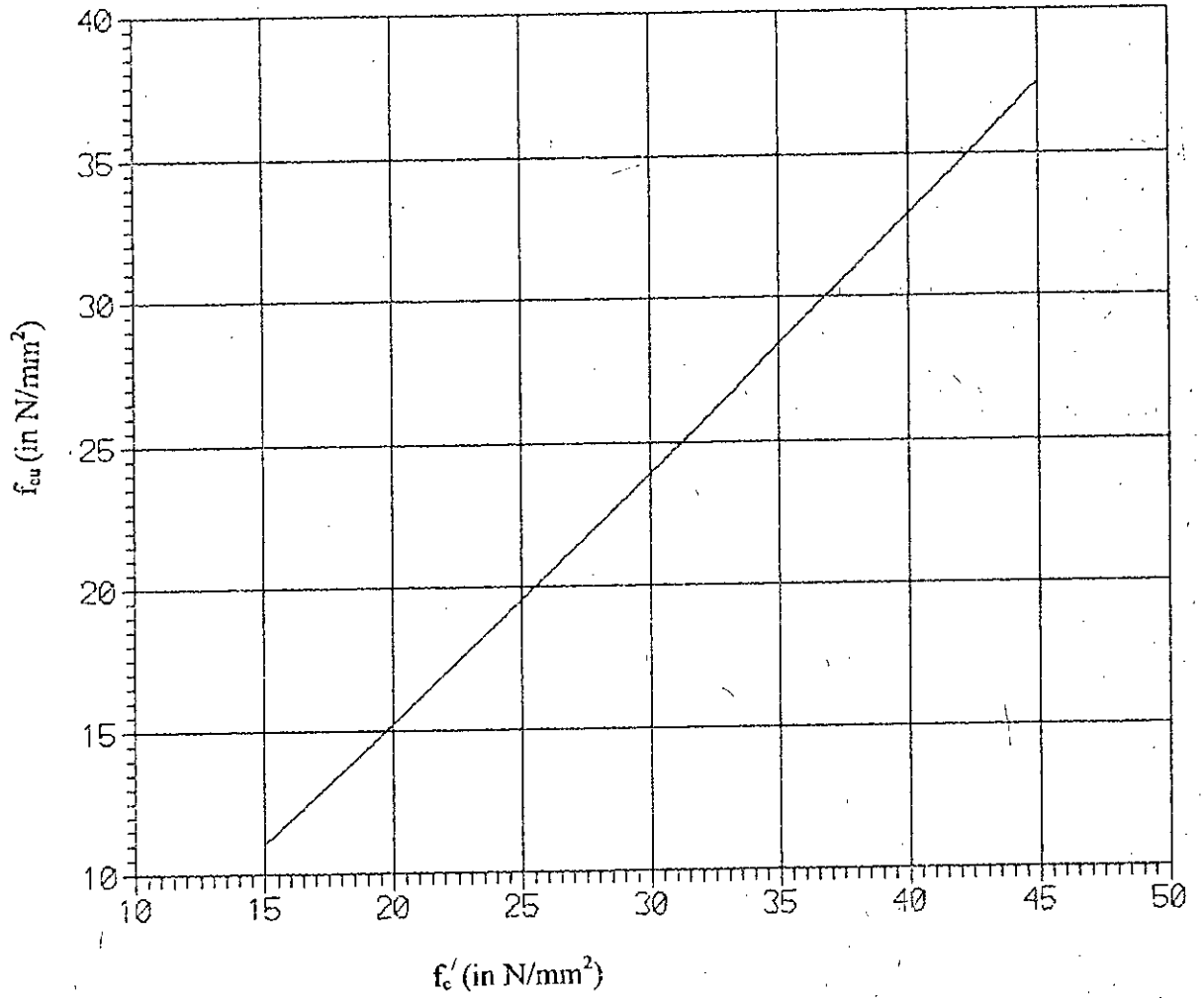


Fig. 5.27 Conversion factor from  $f'_c$  to  $f_{cu}$

$$t_f = 150 \text{ to } 400 \text{ mm.}$$

$$d = 100 \text{ to } 250 \text{ mm.}$$

$$Z = 200 \text{ to } 1000 \text{ mm.}$$

$$W = 400 \text{ to } 1000 \text{ mm.}$$

$$L = 2000 \text{ to } 4000 \text{ mm.}$$

$$f_c' = 15 \text{ to } 45 \text{ N/mm}^2$$

The flow diagram for calculation of punching shear strength is given in Fig. 5.28. To explain the procedure of consulting the graph, two numerical examples are given below.

#### 5.4.4.6.1 Example 1: Flanged Shear Wall

Let the various parameters for the example ( $C_1$  of Fig. 5.29) be  $t_f = 250$  mm,  $d = 150$  mm,  $Z = 400$  mm,  $W = 1000$  mm,  $L = 3000$  mm and  $f_c' = 25$  N/mm<sup>2</sup>. To find out the punching shear strength,  $b_p/d$  and  $V_e/V_0$  is to be calculated from the graph. The sequence to be followed is:

- For calculating  $b_p/d$ , values for different ratios  $d/t_f$ ,  $d/Z$  and  $t_f/W$  are to be calculated. The values of these ratios for the present example are  $d/t_f = 0.60$ ,  $d/Z = 0.375$  and  $t_f/W = 0.25$ . Depending on the value of  $d/t_f$ , the relevant curve (for this example, Figs. 5.10 & 5.11) is to be consulted. Interpolation is to be done for intermediate values.
- For  $d/t_f = 0.50$ ,  $d/Z = 0.375$  and  $t_f/W = 0.25$ ,  $b_p/d = 21.00$  and for  $d/t_f = 0.70$ ,  $d/Z = 0.375$  and  $t_f/W = 0.25$ ,  $b_p/d = 16.50$ . By interpolation the value of  $b_p/d$  for  $d/t_f = 0.60$ ,  $d/Z = 0.375$  and  $t_f/W = 0.25$  is 18.75.
- Whatever may be the value of  $L$ , at first the punching shear strength for  $L$  equals to 2000 mm and  $f_c' = 15$  N/mm<sup>2</sup> is to be calculated, keeping the value of all other parameters same. Once the punching shear strength for  $L$  equals to 2000 mm and  $f_c' = 15$  N/mm<sup>2</sup> is calculated, for other values of  $L$  and  $f_c'$ , Figs. 5.25 & 5.26 is to be consulted.

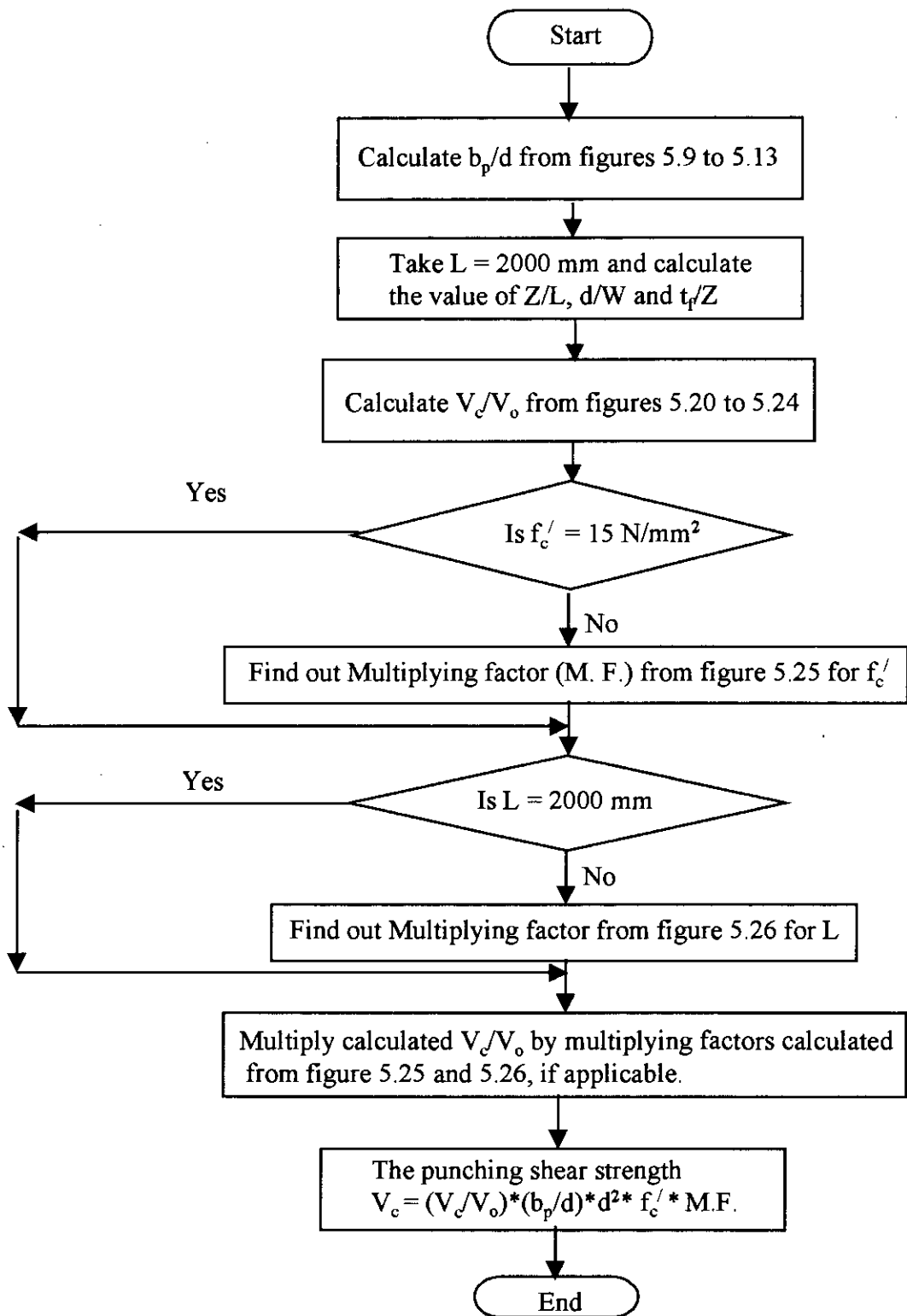


Fig. 5.28 Flow diagram for calculation of punching shear strength of shear wall and edge column-slab connection by using graph

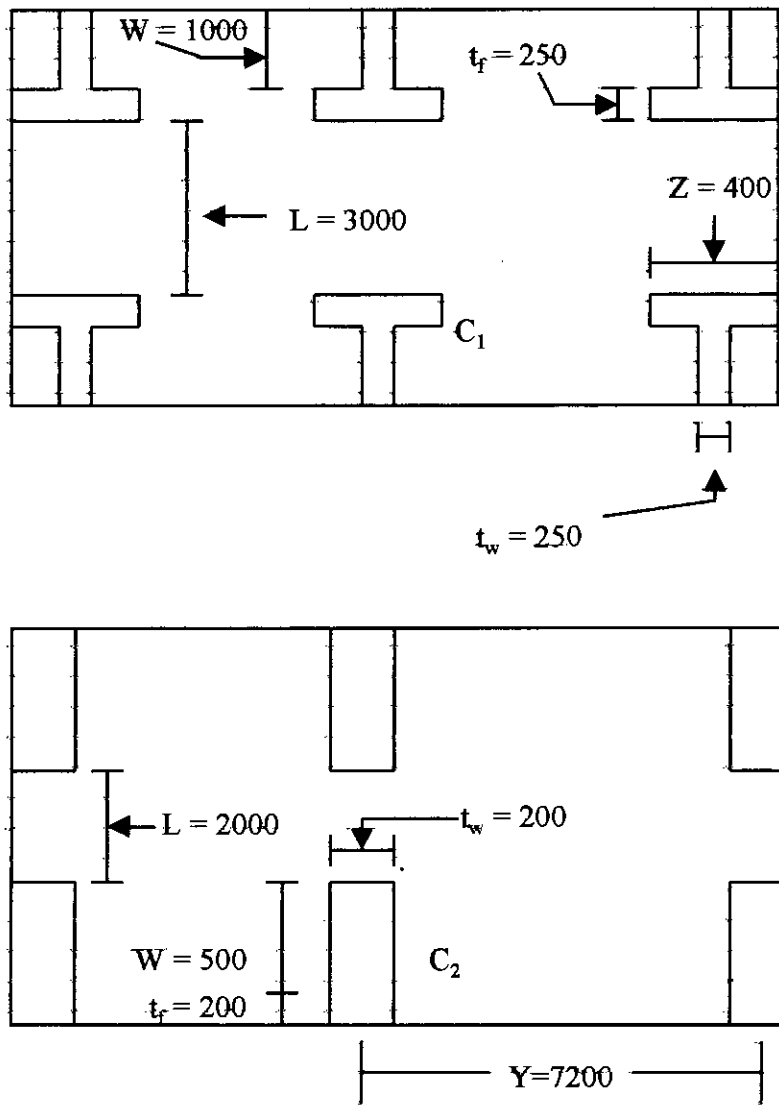


Fig. 5.29 Typical plan of a shear wall structure  
(all dimensions are in mm)



- Values for different ratios  $Z/L$ ,  $d/W$  and  $t_f/Z$  are to be calculated. The values of these ratios for the present example are  $Z/L = 0.20$ ,  $d/W = 0.15$  and  $t_f/Z = 0.625$ . Depending on the value of  $Z/L$ , the relevant curve (for this example, Figs. 5.21) is to be consulted.
- For  $d/W = 0.15$  and  $t_f/Z = 0.625$ , the value of  $V_c/V_0$  is 0.0399.
- The calculated punching shear strength ratio,  $V_c/V_0$  is 0.0399 for  $f_c'$  equal to 15  $\text{N/mm}^2$ . For calculating the punching shear strength for  $f_c'$  equal to 25  $\text{N/mm}^2$ , the value of  $V_c/V_0$  obtained from the graph should be multiplied by a multiplying factor. The multiplying factor for different values of  $f_c'$  can be calculated from Fig. 5.25. From the Fig. 5.25, the multiplying factor is 0.703 for  $f_c'$  equal to 25  $\text{N/mm}^2$ . So the punching shear strength ratio  $V_c/V_0$ , for  $f_c'$  equal to 25  $\text{N/mm}^2$  is  $0.0399 \times 0.703 = 0.028$ .
- Now the multiplying factor for  $L = 3000$  mm is to be considered. The multiplying factor for  $L = 3000$  mm is 0.775. So the punching shear strength ratio  $V_c/V_0$ , for  $f_c'$  equal to 25  $\text{N/mm}^2$  and  $L = 3000$  mm is  $0.028 \times 0.775 = 0.02174$ .
- Therefore the punching shear strength,  $V_c$  is  $0.02174 \times 18.75 \times 150 \times 150 \times 25 = 229289$  N or 229.3 KN for the said example.
- For this example i.e. when  $t_f = 250$  mm,  $d = 150$  mm,  $Z = 400$  mm,  $W = 1000$  mm,  $L = 3000$  mm and  $f_c' = 25$   $\text{N/mm}^2$ , if the punching shear strength ( $V_c$ ) is calculated by design equations, the calculated punching shear strength is 246.55 KN. The percentage difference between the values calculated by graph and formula is 7%.

#### 5.4.4.6.2 Example 2: Plane Shear Wall

Let the various parameters for the second example ( $C_2$  of Fig. 5.29) be  $t_f = 200$  mm,  $d = 140$  mm,  $Z = 200$  mm,  $W = 500$  mm,  $L = 2000$  mm and  $f_c' = 20$   $\text{N/mm}^2$ . To find out the punching shear strength,  $b_p/d$  and  $V_c/V_0$  is to be calculated from the graph. The sequence to be followed is:

- For calculating  $b_p/d$ , values for different ratios  $d/t_f$ ,  $d/Z$  and  $t_f/W$  are to be calculated. The values of these ratios for the present example are  $d/t_f = 0.70$ ,  $d/Z = 0.70$  and  $t_f/W = 0.40$ . Depending on the value of  $d/t_f$ , the relevant curve (for this example, Fig. 5.11) is to be consulted.

- For  $d/t_f = 0.70$ ,  $d/Z = 0.70$  and  $t_f/W = 0.40$ , the value of  $b_p/d$  is 12.70.
- The values of the ratios  $Z/L$ ,  $d/W$  and  $t_f/Z$  for this example are 0.10, 0.28 and 1.00 respectively. For  $Z/L = 0.10$ , the relevant curve (Figs. 5.20) is to be consulted.
- For  $d/W = 0.28$  and  $t_f/Z = 1.00$ , the value of  $V_c/V_0$  is 0.0351.
- The calculated punching shear strength ratio,  $V_c/V_0$  is 0.0351 for  $f_c'$  equal to 15 N/mm<sup>2</sup>. For calculating the punching shear strength for  $f_c'$  equal to 20 N/mm<sup>2</sup>, the value of  $V_c/V_0$  obtained from the graph should be multiplied by a multiplying factor. The multiplying factor for different values of  $f_c'$  can be calculated from Fig. 5.25. From the Fig. 5.25, the multiplying factor is 0.8189 for  $f_c'$  equal to 20 N/mm<sup>2</sup>. So the punching shear strength ratio  $V_c/V_0$ , for  $f_c'$  equal to 20 N/mm<sup>2</sup> is  $0.0351 \times 0.8189 = 0.02874$ .
- Therefore the punching shear strength,  $V_c$  is  $0.02874 \times 12.70 \times 140 \times 140 \times 20 = 143062$  N or 143.06 KN for the said example.
- The punching shear strength,  $V_c$  for  $t_f = 200$  mm,  $d = 140$  mm,  $Z = 200$  mm,  $W = 500$  mm,  $L = 2000$  mm and  $f_c' = 20$  N/mm<sup>2</sup> is 138.16 KN when calculated by design equations. The percentage difference between the values calculated by graph and formula is 3.42%.

## 5.5 Computer Program

There are two different sets of program. These are:

- First set of program consists of two files: 5a.wt and 5a.exe files. These are used to calculate the critical perimeter for punching shear. The listing of files 5a.wt and 5a.exe are given in appendix C.
- Second set of program consists of two files: 5b.wt and 5b.exe files. These are used to calculate the shear strength for punching shear. The listing of files 5b.wt and 5b.exe are given in appendix D.

### *Use of the computer program:*

Once the program files are copied, we can start it by simply typing 5a or 5b (as applicable) at the root directory and pressing **Enter**.

“Test output file” writing will appear on the screen. Here the output file name is to be given. File name can be alphabetical or numerical. File name will have an extension “out”. Example of file name: A.out or 1.out. After typing output file name **Enter** is to be pressed.

“HN” writing will appear on the screen. Number of hidden neurones, which was used during training must be given here. Otherwise output value will not be correct. The value of HN to calculate critical perimeter for punching shear is 15 and the value of HN to calculate the shear strength for punching shear is 12. After typing 15 or 12 **Enter** is to be pressed.

“Loop no” and “Give data ... 1” writing will appear on the screen. It is the number of sets of data one wants to calculate. After loop number input data is given. During data input, input serial must be maintained, input serial will appear on the screen. Otherwise output value will not be correct. After typing first input data **Enter** is to be pressed. “Give data ... 2” writing will appear on the screen. Here second input data is given and **Enter** is to be pressed. “Give data ...” writing will continue to appear on the screen until data input is completed.

Output writing along with output will appear on the screen. Output is given in the same sequence of loop number. The output for the critical perimeter for punching shear is in the form of  $b_p/(40*d)$ . To find out the critical perimeter for punching shear the computed value should be multiplied by 40 times the effective depth or  $40*d$ . The output for the shear strength for punching shear is in the form of  $12*V_d/(f_c'*b_p*d)$  for  $L = 2000$  mm and  $f_c' = 15$  N/mm<sup>2</sup>. So to get the shear strength for punching shear for  $L = 2000$  mm and  $f_c' = 15$  N/mm<sup>2</sup> the computed value should be multiplied by  $(f_c'*b_p*d)/12$ . If  $f_c'$  is other than 15 N/mm<sup>2</sup> or  $L$  is other than 2000 mm, the computed value should be again multiplied by multiplying factors, which can be obtained from Fig. 5.25 and 5.26 respectively.

# CHAPTER SIX

## CONCLUSIONS AND RECOMMENDATIONS

### 6.1 General

In this thesis, single layered neural network have been developed to produce non-dimensional design curves to determine the effective slab width of floor slab, critical perimeter and punching shear strength of wall-slab connections. Empirical equations proposed by Coull & Wong [2] to determine the effective slab width of floor slab and the design equations proposed by Bari. M. S. [6] to determine the critical perimeter and punching shear strength of wall-slab connections have been used to generate the input data for training the networks.

Backpropagation training algorithm for feedforward network is used to obtain the network weights. The developed networks have been tested by using different sets of data which were not used during the training. The output response is found very good.

### 6.2 Effective Slab Width of Floor Slab

- The set of curves given in Figs. 4.8 to 4.10 show the variation of effective width ratio ( $Y_e/Y$ ) for a range of wall opening ratios  $L/X$  for varying wall thickness ratio  $t/Y$  for plane wall. Figs. 4.16 to 4.18 show the variation of effective width ratio ( $Y_e/Y$ ) for a range of wall opening ratios  $L/X$  for varying flange thickness ratio  $Z/Y$  for equal flanged wall. The effective width ratio predicted by ANN for plane wall configurations, is found slightly higher than the values given by Coull & Wong [2] and Hossain M. A. [4]. In ANN wall thickness has been considered but Coull & Wong [2] and Hossain M. A. [4] neglected the wall thickness, this may be one of the reasons of slight variation of results. For flanged wall configurations, the ANN results are compared with the finite element results [23] and the results agree within 3.5%. Using the

developed artificial neural network, the effective width ratio ( $Y_e/Y$ ) can be found out accurately and within fraction of minute, when the required input parameters such as  $Y/X$ ,  $L/X$ ,  $t/Y$  or  $Z/Y$  and  $L/Y$  are known for a particular problem.

- From the figures it can be concluded that the effective width ratio increases with the increase of wall thickness. The thickness of the wall can have a considerable stiffening effect on the slab, the influence being relatively more significant with smaller wall opening ratios. The influence of the finite wall thickness and flange width is practically identical.

### 6.3 Punching Shear Strength of Wall-Slab Connections

To the best of author's knowledge no non-dimensional design curves are available to determine the critical perimeter and punching shear strength of wall-slab connections. These curves can also be used for exterior column - slab connections. The design curves given in Figs. 5.20 to 5.24 show the variation of punching shear strength ratio ( $V_e/V_0$ ) for a range of flange width ratios  $Z/L$  for varying flange thickness ratio  $t_f/Z$  and varying slab thickness ratio  $d/W$  for a constant  $f'_c = 15$  N/mm<sup>2</sup> and  $L = 2000$  mm. Fig. 5.25 and Fig. 5.26 gives the multiplication factor for other concrete strength ( $f'_c = 15$  to 45 N/mm<sup>2</sup>) and different slab opening length ( $L = 2000$  to 4000 mm) respectively.

- The non-dimensional design curves developed by ANN can evaluate the ultimate shear strength of junctions for both plane and flanged shear walls. ANN is found quite safe and consistent when compared with the design equation proposed in Ref. 6. The test results [6] also show that the punching shear strength is very close to the value calculated by ANN.

- The punching shear strength of wall-slab connections calculated by British Code (assuming shear wall as an edge column) gives much higher value (table 5.8) than the value calculated by the design equation or ANN. The calculated (by British Code) punching shear strength is around 328% higher than the design equation or ANN when ratio of long side to short side is 5. ACI Code can predict the punching shear strength of wall-slab connections (assuming shear wall as an edge column) when ratio of long side to short side is less than or equal to 3. But the calculated punching shear strength is around 65% higher than the design equation or ANN when ratio of long side to short side is 5. Hence recommendations of BS 8110 for the prediction of the strength of slab-edge column connections are unsuitable for estimating the strength of wall-slab connections, assuming shear wall as an edge column.

#### **6.4 Recommendations for Future Study**

The following recommendations are made for future study:

- More investigation should be done with various types of shear walls specially lift core walls as in this study only planar and equal flanged shear wall is considered.
- Investigations can be done with multiple bands of openings in the shear wall as in this study only one band of opening is studied.
- Non-dimensional design curves have been drawn only for shear wall-flat plate connections. These curves can also be used for exterior column-slab connections. Using ANN, non-dimensional design curves can be obtained for interior slab-column connections as well as slab with drop panel or column capital.

- In developing the ANN, backpropagation training algorithm has been used. Using adaptive architectures with cascade correlation [1] non-dimensional design curves can be obtained for shear wall-floor slab connections. In cascade correlation input units are connected directly to output units with adjustable weighted connections. Connections from inputs to a hidden unit are trained when the hidden unit is added to the net and are then frozen. Connections from the hidden units to the output units are adjustable. Design curves obtained by cascade correlation may further reduce the error.
- When the weights varies too much from one another then weight smoothing feed forward network can be used to smoothen the wide variation of weight. The use of weight smoothing feed forward network algorithm [25] may give better result in such cases. The weight smoothing feed forward network can be used to train the net for obtaining the non-dimensional graphs.

## REFERENCES

1. Fausett L., "Fundamentals of Neural Networks" Prentice Hall, Englewood Cliffs, NJ 07632.
2. Coull A. & Wong, Y. C., "Bending Stiffness of Floor Slabs in Cross-Wall Structures," Proceedings The Institute of Civil Engineers, Part 2, 1981, pp. 17-35.
3. Tso W. and Mahmoud A., "Effective Width of Coupling Slabs in Shear Wall Buildings", Journal of the Structural Division, ASCE, Vol.103, No.ST3, Proceeding paper 12817, March 1977, pp. 573-586.
4. Hossain M. A., " Non-linear Behaviour of Slabs in Coupled Shear Wall Structures" M.Sc. Thesis, BUET, Dhaka, January 1990.
5. Rosman R., "Approximate analysis of Shear Walls Subjected to Lateral Loads", Journal of the American Concrete Institute, Proceedings, Vol.61, No.6, June 1964, pp. 717-734.
6. Bari M. S., "Design of Shear Wall-Floor Slab Connections using Shear Reinforcement" Ph. D. thesis, University of Glasgow, October 1987.
7. Hawkins N. M., "Shear Strength of Slabs with Shear Reinforcement", ACI special publication - Shear in Reinforced Concrete - SP 42, Vol.1, Detroit, American Concrete Institute, 1974, pp. 758-815.
8. ASCE-ACI Committee 426, "The Shear Strength of Reinforced Concrete Member-Slab", Journal of the Structural Division, ASCE, Vol.100, No.ST8, August 1974, pp. 1543-1591.
9. ACI Committee 318, "Commentary on Building Code Requirements for Reinforced Concrete (ACI 318-63)", Publication SP-10, American Concrete Institute, Michigan, 1965.
10. Distasio J. and Van Buren M. R., " Transfer of Bending Moment Between Flat Plate Floor and Column", Journal of the American Concrete Institute, Proceedings, Vol.53, No.3, September 1960, pp. 299-314.



11. Moe J., "Shearing Strength of Reinforced Concrete Slabs and Footings Under Concentrated Loads", Development Department Bulletin D47, Portland Cement Association, April 1961, pp. 130.
12. Hanson N. W. and Hanson J. M., "Shear and Moment Transfer Between Concrete Slabs and Columns", Journal of the Portland Cement Association, Research and Development Laboratories, Vol.10, No.1. January 1968, pp. 2-16.
13. Akiyama H. and Hawkins N. M., "Response of Flat Plate Concrete Structures to Seismic and Wind forces", Progress Report on National Science Foundation Earthquake Hazards Mitigation Program, Grant No. ENN 72-03585, University of Washington, Seattle, July 1984.
14. Regan P. E., "Behaviour of Reinforced and Prestressed Concrete Subjected to Shear Forces," Paper 7441 S, Proceedings, The Institute of Civil Engineers, Vol. 50, December 1971, pp. 527, Supplement (xvii), pp. 337-364.
15. British Standards Institution, " The Structural Use of Concrete", Unified British Code for Structural Use of Concrete in Buildings, CP110, London, 1972.
16. British Standards Institution, " The Structural use of Concrete", Unified British Code for Structural Use of Concrete in Buildings, BS 8110, London, 1985.
17. Wen Y. K., Ghaboussi J., Venini P. and Nikzad K., "Control of Structures using Neural Networks" In: Proceedings, US/Italy/Japan Workshop on Structural Control and Intelligent Systems, Sorrento, Italy, 1992, pp. 232-251.
18. Mukherjee A. & Deshpande J. M., "Application of Artificial Neural Networks in Structural Design Expert System" Computers & Structures Vol. 54, No. 3, 1995, pp. 367-375.
19. Adeli H. & Park H. S., "A Neural Dynamics Model for Structural Optimisation-Theory" and Park H. S & Adeli H., "A Neural Dynamics Model for Structural Optimisation-Application to Plastic Design of Structures" Computers & Structures Vol. 57, No. 3, 1995, pp. 383-399.

20. Ramasamy J. V. & Rajasekaran S., "Artificial Neural Network and Genetic Algorithm for the Design Optimisation of Industrial Roofs-A comparison" *Computers & Structures* Vol. 58, No. 4, 1996, pp. 747-755.
21. Yu Tang, "Active Control of SDF Systems Using Artificial Neural Networks" *Computers & Structures* Vol. 60, No. 5, 1996, pp. 695-703.
22. Freeman J. A. and Skapura D. M., "Neural Networks : Algorithms, Applications, and Programming Techniques ", Addison-Wesley Publishing Company, 1991.
23. Wong Y. C., " Interaction between Floor Slabs and Shear Walls in Tall Building" Ph. D. thesis, University of Strathclyde, 1979 [Adopted from Ref. 2]
24. Neville A. M., "Properties of Concrete", Third Edition, Longmont Scientific and Technical, U. K., 1981.
25. Thomson A., Brown J. C., Kay J. W. and Titterington D. M., "A Study of Methods of Choosing the Smoothing Parameter un Image Restoration by Regularisation," *IEEE Trans. Pattern Anal. Machine Intell.*, Vol. 13, No.4, pp. 326-339,1991.

# **APPENDIX - A**

# INPUT FILE FOR ANN FOR PLANE WALL CONFIGURATIONS

INPUT				OUTPUT
Y/X	L/X	L/1.6Y	t/Y	Y <sub>o</sub> /Y
0.6000	0.9167	0.9549	0.0694	0.7733
0.6000	0.9167	0.9549	0.0556	0.7665
0.6000	0.9167	0.9549	0.0417	0.7595
0.6000	0.9167	0.9549	0.0278	0.7525
0.6000	0.8333	0.8681	0.0556	0.7431
0.6000	0.8333	0.8681	0.0417	0.7355
0.6000	0.8333	0.8681	0.0278	0.7278
0.6000	0.8333	0.8681	0.0139	0.7199
0.6000	0.7500	0.7813	0.0694	0.7229
0.6000	0.7500	0.7813	0.0417	0.7061
0.6000	0.7500	0.7813	0.0278	0.6975
0.6000	0.7500	0.7813	0.0139	0.6888
0.6000	0.6667	0.6944	0.0694	0.6883
0.6000	0.6667	0.6944	0.0556	0.6789
0.6000	0.6667	0.6944	0.0417	0.6694
0.6000	0.6667	0.6944	0.0278	0.6597
0.6000	0.6667	0.6944	0.0139	0.6499
0.6000	0.5833	0.6076	0.0556	0.6330
0.6000	0.5833	0.6076	0.0417	0.6221
0.6000	0.5833	0.6076	0.0278	0.6111
0.6000	0.5833	0.6076	0.0139	0.6027
0.6000	0.5000	0.5208	0.0694	0.6043
0.6000	0.5000	0.5208	0.0556	0.5948
0.6000	0.5000	0.5208	0.0417	0.5851
0.6000	0.5000	0.5208	0.0278	0.5754
0.6000	0.5000	0.5208	0.0139	0.5655
0.6000	0.4167	0.4340	0.0694	0.5566
0.6000	0.4167	0.4340	0.0556	0.5458
0.6000	0.4167	0.4340	0.0417	0.5348
0.6000	0.4167	0.4340	0.0278	0.5238
0.6000	0.4167	0.4340	0.0139	0.5127
0.6000	0.3333	0.3472	0.0694	0.4923
0.6000	0.3333	0.3472	0.0556	0.4804
0.6000	0.3333	0.3472	0.0417	0.4684
0.6000	0.3333	0.3472	0.0278	0.4563
0.6000	0.3333	0.3472	0.0139	0.4442
0.6000	0.2500	0.2604	0.0694	0.4115
0.6000	0.2500	0.2604	0.0556	0.3987

INPUT				OUTPUT
Y/X	L/X	L/1.6Y	t/Y	Y <sub>e</sub> /Y
0.6000	0.1667	0.1736	0.0417	0.2872
0.6000	0.1667	0.1736	0.0278	0.2738
0.6000	0.1667	0.1736	0.0139	0.2604
0.6000	0.0833	0.0868	0.0694	0.2000
0.6000	0.0833	0.0868	0.0556	0.1863
0.6000	0.0833	0.0868	0.0417	0.1725
0.6000	0.0833	0.0868	0.0278	0.1587
0.6000	0.0833	0.0868	0.0139	0.1450
0.6000	0.2500	0.2604	0.0417	0.3859
0.6000	0.2500	0.2604	0.0278	0.3730
0.6000	0.2500	0.2604	0.0139	0.3601
0.6000	0.1667	0.1736	0.0694	0.3141
0.6000	0.1667	0.1736	0.0556	0.3007
0.8333	0.0833	0.0625	0.0100	0.1060
0.8333	0.0833	0.0625	0.0300	0.1259
0.8333	0.0833	0.0625	0.0400	0.1358
0.8333	0.0833	0.0625	0.0500	0.1458
0.8333	0.1667	0.1250	0.0200	0.2037
0.8333	0.1667	0.1250	0.0300	0.2135
0.8333	0.1667	0.1250	0.0400	0.2233
0.8333	0.1667	0.1250	0.0500	0.2332
0.8333	0.2500	0.1875	0.0100	0.2736
0.8333	0.2500	0.1875	0.0200	0.2833
0.8333	0.2500	0.1875	0.0300	0.2929
0.8333	0.2500	0.1875	0.0500	0.3121
0.8333	0.3333	0.2500	0.0100	0.3454
0.8333	0.3333	0.2500	0.0200	0.3547
0.8333	0.3333	0.2500	0.0300	0.3640
0.8333	0.3333	0.2500	0.0400	0.3733
0.8333	0.4167	0.3125	0.0100	0.4090
0.8333	0.4167	0.3125	0.0200	0.4180
0.8333	0.4167	0.3125	0.0400	0.4358
0.8333	0.4167	0.3125	0.0500	0.4447
0.8333	0.5000	0.3750	0.0200	0.4731
0.8333	0.5000	0.3750	0.0300	0.4815
0.8333	0.5000	0.3750	0.0400	0.4900
0.8333	0.5000	0.3750	0.0500	0.4984
0.8333	0.5833	0.4375	0.0100	0.5120
0.8333	0.5833	0.4375	0.0200	0.5200
0.8333	0.5833	0.4375	0.0300	0.5279
0.8333	0.5833	0.4375	0.0500	0.5437

INPUT				OUTPUT
Y/X	L/X	L/1.6Y	t/Y	Y/Y
0.8333	0.6667	0.5000	0.0100	0.5514
0.8333	0.6667	0.5000	0.0200	0.5588
0.8333	0.6667	0.5000	0.0300	0.5661
0.8333	0.6667	0.5000	0.0400	0.5733
0.8333	0.6667	0.5000	0.0500	0.5805
0.8333	0.7500	0.5625	0.0100	0.5827
0.8333	0.7500	0.5625	0.0200	0.5894
0.8333	0.7500	0.5625	0.0300	0.5960
0.8333	0.7500	0.5625	0.0400	0.6025
0.8333	0.7500	0.5625	0.0500	0.6089
0.8333	0.8333	0.6250	0.0100	0.6080
0.8333	0.8333	0.6250	0.0200	0.6158
0.8333	0.8333	0.6250	0.0300	0.6236
0.8333	0.8333	0.6250	0.0400	0.6314
0.8333	0.9167	0.6875	0.0200	0.6508
0.8333	0.9167	0.6875	0.0300	0.6579
0.8333	0.9167	0.6875	0.0400	0.6649
0.8333	0.9167	0.6875	0.0500	0.6718
0.9999	0.0833	0.0521	0.0083	0.0889
0.9999	0.0833	0.0521	0.0167	0.0972
0.9999	0.0833	0.0521	0.0250	0.1055
0.9999	0.0833	0.0521	0.0333	0.1138
0.9999	0.1667	0.1042	0.0250	0.1803
0.9999	0.1667	0.1042	0.0333	0.1885
0.9999	0.1667	0.1042	0.0417	0.1967
0.9999	0.2500	0.1562	0.0083	0.2331
0.9999	0.2500	0.1562	0.0167	0.2412
0.9999	0.2500	0.1562	0.0250	0.2494
0.9999	0.2500	0.1562	0.0417	0.2656
0.9999	0.3333	0.2083	0.0083	0.2968
0.9999	0.3333	0.2083	0.0167	0.3048
0.9999	0.3333	0.2083	0.0250	0.3127
0.9999	0.3333	0.2083	0.0333	0.3207
0.9999	0.3333	0.2083	0.0417	0.3286
0.9999	0.4167	0.2604	0.0083	0.3550
0.9999	0.4167	0.2604	0.0167	0.3627
0.9999	0.4167	0.2604	0.0250	0.3704
0.9999	0.4167	0.2604	0.0333	0.3782
0.9999	0.4167	0.2604	0.0417	0.3859
0.9999	0.5000	0.3125	0.0083	0.4075
0.9999	0.5000	0.3125	0.0167	0.4150

INPUT				OUTPUT
Y/X	L/X	L/1.6Y	t/Y	Y <sub>o</sub> /Y
0.9999	0.5000	0.3125	0.0250	0.4224
0.9999	0.5000	0.3125	0.0333	0.4299
0.9999	0.5000	0.3125	0.0417	0.4373
0.9999	0.5833	0.3646	0.0083	0.4544
0.9999	0.5833	0.3646	0.0167	0.4616
0.9999	0.5833	0.3646	0.0250	0.4687
0.9999	0.5833	0.3646	0.0333	0.4759
0.9999	0.5833	0.3646	0.0417	0.4830
0.9999	0.6667	0.4167	0.0083	0.4957
0.9999	0.6667	0.4167	0.0167	0.5025
0.9999	0.6667	0.4167	0.0250	0.5093
0.9999	0.6667	0.4167	0.0333	0.5161
0.9999	0.7500	0.4688	0.0167	0.5379
0.9999	0.7500	0.4688	0.0250	0.5442
0.9999	0.7500	0.4688	0.0333	0.5506
0.9999	0.7500	0.4688	0.0417	0.5569
0.9999	0.8333	0.5208	0.0083	0.5616
0.9999	0.8333	0.5208	0.0167	0.5675
0.9999	0.8333	0.5208	0.0250	0.5734
0.9999	0.8333	0.5208	0.0417	0.5851
0.9999	0.9167	0.5729	0.0083	0.5861
0.9999	0.9167	0.5729	0.0167	0.5915
0.9999	0.9167	0.5729	0.0333	0.6023
0.9999	0.9167	0.5729	0.0417	0.6076
0.6000	0.1250	0.1302	0.0208	0.2114
0.6000	0.1250	0.1302	0.0417	0.2319
0.6000	0.1250	0.1302	0.0833	0.2727
0.6000	0.1250	0.1302	0.1042	0.2931
0.6000	0.2500	0.2604	0.0208	0.3666
0.6000	0.2500	0.2604	0.0625	0.4051
0.6000	0.2500	0.2604	0.0833	0.4242
0.6000	0.2500	0.2604	0.1042	0.4433
0.6000	0.3750	0.3906	0.0417	0.5036
0.6000	0.3750	0.3906	0.0625	0.5208
0.6000	0.3750	0.3906	0.0833	0.5379
0.6000	0.3750	0.3906	0.1042	0.5547
0.6000	0.5000	0.5208	0.0208	0.5705
0.6000	0.5000	0.5208	0.0417	0.5851
0.6000	0.5000	0.5208	0.0833	0.6136
0.6000	0.5000	0.5208	0.1042	0.6274
0.6000	0.6250	0.6510	0.0208	0.6318

INPUT				OUTPUT
Y/X	L/X	L/1.6Y	t/Y	Y <sub>o</sub> /Y
0.6000	0.6250	0.6510	0.0625	0.6625
0.6000	0.6250	0.6510	0.0833	0.6773
0.6000	0.6250	0.6510	0.1042	0.6918
0.6000	0.7500	0.7812	0.0208	0.6932
0.6000	0.7500	0.7812	0.0417	0.7061
0.6000	0.7500	0.7812	0.0833	0.7311
0.6000	0.7500	0.7812	0.1042	0.7432
0.6000	0.8750	0.9115	0.0208	0.7370
0.6000	0.8750	0.9115	0.0625	0.7589
0.6000	0.8750	0.9115	0.0833	0.7695
0.6000	0.8750	0.9115	0.1042	0.7799
0.8000	0.1250	0.0977	0.0156	0.1620
0.8000	0.1250	0.0977	0.0469	0.1929
0.8000	0.1250	0.0977	0.0625	0.2083
0.8000	0.1250	0.0977	0.0781	0.2238
0.8000	0.2500	0.1953	0.0156	0.2884
0.8000	0.2500	0.1953	0.0312	0.3034
0.8000	0.2500	0.1953	0.0625	0.3333
0.8000	0.2500	0.1953	0.0781	0.3483
0.8000	0.3750	0.2930	0.0156	0.3951
0.8000	0.3750	0.2930	0.0312	0.4093
0.8000	0.3750	0.2930	0.0469	0.4234
0.8000	0.3750	0.2930	0.0781	0.4515
0.8000	0.5000	0.3906	0.0156	0.4819
0.8000	0.5000	0.3906	0.0312	0.4950
0.8000	0.5000	0.3906	0.0469	0.5079
0.8000	0.5000	0.3906	0.0625	0.5208
0.8000	0.6250	0.4883	0.0312	0.5605
0.8000	0.6250	0.4883	0.0469	0.5720
0.8000	0.6250	0.4883	0.0625	0.5833
0.8000	0.6250	0.4883	0.0781	0.5945
0.8000	0.7500	0.5859	0.0156	0.5960
0.8000	0.7500	0.5859	0.0312	0.6058
0.8000	0.7500	0.5859	0.0469	0.6155
0.8000	0.7500	0.5859	0.0625	0.6250
0.8000	0.8750	0.6836	0.0312	0.6568
0.8000	0.8750	0.6836	0.0469	0.6678
0.8000	0.8750	0.6836	0.0625	0.6786
0.8000	0.8750	0.6836	0.0781	0.6892
0.9999	0.1250	0.0781	0.0125	0.1312
0.9999	0.1250	0.0781	0.0375	0.1560



INPUT				OUTPUT
Y/X	L/X	L/1.6Y	t/Y	Y/Y
0.9999	0.1250	0.0781	0.0500	0.1684
0.9999	0.1250	0.0781	0.0625	0.1808
0.9999	0.2500	0.1562	0.0125	0.2372
0.9999	0.2500	0.1562	0.0250	0.2494
0.9999	0.2500	0.1562	0.0375	0.2615
0.9999	0.2500	0.1562	0.0625	0.2858
0.9999	0.3750	0.2344	0.0125	0.3305
0.9999	0.3750	0.2344	0.0250	0.3423
0.9999	0.3750	0.2344	0.0375	0.3541
0.9999	0.3750	0.2344	0.0500	0.3658
0.9999	0.5000	0.3125	0.0125	0.4112
0.9999	0.5000	0.3125	0.0250	0.4224
0.9999	0.5000	0.3125	0.0375	0.4336
0.9999	0.5000	0.3125	0.0500	0.4447
0.9999	0.7500	0.4688	0.0125	0.5347
0.9999	0.7500	0.4688	0.0250	0.5442
0.9999	0.7500	0.4688	0.0375	0.5537
0.9999	0.7500	0.4688	0.0625	0.5725
0.9999	0.8750	0.5469	0.0125	0.5774
0.9999	0.8750	0.5469	0.0250	0.5859
0.9999	0.8750	0.5469	0.0375	0.5943
0.9999	0.8750	0.5469	0.0625	0.6108
0.6000	0.0625	0.0651	0.0104	0.1102
0.6000	0.0625	0.0651	0.0312	0.1309
0.6000	0.0625	0.0651	0.0417	0.1413
0.6000	0.0625	0.0651	0.0521	0.1517
0.6000	0.1875	0.1953	0.0104	0.2834
0.6000	0.1875	0.1953	0.0312	0.3034
0.6000	0.1875	0.1953	0.0417	0.3134
0.6000	0.1875	0.1953	0.0521	0.3234
0.6000	0.3125	0.3255	0.0104	0.4216
0.6000	0.3125	0.3255	0.0208	0.4309
0.6000	0.3125	0.3255	0.0312	0.4401
0.6000	0.3125	0.3255	0.0521	0.4584
0.6000	0.4375	0.4557	0.0104	0.5247
0.6000	0.4375	0.4557	0.0208	0.5328
0.6000	0.4375	0.4557	0.0312	0.5409
0.6000	0.4375	0.4557	0.0417	0.5489
0.6000	0.5625	0.5859	0.0208	0.5993
0.6000	0.5625	0.5859	0.0312	0.6058
0.6000	0.5625	0.5859	0.0417	0.6123

INPUT				OUTPUT
Y/X	L/X	L/1.6Y	t/Y	Y <sub>o</sub> /Y
0.6000	0.5625	0.5859	0.0521	0.6187
0.6000	0.6875	0.7161	0.0312	0.6724
0.6000	0.6875	0.7161	0.0417	0.6794
0.6000	0.6875	0.7161	0.0521	0.6863
0.6000	0.8125	0.8464	0.0104	0.7107
0.6000	0.8125	0.8464	0.0208	0.7168
0.6000	0.8125	0.8464	0.0417	0.7287
0.6000	0.8125	0.8464	0.0521	0.7346
0.6000	0.9375	0.9766	0.0104	0.7493
0.6000	0.9375	0.9766	0.0208	0.7546
0.6000	0.9375	0.9766	0.0312	0.7597
0.6000	0.9375	0.9766	0.0417	0.7649
0.8000	0.0625	0.0488	0.0156	0.0913
0.8000	0.0625	0.0488	0.0234	0.0991
0.8000	0.0625	0.0488	0.0312	0.1069
0.8000	0.0625	0.0488	0.0391	0.1146
0.8000	0.1875	0.1465	0.0078	0.2200
0.8000	0.1875	0.1465	0.0234	0.2353
0.8000	0.1875	0.1465	0.0312	0.2429
0.8000	0.1875	0.1465	0.0391	0.2506
0.8000	0.3125	0.2441	0.0078	0.3369
0.8000	0.3125	0.2441	0.0156	0.3442
0.8000	0.3125	0.2441	0.0234	0.3516
0.8000	0.3125	0.2441	0.0312	0.3589
0.8000	0.4375	0.3418	0.0156	0.4410
0.8000	0.4375	0.3418	0.0234	0.4478
0.8000	0.4375	0.3418	0.0312	0.4546
0.8000	0.4375	0.3418	0.0391	0.4614
0.8000	0.5625	0.4395	0.0078	0.5116
0.8000	0.5625	0.4395	0.0156	0.5179
0.8000	0.5625	0.4395	0.0312	0.5302
0.8000	0.5625	0.4395	0.0391	0.5364
0.8000	0.6875	0.5371	0.0156	0.5749
0.8000	0.6875	0.5371	0.0234	0.5803
0.8000	0.6875	0.5371	0.0312	0.5857
0.8000	0.6875	0.5371	0.0391	0.5910
0.8000	0.8125	0.6348	0.0078	0.6123
0.8000	0.8125	0.6348	0.0156	0.6184
0.8000	0.8125	0.6348	0.0234	0.6244
0.8000	0.8125	0.6348	0.0312	0.6304
0.8000	0.9375	0.7324	0.0156	0.6693

INPUT				OUTPUT
Y/X	L/X	L/1.6Y	t/Y	Y <sub>c</sub> /Y
0.8000	0.9375	0.7324	0.0234	0.6745
0.8000	0.9375	0.7324	0.0312	0.6797
0.8000	0.9375	0.7324	0.0391	0.6848
0.9999	0.0625	0.0391	0.0063	0.0672
0.9999	0.0625	0.0391	0.0125	0.0734
0.9999	0.0625	0.0391	0.0250	0.0859
0.9999	0.0625	0.0391	0.0312	0.0921
0.9999	0.1875	0.1172	0.0063	0.1796
0.9999	0.1875	0.1172	0.0188	0.1919
0.9999	0.1875	0.1172	0.0250	0.1981
0.9999	0.1875	0.1172	0.0312	0.2042
0.9999	0.3125	0.1953	0.0063	0.2794
0.9999	0.3125	0.1953	0.0125	0.2854
0.9999	0.3125	0.1953	0.0188	0.2914
0.9999	0.3125	0.1953	0.0312	0.3034
0.9999	0.4375	0.2734	0.0063	0.3667
0.9999	0.4375	0.2734	0.0188	0.3782
0.9999	0.4375	0.2734	0.0250	0.3840
0.9999	0.4375	0.2734	0.0312	0.3897
0.9999	0.5625	0.3516	0.0063	0.4414
0.9999	0.5625	0.3516	0.0125	0.4468
0.9999	0.5625	0.3516	0.0188	0.4523
0.9999	0.5625	0.3516	0.0312	0.4631
0.9999	0.6875	0.4297	0.0063	0.5035
0.9999	0.6875	0.4297	0.0125	0.5085
0.9999	0.6875	0.4297	0.0188	0.5136
0.9999	0.6875	0.4297	0.0250	0.5186
0.9999	0.8125	0.5078	0.0125	0.5576
0.9999	0.8125	0.5078	0.0188	0.5621
0.9999	0.8125	0.5078	0.0250	0.5667
0.9999	0.8125	0.5078	0.0312	0.5712
0.9999	0.9375	0.5859	0.0063	0.5900
0.9999	0.9375	0.5859	0.0188	0.5980
0.9999	0.9375	0.5859	0.0250	0.6019
0.9999	0.9375	0.5859	0.0312	0.6058

## NETWORK WEIGHTS AND BIAS

Weights between input layer and hidden layer				Bias
$W_{11}^h = 0.449022$	$W_{12}^h = 5.854579$	$W_{13}^h = 5.730213$	$W_{14}^h = 5.703676$	0.741966
$W_{21}^h = -0.273461$	$W_{22}^h = -0.015850$	$W_{23}^h = -0.271046$	$W_{24}^h = 0.166977$	-0.568017
$W_{31}^h = -0.819033$	$W_{32}^h = -0.015588$	$W_{33}^h = 0.758726$	$W_{34}^h = 0.515037$	-0.816233
$W_{41}^h = -0.867501$	$W_{42}^h = 0.309323$	$W_{43}^h = 0.786244$	$W_{44}^h = 0.842238$	-0.930521
$W_{51}^h = 0.387922$	$W_{52}^h = 0.150351$	$W_{53}^h = -0.544479$	$W_{54}^h = -1.793884$	-0.556328
$W_{61}^h = -0.714520$	$W_{62}^h = -0.307530$	$W_{63}^h = -0.244367$	$W_{64}^h = 0.008941$	-0.460839
$W_{71}^h = -0.298631$	$W_{72}^h = -0.799401$	$W_{73}^h = -0.483834$	$W_{74}^h = -1.260038$	-0.773212
$W_{81}^h = -0.199060$	$W_{82}^h = -0.620726$	$W_{83}^h = 0.015931$	$W_{84}^h = -0.786501$	-0.334915
$W_{91}^h = -0.725541$	$W_{92}^h = -0.252499$	$W_{93}^h = -0.619560$	$W_{94}^h = 0.576299$	-0.171466
$W_{101}^h = -0.091051$	$W_{102}^h = -0.425930$	$W_{103}^h = -0.539212$	$W_{104}^h = -0.539088$	-0.067252
$W_{111}^h = 0.953866$	$W_{112}^h = -2.426488$	$W_{113}^h = -2.583926$	$W_{114}^h = -2.600847$	-1.109742
$W_{121}^h = 0.379280$	$W_{122}^h = 0.100271$	$W_{123}^h = -1.185476$	$W_{124}^h = -1.092074$	0.066256
$W_{131}^h = -0.422178$	$W_{132}^h = -0.980399$	$W_{133}^h = -0.546517$	$W_{134}^h = 0.010941$	-0.285676
$W_{141}^h = 0.391672$	$W_{142}^h = 0.551259$	$W_{143}^h = -0.686205$	$W_{144}^h = -2.608370$	-0.814778
$W_{151}^h = -0.369621$	$W_{152}^h = -0.430251$	$W_{153}^h = -0.260492$	$W_{154}^h = -0.061971$	-0.702564

Weights between hidden layer and output layer	Bias
$W_{11}^o = 5.014238$	-1.642177
$W_{12}^o = -0.243044$	
$W_{13}^o = 0.381613$	
$W_{14}^o = 0.684880$	
$W_{15}^o = -1.547807$	
$W_{16}^o = -0.412582$	
$W_{17}^o = -1.611403$	
$W_{18}^o = -0.927998$	
$W_{19}^o = -0.316539$	
$W_{110}^o = -0.936209$	
$W_{111}^o = -2.864733$	
$W_{112}^o = -1.399910$	
$W_{113}^o = -0.955594$	
$W_{114}^o = -2.053954$	
$W_{115}^o = -0.568204$	

# **APPENDIX - B**

**INPUT FILE FOR ANN FOR FLANGED WALL  
CONFIGURATIONS**

INPUT				OUTPUT
Y/X	L/X	L/2.5Y	Z/Y	Y <sub>o</sub> /Y
0.0833	0.0833	0.4000	0.1000	0.6760
0.1667	0.0833	0.2000	0.0500	0.4447
0.1667	0.2500	0.6000	0.0500	0.7593
0.2500	0.0833	0.1333	0.0333	0.3207
0.2500	0.2500	0.4000	0.0333	0.6262
0.2500	0.4167	0.6667	0.0333	0.7757
0.2500	0.5833	0.9333	0.0333	0.8398
0.3333	0.0833	0.1000	0.0250	0.2494
0.3333	0.4167	0.5000	0.0250	0.6958
0.3333	0.5833	0.7000	0.0250	0.7827
0.3333	0.7500	0.9000	0.0250	0.8310
0.4167	0.0833	0.0800	0.0200	0.2037
0.4167	0.2500	0.2400	0.0200	0.4731
0.4167	0.5833	0.5600	0.0200	0.7256
0.4167	0.7500	0.7200	0.0200	0.7866
0.5000	0.0833	0.0667	0.0167	0.1720
0.5000	0.2500	0.2000	0.0167	0.4150
0.5000	0.4167	0.3333	0.0167	0.5675
0.5000	0.5833	0.4667	0.0167	0.6685
0.5000	0.7500	0.6000	0.0167	0.7421
0.5833	0.0833	0.0571	0.0143	0.1489
0.5833	0.2500	0.1714	0.0143	0.3683
0.5833	0.5833	0.4000	0.0143	0.6113
0.5833	0.7500	0.5143	0.0143	0.6977
0.6667	0.0833	0.0500	0.0125	0.1312
0.6667	0.2500	0.1500	0.0125	0.3305
0.6667	0.4167	0.2500	0.0125	0.4793
0.6667	0.7500	0.4500	0.0125	0.6533
0.7500	0.0833	0.0444	0.0111	0.1172
0.7500	0.2500	0.1333	0.0111	0.2995
0.7500	0.4167	0.2222	0.0111	0.4418
0.7500	0.7500	0.4000	0.0111	0.6088
0.0833	0.0833	0.4000	0.3000	0.8040
0.1667	0.0833	0.2000	0.1500	0.5324
0.1667	0.2500	0.6000	0.1500	0.8073
0.2500	0.0833	0.1333	0.1000	0.3840
0.2500	0.2500	0.4000	0.1000	0.6760

INPUT				OUTPUT
Y/X	L/X	L/2.5Y	Z/Y	Y <sub>2</sub> /Y
0.2500	0.4167	0.6667	0.1000	0.8056
0.2500	0.5833	0.9333	0.1000	0.8611
0.3333	0.0833	0.1000	0.0750	0.2980
0.3333	0.4167	0.5000	0.0750	0.7262
0.3333	0.5833	0.7000	0.0750	0.8044
0.3333	0.7500	0.9000	0.0750	0.8479
0.4167	0.0833	0.0800	0.0600	0.2430
0.4167	0.2500	0.2400	0.0600	0.5068
0.4167	0.5833	0.5600	0.0600	0.7475
0.4167	0.7500	0.7200	0.0600	0.8036
0.5000	0.0833	0.0667	0.0500	0.2050
0.5000	0.2500	0.2000	0.0500	0.4447
0.5000	0.5833	0.4667	0.0500	0.6906
0.5000	0.7500	0.6000	0.0500	0.7593
0.5833	0.0833	0.0571	0.0429	0.1772
0.5833	0.2500	0.1714	0.0429	0.3947
0.5833	0.5833	0.4000	0.0429	0.6336
0.5833	0.7500	0.5143	0.0429	0.7150
0.6667	0.0833	0.0500	0.0375	0.1560
0.6667	0.2500	0.1500	0.0375	0.3541
0.6667	0.4167	0.2500	0.0375	0.5002
0.6667	0.7500	0.4500	0.0375	0.6706
0.7500	0.0833	0.0444	0.0333	0.1393
0.7500	0.2500	0.1333	0.0333	0.3207
0.7500	0.4167	0.2222	0.0333	0.4612
0.7500	0.5833	0.3111	0.0333	0.5608
0.7500	0.7500	0.4000	0.0333	0.6262
0.0833	0.0833	0.4000	0.5000	0.9000
0.1667	0.0833	0.2000	0.2500	0.6167
0.1667	0.2500	0.6000	0.2500	0.8500
0.0917	0.0833	0.3636	0.9091	0.9964
0.1667	0.0833	0.2000	0.2500	0.6167
0.1667	0.2500	0.6000	0.2500	0.8500
0.1667	0.0833	0.2000	0.5000	0.8000
0.1667	0.2500	0.6000	0.5000	0.9333
0.1667	0.0833	0.2000	0.7500	0.9500
0.1667	0.2500	0.6000	0.7500	0.9833
0.2500	0.0833	0.1333	0.1667	0.4467
0.2500	0.2500	0.4000	0.1667	0.7222
0.2500	0.4167	0.6667	0.1667	0.8333
0.2500	0.5833	0.9333	0.1667	0.8810
0.3333	0.0833	0.1000	0.1250	0.3464

INPUT				OUTPUT
Y/X	L/X	L/2.5Y	Z/Y	Y <sub>o</sub> /Y
0.3333	0.2500	0.3000	0.1250	0.6179
0.3333	0.5833	0.7000	0.1250	0.8250
0.4167	0.0833	0.0800	0.1000	0.2822
0.4167	0.2500	0.2400	0.1000	0.5400
0.4167	0.4167	0.4000	0.1000	0.6760
0.4167	0.5833	0.5600	0.1000	0.7686
0.5000	0.0833	0.0667	0.0833	0.2379
0.5000	0.2500	0.2000	0.0833	0.4742
0.5000	0.4167	0.3333	0.0833	0.6136
0.5000	0.5833	0.4667	0.0833	0.7119
0.5833	0.0833	0.0571	0.0714	0.2055
0.5833	0.2500	0.1714	0.0714	0.4209
0.5833	0.4167	0.2857	0.0714	0.5659
0.5833	0.5833	0.4000	0.0714	0.6551
0.6667	0.0833	0.0500	0.0625	0.1808
0.6667	0.2500	0.1500	0.0625	0.3775
0.6667	0.4167	0.2500	0.0625	0.5208
0.6667	0.5833	0.3500	0.0625	0.6108
0.7500	0.0833	0.0444	0.0556	0.1614
0.7500	0.2500	0.1333	0.0556	0.3418
0.7500	0.5833	0.3111	0.0556	0.5771
0.7500	0.7500	0.4000	0.0556	0.6432
0.2500	0.0833	0.1333	0.3333	0.6000
0.2500	0.2500	0.4000	0.3333	0.8222
0.2500	0.4167	0.6667	0.3333	0.8933
0.2500	0.5833	0.9333	0.3333	0.9238
0.3333	0.0833	0.1000	0.2500	0.4667
0.3333	0.4167	0.5000	0.2500	0.8200
0.3333	0.5833	0.7000	0.2500	0.8714
0.4167	0.0833	0.0800	0.2000	0.3800
0.4167	0.2500	0.2400	0.2000	0.6200
0.4167	0.4167	0.4000	0.2000	0.7440
0.4167	0.5833	0.5600	0.2000	0.8171
0.5000	0.0833	0.0667	0.1667	0.3200
0.5000	0.2500	0.2000	0.1667	0.5467
0.5000	0.4167	0.3333	0.1667	0.6667
0.5000	0.5833	0.4667	0.1667	0.7619
0.5833	0.0833	0.0571	0.1429	0.2762
0.5833	0.2500	0.1714	0.1429	0.4857
0.5833	0.4167	0.2857	0.1429	0.6190
0.5833	0.5833	0.4000	0.1429	0.7061



INPUT				OUTPUT
Y/X	L/X	L/2.5Y	Z/Y	Y <sub>J</sub> /Y
0.6667	0.0833	0.0500	0.1250	0.2429
0.6667	0.2500	0.1500	0.1250	0.4357
0.6667	0.4167	0.2500	0.1250	0.5714
0.6667	0.5833	0.3500	0.1250	0.6500
0.7500	0.0833	0.0444	0.1111	0.2167
0.7500	0.2500	0.1333	0.1111	0.3944
0.7500	0.4167	0.2222	0.1111	0.5278
0.7500	0.5833	0.3111	0.1111	0.6167
0.7500	0.7500	0.4000	0.1111	0.6840
0.2500	0.0833	0.1333	0.5000	0.7444
0.2500	0.2500	0.4000	0.5000	0.9000
0.2500	0.4167	0.6667	0.5000	0.9400
0.2500	0.5833	0.9333	0.5000	0.9571
0.3333	0.0833	0.1000	0.3750	0.5850
0.3333	0.2500	0.3000	0.3750	0.7917
0.3333	0.4167	0.5000	0.3750	0.8750
0.3333	0.5833	0.7000	0.3750	0.9107
0.4167	0.0833	0.0800	0.3000	0.4771
0.4167	0.2500	0.2400	0.3000	0.6943
0.4167	0.4167	0.4000	0.3000	0.8040
0.4167	0.5833	0.5600	0.3000	0.8600
0.5000	0.0833	0.0667	0.2500	0.4019
0.5000	0.2500	0.2000	0.2500	0.6167
0.5000	0.4167	0.3333	0.2500	0.7300
0.5000	0.5833	0.4667	0.2500	0.8071
0.5833	0.0833	0.0571	0.2143	0.3468
0.5833	0.2500	0.1714	0.2143	0.5494
0.5833	0.4167	0.2857	0.2143	0.6688
0.5833	0.5833	0.4000	0.2143	0.7531
0.6667	0.0833	0.0500	0.1875	0.3048
0.6667	0.2500	0.1500	0.1875	0.4933
0.6667	0.4167	0.2500	0.1875	0.6202
0.6667	0.5833	0.3500	0.1875	0.6982
0.7500	0.0833	0.0444	0.1667	0.2719
0.7500	0.2500	0.1333	0.1667	0.4467
0.7500	0.4167	0.2222	0.1667	0.5741
0.7500	0.5833	0.3111	0.1667	0.6541
0.7500	0.7500	0.4000	0.1667	0.7222
0.2500	0.0833	0.1333	0.6667	0.8667
0.2500	0.2500	0.4000	0.6667	0.9556
0.2500	0.4167	0.6667	0.6667	0.9733

INPUT				OUTPUT
Y/X	L/X	L/2.5Y	Z/Y	Y <sub>2</sub> /Y
0.2500	0.5833	0.9333	0.6667	0.9810
0.3333	0.0833	0.1000	0.5000	0.7000
0.3333	0.2500	0.3000	0.5000	0.8667
0.3333	0.4167	0.5000	0.5000	0.9200
0.3333	0.5833	0.7000	0.5000	0.9429
0.4167	0.0833	0.0800	0.4000	0.5733
0.4167	0.2500	0.2400	0.4000	0.7600
0.4167	0.4167	0.4000	0.4000	0.8560
0.4167	0.5833	0.5600	0.4000	0.8971
0.5000	0.0833	0.0667	0.3333	0.4833
0.5000	0.2500	0.2000	0.3333	0.6833
0.5000	0.4167	0.3333	0.3333	0.7867
0.5000	0.5833	0.4667	0.3333	0.8476
0.5833	0.0833	0.0571	0.2857	0.4171
0.5833	0.2500	0.1714	0.2857	0.6114
0.5833	0.4167	0.2857	0.2857	0.7143
0.5833	0.5833	0.4000	0.2857	0.7959
0.6667	0.0833	0.0500	0.2500	0.3667
0.6667	0.2500	0.1500	0.2500	0.5500
0.6667	0.4167	0.2500	0.2500	0.6667
0.6667	0.5833	0.3500	0.2500	0.7429
0.7500	0.0833	0.0444	0.2222	0.3270
0.7500	0.2500	0.1333	0.2222	0.4984
0.7500	0.4167	0.2222	0.2222	0.6190
0.7500	0.5833	0.3111	0.2222	0.6889
0.7500	0.7500	0.4000	0.2222	0.7580
0.2500	0.0833	0.1333	0.8333	0.9667
0.2500	0.2500	0.4000	0.8333	0.9889
0.2500	0.4167	0.6667	0.8333	0.9933
0.2500	0.5833	0.9333	0.8333	0.9952
0.3333	0.0833	0.1000	0.6250	0.8083
0.3333	0.2500	0.3000	0.6250	0.9250
0.3333	0.4167	0.5000	0.6250	0.9550
0.3333	0.5833	0.7000	0.6250	0.9679
0.4167	0.0833	0.0800	0.5000	0.6680
0.4167	0.2500	0.2400	0.5000	0.8333
0.4167	0.4167	0.4000	0.5000	0.9000
0.4167	0.5833	0.5600	0.5000	0.9286
0.5000	0.0833	0.0667	0.4167	0.5643
0.5000	0.2500	0.2000	0.4167	0.7452
0.5000	0.4167	0.3333	0.4167	0.8367

INPUT				OUTPUT
Y/X	L/X	L/2.5Y	Z/Y	Y <sub>o</sub> /Y
0.5000	0.5833	0.4667	0.4167	0.8833
0.5833	0.0833	0.0571	0.3571	0.4873
0.5833	0.2500	0.1714	0.3571	0.6714
0.5833	0.4167	0.2857	0.3571	0.7686
0.5833	0.5833	0.4000	0.3571	0.8347
0.6667	0.0833	0.0500	0.3125	0.4284
0.6667	0.4167	0.2500	0.3125	0.7102
0.6667	0.5833	0.3500	0.3125	0.7839
0.7500	0.0833	0.0444	0.2778	0.3821
0.7500	0.2500	0.1333	0.2778	0.5496
0.7500	0.4167	0.2222	0.2778	0.6624
0.7500	0.5833	0.3111	0.2778	0.7317
0.7500	0.7500	0.4000	0.2778	0.7914
0.3333	0.0833	0.1000	0.7500	0.9000
0.3333	0.2500	0.3000	0.7500	0.9667
0.3333	0.4167	0.5000	0.7500	0.9800
0.3333	0.5833	0.7000	0.7500	0.9857
0.4167	0.0833	0.0800	0.6000	0.7600
0.4167	0.2500	0.2400	0.6000	0.8933
0.4167	0.4167	0.4000	0.6000	0.9360
0.4167	0.5833	0.5600	0.6000	0.9543
0.5000	0.0833	0.0667	0.5000	0.6444
0.5000	0.4167	0.3333	0.5000	0.8800
0.5000	0.5833	0.4667	0.5000	0.9143
0.5833	0.0833	0.0571	0.4286	0.5571
0.5833	0.2500	0.1714	0.4286	0.7286
0.5833	0.4167	0.2857	0.4286	0.8171
0.5833	0.5833	0.4000	0.4286	0.8694
0.6667	0.0833	0.0500	0.3750	0.4900
0.6667	0.2500	0.1500	0.3750	0.6600
0.6667	0.4167	0.2500	0.3750	0.7500
0.6667	0.5833	0.3500	0.3750	0.8214
0.7500	0.0833	0.0444	0.3333	0.4370
0.7500	0.2500	0.1333	0.3333	0.6000
0.7500	0.4167	0.2222	0.3333	0.7037
0.7500	0.5833	0.3111	0.3333	0.7714
0.7500	0.7500	0.4000	0.3333	0.8222
0.3333	0.0833	0.1000	0.8750	0.9750
0.3333	0.2500	0.3000	0.8750	0.9917
0.3333	0.4167	0.5000	0.8750	0.9950
0.3333	0.5833	0.7000	0.8750	0.9964

INPUT				OUTPUT
Y/X	L/X	L/2.5Y	Z/Y	Y <sub>o</sub> /Y
0.3333	0.7500	0.9000	0.8750	0.9972
0.4167	0.0833	0.0800	0.7000	0.8467
0.4167	0.2500	0.2400	0.7000	0.9400
0.4167	0.4167	0.4000	0.7000	0.9640
0.4167	0.5833	0.5600	0.7000	0.9743
0.4167	0.7500	0.7200	0.7000	0.9800
0.5000	0.0833	0.0667	0.5833	0.7233
0.5000	0.4167	0.3333	0.5833	0.9167
0.5000	0.5833	0.4667	0.5833	0.9405
0.5000	0.7500	0.6000	0.5833	0.9537
0.5833	0.0833	0.0571	0.5000	0.6265
0.5833	0.2500	0.1714	0.5000	0.7816
0.5833	0.4167	0.2857	0.5000	0.8600
0.5833	0.5833	0.4000	0.5000	0.9000
0.5833	0.7500	0.5143	0.5000	0.9222
0.6667	0.0833	0.0500	0.4375	0.5514
0.6667	0.2500	0.1500	0.4375	0.7125
0.6667	0.4167	0.2500	0.4375	0.7975
0.6667	0.5833	0.3500	0.4375	0.8554
0.6667	0.7500	0.4500	0.4375	0.8875
0.7500	0.0833	0.0444	0.3889	0.4919
0.7500	0.2500	0.1333	0.3889	0.6495
0.7500	0.4167	0.2222	0.3889	0.7424
0.7500	0.5833	0.3111	0.3889	0.8079
0.7500	0.7500	0.4000	0.3889	0.8506
0.3750	0.0833	0.0889	0.8889	0.9778
0.3750	0.2500	0.2667	0.8889	0.9926
0.3750	0.5833	0.6222	0.8889	0.9968
0.3750	0.7500	0.8000	0.8889	0.9975
0.5000	0.0833	0.0667	0.6667	0.8000
0.5000	0.2500	0.2000	0.6667	0.9111
0.5000	0.4167	0.3333	0.6667	0.9467
0.5000	0.5833	0.4667	0.6667	0.9619
0.5000	0.7500	0.6000	0.6667	0.9704
0.5833	0.0833	0.0571	0.5714	0.6952
0.5833	0.2500	0.1714	0.5714	0.8286
0.5833	0.4167	0.2857	0.5714	0.8971
0.5833	0.5833	0.4000	0.5714	0.9265
0.5833	0.7500	0.5143	0.5714	0.9429
0.6667	0.0833	0.0500	0.5000	0.6125
0.6667	0.2500	0.1500	0.5000	0.7625

INPUT				OUTPUT
Y/X	L/X	L/2.5Y	Z/Y	Y <sub>e</sub> /Y
0.6667	0.4167	0.2500	0.5000	0.8400
0.6667	0.5833	0.3500	0.5000	0.8857
0.6667	0.7500	0.4500	0.5000	0.9111
0.7500	0.0833	0.0444	0.4444	0.5467
0.7500	0.4167	0.2222	0.4444	0.7778
0.7500	0.5833	0.3111	0.4444	0.8413
0.7500	0.7500	0.4000	0.4444	0.8765
0.8333	0.0833	0.0400	0.0100	0.1060
0.8333	0.0833	0.0400	0.0300	0.1259
0.8333	0.0833	0.0400	0.0500	0.1458
0.8333	0.0833	0.0400	0.1000	0.1956
0.8333	0.0833	0.0400	0.1500	0.2453
0.8333	0.0833	0.0400	0.2000	0.2950
0.8333	0.0833	0.0400	0.2500	0.3447
0.8333	0.0833	0.0400	0.3000	0.3943
0.8333	0.0833	0.0400	0.3500	0.4438
0.8333	0.0833	0.0400	0.4000	0.4933
0.8333	0.2500	0.1200	0.0100	0.2736
0.8333	0.2500	0.1200	0.0300	0.2929
0.8333	0.2500	0.1200	0.0500	0.3121
0.8333	0.2500	0.1200	0.1000	0.3600
0.8333	0.2500	0.1200	0.1500	0.4076
0.8333	0.2500	0.1200	0.2000	0.4550
0.8333	0.2500	0.1200	0.2500	0.5020
0.8333	0.2500	0.1200	0.3000	0.5486
0.8333	0.4167	0.2000	0.0100	0.4090
0.8333	0.4167	0.2000	0.0300	0.4269
0.8333	0.4167	0.2000	0.0500	0.4447
0.8333	0.4167	0.2000	0.1000	0.4889
0.8333	0.4167	0.2000	0.1500	0.5324
0.8333	0.4167	0.2000	0.2000	0.5750
0.8333	0.4167	0.2000	0.2500	0.6167
0.8333	0.4167	0.2000	0.3000	0.6571
0.8333	0.4167	0.2000	0.3500	0.6962
0.8333	0.4167	0.2000	0.4000	0.7333
0.8333	0.5833	0.2800	0.0100	0.5120
0.8333	0.5833	0.2800	0.0300	0.5279
0.8333	0.5833	0.2800	0.0500	0.5437
0.8333	0.5833	0.2800	0.1000	0.5822
0.8333	0.5833	0.2800	0.1500	0.6194
0.8333	0.5833	0.2800	0.2000	0.6550

INPUT				OUTPUT
Y/X	L/X	L/2.5Y	Z/Y	Y <sub>o</sub> /Y
0.8333	0.5833	0.2800	0.2500	0.6887
0.8333	0.5833	0.2800	0.3000	0.7200
0.8333	0.5833	0.2800	0.3500	0.7586
0.8333	0.5833	0.2800	0.4000	0.7943
0.8333	0.7500	0.3600	0.0100	0.5827
0.8333	0.7500	0.3600	0.0300	0.5960
0.8333	0.7500	0.3600	0.0500	0.6089
0.8333	0.7500	0.3600	0.1000	0.6400
0.8333	0.7500	0.3600	0.1500	0.6789
0.8333	0.7500	0.3600	0.2000	0.7156
0.8333	0.7500	0.3600	0.2500	0.7500
0.8333	0.7500	0.3600	0.3000	0.7822
0.8333	0.7500	0.3600	0.3500	0.8122
0.8333	0.7500	0.3600	0.4000	0.8400



## NETWORK WEIGHTS AND BIAS

Weights between input layer and hidden layer				Bias
$W_{11}^h = 1.488627$	$W_{12}^h = 1.976991$	$W_{13}^h = 8.163399$	$W_{14}^h = 0.141912$	1.140950
$W_{21}^h = -0.615855$	$W_{22}^h = 0.214111$	$W_{23}^h = 0.360304$	$W_{24}^h = 1.157274$	-1.685776
$W_{31}^h = -2.738613$	$W_{32}^h = 3.153483$	$W_{33}^h = 3.787693$	$W_{34}^h = 3.196568$	-2.728988
$W_{41}^h = -0.444690$	$W_{42}^h = 0.924305$	$W_{43}^h = 0.302792$	$W_{44}^h = 7.854577$	-8.109278
$W_{51}^h = 0.270132$	$W_{52}^h = -0.099742$	$W_{53}^h = -1.143788$	$W_{54}^h = -1.031389$	-1.536230
$W_{61}^h = -1.297126$	$W_{62}^h = -0.277256$	$W_{63}^h = -0.028983$	$W_{64}^h = -0.015409$	-1.125393
$W_{71}^h = 1.663180$	$W_{72}^h = -2.181187$	$W_{73}^h = -5.225489$	$W_{74}^h = -0.979957$	-0.700361
$W_{81}^h = 0.214940$	$W_{82}^h = 0.144240$	$W_{83}^h = 0.463945$	$W_{84}^h = -2.293488$	-2.046359
$W_{91}^h = -1.359411$	$W_{92}^h = -0.158491$	$W_{93}^h = 0.324259$	$W_{94}^h = 0.906778$	-0.729572
$W_{101}^h = -0.128586$	$W_{102}^h = -0.269310$	$W_{103}^h = -0.553249$	$W_{104}^h = -0.760930$	-1.148345
$W_{111}^h = 0.575870$	$W_{112}^h = -3.931171$	$W_{113}^h = -5.172261$	$W_{114}^h = -7.926411$	-1.638387
$W_{121}^h = 0.102414$	$W_{122}^h = -0.076516$	$W_{123}^h = -1.343205$	$W_{124}^h = -0.938524$	-1.238940
$W_{131}^h = -0.158711$	$W_{132}^h = -0.798186$	$W_{133}^h = -1.353791$	$W_{134}^h = -0.172443$	-1.281352
$W_{141}^h = -1.769211$	$W_{142}^h = 1.418651$	$W_{143}^h = -1.275641$	$W_{144}^h = -3.054893$	2.510835
$W_{151}^h = -0.547203$	$W_{152}^h = -0.319943$	$W_{153}^h = -0.260599$	$W_{154}^h = -0.193454$	-1.381679

Weights between hidden layer and output layer	Bias
$W_{11}^o = 4.033976$	-1.466577
$W_{12}^o = 0.805513$	
$W_{13}^o = 1.189989$	
$W_{14}^o = 6.479342$	
$W_{15}^o = -1.034497$	
$W_{16}^o = 0.495877$	
$W_{17}^o = -2.332311$	
$W_{18}^o = -1.631959$	
$W_{19}^o = 0.882151$	
$W_{110}^o = -0.466208$	
$W_{111}^o = -5.698292$	
$W_{112}^o = -0.728227$	
$W_{113}^o = -0.447718$	
$W_{114}^o = -2.374859$	
$W_{115}^o = -0.051743$	

# **APPENDIX - C**



**INPUT FILE FOR ANN FOR CALCULATION OF CRITICAL  
PERIMETER**

INPUT			OUTPUT
$d/(1.5*t_f)$	$d/(1.5*Z)$	$t_f/W$	$b_p/(40*d)$
0.5000	0.5000	0.4000	0.3185
0.6667	0.6667	0.4000	0.2525
0.8333	0.8333	0.4000	0.2131
1.0000	1.0000	0.4000	0.1870
0.3333	0.5000	0.6000	0.3502
0.4444	0.6667	0.6000	0.2756
0.5556	0.8333	0.6000	0.2311
0.6667	1.0000	0.6000	0.2017
0.2500	0.5000	0.8000	0.3835
0.3333	0.6667	0.8000	0.3000
0.4167	0.8333	0.8000	0.2501
0.5000	1.0000	0.8000	0.2171
0.2000	0.5000	1.0000	0.4185
0.2667	0.6667	1.0000	0.3256
0.3333	0.8333	1.0000	0.2701
0.4000	1.0000	1.0000	0.2333
0.5000	0.2500	0.4000	0.3599
0.6667	0.3333	0.4000	0.2846
0.8333	0.4167	0.4000	0.2397
1.0000	0.5000	0.4000	0.2098
0.3333	0.2500	0.6000	0.3885
0.4444	0.3333	0.6000	0.3055
0.5556	0.4167	0.6000	0.2559
0.6667	0.5000	0.6000	0.2231
0.2500	0.2500	0.8000	0.4185
0.3333	0.3333	0.8000	0.3275
0.4167	0.4167	0.8000	0.2731
0.5000	0.5000	0.8000	0.2370
0.2000	0.2500	1.0000	0.4502
0.2667	0.3333	1.0000	0.3506
0.3333	0.4167	1.0000	0.2911
0.4000	0.5000	1.0000	0.2517
0.5000	0.1667	0.4000	0.4069
0.6667	0.2222	0.4000	0.3208
0.8333	0.2778	0.4000	0.2693

INPUT			OUTPUT
$d/(1.5*t_f)$	$d/(1.5*Z)$	$t_f/W$	$b_p/(40*d)$

1.0000	0.3333	0.4000	0.2351
0.3333	0.1667	0.6000	0.4328
0.4444	0.2222	0.6000	0.3398
0.5556	0.2778	0.6000	0.2841
0.6667	0.3333	0.6000	0.2472
0.2500	0.1667	0.8000	0.4599
0.3333	0.2222	0.8000	0.3596
0.4167	0.2778	0.8000	0.2997
0.5000	0.3333	0.8000	0.2598
0.2000	0.1667	1.0000	0.4885
0.2667	0.2222	1.0000	0.3805
0.3333	0.2778	1.0000	0.3159
0.4000	0.3333	1.0000	0.2731
0.5000	0.1250	0.4000	0.4578
0.6667	0.1667	0.4000	0.3597
0.8333	0.2083	0.4000	0.3010
1.0000	0.2500	0.4000	0.2619
0.3333	0.1250	0.6000	0.4821
0.4444	0.1667	0.6000	0.3776
0.5556	0.2083	0.6000	0.3150
0.6667	0.2500	0.6000	0.2734
0.2500	0.1250	0.8000	0.5069
0.3333	0.1667	0.8000	0.3958
0.4167	0.2083	0.8000	0.3293
0.5000	0.2500	0.8000	0.2851
0.2000	0.1250	1.0000	0.5328
0.2667	0.1667	1.0000	0.4148
0.3333	0.2083	1.0000	0.3441
0.4000	0.2500	1.0000	0.2972
0.5000	0.1000	0.4000	0.4884
0.6667	0.1333	0.4000	0.3837
0.8333	0.1667	0.4000	0.3209
1.0000	0.2000	0.4000	0.2791
0.3333	0.1000	0.6000	0.5354
0.4444	0.1333	0.6000	0.4182
0.5556	0.1667	0.6000	0.3479
0.6667	0.2000	0.6000	0.3012
0.2500	0.1000	0.8000	0.5583
0.3333	0.1333	0.8000	0.4351
0.4167	0.1667	0.8000	0.3612

INPUT			OUTPUT
$d/(1.5*t_f)$	$d/(1.5*Z)$	$t_f/W$	$b_p/(40*d)$

0.5000	0.2000	0.8000	0.3121
0.2000	0.1000	1.0000	0.5821
0.2667	0.1333	1.0000	0.4526
0.3333	0.1667	1.0000	0.3750
0.4000	0.2000	1.0000	0.3234
0.5000	0.5000	0.2667	0.3194
0.6667	0.6667	0.2667	0.2531
0.8333	0.8333	0.2667	0.2136
1.0000	1.0000	0.2667	0.1874
0.3333	0.5000	0.4000	0.3791
0.4444	0.6667	0.4000	0.2972
0.5556	0.8333	0.4000	0.2483
0.6667	1.0000	0.4000	0.2159
0.2500	0.5000	0.5333	0.4282
0.3333	0.6667	0.5333	0.3335
0.4167	0.8333	0.5333	0.2769
0.5000	1.0000	0.5333	0.2393
0.2000	0.5000	0.6667	0.4728
0.2667	0.6667	0.6667	0.3665
0.3333	0.8333	0.6667	0.3029
0.4000	1.0000	0.6667	0.2607
0.5000	0.2500	0.2667	0.4017
0.6667	0.3333	0.2667	0.3156
0.8333	0.4167	0.2667	0.2640
1.0000	0.5000	0.2667	0.2298
0.3333	0.2500	0.4000	0.4701
0.4444	0.3333	0.4000	0.3662
0.5556	0.4167	0.4000	0.3040
0.6667	0.5000	0.4000	0.2627
0.2500	0.2500	0.5333	0.5012
0.3333	0.3333	0.5333	0.3892
0.4167	0.4167	0.5333	0.3221
0.5000	0.5000	0.5333	0.2775
0.2000	0.2500	0.6667	0.5335
0.2667	0.3333	0.6667	0.4129
0.3333	0.4167	0.6667	0.3407
0.4000	0.5000	0.6667	0.2928
0.5000	0.1667	0.2667	0.4351
0.6667	0.2222	0.2667	0.3415

INPUT			OUTPUT
$d/(1.5*t_f)$	$d/(1.5*Z)$	$t_f/W$	$b_p/(40*d)$

0.8333	0.2778	0.2667	0.2856
1.0000	0.3333	0.2667	0.2484
0.3333	0.1667	0.4000	0.5110
0.4444	0.2222	0.4000	0.3976
0.5556	0.2778	0.4000	0.3298
0.6667	0.3333	0.4000	0.2846
0.2500	0.1667	0.5333	0.5400
0.3333	0.2222	0.5333	0.4191
0.4167	0.2778	0.5333	0.3466
0.5000	0.3333	0.5333	0.2984
0.2000	0.1667	0.6667	0.5701
0.2667	0.2222	0.6667	0.4412
0.3333	0.2778	0.6667	0.3640
0.4000	0.3333	0.6667	0.3127
0.5000	0.1250	0.2667	0.4578
0.6667	0.1667	0.2667	0.3597
0.8333	0.2083	0.2667	0.3010
1.0000	0.2500	0.2667	0.2619
0.3333	0.1250	0.4000	0.5558
0.4444	0.1667	0.4000	0.4319
0.5556	0.2083	0.4000	0.3577
0.6667	0.2500	0.4000	0.3083
0.2500	0.1250	0.5333	0.5829
0.3333	0.1667	0.5333	0.4519
0.4167	0.2083	0.5333	0.3735
0.5000	0.2500	0.5333	0.3213
0.2000	0.1250	0.6667	0.6110
0.2667	0.1667	0.6667	0.4726
0.3333	0.2083	0.6667	0.3898
0.4000	0.2500	0.6667	0.3346
0.5000	0.1000	0.2667	0.4884
0.6667	0.1333	0.2667	0.3837
0.8333	0.1667	0.2667	0.3209
1.0000	0.2000	0.2667	0.2791
0.3333	0.1000	0.4000	0.6040
0.4444	0.1333	0.4000	0.4687
0.5556	0.1667	0.4000	0.3876
0.6667	0.2000	0.4000	0.3336
0.2500	0.1000	0.5333	0.6295

INPUT			OUTPUT
$d/(1.5*t_f)$	$d/(1.5*Z)$	$t_f/W$	$b_p/(40*d)$

0.3333	0.1333	0.5333	0.4875
0.4167	0.1667	0.5333	0.4024
0.5000	0.2000	0.5333	0.3458
0.2000	0.1000	0.6667	0.6558
0.2667	0.1333	0.6667	0.5069
0.3333	0.1667	0.6667	0.4177
0.4000	0.2000	0.6667	0.3583
0.5000	0.5000	0.2000	0.3194
0.6667	0.6667	0.2000	0.2531
0.8333	0.8333	0.2000	0.2136
1.0000	1.0000	0.2000	0.1874
0.3333	0.5000	0.3000	0.3791
0.4444	0.6667	0.3000	0.2972
0.5556	0.8333	0.3000	0.2483
0.6667	1.0000	0.3000	0.2159
0.2500	0.5000	0.4000	0.4282
0.3333	0.6667	0.4000	0.3335
0.4167	0.8333	0.4000	0.2769
0.5000	1.0000	0.4000	0.2393
0.2000	0.5000	0.5000	0.4728
0.2667	0.6667	0.5000	0.3665
0.3333	0.8333	0.5000	0.3029
0.4000	1.0000	0.5000	0.2607
0.5000	0.2500	0.2000	0.4017
0.6667	0.3333	0.2000	0.3156
0.8333	0.4167	0.2000	0.2640
1.0000	0.5000	0.2000	0.2298
0.3333	0.2500	0.3000	0.5066
0.4444	0.3333	0.3000	0.3934
0.5556	0.4167	0.3000	0.3257
0.6667	0.5000	0.3000	0.2806
0.2500	0.2500	0.4000	0.5843
0.3333	0.3333	0.4000	0.4512
0.4167	0.4167	0.4000	0.3716
0.5000	0.5000	0.4000	0.3185
0.2000	0.2500	0.5000	0.6168
0.2667	0.3333	0.5000	0.4753
0.3333	0.4167	0.5000	0.3906
0.4000	0.5000	0.5000	0.3342

INPUT			OUTPUT
$d/(1.5*t_f)$	$d/(1.5*Z)$	$t_f/W$	$b_p/(40*d)$

0.5000	0.1667	0.2000	0.4351
0.6667	0.2222	0.2000	0.3415
0.8333	0.2778	0.2000	0.2856
1.0000	0.3333	0.2000	0.2484
0.3333	0.1667	0.3000	0.5744
0.4444	0.2222	0.3000	0.4448
0.5556	0.2778	0.3000	0.3672
0.6667	0.3333	0.3000	0.3156
0.2500	0.1667	0.4000	0.6217
0.3333	0.2222	0.4000	0.4800
0.4167	0.2778	0.4000	0.3950
0.5000	0.3333	0.4000	0.3385
0.2000	0.1667	0.5000	0.6526
0.2667	0.2222	0.5000	0.5028
0.3333	0.2778	0.5000	0.4130
0.4000	0.3333	0.5000	0.3533
0.5000	0.1250	0.2000	0.4578
0.6667	0.1667	0.2000	0.3597
0.8333	0.2083	0.2000	0.3010
1.0000	0.2500	0.2000	0.2619
0.3333	0.1250	0.3000	0.6105
0.4444	0.1667	0.3000	0.4725
0.5556	0.2083	0.3000	0.3898
0.6667	0.2500	0.3000	0.3348
0.2500	0.1250	0.4000	0.6624
0.3333	0.1667	0.4000	0.5110
0.4167	0.2083	0.4000	0.4203
0.5000	0.2500	0.4000	0.3599
0.2000	0.1250	0.5000	0.6917
0.2667	0.1667	0.5000	0.5327
0.3333	0.2083	0.5000	0.4374
0.4000	0.2500	0.5000	0.3740
0.5000	0.1000	0.2000	0.4884
0.6667	0.1333	0.2000	0.3837
0.8333	0.1667	0.2000	0.3209
1.0000	0.2000	0.2000	0.2791
0.3333	0.1000	0.3000	0.6331
0.4444	0.1333	0.3000	0.4902
0.5556	0.1667	0.3000	0.4046
0.6667	0.2000	0.3000	0.3475

INPUT			OUTPUT
$d/(1.5*t_f)$	$d/(1.5*Z)$	$t_f/W$	$b_p/(40*d)$

0.2500	0.1000	0.4000	0.7060
0.3333	0.1333	0.4000	0.5443
0.4167	0.1667	0.4000	0.4473
0.5000	0.2000	0.4000	0.3828
0.2000	0.1000	0.5000	0.7338
0.2667	0.1333	0.5000	0.5649
0.3333	0.1667	0.5000	0.4636
0.4000	0.2000	0.5000	0.3962

## NETWORK WEIGHTS AND BIAS

Weights-between input layer and hidden layer					Bias	
$W_{11}^h = -0.168652$	$W_{12}^h$	0.905278	$W_{13}^h$	4.213480	-0.002187	
$W_{21}^h = -1.630110$	$W_{22}^h$	14.199407	$W_{23}^h$	-1.475853	2.308174	
$W_{31}^h = -2.199148$	$W_{32}^h$	-1.340044	$W_{33}^h$	-0.070037	1.012040	
$W_{41}^h = -0.481182$	$W_{42}^h$	2.804458	$W_{43}^h$	0.301263	0.836645	
$W_{51}^h = -0.947066$	$W_{52}^h$	3.141695	$W_{53}^h$	5.818547	-2.176270	
$W_{61}^h = -0.005194$	$W_{62}^h$	0.652035	$W_{63}^h$	-0.500801	-0.202923	
$W_{71}^h = -8.705182$	$W_{72}^h$	-3.645303	$W_{73}^h$	-3.854653	2.072483	
$W_{81}^h = -0.329300$	$W_{82}^h$	-0.231012	$W_{83}^h$	-0.511999	-0.071258	
$W_{91}^h = -0.009389$	$W_{92}^h$	-0.253812	$W_{93}^h$	-0.904615	0.405545	
$W_{101}^h = -0.379607$	$W_{102}^h$	-0.009435	$W_{103}^h$	-0.428561	-0.650237	
$W_{111}^h = 11.281569$	$W_{112}^h$	-0.729892	$W_{113}^h$	-0.579828	0.810883	
$W_{121}^h$	-0.120730	$W_{122}^h$	-0.244816	$W_{123}^h$	-0.105662	-0.449513
$W_{131}^h$	0.014882	$W_{132}^h$	-0.071931	$W_{133}^h$	-0.302361	-0.671853
$W_{141}^h$	0.016647	$W_{142}^h$	0.386277	$W_{143}^h$	-0.305617	-0.546815
$W_{151}^h$	-0.914941	$W_{152}^h$	-0.581690	$W_{153}^h$	-0.663085	-0.160377

Weights between hidden layer and output layer		Bias
$W_{11}^o$	3.464911	1.962479
$W_{12}^o$	-4.733091	
$W_{13}^o$	2.054119	
$W_{14}^o$	1.717033	
$W_{15}^o$	-1.506408	
$W_{16}^o$	0.739126	
$W_{17}^o$	5.541857	
$W_{18}^o$	0.877159	
$W_{19}^o$	1.220644	
$W_{110}^o$	0.599265	
$W_{111}^o$	-4.383450	
$W_{112}^o$	0.389613	
$W_{113}^o$	0.616570	
$W_{114}^o$	0.552878	
$W_{115}^o$	1.059260	



# **APPENDIX - D**

## INPUT FILE FOR CALCULATION OF PUNCHING SHEAR STRENGTH

INPUT			OUTPUT
Z/(2*L)	d/W	t <sub>p</sub> /(3*Z)	12*V <sub>d</sub> /V <sub>0</sub>
0.0500	0.2500	0.2500	0.3571
0.0500	0.3750	0.2500	0.3777
0.0500	0.5000	0.2500	0.3979
0.0500	0.2500	0.3333	0.3526
0.0500	0.3750	0.3333	0.3918
0.0500	0.5000	0.3333	0.4115
0.0500	0.6250	0.3333	0.4310
0.0625	0.2500	0.2000	0.3699
0.0625	0.3750	0.2000	0.3901
0.0625	0.5000	0.2000	0.4100
0.0625	0.2500	0.2667	0.3846
0.0625	0.3750	0.2667	0.4043
0.0625	0.5000	0.2667	0.4238
0.0625	0.2500	0.3333	0.3982
0.0625	0.3750	0.3333	0.4173
0.0625	0.5000	0.3333	0.4362
0.0625	0.6250	0.2667	0.4433
0.0625	0.6250	0.3333	0.4551
0.1375	0.2500	0.0909	0.4364
0.1375	0.3750	0.0909	0.4574
0.1375	0.5000	0.0909	0.4792
0.1375	0.2500	0.1212	0.4540
0.1375	0.3750	0.1212	0.4748
0.1375	0.5000	0.1212	0.4963
0.1375	0.2500	0.1515	0.4688
0.1375	0.3750	0.1515	0.4891
0.1375	0.5000	0.1515	0.5102
0.1375	0.2500	0.1818	0.4813
0.1375	0.3750	0.1818	0.5011
0.1375	0.5000	0.1818	0.5216
0.1375	0.2500	0.2121	0.4921
0.1375	0.3750	0.2121	0.5112
0.1375	0.5000	0.2121	0.5310
0.1375	0.2500	0.2424	0.5017
0.1375	0.3750	0.2424	0.5200
0.1375	0.5000	0.2424	0.5389
0.2000	0.2500	0.0833	0.5104
0.2000	0.3750	0.0833	0.5345

INPUT			OUTPUT
Z/(2*L)	d/W	t <sub>p</sub> /(3*Z)	12*V <sub>c</sub> /V <sub>0</sub>
0.2000	0.5000	0.0833	0.5595
0.2000	0.6250	0.0833	0.5855
0.2000	0.2500	0.1042	0.5297
0.2000	0.3750	0.1042	0.5535
0.2000	0.5000	0.1042	0.5782
0.2000	0.6250	0.1042	0.6039
0.2000	0.2500	0.1250	0.5450
0.2000	0.3750	0.1250	0.5684
0.2000	0.5000	0.1250	0.5928
0.2000	0.6250	0.1250	0.6181
0.2000	0.2500	0.1458	0.5570
0.2000	0.3750	0.1458	0.5799
0.2000	0.5000	0.1458	0.6038
0.2000	0.6250	0.1458	0.6286
0.2000	0.2500	0.1667	0.5664
0.2000	0.3750	0.1667	0.5887
0.2000	0.5000	0.1667	0.6119
0.2000	0.6250	0.1667	0.6361
0.2500	0.2500	0.0667	0.5578
0.2500	0.3750	0.0667	0.5862
0.2500	0.5000	0.0667	0.6158
0.2500	0.6250	0.0667	0.6465
0.2500	0.2500	0.0833	0.5813
0.2500	0.3750	0.0833	0.6084
0.2500	0.5000	0.0833	0.6367
0.2500	0.6250	0.0833	0.6660
0.2500	0.2500	0.1000	0.6014
0.2500	0.3750	0.1000	0.6283
0.2500	0.5000	0.1000	0.6562
0.2500	0.6250	0.1000	0.6852
0.2500	0.2500	0.1167	0.6168
0.2500	0.3750	0.1167	0.6433
0.2500	0.5000	0.1167	0.6708
0.2500	0.6250	0.1167	0.6994
0.2500	0.2500	0.1333	0.6282
0.2500	0.3750	0.1333	0.6542
0.2500	0.5000	0.1333	0.6812
0.2500	0.6250	0.1333	0.7094
0.0500	0.1667	0.2500	0.3541
0.0500	0.2500	0.2500	0.3861
0.0500	0.3333	0.2500	0.4056

INPUT			OUTPUT
Z/(2*L)	d/W	t <sub>p</sub> /(3*Z)	12*V <sub>J</sub> /V <sub>0</sub>
0.0500	0.1667	0.3333	0.3462
0.0500	0.2500	0.3333	0.3911
0.0500	0.3333	0.3333	0.4358
0.0500	0.4167	0.3333	0.4543
0.0625	0.1667	0.2000	0.3870
0.0625	0.2500	0.2000	0.4061
0.0625	0.3333	0.2000	0.4247
0.0625	0.1667	0.2667	0.3886
0.0625	0.2500	0.2667	0.4321
0.0625	0.3333	0.2667	0.4609
0.0625	0.4167	0.2667	0.4774
0.0625	0.1667	0.3333	0.3837
0.0625	0.2500	0.3333	0.4246
0.0625	0.3333	0.3333	0.4652
0.0625	0.4167	0.3333	0.4972
0.1375	0.1667	0.0909	0.4364
0.1375	0.2500	0.0909	0.4574
0.1375	0.3333	0.0909	0.4792
0.1375	0.1667	0.1212	0.4947
0.1375	0.2500	0.1212	0.5097
0.1375	0.3333	0.1212	0.5246
0.1375	0.4167	0.1212	0.5394
0.1375	0.1667	0.1515	0.5071
0.1375	0.2500	0.1515	0.5219
0.1375	0.3333	0.1515	0.5365
0.1375	0.4167	0.1515	0.5511
0.1375	0.1667	0.1818	0.5185
0.1375	0.2500	0.1818	0.5329
0.1375	0.3333	0.1818	0.5473
0.1375	0.4167	0.1818	0.5617
0.1375	0.1667	0.2121	0.5290
0.1375	0.2500	0.2121	0.5432
0.1375	0.3333	0.2121	0.5572
0.1375	0.1667	0.2424	0.5389
0.1375	0.2500	0.2424	0.5526
0.1375	0.3333	0.2424	0.5663
0.1375	0.4167	0.2424	0.5800
0.2000	0.1667	0.0833	0.5172
0.2000	0.2500	0.0833	0.5355
0.2000	0.3333	0.0833	0.5542
0.2000	0.4167	0.0833	0.5733
0.2000	0.1667	0.1042	0.5474

INPUT			OUTPUT
Z/(2*L)	d/W	t <sub>f</sub> /(3*Z)	12*V <sub>c</sub> /V <sub>0</sub>
0.2000	0.2500	0.1042	0.5622
0.2000	0.3333	0.1042	0.5772
0.2000	0.4167	0.1042	0.5924
0.2000	0.1667	0.1250	0.5598
0.2000	0.2500	0.1250	0.5744
0.2000	0.3333	0.1250	0.5892
0.2000	0.4167	0.1250	0.6041
0.2000	0.1667	0.1458	0.5709
0.2000	0.2500	0.1458	0.5852
0.2000	0.3333	0.1458	0.5997
0.2000	0.4167	0.1458	0.6143
0.2000	0.1667	0.1667	0.5808
0.2000	0.2500	0.1667	0.5948
0.2000	0.3333	0.1667	0.6089
0.2000	0.4167	0.1667	0.6233
0.2500	0.1667	0.0667	0.5578
0.2500	0.2500	0.0667	0.5862
0.2500	0.3333	0.0667	0.6158
0.2500	0.4167	0.0667	0.6465
0.2500	0.1667	0.0833	0.5771
0.2500	0.2500	0.0833	0.5927
0.2500	0.3333	0.0833	0.6085
0.2500	0.4167	0.0833	0.6245
0.2500	0.1667	0.1000	0.5912
0.2500	0.2500	0.1000	0.6065
0.2500	0.3333	0.1000	0.6221
0.2500	0.4167	0.1000	0.6379
0.2500	0.1667	0.1167	0.6035
0.2500	0.2500	0.1167	0.6185
0.2500	0.3333	0.1167	0.6338
0.2500	0.4167	0.1167	0.6493
0.2500	0.1667	0.1333	0.6142
0.2500	0.2500	0.1333	0.6289
0.2500	0.3333	0.1333	0.6439
0.2500	0.4167	0.1333	0.6592
0.0500	0.1250	0.2500	0.3541
0.0500	0.1875	0.2500	0.3861
0.0500	0.2500	0.2500	0.4056
0.0500	0.1250	0.3333	0.3462
0.0500	0.1875	0.3333	0.3911
0.0500	0.2500	0.3333	0.4358

INPUT			OUTPUT
Z/(2*L)	d/W	t <sub>p</sub> /(3*Z)	12*V <sub>J</sub> /V <sub>0</sub>
0.0500	0.3125	0.3333	0.4543
0.0625	0.1250	0.2000	0.3870
0.0625	0.1875	0.2000	0.4061
0.0625	0.2500	0.2000	0.4247
0.0625	0.1250	0.2667	0.3886
0.0625	0.1875	0.2667	0.4321
0.0625	0.2500	0.2667	0.4609
0.0625	0.3125	0.2667	0.4774
0.0625	0.1250	0.3333	0.3825
0.0625	0.1875	0.3333	0.4227
0.0625	0.2500	0.3333	0.4626
0.0625	0.3125	0.3333	0.5020
0.1375	0.1250	0.0909	0.4364
0.1375	0.1875	0.0909	0.4574
0.1375	0.2500	0.0909	0.4792
0.1375	0.1250	0.1212	0.4974
0.1375	0.1875	0.1212	0.5122
0.1375	0.2500	0.1212	0.5268
0.1375	0.3125	0.1212	0.5415
0.1375	0.1250	0.1515	0.5451
0.1375	0.1875	0.1515	0.5578
0.1375	0.2500	0.1515	0.5702
0.1375	0.3125	0.1515	0.5824
0.1375	0.1250	0.1818	0.5567
0.1375	0.1875	0.1818	0.5692
0.1375	0.2500	0.1818	0.5813
0.1375	0.3125	0.1818	0.5932
0.1375	0.1250	0.2121	0.5661
0.1375	0.1875	0.2121	0.5783
0.1375	0.2500	0.2121	0.5903
0.1375	0.3125	0.2121	0.6020
0.1375	0.1250	0.2424	0.5750
0.1375	0.1875	0.2424	0.5870
0.1375	0.2500	0.2424	0.5987
0.1375	0.3125	0.2424	0.6102
0.2000	0.1250	0.0833	0.5172
0.2000	0.1875	0.0833	0.5355
0.2000	0.2500	0.0833	0.5542
0.2000	0.3125	0.0833	0.5733
0.2000	0.1250	0.1042	0.5681
0.2000	0.1875	0.1042	0.5807

INPUT			OUTPUT
Z/(2*L)	d/W	t <sub>f</sub> /(3*Z)	12*V <sub>c</sub> /V <sub>0</sub>
0.2000	0.2500	0.1042	0.5933
0.2000	0.3125	0.1042	0.6060
0.2000	0.1250	0.1250	0.5919
0.2000	0.1875	0.1250	0.6035
0.2000	0.2500	0.1250	0.6149
0.2000	0.3125	0.1250	0.6263
0.2000	0.1250	0.1458	0.6015
0.2000	0.1875	0.1458	0.6129
0.2000	0.2500	0.1458	0.6242
0.2000	0.3125	0.1458	0.6354
0.2000	0.1250	0.1667	0.6105
0.2000	0.1875	0.1667	0.6216
0.2000	0.2500	0.1667	0.6327
0.2000	0.3125	0.1667	0.6437
0.2500	0.1250	0.0667	0.5578
0.2500	0.1875	0.0667	0.5862
0.2500	0.2500	0.0667	0.6158
0.2500	0.3125	0.0667	0.6465
0.2500	0.1250	0.0833	0.5797
0.2500	0.1875	0.0833	0.5947
0.2500	0.2500	0.0833	0.6097
0.2500	0.3125	0.0833	0.6250
0.2500	0.1250	0.1000	0.6164
0.2500	0.1875	0.1000	0.6279
0.2500	0.2500	0.1000	0.6393
0.2500	0.3125	0.1000	0.6507
0.2500	0.1250	0.1167	0.6266
0.2500	0.1875	0.1167	0.6378
0.2500	0.2500	0.1167	0.6491
0.2500	0.3125	0.1167	0.6603
0.2500	0.1250	0.1333	0.6359
0.2500	0.1875	0.1333	0.6469
0.2500	0.2500	0.1333	0.6580
0.2500	0.3125	0.1333	0.6690
0.0500	0.1000	0.3333	0.3462
0.0500	0.1500	0.3333	0.3911
0.0500	0.2000	0.3333	0.4358
0.0500	0.2500	0.3333	0.4543
0.0625	0.1000	0.2000	0.3870
0.0625	0.1500	0.2000	0.4061
0.0625	0.2000	0.2000	0.4247

INPUT			OUTPUT
Z/(2*L)	d/W	t <sub>f</sub> /(3*Z)	12*V <sub>c</sub> /V <sub>0</sub>
0.0625	0.1000	0.2667	0.3886
0.0625	0.1500	0.2667	0.4321
0.0625	0.2000	0.2667	0.4609
0.0625	0.2500	0.2667	0.4774
0.0625	0.1000	0.3333	0.3825
0.0625	0.1500	0.3333	0.4227
0.0625	0.2000	0.3333	0.4626
0.0625	0.2500	0.3333	0.5020
0.1375	0.1000	0.0909	0.4364
0.1375	0.1500	0.0909	0.4574
0.1375	0.2000	0.0909	0.4792
0.1375	0.1000	0.1212	0.4974
0.1375	0.1500	0.1212	0.5122
0.1375	0.2000	0.1212	0.5268
0.1375	0.2500	0.1212	0.5415
0.1375	0.1000	0.1515	0.5451
0.1375	0.1500	0.1515	0.5578
0.1375	0.2000	0.1515	0.5702
0.1375	0.2500	0.1515	0.5824
0.1375	0.1000	0.1818	0.5810
0.1375	0.1500	0.1818	0.5927
0.1375	0.2000	0.1818	0.6039
0.1375	0.2500	0.1818	0.6148
0.1375	0.1000	0.2121	0.5733
0.1375	0.1500	0.2121	0.6043
0.1375	0.2000	0.2121	0.6216
0.1375	0.2500	0.2121	0.6320
0.1375	0.1000	0.2424	0.5691
0.1375	0.1500	0.2424	0.5994
0.1375	0.2000	0.2424	0.6293
0.1375	0.2500	0.2424	0.6395
0.2000	0.1000	0.0833	0.5172
0.2000	0.1500	0.0833	0.5355
0.2000	0.2000	0.0833	0.5542
0.2000	0.2500	0.0833	0.5733
0.2000	0.1000	0.1042	0.5681
0.2000	0.1500	0.1042	0.5807
0.2000	0.2000	0.1042	0.5933
0.2000	0.2500	0.1042	0.6060
0.2000	0.1000	0.1250	0.6124
0.2000	0.1500	0.1250	0.6229



INPUT			OUTPUT
$Z/(2*L)$	$d/W$	$t_f/(3*Z)$	$12*V_c/V_0$
0.2000	0.2000	0.1250	0.6332
0.2000	0.2500	0.1250	0.6434
0.2000	0.1000	0.1667	0.6402
0.2000	0.1500	0.1667	0.6500
0.2000	0.2000	0.1667	0.6595
0.2000	0.2500	0.1667	0.6689
0.2500	0.1000	0.0667	0.5578
0.2500	0.1500	0.0667	0.5862
0.2500	0.2000	0.0667	0.6158
0.2500	0.2500	0.0667	0.6465
0.2500	0.1000	0.0833	0.5797
0.2500	0.1500	0.0833	0.5947
0.2500	0.2000	0.0833	0.6097
0.2500	0.2500	0.0833	0.6250
0.2500	0.1000	0.1000	0.6236
0.2500	0.1500	0.1000	0.6344
0.2500	0.2000	0.1000	0.6452
0.2500	0.2500	0.1000	0.6560
0.2500	0.1000	0.1167	0.6544
0.2500	0.1500	0.1167	0.6638
0.2500	0.2000	0.1167	0.6731
0.2500	0.2500	0.1167	0.6823
0.2500	0.1000	0.1333	0.6625
0.2500	0.1500	0.1333	0.6718
0.2500	0.2000	0.1333	0.6809
0.2500	0.2500	0.1333	0.6900

## NETWORK WEIGHTS AND BIAS

Weights between input layer and hidden layer			Bias
$W^h_{11} = -3.958761$	$W^h_{12} = 0.406037$	$W^h_{13} = 0.677140$	-1.393859
$W^h_{21} = 0.209075$	$W^h_{22} = 0.475374$	$W^h_{23} = 0.269611$	-0.024879
$W^h_{31} = -0.517618$	$W^h_{32} = -0.085542$	$W^h_{33} = -1.897582$	0.301181
$W^h_{41} = 0.212203$	$W^h_{42} = 0.450770$	$W^h_{43} = -0.381177$	0.195944
$W^h_{51} = 1.008906$	$W^h_{52} = 0.194557$	$W^h_{53} = 1.846377$	-0.248513
$W^h_{61} = 0.096303$	$W^h_{62} = 0.274760$	$W^h_{63} = -0.874169$	-0.068009
$W^h_{71} = -0.698987$	$W^h_{72} = -0.253247$	$W^h_{73} = -2.327243$	0.131168
$W^h_{81} = -0.473679$	$W^h_{82} = -0.055493$	$W^h_{83} = -0.858274$	-0.028703
$W^h_{91} = 6.267336$	$W^h_{92} = -0.019519$	$W^h_{93} = -2.590382$	1.320040
$W^h_{101} = 0.352038$	$W^h_{102} = 0.223010$	$W^h_{103} = -0.094207$	0.192068
$W^h_{111} = 0.263542$	$W^h_{112} = -0.279114$	$W^h_{113} = 0.066704$	0.145694
$W^h_{121} = -0.870592$	$W^h_{122} = -0.530689$	$W^h_{123} = -0.854730$	0.114777

Weights between hidden layer and output layer	Bias
$W^o_{11} = -2.977979$	-0.558847
$W^o_{12} = 0.140285$	
$W^o_{13} = -2.068480$	
$W^o_{14} = -0.393881$	
$W^o_{15} = 1.929795$	
$W^o_{16} = -0.905729$	
$W^o_{17} = -2.539250$	
$W^o_{18} = -1.214428$	
$W^o_{19} = 4.529062$	
$W^o_{110} = -0.097868$	
$W^o_{111} = -0.111538$	
$W^o_{112} = -1.408480$	

